SHRP-A-637

Analysis of the Integrated Model of Climatic Effects on Pavements

Mansour Solaimanian
Pablo Bolzan

The University of Texas at Austin

Strategic Highway Research Program
National Research Council
Washington, DC 1993

SHRP–A–637
Contract A-001

Program Manager: *Edward T. Harrigan*
Project Manager: *Edward T. Harrigan*
Production Editor: *Cara J. Tate*
Program Area Secretary: *Juliet Narsiah*

June 1993

key words:
air temperature
design temperature
Environmental Effects Model
pavement temperature
performance prediction
SUPERPAVE™

Strategic Highway Research Program
National Academy of Sciences
2101 Constitution Avenue N.W.
Washington, DC 20418

(202) 334-3774

350/NAP/693

Acknowledgements

The research described herein was supported by the Strategic Highway Research Program (SHRP). SHRP is a unit of the National Research Council that was authorized by section 128 of the Surface Transportation and Uniform Relocation Assistance Act of 1987.

The draft of this report was reviewed by Mr. James S. Moulthrop whose valuable comments are greatly appreciated. The help of the SHRP A-001 staff in typing the manuscript is also acknowledged.

Table of Contents

Abstract

One of the functions of the FHWA Integrated model of climatic effects on pavements is simulation of the pavement temperature. The model was applied to certain field cases for which pavement temperature measurements were available. The model seems to be capable of providing a reasonable estimate of pavement temperature if realistic input variables, particularly appropriate thermal properties, are utilized.

A sensitivity analysis was also carried out to evaluate the influence of variations in the air temperature, solar radiation, percent sunshine, and thermal properties on the calculated pavement temperatures.

Executive Summary

This report deals with the evaluation and sensitivity analysis of the FHWA integrated model of the environmental effects on pavement temperature. The asphalt concrete pavement temperature is required as one of the input variables to the performance model being developed by the Strategic Highway Research Program (SHRP). It is also required for both the SHRP asphalt binder and asphalt-aggregate mixture specifications.

The study was centered on the calculation of multilayered flexible pavement temperature profiles for certain locations and days of the year for which field measurements were available.

Two different types of analysis were carried out. First, a sensitivity analysis was performed to evaluate the effects of various environmental parameters and pavement thermal properties on the predicted pavement temperature profile. Environmental parameters included air temperature, percent sunshine and solar radiation. Thermal properties studied in this report were pavement emissivity, absorptivity and thermal conductivity.

The second type of analysis included a comparison between the model outputs and measured pavement temperature profiles. The analysis was performed for a number of cities in the USA and Canada during both Summer and Winter seasons.

In general, it was found that the model can provide satisfactory results depending upon a proper selection of the input parameters. Boundary conditions, climatic parameters, and material properties must be properly characterized in order to obtain a reasonable output.

A good agreement between measured and predicted pavement surface temperatures was observed.

No underprediction or overprediction higher than 2°F (1.1°C) was found on pavement surface temperature.

The sensitivity to environmental parameters indicated that air temperature was the most influential factor regarding the pavement temperature. The difference between air temperature and pavement surface temperature encountered was as low as 10°F to 15°F (6 to 8°C), or as high as 40 to 50°F (22 to 28°C) depending upon solar radiation and percent sunshine and the season.

The sensitivity analysis of the materials thermal properties showed that their influence on pavement surface temperature is more pronounced in summer than in winter. It was also found that small differences in both absorptivity and emissivity, and a rather large difference in thermal conductivity of the asphalt layer can result in a significant change in the pavement temperature profile.

Finally, it is recommended that the user interface of the model be modified in order to make it more efficient. A large number of input variables are required by the model. The complexity of the input interface, as it presently exists, will be reduced. Those variables which do not influence results to a measurable level are either eliminated or defaulted so that users do not have to interact with them. It is also necessary to modify the model to remove the effect of the wind velocity into account as, at this point, the output of the model is insensitive to the variations in the wind velocity.

Chapter 1 Introduction

The Integrated Model

The FHWA integrated model (Ref. 1), as the name implies, integrates three previously developed models, with some modifications, to investigate the environmental effects on the pavement. The first is the Infiltration and Drainage Model (ID Model), developed at the Texas A&M University, that evaluates the effect of rainfall on the pavement. The second is the Climatic-Materials-Structural Model (CMS Model), developed at the University of Illinois, which simulates environmental conditions controlling temperature and moisture in the pavement, and predicts pavement temperatures. The third is the CRREL model, developed at the United States Army Cold Region Research and Engineering Laboratory, which computes the heat and moisture flow at various temperatures and predicts the depth of frost and thaw penetration.

Weather patterns and materials properties are selected as input. It is possible to use the default values provided in the Integrated Model to simulate infiltration and drainage, moisture and temperature profiles, and frost depth and heaving throughout an entire year. With this data, the variation of pavement material properties can be followed from the beginning to the end of the year according to the changes produced in the weather conditions. A detailed explanation of the mechanics of the model can be found in Reference 1.

The Input Data for the Integrated Model

The following seven data files are required to run the integrated environmental model:

1. *Structural File*

This file includes data concerning thickness of different layers, thermal properties of different layers, unit weights, etc. It also includes information concerning initial temperature and suction profiles, location of nodes, and the time increment used in finite difference calculations.

2. *Temperature Data File*

This file includes minimum and maximum daily temperatures for a one year period. The user can make use of the temperature data files already available for different regions, or one may choose to enter his own data. In this case, during input procedure, he will be prompted to enter 12 numbers representing the average monthly minimum and maximum temperatures. The program will then create a one-year temperature data file through interpolation using these monthly values. Another alternative for the user is to create the one-year temperature data file directly. The average daily minimum and maximum air temperature for a one year period are already provided and available based on thirty years of data records for nine different climatic regions defined in the model.

3. *Wind/Sunshine File*

This file contains average monthly wind speed, average monthly percent sunshine, and the

corresponding standard deviation for each month of the year. Daily wind speed and sunshine are obtained through linear interpolation using average monthly values. Another alternative is to create the one year data file directly without using monthly values.

4. *Sunrise/Sunset, Radiation File*

This data file includes information concerning time of sunrise, time of sunset, and solar radiation for each day of the year. There is a routine in the program that calculates these three parameters for each day of the year once the latitude of the location is known.

5. *Lower Boundary Condition Suction File*

This file contains the lower boundary suction values (at the interface between base course and subgrade) at two week intervals for a period of one year.

6. *Infiltration, Drainage Files*

This file includes field data for the base course and subgrade. It includes data such as the amount and type of material used in the base and the width and slope of the base. The data is used to evaluate drainage capabilities of the pavement structure.

7. *Rainfall Data File*

This file contains data on monthly rainfall, number of wet days, number of thunderstorms, and average monthly temperature. Based on

statistics (such as average amount of rainfall, average number of wet days, number of thunderstorms, and standard deviation of each of these parameters) and probability considerations, the distribution of wet days in a month and the amount of rainfall for each wet day is determined. Heat flux resulting from rainfall is not incorporated into the energy balance in this model.

The Analysis Procedure

The following procedure is followed to evaluate this model in predicting the pavement temperature:

1. *Sensitivity Analysis*

   An analysis is performed to evaluate how sensitive the predicted pavement temperature is to the environmental and material thermal properties input data.

2. *Simulation of the Pavement Temperature*

   How well does the model simulate the pavement temperature? The predicted pavement temperatures are compared with the existing field data to answer this question. Previous comparisons cited in the FHWA final report on the integrated model indicate a close match between predicted and measured pavement temperatures.

The sensitivity analysis and pavement temperature prediction was performed for both summer time and winter time. Part 1 includes the high temperature sensitivity analysis (Chapter 1) and maximum pavement temperature prediction (Chapter 2) during the summer time, while Part 2 covers the low temperature sensitivity analysis (Chapter 3)

and minimum pavement temperature prediction (Chapter 4) during the winter time.

Chapter 2 Sensitivity Analysis For Maximum Pavement Temperature

It is important to know the sensitivity of the model to various input parameters, one reason being that the exact values of these parameters are not known in most cases. The sensitivity analysis reported here was performed in two parts. In the first part, the effect of variation of environmental parameters on the calculated pavement temperature was investigated. The environmental factors covered in this part of the analysis included daily maximum temperature, percent sunshine, average wind velocity, and solar radiation. The second part of the study included the effect of material thermal properties on the calculated pavement temperature. The surface absorptivity to solar radiation, emissivity, and thermal conductivity were the variables included in this part of the analysis.

Selection of Values for Environmental Factors

As a first step to perform a sensitivity analysis, it was decided that the pavement temperature in July should be calculated for a reasonable number of different values of input variables (i.e. for various environmental conditions). Four different daily maximum temperatures 80, 90, 100, 110, F°(27, 32, 38, 43 °C) were selected. This range covers typical values for maximum temperature throughout the United States during the Summer.

An overview of percent sunshine reported for 174 weather stations indicates that, in the month of July, the average percent sunshine for most cities is in the range of 60 to 80 percent. Sunshine distributions for these stations for the months of January and July are

shown in Figures I-1 and I-2, respectively. Three values of 45%, 70%, and 90% were selected for the analyses purposes.

Again, based on weather station records for 273 cities, the average wind velocity for July was found to be in the range of 3 mph to 12 mph. Three values of 3, 10, and 18 mph were selected for input to the model. Wind velocity distribution for 120 stations through the U.S. is shown in Figures I-3 and I-4, respectively.

Extraterrestrial solar radiation varies considerably depending upon location and time of the year (about 500 BTU/sq. ft./day to about 4000 BTU/sq. ft./day). However, during a particular month, the differences in solar radiation for various places is much less variable. For July, 3000 to 4000 BTU/sq. ft./day seems to be a reasonable range. The selected values for analysis were 3000, 3500, and 4000 BTU/sq. ft./day.

Figure I-5 shows distribution of extraterrestrial solar radiation as a function of time of the year for different latitudes. It can be seen that during the summer time, the difference between total daily radiation for different latitudes is negligible. This conclusion is more clearly observed considering Figure I-6 which indicates a small variation in extraterrestrial radiation as a function of latitude for a particular day of the year (July 4th).

However, because of significant differences in the time of sunrise and sunset for different latitudes (as shown in Figures I-7 and I-8), the day time duration is longer during summer time for higher latitudes (Figure I-9). Therefore, the average hourly radiation will be smaller as shown in Figure I-10.

In summary, the following values were selected for input variables to give a combination of 81 different cases.

Daily maximum temperature (4 values):	80, 90, 100, 110 °F (27, 32, 38, 43 °C)
Percent sunshine (3 values):	45, 70, 90
Extraterrestrial solar radiation (3 values):	3000, 3500, 4000 BTU/sq.ft./day
Wind velocity (3 values) :	3, 10, 18 mph

In addition, the thermal parameters which were kept constant during this part of the analysis were the following:

Thermal conductivity	0.80 BTU/Hr.Ft. °F
Emissivity factor	0.93
Surface short-wave absorptivity	0.85

Selection of Values for Thermal Properties

In general, absorptivity of long wave radiation can be different from that of shortwave radiation for various materials. The absorptivity of an asphalt concrete surface is reported to be about 0.93 (Ref. 1). This is the absorptivity for long wave radiation received from a black body. However, it appears that absorptivity of the asphalt for short wave solar radiation is also about 0.93. In general, absorptivity of the asphalt concrete depends on the type of aggregates used, the color and the texture of the mix and probably some other factors. Values of 0.7, 0.8, and 0.9 were selected for sensitivity analysis.

Emissivity and absorptivity are identical for black radiation from a source at the same temperature. However, in general, solar absorptivity of a surface can be different from its emissivity for radiation to the atmosphere. Typical values for asphalt concrete emissivity are reported to be about 0.9. Three values of 0.7, 0.8, and 0.9 were selected

for analysis of sensitivity to emissivity.

Reports on thermal conductivity of asphalt concrete indicate a variation of 0.43 to 1.67 BTU/Hr.Ft. °F for this parameter (Ref. 7). In most cases a value of 0.8 BTU/Hr.Ft. °F is used. Apparently, thermal properties of the aggregate which is the predominant component of the mix significantly influence thermal conductivity of the asphalt concrete. Three values of 0.3, 0.6, and 0.9 were selected to analyze sensitivity of the environmental effects integrated model to thermal conductivity.

Using the following values for each of the thermal parameters a total of twenty-seven different conditions were created to be analyzed:

Thermal conductivity of unfrozen asphalt (3 levels)	0.3, 0.6, 0.9 BTU/Hr.Ft. °F
Emissivity factor (3 levels)	0.7, 0.8, 0.9
Surface short-wave absorptivity (3 levels)	0.7, 0.8, 0.9
Daily maximum air temperature	82°F (28°C)
Extraterrestrial solar radiation	3775 BTU/sq.ft./day
Percent sunshine	90

Results of Analysis

The results showing the effect of various environmental factors on the predicted pavement temperature are demonstrated in Figures I-11 through I-22. The results are for the pavement surface. The same trend is expected for temperatures at any other depth, as can be seen in Figures I-23 through I-25, except the fact that the difference between air and pavement temperature will be smaller. It should also be noticed that all these results are for the same structural properties. These figures indicate that there is nearly a linear relationship between predicted pavement temperature and maximum air temperature within the range of values applied in this analysis. Figures I-26 through I-52 indicate the influence of variations in thermal properties on the predicted pavement temperature. The figures represent different temperature profiles as a function of depth

different values of thermal conductivity, solar absorptivity, and emissivity.

The model did not indicate any sensitivity to changes in the wind velocity. Regardless of the magnitude of the wind velocity, the same pavement temperature is calculated by the model. Obviously this cannot be the case. At the time this analysis was done, it was not clear whether this problem was due to a programming error or some other factor.

Conclusions

The following conclusions can be drawn based on the results obtained from this analysis.

Sensitivity to Environmental Parameters

1. The air temperature is the most influential factor regarding the pavement temperature.
2. The difference between air temperature and pavement surface temperature can be as low as 10 to 15 °F (-12 to -9 °C), or as high as 40-50 °F (4° to 10 °C) depending on solar radiation and percent sunshine. Some previous field evidence indicated differences in excess of 50 °F (10 °C).
3. The relationship between air temperature and pavement temperature is nearly linear as long as percent sunshine and solar radiation remain the same.
4. For an increase in solar radiation from 3000 to 4000 BTU/sq. ft./day, there is a 8-10 °F (5 to 6 °C) increase in the pavement temperature.
5. For an increase in percent sunshine from 45% to 90%, there is at 8-10 °F (5 to 6 °C) increase in the pavement temperature .

Sensitivity to Thermal Parameters

1. A change in absorptivity from 0.7 to 0.8 or from 0.8 to 0.9 reduces the temperature at any depth by 5 °F (2.8°C).
2. A change in emissivity from 0.7 to 0.8 or from 0.8 to 0.9 increases the temperature at any depth by 5 °F (2.8°C).
3. As expected, a lower thermal conductivity results in a higher surface temperature and a higher temperature gradient with depth.
4. A change in thermal conductivity from 0.3 to 0.6 BTU/Hr.Ft. 2°F/ft. results in nearly a 3 °F (1.7°C) drop in the surface temperature. A change from 0.6 to 0.9 BTU/Hr.Ft.^{2} °F/ft., on the average, results in nearly a 2 °F (1.1 °C) drop in the surface temperature.
5. For changes in thermal conductivity, larger pavement temperature changes are observed at larger depths.
6. At a depth of about 6 inches, a change in thermal conductivity from 0.3 to 0.6 BTU/Hr.Ft. °F may result in a 6 to 7 °F (3.4 to 4°C) increase in temperature while a change of 0.6 to 0.9 BTU/Hr.Ft. °F may cause nearly a 3°F (1.7°C) increase in temperature.

Chapter 3 Maximum Pavement Temperature Prediction

Model and Prediction of Pavement Temperature

In the Texas Transportation Institute report to the Federal Highway Administration on integrated climatic effects model (Ref. 1), it is mentioned that *"it should not be the objective of the use of this program to duplicate field measurements but rather to be able to generate patterns and ranges of the values that realistically match those measured in the field, for that is what is important in design."* It is important to keep this concept in mind when utilizing this program. As discussed earlier numerous input variables are needed for this model, and in most cases, not all these variables are known exactly. Therefore, assumptions need to be made which will be one of sources of expected discrepancies between measured and predicted values. The model was applied to predict the maximum pavement temperature for some field studies for which measured pavement temperatures were available. Most computations were made for specific days in June, July and August. The output was obtained for 2:00 p.m. or 3:00 p.m. where the pavement temperature is expected to be maximum. Of the seven input files discussed before, the first five contain data which influence the predicted pavement temperature. For all field cases studied, assumptions had to be made since not all input variables were available. The thermal properties of asphalt concrete do not vary within a wide range, and reasonable assumptions were made regarding these variables based on existing data in the literature and the model itself. The initial temperature and suction profiles heavily influence the first day results. These data were not available for any of the cases. Therefore, reasonable assumptions were made. The effect of these initial profiles on the pavement temperature output, beyond the first couple of days, is negligible. In other

words, no matter what values are used for the initial profile, the results will not significantly change beyond the second day. For this reason, if the objective was to predict the maximum pavement temperature on July 28th, the analysis was started on July 25th to keep the initial profile sufficiently far from the intended day of analysis.

Extraterrestrial solar radiation, sunrise time, and sunset time for each location were calculated based on the latitude. The percent sunshine in some cases was estimated based on the best available evidence. If the intention was to use a 90% sunshine for July 28, then the average monthly sunshine for several months in a row (May, June, July, August, September) was input as 90% so that after the internal interpolation of sunshine is performed by the program, the percent sunshine for the intended day of analysis (i.e. July 28th) remained at 90. In the present report, interest was centered on the prediction of the temperature profile for asphalt concrete pavements located in different environmental regions using the Integrated Model. The CMS model is the one that calculates the temperature profiles and takes into account the heat flux boundary condition at the surface. Field data from different locations in the USA were compared to the predicted values obtained from the Integrated Model.

Asphalt Pavement Thermal Property Parameters

In studying the sensitivity of the CMS model to the asphalt pavement thermal properties, accounted for by the thermal conductivity of unfrozen asphalt (K), the emissivity factor (ϵ), and the surfaceshort-wave absorptivity (α), it was found that variation in these three parameters can produce a significant change in the predicted pavement temperatures obtained by the CMS model. In the FHWA report on the climatic effects on pavements, the sensitivity of the CMS model to short-wave absorptivity is reported moderate while its sensitivity to emissivity and thermal conductivity is reported low. In the absence of the actual thermal measurements in each case studied, a set of values for the above mentioned parameters (named prediction 1 in the corresponding graphs) were adopted

on the basis of suggested values reported by the FHWA-Integrated Model. Thermal conductivity of 0.80 BTU/Hr-Ft-°F, emissivity factor of 0.93, and absorptivity of 0.85 were used in the first stage of the analysis. The results obtained, as it will be analyzed later in the report, were far from satisfactory. It was then thought advisable to rerun the program using a new set of thermal parameters, still pertaining to the asphalt pavement materials properties range, but that would reflect a better matching with the measured temperature profile. A thirty-five percent reduction in thermal conductivity, a ten percent reduction in the emissivity, and nearly a ten percent increase in absorptivity resulted in a much better match between measured and predicted values. Average values of these parameters were as follows: conductivity of 0.52 BTU/Hr-Ft-° F, emissivity of 0.84, and absorptivity of 0.92.

The results obtained with this new set of parameters (indicated as prediction 2 in the graphs) were better than those obtained from the typical values reported for these parameters. However, it must be noted that none of those values are the actual data. Later in this report, each case will be described in detail.

Some discrepancies were found in some of the cases studied. A different set of thermal parameters for the same pavement structure with different measured temperature profiles were needed in order to obtain the same degree of matching. This was due to the different temperature profiles with different shapes and slopes in the same season (generally in July). Each individual case will be discussed subsequently.

Applying the Model to Field Data

Comparison between Predicted and Measured Maximum Pavement Temperatures

CASE I: Test Site in College Park, Maryland.

Air and pavement temperatures were reported by Kallas (Ref. 2) on pavement test sections located at College Park, Maryland in June 1964. Asphalt concrete sections with two different thicknesses (12 in. and 6 in. thick) were constructed in order to monitor the temperature profile at different depths. Among the findings encountered, the author mentioned that temperatures at the same depths in both the 6 in. and the 12 in. thick asphalt concrete were virtually the same. The maximum pavement temperatures recorded were obtained on June 30, 1964. The temperature on the surface was 142 °F (61°C) at 3:00 pm when the air temperature reached 99 °F (37°C). There is not enough information about the pavement structure nor about other environmental parameters such as radiation, sunshine, etc. to be used as input to the model.

Extraterrestrial radiation was calculated using the latitude of College Park and sunshine was adopted as 95%, bearing in mind that according to the hourly-temperature data there is no reason to think that the day was not sunny. The extraterrestrial radiation corresponding to College Park for June is about 3700 BTU/sq ft/day. Wind speed was not taken into account since the Integrated Model indicated the simulated temperature not to be sensitive to this parameter.

The program was run for June 30th using the values for radiation and sunshine mentioned above and for the maximum temperature of 99 °F (37°C) at 3:00 p.m.

An asphaltic pavement structure 12 in. thick was adopted using the following values: thermal conductivity of unfrozen asphalt of 0.8 BTU/Hr-Ft °F/ft., heat capacity of 0.22 Btu/lb-°F; unit weight of unfrozen asphalt of 140 pcf, air content of the asphalt layer of 4%, and 80% coarse aggregate content.

The predicted temperature profile is shown in Figure II-1. The surface temperature is

underestimated by 11 degrees (about 8% difference). The predicted temperature at 2-in. depth is about 6 degrees less than the measured value. At lower depths, the match is closer, although it seems that the prediction curve starts to flatten out at a higher rate.

These results were obtained using a thermal conductivity of 0.80 BTU/Hr-Ft °F, emissivity factor of 0.93, and absorptivity of 0.85 (prediction 1 in Figure). However, when a different set of thermal parameters were adopted (conductivity of 0.45, emissivity factor of 0.80, and absorptivity of 0.95), the results were significantly improved, as can be observed in Figure 1 (prediction 2). The shape of the measured and predicted curves are quite similar and the differences in temperature are minimal.

In all the cases, the pore pressure transfer coefficient "r" was kept constant and equal to 0.01 in^{-1}. The lower boundary water pressure was held constant as well for all the cases since both parameters did not indicate a significant difference in the final results.

CASE II: Test Site in Potsdam, N.Y., Clarkson College Campus.

Straub et al (Ref. 3) studied the variations of asphalt concrete pavement temperatures occurring in Potsdam which is located in the northern part of New York State.

The asphalt concrete test section was built with two thicknesses: 6 in. and 12 in. Once more, there was virtually no difference between measurements for both thicknesses at the same depth.

At this site, the data recorded on June 28, 1967 was compared with the predicted data from the Integrated Model. The maximum air temperature reported was 83°F (28°C), and the maximum temperature measured on the pavement surface was 144°F (62°C). A 3700 BTU/sq. ft./day radiation value was adopted. A ninety-five percent sunshine was selected assuming a sunny day.

The predicted profile displayed a surface temperature 31 degree less (22% error) as can be seen in Figure II-2. The temperature difference was 17°F at 2-in. depth tending to approach the measured profile at deeper levels. The difference between air temperature and measured surface temperature was 61°F (16°C).

Considerable enhancement was achieved on the surface temperature prediction using a 50% less conductivity, lower emissivity and higher absorptivity, as illustrated in Figure 2 (prediction 2). Nonetheless, predicted temperature profile still show a gap of about 10°F (5.6°C). This is a very peculiar case since the measured temperature seems to be considerably high. The difference between air temperature and surface temperature is 61°F (34°C) which seems to be too high when compared with the other cases and according to what one can expect from field measurements. Consequently, no reasonable thermal parameters could improve the matching between predicted and measured values.

Running the program using 100% sunshine instead of 90% gave a surface temperature of 5°F (2.8°C) higher when keeping the rest of the parameters constant. Below 2 in. depth, the increase is nearly 3°F (1.7°C). These results agree with the ones found in the sensitivity analysis for the surface temperature. Typical temperature profiles indicate that, as the depth increases, the temperature tends to stabilize. In other words, the curve tends to have a decreasing slope with depth.

CASE III: Test Site in Hybla Valley, Virginia

The data was taken from a paper written by Barber (Ref. 4) who presented a relationship between pavement temperature and weather parameters (wind, precipitation, solar radiation and air temperature). In that article, there is no mention of the method used to measure the pavement temperature on the surface. Moreover, the variation in the radiation values reported was very high due to cloudiness and rainstorms on some of the days in which the measurements were taken.

The daily range in air temperatures registered from May 21 to May 30 spanned from 7 to 37°F (-14 to 3°C) according to this reference. Figure III-3 indicates the measured and predicted maximum pavement temperatures at surface for this site. The results obtained with the default values already available in the Integrated Model underpredict the measured surface pavement temperatures. The differences range from 7 to 22°F (4 to 12°C) (difference between 6.8% and 18% ; average difference 12%). In some cases the measured radiation was very low indicating a cloudy day or even a rainy day.

It is important to note that the largest difference encountered on May 29 and May 30 could be caused either by the low radiation reported or the daily air temperature range which was the largest for May 29. Moreover, on May 30 the radiation reported corresponds to that obtained before a rainstorm which started at 2 pm.

Despite the underprediction using the Environmental Effects Integrated Model (average 13.7°F or 7.7°C), the predicted curve follows the shape of the observed curve very closely.

Using a different input for the thermal parameters, namely conductivity 0.45 BTU/Hr-Ft-°F, emissivity of 0.80, and absorptivity of 0.95, the agreement is fairly good with the exception of May 28, 29 and 30.

CASE IV: Test Site in Tucson, AZ.

In this case taken from the Asphalt Institute files, and reported by Rumney et al. (Ref. 5) local climatological data from Tucson, for July 1969 was available along with air temperature, surface pavement temperature, and depth profile for a 6-in thick layer and a 12-in thick layer. The method used in the measurements is not known.

Three sunny, warm days were selected: 19, 22 and 27th of July 1969. An extraterrestrial solar radiation of 3700 BTU/sq. ft./day was chosen to be realistic for this time of the year. The sunshine was selected at 95%. The lower boundary conditions and the pore

pressure remained the same in all cases.

Figures II-4 through II-6 show the measured and predicted temperature profiles for this site. In all these cases, the surface temperature is underestimated: 11°F (6.2°C) on July 19 (8% difference), 17°F (9.5°C) on July 22 (11% difference), and 11°F (6.2°C) on July 27 (8% difference). The two profiles approach each other at higher depths. While slight overprediction is observed for July 19 for depths below 4 inches, some underprediction is still noticeable for the other two dates. The shape of the measured profile for July 19 indicates a higher temperature gradient compared to the other two dates.

A clearer picture can be observed on both July the 22nd and July the 27th when the model gives an underpredicted curve with a maximum difference on the surface temperature gradually approaching the measured values with depth. The predicted temperature at the surface was 17°F (9.5°C) less than the measured one (18% difference). Below a 2-in depth, the difference was (6.7°C) (9% difference).

Similar results were obtained on July 27. The difference between measured and predicted temperatures was 18°F (10°C) at the surface (12% difference) and 11°F (6.2°C) at the 2-in. depth (8% difference).

Using different thermal coefficients on July 22 and 27 (conductivity = 0.60 BTU/Hr-Ft.°F, emissivity = 0.70 and absorptivity = 0.95), the results indicated a much closer agreement between predicted and measured values as can be seen in Figures II-5 and II-6. For July 19, this set of coefficients did not result in a close match. It is interesting to note that the measured temperature profile of that particular day is quite different from that of the other two days. For this reason, it was necessary to select another set of thermal coefficients in order to obtain a better match. Obviously, it is not correct to use different thermal properties for the same pavement structure built with the same materials.

Prediction 2 on July 19 with a different set of thermal coefficients produced a better fit between calculated and measured temperature profiles. Even though all three days were considered sunny, other environmental factors (such as strong wind at the surface, etc.) might have contributed to differences in measured temperature profiles for different dates.

CASE V: Test Site in Saskatchewan, Canada

In order to develop a computer model to predict pavement layer temperatures, Huber et al. (Ref. 6) collected field data on pavement temperatures at different depths.

The temperatures in this case were reported to be measured bi-hourly in a 10-in. full depth pavement constructed in the Fall of 1974. Temperatures were recorded in the Summer of 1975. In accordance with the latitude of Saskatchewan in July, the radiation is approximately 3763 BTU/sq. ft./day. Several days in June and July were chosen for comparison. The sunshine was taken as 95% in all cases assuming sunny warm days. The maximum temperature difference between air and surface was approximately 40°F (4°C). At 2-in. depth, the difference was less and ranged between 15 and 25°F (-9 and -4°C). There was no sunshine or cloudiness data available nor was the air temperature range available for each day.

From June 21st to June 25th, the measured pavement temperature profiles were compared with the ones predicted using the FHWA-Integrated Model. The same was done for July 2nd through the 6th and for July 12th through July 16th. Profiles can be seen in Figures II-7 through II-21. The general trend in the results indicates a closer agreement than in the former cases. Both radiation and sunshine values adopted were the highest possible values for sunny days during the Summer time.

A substantial improvement was achieved using different values of the thermal parameters. The average values were thermal conductivity of 0.52 BTU/Hr-Ft-°F,

emissivity of 0.87, and absorptivity of 0.91; although in every case they varied slightly in order to approach the best fit. In general, the predicted profiles do not follow exactly the shape of the measured ones. In two cases, prediction 1 parameters (with the CMS suggested parameters) were adequate to obtain a good agreement as can be seen in Figures II-10 and II-11. It is noteworthy to observe that the measured temperature profiles for Saskatchewan in general do not follow the typical smooth decreasing curve as noted in the other cases.

The predicted and measured maximum surface temperatures are shown in Figure II-22 through II-24. In nearly every case,the surface temperature is underestimated.

The largest difference between predicted and measured pavement surface temperatures was 13°F (7.3°C) underprediction (11% difference), and the average difference was 4°F (2.2°C). In one case, June the 24th, predicted pavement surface temperature matched the measured temperature. The average difference was found to be around 4%. The lowest difference encountered (3%) was on the week of July 12.

With the second set of parameters (lower conductivity and emissivity and higher absorptivity), the curves shifted towards a higher maximum pavement temperature (about 5°F) (2.8°C). The predicted profiles match the measurements more closely as can be seen in the above mentioned Figures.

Conclusions

The following conclusions can be drawn based on the analysis carried out in this study.

1. Applying typical values of 0.8 BTU/Hr-Ft-°F for thermal conductivity, 0.85 for absorptivity, and 0.93 for emissivity resulted in underprediction of pavement temperature for most of the field cases studied in this report.

2. It was found that underprediction ranged between 4 and 18% (average difference of 8%) under the conditions imposed. However, the temperature prediction is improved below the 2-in. depth.

3. Average values of 0.52 BTU/Hr-Ft-°F for thermal conductivity, 0.92 for absorptivity and 0.84 for emissivity significantly improved predictions.

4. More field data with more comprehensive measurements on environmental conditions need to be analyzed to establish the best values for thermal properties, and to investigate the reliability of the model in simulating the pavement temperature.

Chapter 4 Sensitivity Analysis For Minimum Pavement Temperature

In this section, a study of the prediction of pavement temperatures using the FHWA Integrated Model was conducted to determine the pavement temperature profile under low temperature environmental conditions. First, a sensitivity analysis was performed on one pavement profile using the CMS model for different climatic inputs at four different temperatures. Secondly, a thermal parameters sensitivity analysis was also conducted on the same pavement profile at two different temperatures.

Selection of Values for Environmental Factors

January was the time of the year selected to perform the sensitivity analysis for low temperatures using average typical environmental parameters. The following values were selected for climatic input variables resulting in a combination of 48 different cases,

Daily minimum air temperature (4 values):	-30, 20, -10, 0°F
	(-34, -29, -23, -18°C)
Percent sunshine (2 values):	30, 70
Extraterrestrial solar radiation (2 values):	1000, 2000 Btu/sq.ft. day
Wind velocity (2 values):	3, 18 mph

In addition the thermal parameters used were the following:

Thermal conductivity of surface asphalt	0.8 BTU/Hr-Ft-°F
Emissivity Factor	0.93
Surface short-wave absorptivity	0.85

Selection of Values for Thermal Properties

Among the material properties that can affect pavement temperature are the thermal properties defined in the model as the emissivity factor, the surface short-wave absorptivity, and thermal conductivity of unfrozen, freezing, and frozen asphalt. The sensitivity analysis was carried out with the following input values giving a combination of 24 different cases:

Thermal conductivity of unfrozen asphalt (3 levels):	0.3, 0.6, 0.9 BTU/Hr-Ft-°F
Emissivity factor (2 levels):	0.7, 0.9
Surface short-wave absorptivity (2 levels)	0.7, 0.9
Daily minimum air temperature (2 levels) :	-10, 40°F (-23, 4°C)
Extraterrestrial solar radiation	1000 BTU/sq. ft./day
Percent sunshine	50

The same values of thermal conductivity were adopted for freezing and frozen asphalt.

Two temperature levels were adopted because some differences were observed between frozen and unfrozen conditions. Since thermal conductivity is the most likely thermal parameter that can influence pavement temperature profile at low temperatures, three values of that parameter were chosen.

Results of Analysis

Sensitivity to Environmental Parameters

The results of the effect of diverse environmental conditions on the pavement predicted temperature can be observed in Figures III-1 to III-9. In general, it can be said that

there are no noticeable changes caused by the amount of shortwave radiation nor by the percent sunshine. These results were expected since the lowest pavement temperature occurs during early morning when the pavement is not yet exposed to much radiation.

When solar radiation is increased to a 100%, the increase in pavement temperature is approximately 0.5°F (0.3°C) (See Figures III-3 to III-6). Curiously, when the percent sunshine is increased from 30 to 70, the pavement temperature profile shifts downward about 2°F (1.1°C) as can be seen in Figures III-1 and III-2. It is not clear why, with an increase in percent sunshine, a slight decrease in low temperature is observed.

The effect of wind speed is negligible, at least using this model and for the typical range of values for this parameter.

The variation of predicted pavement temperature observed for different climatic inputs (wind speed, solar radiation, percent sunshine, and minimum and maximum temperature) suggests that there is no significant change in the output values when low temperatures are considered. That is to say that, essentially, the minimum pavement surface temperature can be considered very close to the minimum air temperature. In some cases measured minimum pavement surface temperature was found to be 2 or 4°F (1.1 or 2.2°C) higher than the minimum air temperature.

Sensitivity to Thermal Parameters

In general, the surface short-wave absorptivity did not show any significant change in pavement temperature prediction at both temperatures, -10°F (-23°C) and 40°F (4°C) as can be observed in Figures III-10 to III-16. Note that the slope of the pavement temperature versus depth curve is lower at higher temperature.

Thermal conductivity and the emissivity factor have a relatively modest effect on the

predicted pavement temperature at the low temperature -10°F (-23°C) and a slightly higher effect at the high temperature 40°F (4°C). The higher the emissivity, the lower the temperature; for an increase of 0.2 in emissivity the temperature is lowered approximately 3°F (1.7°C) at a daily minimum temperature of (4°C). When that increment occurs at -10°F (-23°C), the decrease in temperature is around 2°F (1.1°C). In both cases the temperature profile varies with depth, and the decrease in temperature is slightly more pronounced at the surface than in depth as depicted in Figures III-17 to III-22.

The pavement temperature variation given by different thermal conductivities is portrayed in Figures III-23 to 26. The predicted temperature profiles with higher conductivity indicate lower variation with depth. The profile temperature has a higher slope at lower temperatures for the same conductivity value. This trend is, in general, the same regardless of the emissivity and absorptivity values, within the values used in this study.

While both absorptivity and emissivity produce a temperature shifting, different conductivities create a rotation around some point below the surface (change of slope). The temperature change on the pavement surface is more noticeable at -10°F (-23°C) than at 40°F (4°C) for changes in conductivity. For instance, as shown in Figure III-25 the pavement surface temperature difference between a profile calculated with a conductivity of 0.3 Btu/Hr-Ft-°F and another with conductivity of 0.9 Btu/Hr-Ft-°F is 3.6°F (2°C). For a change in conductivity from 0.3 Btu/Hr-Ft-°F to 0.6 Btu/Hr-Ft-°F the change in pavement temperature is 2.7°F (1.5°C), while increasing such conductivity from 0.6 Btu/Hr-Ft-°F to 0.9 Btu/Hr-Ft-°F causes a change of 0.9°F (0.5°C). The lower the conductivity, the lower the predicted surface temperature. The impact is more significant for lower conductivity values.

Conclusions

The following conclusions were based on the observations and analysis presented in this study.

Sensitivity to Environmental Parameters

The sensitivity analysis of the climatic inputs (min. and max. air temperature, wind speed, solar radiation, and percent sunshine) in the low temperature region indicates that the minimum pavement surface temperature is very close to air temperature and, as expected, it is little affected by both solar radiation and percent sunshine.

Sensitivity to Thermal Parameters

The sensitivity analysis of the materials thermal properties inputs (thermal conductivity of unfrozen, freezing, and frozen asphalt; emissivity factor, and surface short-wave absorptivity) of the Integrated Model at low temperatures shows.

1. The surface short-wave absorptivity has no impact on the minimum pavement surface temperature within the values used,
2. A change in emissivity factor from 0.7 to 0.9 reduces the temperature at the surface by almost 2°F (1.1°C) when the minimum air temperature is 40°F (4°C); and reduces the surface temperature about 0.5°F (0.3°C) at a minimum air temperature of -10°F (-23°C).
3 A lower thermal conductivity results in a lower surface temperature and the impact is larger for lower conductivities and lower temperature (-10°F), (-23°C).

Chapter 5 Minimum Pavement Temperature Prediction

Measured and predicted lowest temperature data from eight cases located in four different places in the USA and Canada were compared using the Integrated Model.

CASE I : Test Site in College Park, Maryland.

The data from this site was reported by Kallas (Ref. 2) on pavement test sections located at College Park in January, 1965. It is the same test section cited previously in the high temperature analysis.

The minimum air temperature recorded on January 19, 1965 was 6°F at 7 a.m. and on the surface the temperature was 9°F (-13°C). Figure IV-1 shows the temperature variation (both measured and predicted) in the 12-inch thick asphalt concrete layer. The predicted profile matches well with the measured one below 4 inches. There is a 2 °F (1.1°C) overprediction on the pavement surface. Climatic and thermal parameter inputs are indicated on the graph.

CASE III : Test Site in Potsdam, N.Y., Clarkson College Campus.

At this site, (Ref. 3) the minimum pavement temperature was recorded in February 8, 1967. The temperatures were measured at 0.25, 2, 4, 6, 8, 10 and 12 inches at 6 a.m. when the air temperature was -7°F (-22°C). Since there is no surface temperature data available, the prediction was done from 2 inches downwards and it is shown in Figure IV-2. There is a coincidence in temperatures at 2-inches but a growing departure below

this depth. The maximum difference is produced at 8-inch depth where predicted temperature is about 6°F (3.4°C) higher than measured temperature.

CASE III : Test Site in Tucson, Arizona

During January 1970 minimum pavement temperature profiles were recorded in Tucson (Ref. 5). Figures IV-3 to IV-7 show the measured and predicted temperature profiles for different days in January. The results obtained are different in every case despite the fact that the input parameters remained the same. In one case the match between predicted and measured values is very close (January 30). On January 23, the predicted surface temperature was very close to the measured one while the profile presented a gap between 2 and 3°F (1.1 to 1.7°C).

On January 16, there was an underprediction of 3°F (1.7°C) while on January 9 there was an overprediction of about 4°F (2.2°C). Finally, on January 2, there was a slight overprediction on the surface accompanied by an increasing underprediction below 1 inch.

CASE IV : Test Site in Saskatchewan, Canada

The temperature profile data was reported by Huber et al (Ref. 6) and recorded on February 18, 1975 from McLean, Saskatchewan by the Saskatchewan Highway and Transportation Department. The pavement section is a 250 mm Full Depth Asphalt Pavement and the temperatures were measured at depths of 0, 2, 4, 6, 8, 10 and 22 inches. Minimum air temperature reported was 6°F (-14°C) at 6 a.m. and the same temperature magnitude was measured on the surface.

Both measured and predicted temperature gradients are depicted in Figure IV-8. There is an overprediction of 5°F (2.8°C) on the surface and at 2 inch depth.

Conclusions

After applying the FHWA Integrated Model to a limited number of pavement profiles under low temperature environmental conditions the following conclusions can be drawn:

1. In general, there is a good agreement between measured and predicted pavement surface temperature. No underprediction or overprediction higher than 2°F (1.1°C) was observed.
2. Predicted pavement temperature profiles were fairly close to measured asphalt concrete temperature profiles bearing in mind that in some cases some of the materials properties and environmental conditions were not available.
3. It must be taken into consideration that there are some uncertainties with regard to some environmental inputs (for example percentage sunshine in several cases) and thermal properties. The assumptions made in that regard in this study can affect the final results.
4. Further analysis on more field data at low temperature using the FHWA Integrated Model is required in order to reinforce these conclusions.

Chapter 6 General Conclusions And Recommendations

The following conclusions are made based on the results discussed in this report.

1. In general, the model can provide satisfactory results as long as the best estimates of the input parameters are used.
2. The air temperature is the most influential factor regarding the pavement temperature.
3. The difference between air temperature and pavement surface temperature can be as low as 10 to 15°F (6 to 8°C), or as high as 40 to 50°F (22 to 28°C) depending on solar radiation and percent sunshine. Some previous field evidence indicates differences over 50°F (28°C).
4. The relationship between air temperature and pavement temperature is nearly linear as long as percent sunshine and solar radiation remain the same.
5. For an increase in solar radiation from 3000 to 4000 BTU/sq. ft./day, there is almost 8-10°F (4.5 - 5.6°C) increase in the pavement temperature.
6. For an increase in percent sunshine from 45% to 90%, there is almost 8-10°F (4.5 - 5.6°C) increase in the pavement temperature.
7. Applying typical values of 0.8 BTU/Hr-Ft-°F for thermal conductivity, 0.85 for absorptivity, and 0.93 for emissivity resulted in underprediction of pavement temperature for most of the field cases studied in this report.
8. It was found that underprediction ranged between 4 and 18% (average difference of 8%) under the conditions imposed. However, the temperature prediction is improved below the 2-in. depth.
9. Average values of 0.52 BTU/Hr-Ft-°F for thermal conductivity, 0.92 for absorptivity and 0.84 for emissivity significantly improved

predictions.

10. More field data with more comprehensive measurements on environmental conditions need to be analyzed to establish the best values for thermal properties, and to investigate the reliability of the model in simulating pavement temperature.

11. The sensitivity analysis of the climatic inputs (min. and max. air temperature, wind speed, solar radiation, and percent sunshine) in the low temperature region indicates that the minimum pavement surface temperature is very close to air temperature and, as expected, it is little affected by both solar radiation and percent sunshine.

12. The sensitivity analysis of the material thermal properties inputs (thermal conductivity of unfrozen, freezing, and frozen asphalt; emissivity factor, and surface short-wave absorptivity) of the Integrated Model at low temperatures shows:

    a. the surface short-wave absorptivity has no impact on the minimum pavement surface temperature within the values used,

    b. a change in emissivity factor from 0.7 to 0.9 reduces the temperature at the surface by almost 2°F (1.1°C) when the minimum air temperature is 40°F (4°C); and reduces the surface temperature about 0.5°F (0.3°C) at a minimum air temperature of -10°F (-23°C).

    c. a lower thermal conductivity results in a lower surface temperature and the impact is larger for lower conductivities and lower temperatures -10°F (-23°C).

13. In general, there is good agreement between measured and predicted pavement surface temperatures. No underprediction or overprediction higher than 2°F (1.1°C) was observed.

14. Predicted pavement temperature profiles were fairly close to measured asphalt concrete temperature profiles bearing in mind that in some cases some of the materials properties and environmental conditions were not available.

15. It must be taken into consideration that there are some uncertainties with regard to some environmental inputs such as percentage sunshine and thermal properties. The assumptions made in that regard can affect the final results reported in this study.

16. Further analysis on more field data at low temperature using the FHWA Integrated Model is required in order to reinforce these conclusions.

It is recommended that the model be used for simulating pavement response rather than predicting exact values for pavement temperature or any other pavement response.

It appears it is necessary to modify the user interface of the model to make it more efficient. Input phase is to some extent cumbersome and is not flexible enough.

One shortcoming of the model is in the way it takes into account the effect of wind speed on the pavement temperature. Whether the wind velocity is very low or very high, exactly the same result will be obtained for the calculated pavement temperature. It could not be identified if this problem is due to a programming error or shortcomings of the formulas used in the program. Therefore, it seems necessary to modify the model to appropriately take the effect of the wind velocity into account.

List Of References

1. Lytton, R. L., Pufahl, D. E., Michalak, C. H., Liang, H. S., and Dempsey, Bl J., "An Integrated Model of the Climatic Effects on Pavements", Texas Transportation Institute, Texas A & M University, Final Report, February 1990.
2. Kallas, B. F., "Asphalt Pavement Temperatures", Highway Research Record 150, National Research Council, 1966, pp. 1-11.
3. Straub, A. L., Schenck, H.N., and Przybcien, F. E., "Bituminous Pavement Temperature Related to Climate," Highway Research Record 256, Highway Research Board, 1968, pp. 53-77.
4. Barber, E. S., " Calculation of Maximum Pavement Temperatures from Weather Reports", Bulletin 168, Highway Research Board, Washington, D. C., 1957, pp. 1-8.
5. Rumney, T. N. and Jimenez, R. A., "Pavement Temperatures in the Southwest", Highway Research Record 361, National Research Council, 1969, pp. 1-13.
6. Huber, G. A., Heiman, G. H., and Chursinoff, R. W., "Prediction of Pavement Layer Temperature During Winter Months Using a Computer Model", Canadian Technical Asphalt Association, November 1989.
7. Highter, W. H., and Wall, D. J., "Thermal Properties of Some Asphaltic Concrete Mixes", Transportation Research Record 968, TRB, NRC.

Appendix A - Figures

List of Figures

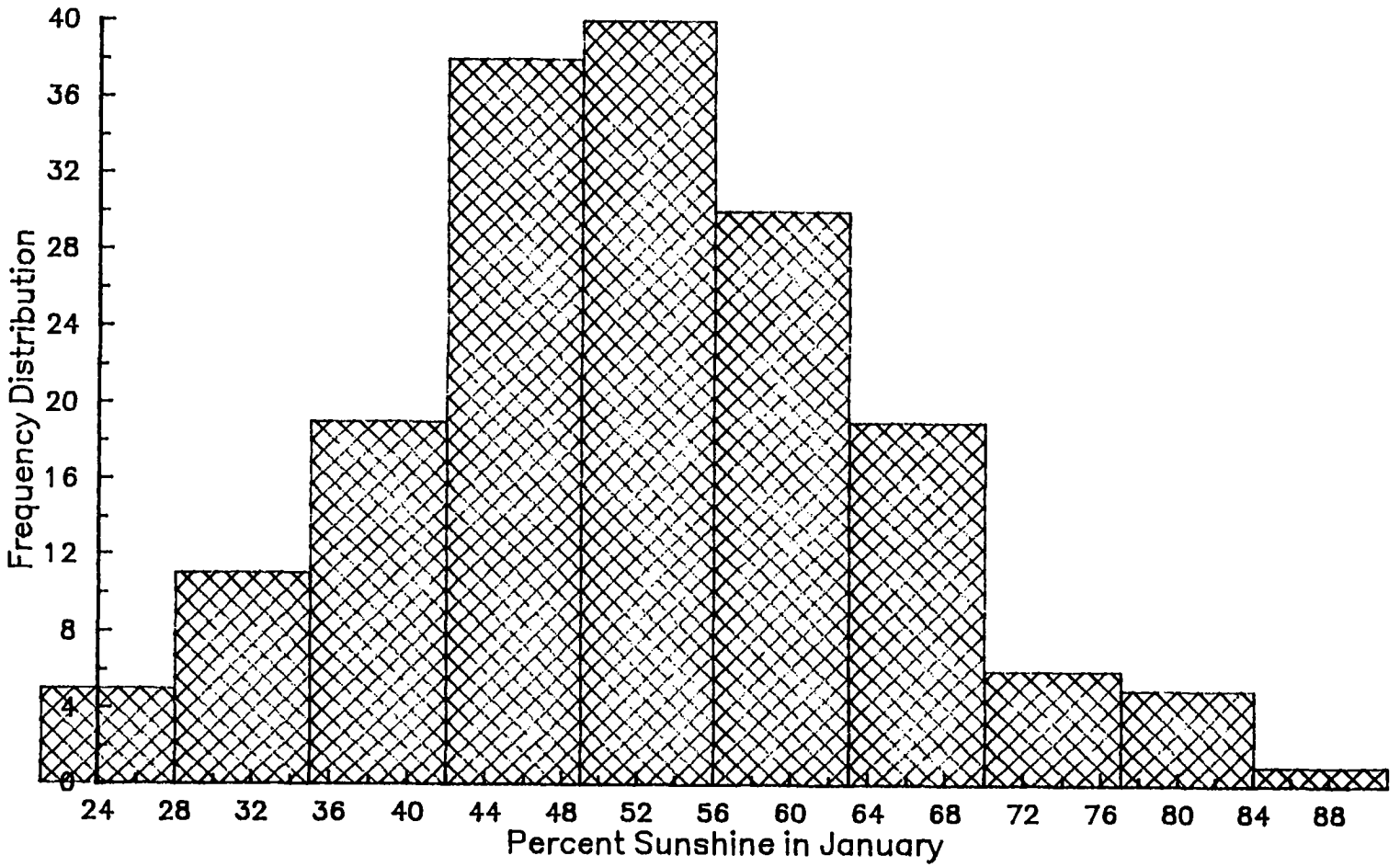

Figure I-1. Frequency Distribution of Average Percent Sunshine in January Measured at 174 Primary Stations in the United States.

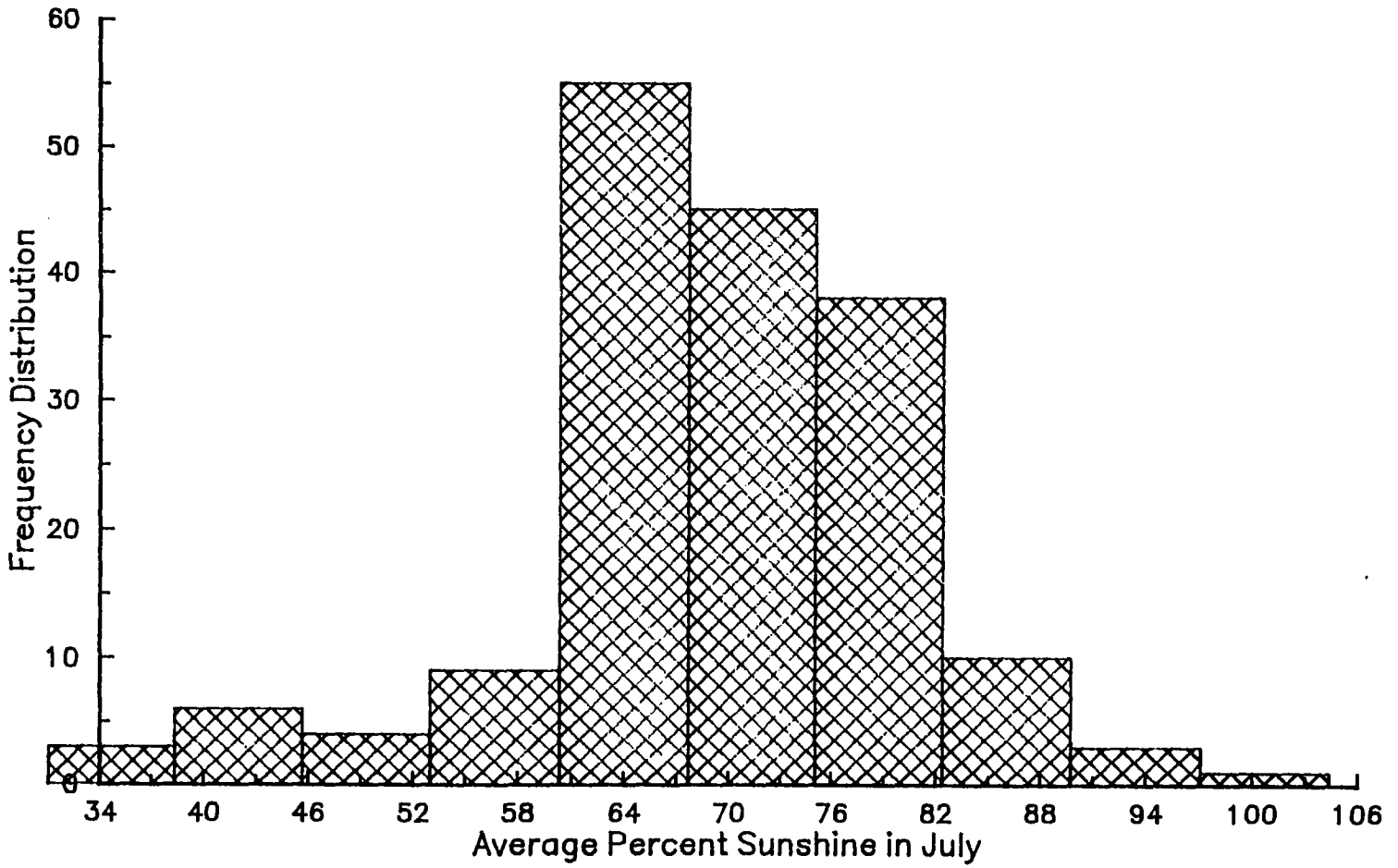

Figure I-2. Frequency Distribution of Average Percent Sunshine in July Measured at 174 Primary Stations in the United States.

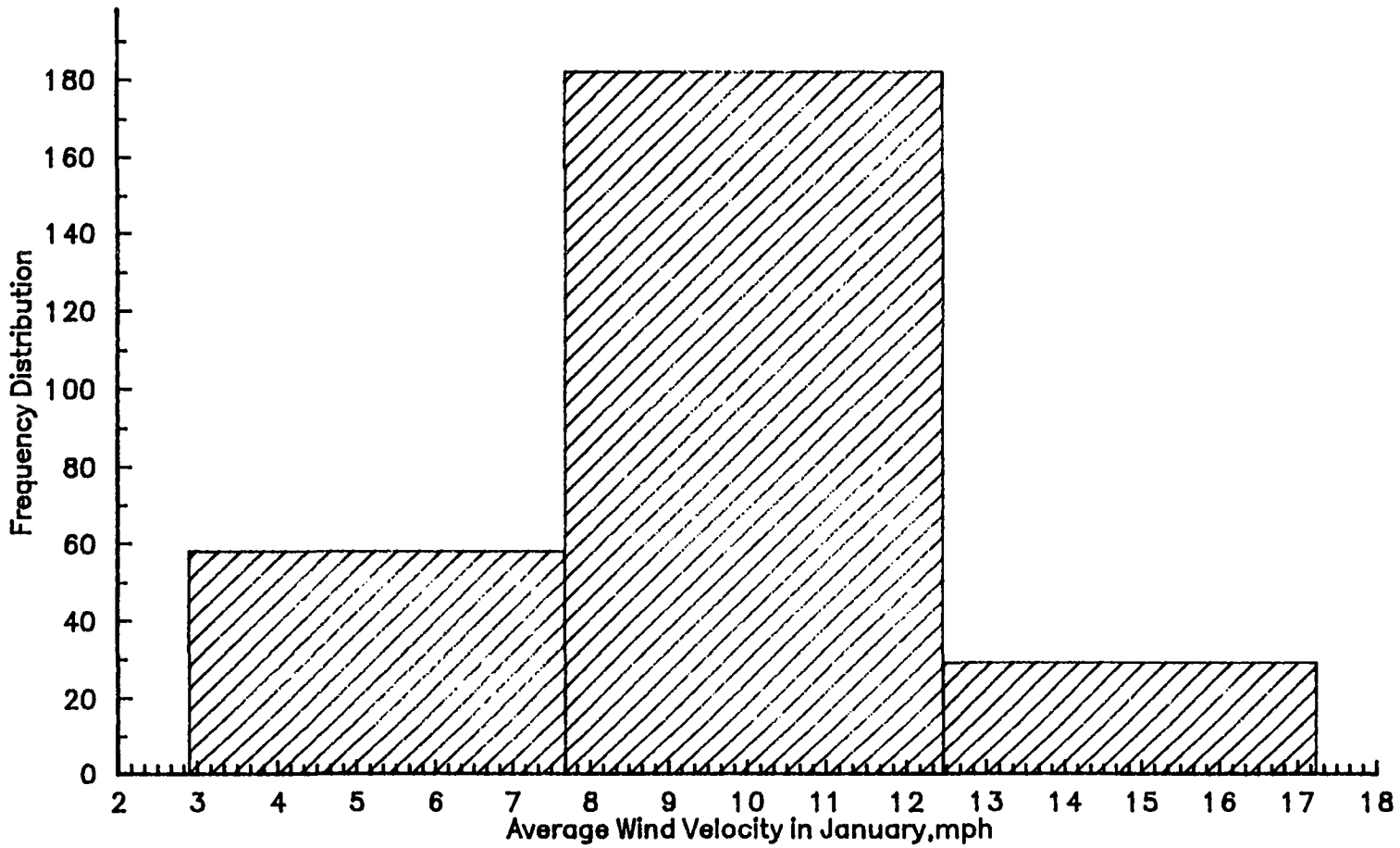

Figure I-3. Frequency Distribution of Average Monthly Wind Velocity in January Measured at 273 Primary Stations in the United States.

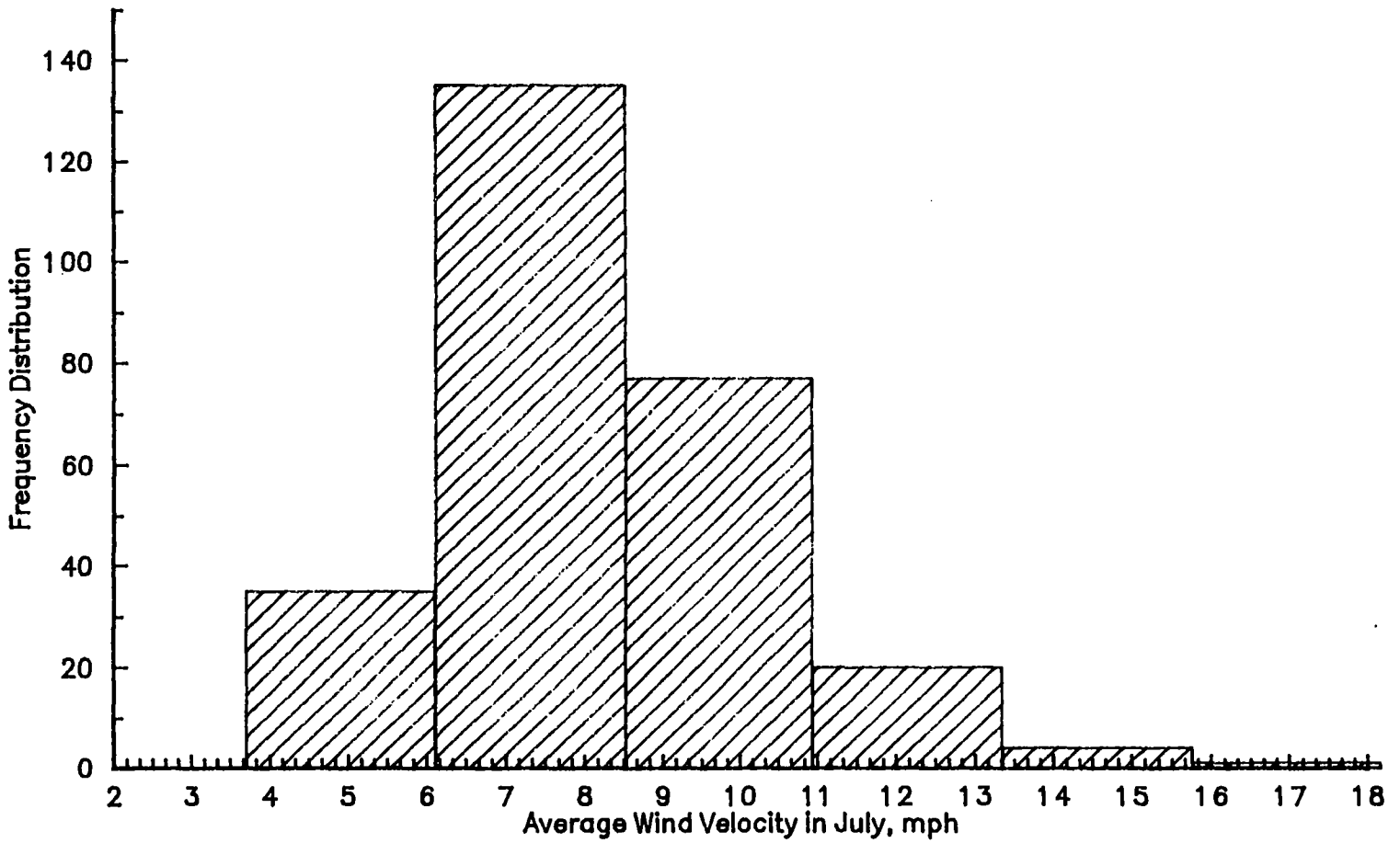

Figure I-4. Frequency Distribution of Average Monthly Wind Velocity in July Measured at 273 Primary Stations in the United States.

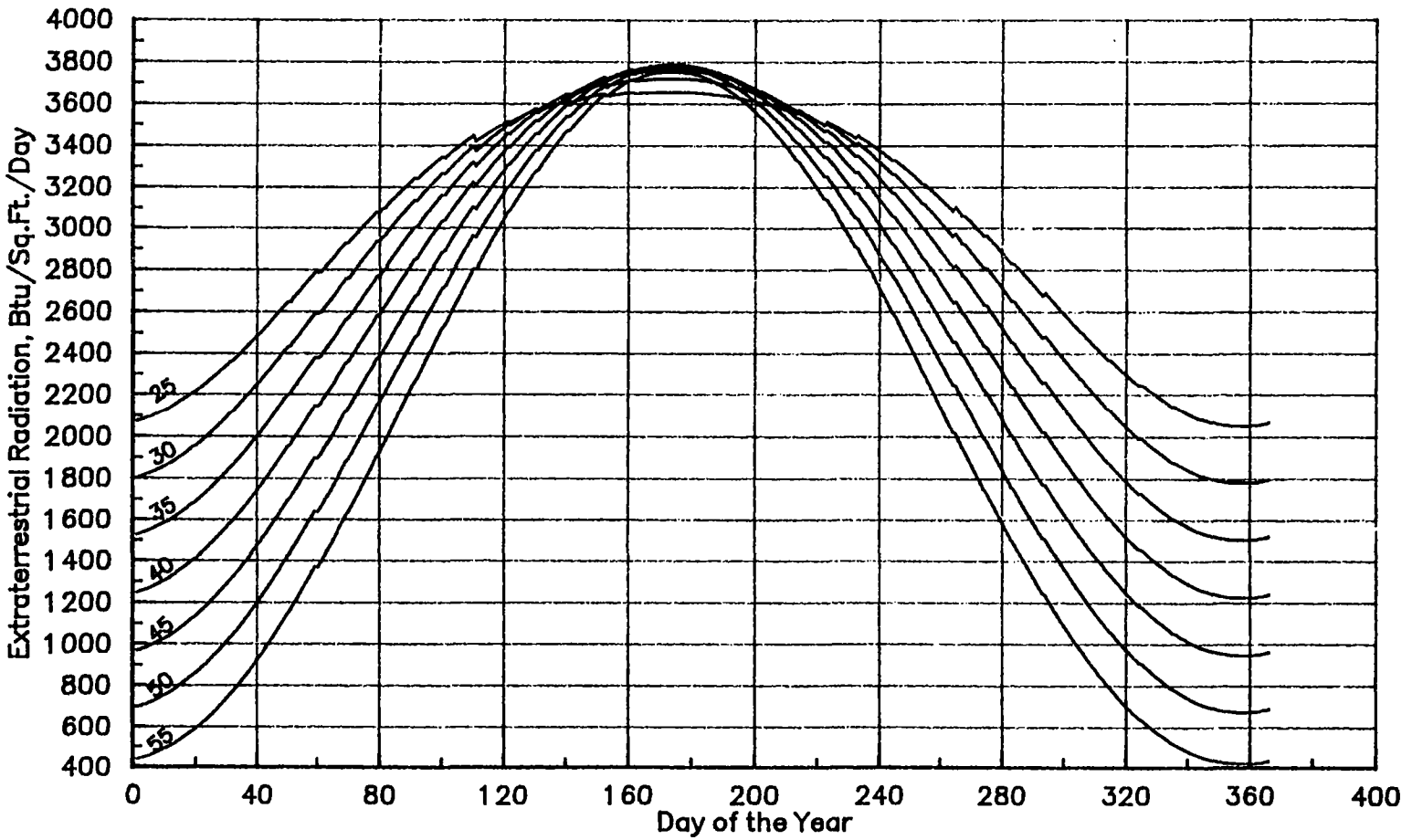

Figure I-5. Extraterrestrial Solar Radiation as a Function of Time of the Year for Different Latitudes.

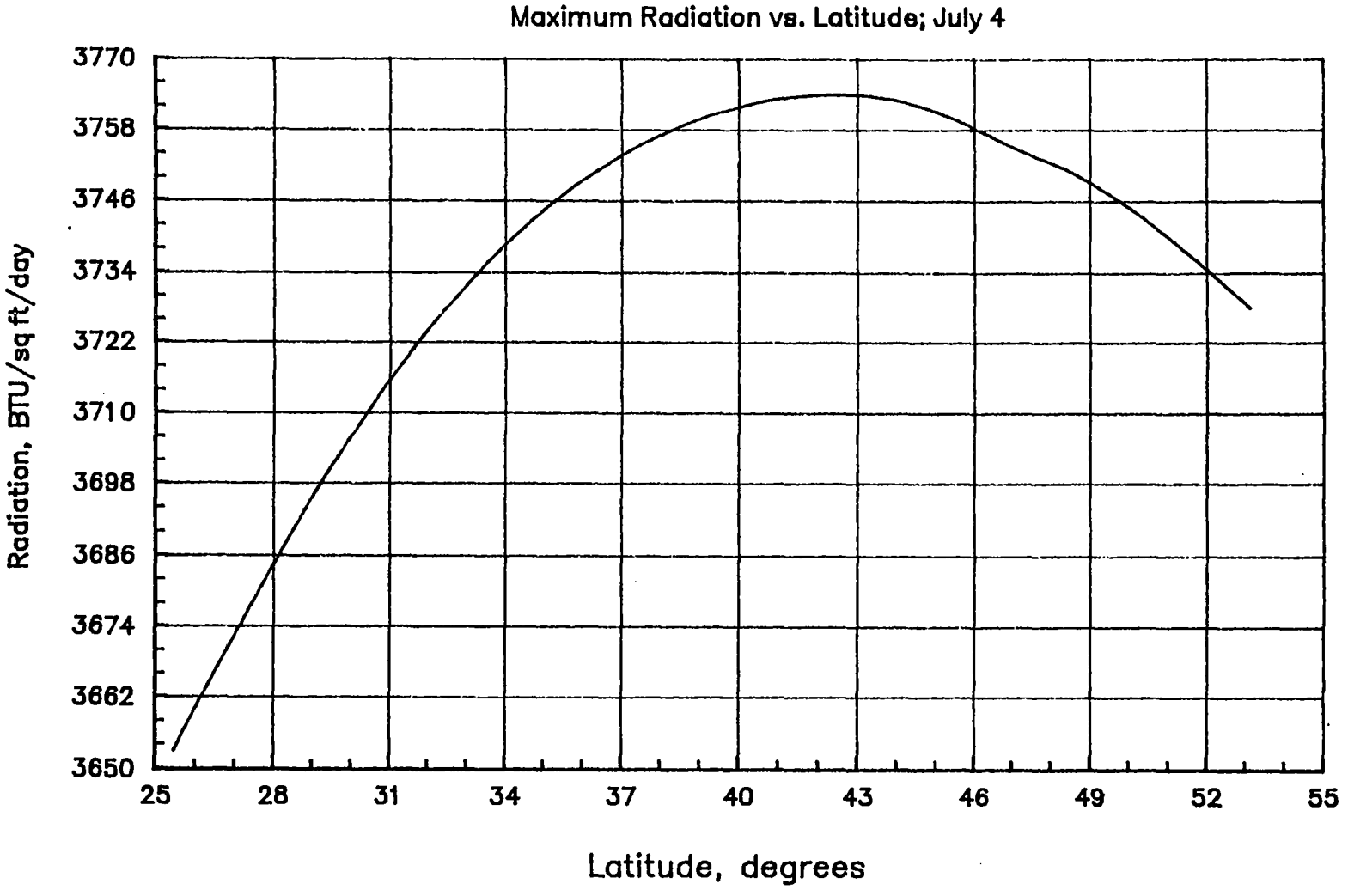

Figure I-6. Extraterrestrial Radiation as a Function of Latitude for a Particular Day of the Year.

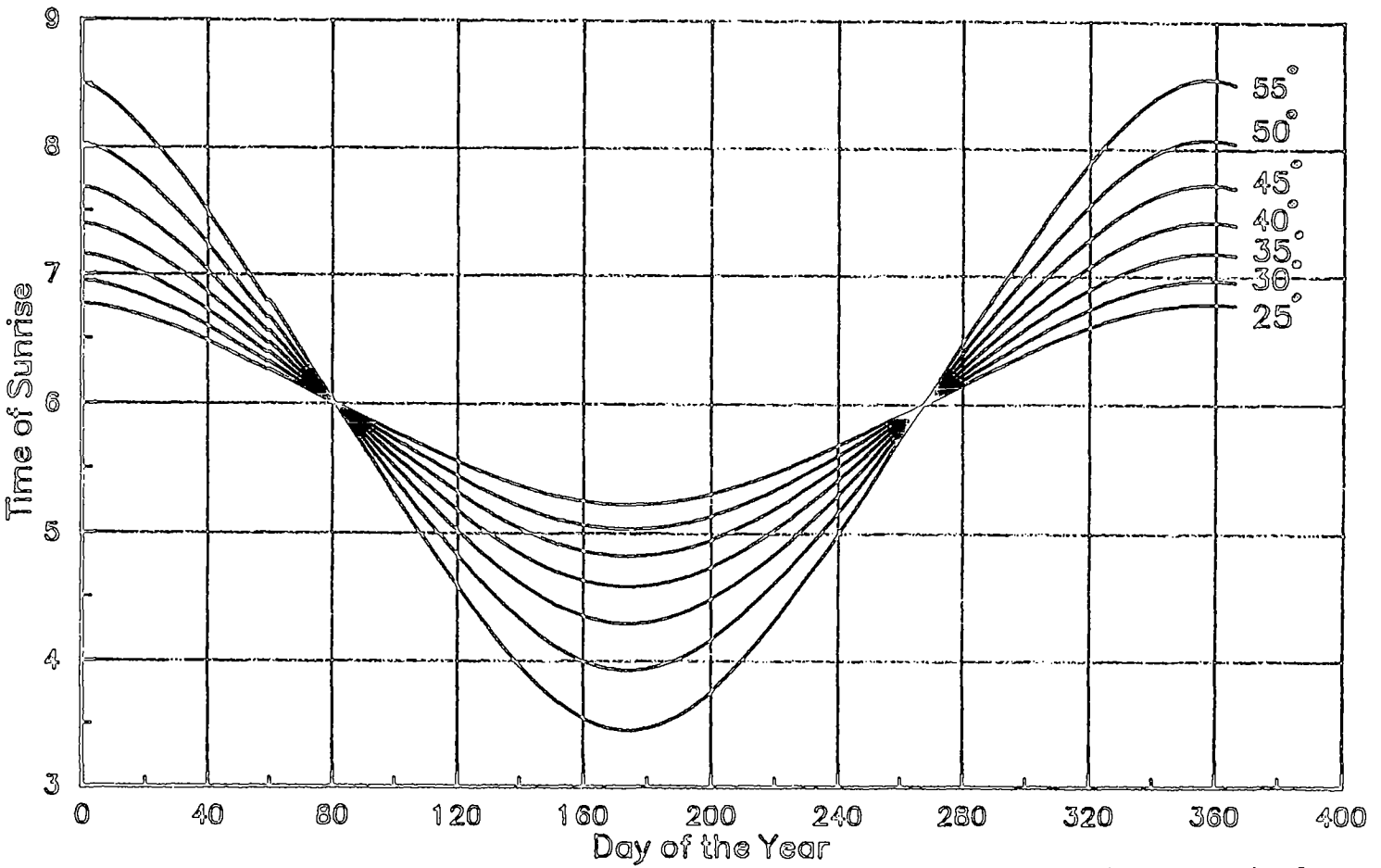

Figure I-7. Time of Sunrise as a Function of Time of the Year for Different Latitudes.

Figure I-8. Time of Sunset as a Fuction of Time of the Year for Different Latitudes.

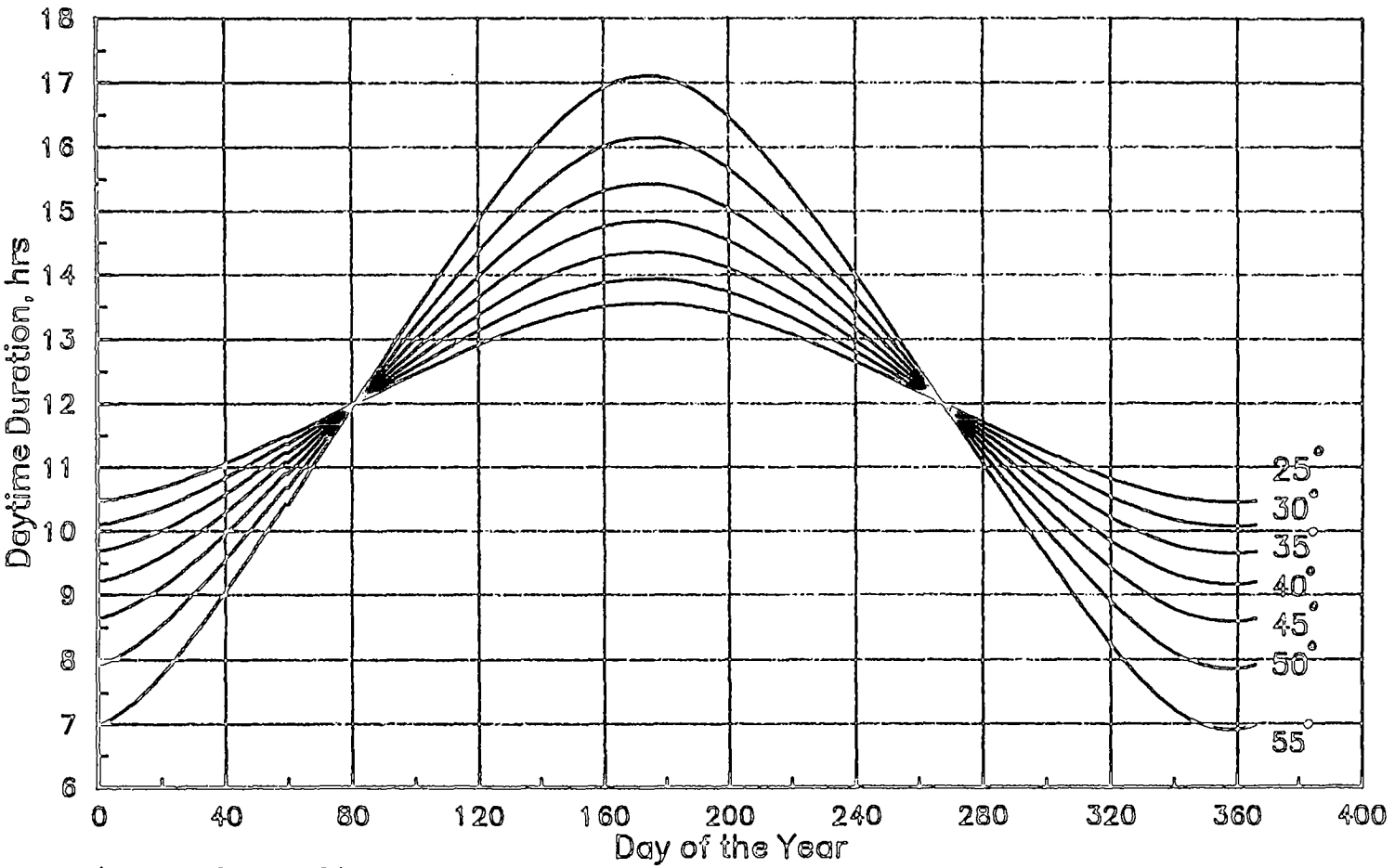

Figure I-9. Daylight Duration as a Function of Time of the Year for Different Latitudes.

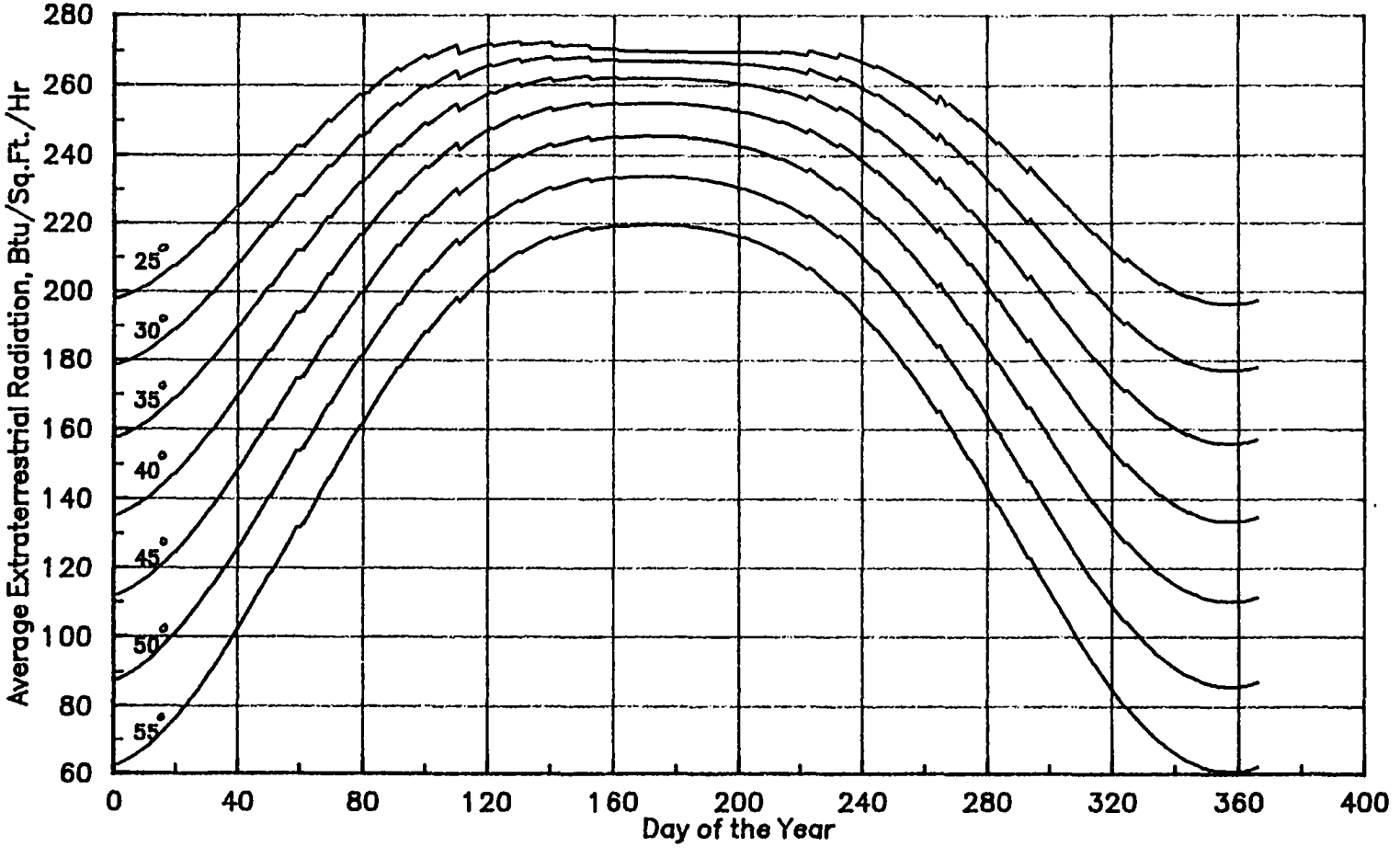

Figure I-10. Average Extraterrestrial Radiation as a Functionof Time of the Year for Different Latitudes.

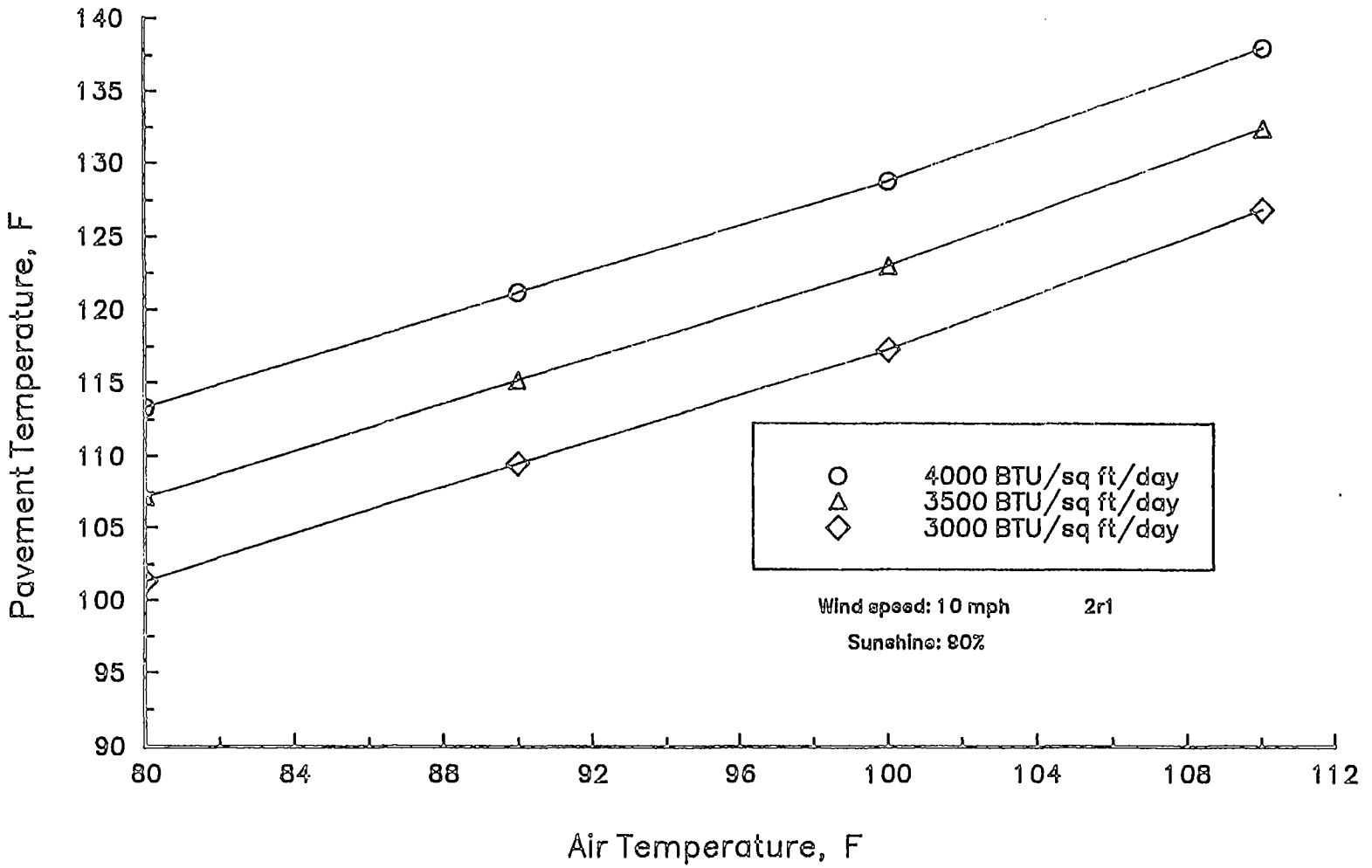

Figure I-11. Predicted Pavement Surface Temperature as a Function of Air Temperature for Different Radiations.

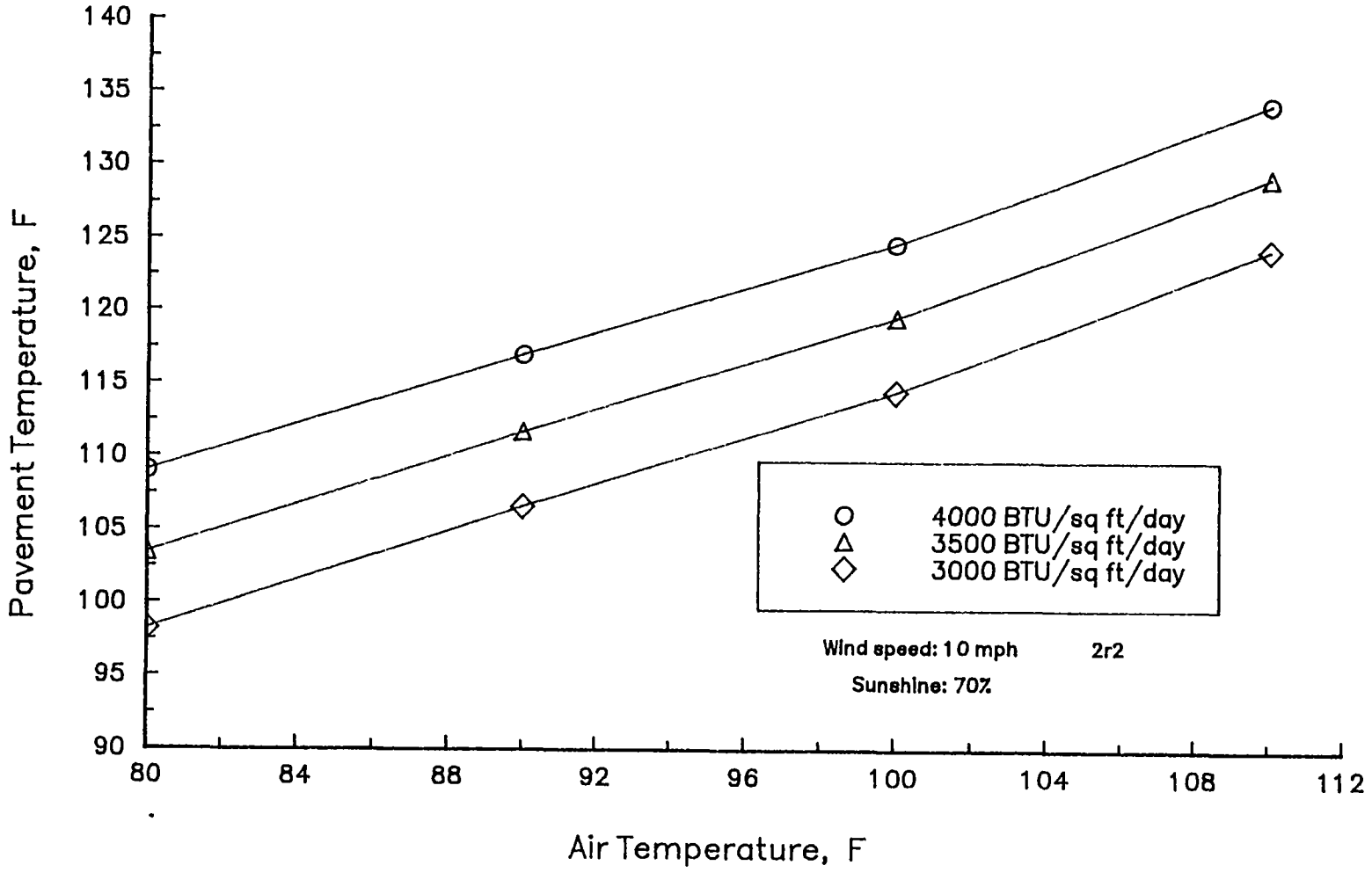

Figure I-12. Predicted Pavement Surface Temperature as a Function of Air Temperature for Different Radiations.

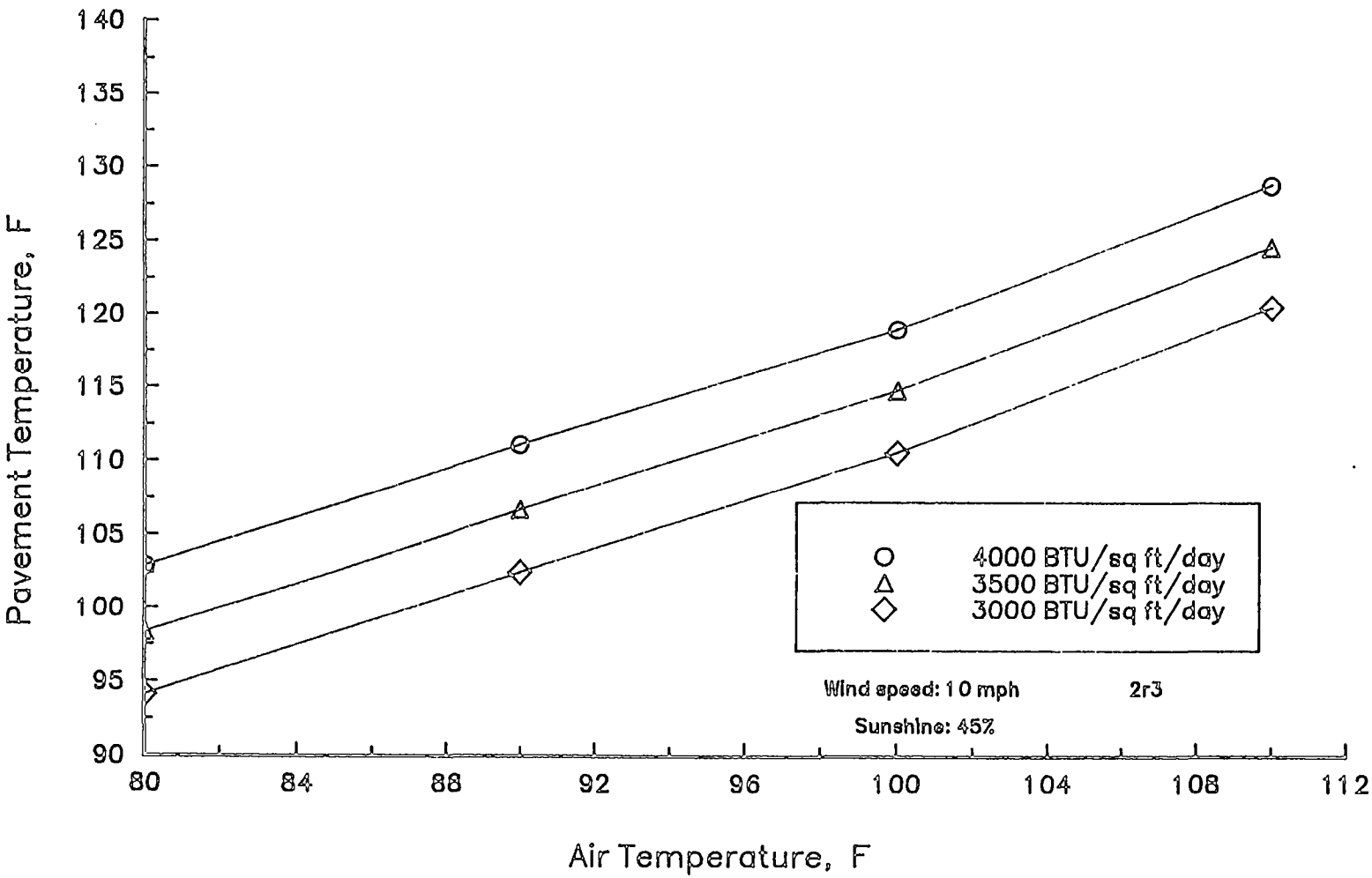

Figure I-13. Predicted Pavement Surface Temperature as a Function of Air Temperature for Different Radiations.

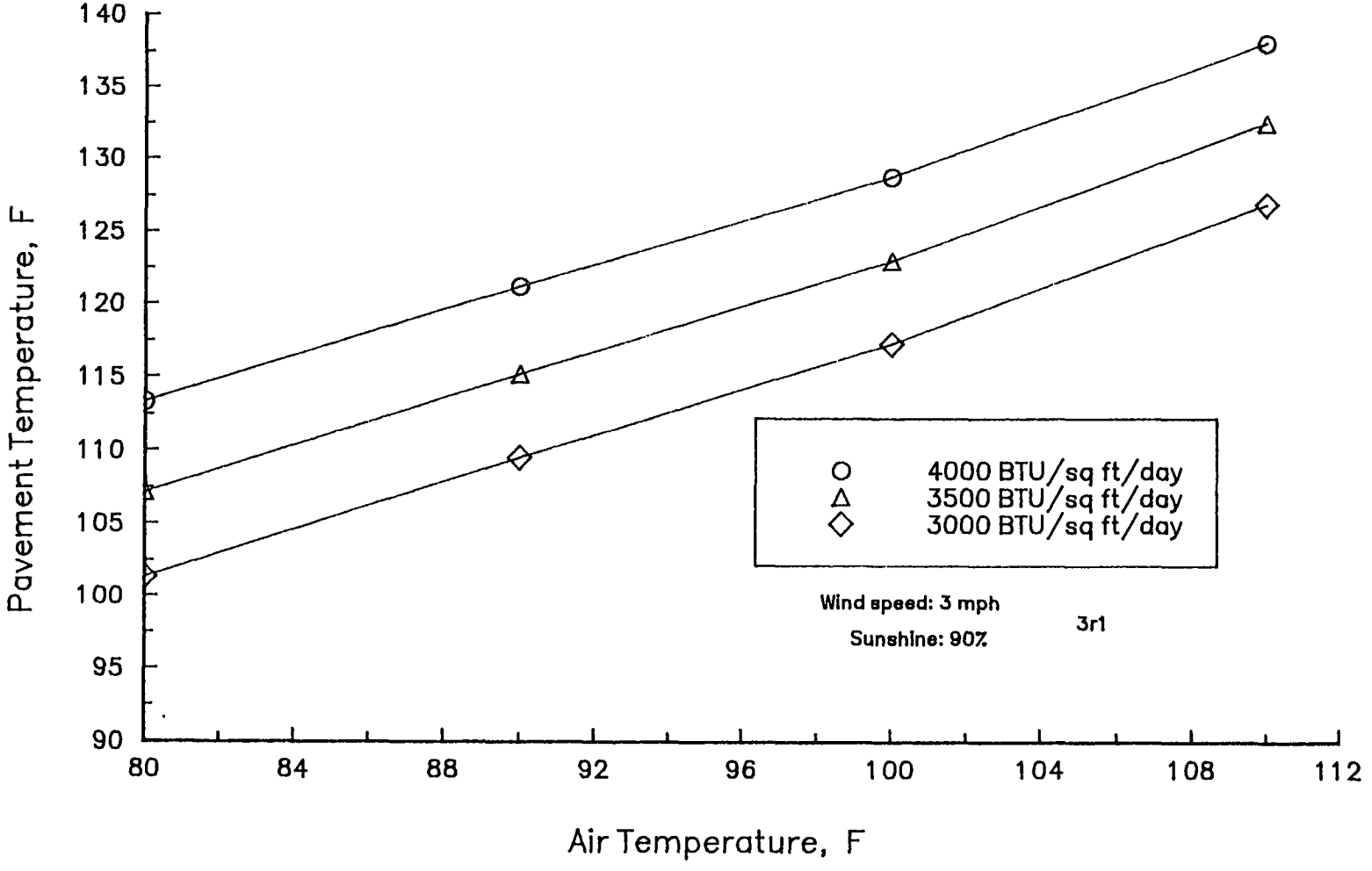

Figure I-14. Predicted Pavement Surface Temperature as Function of Air Temperature for Different Radiations.

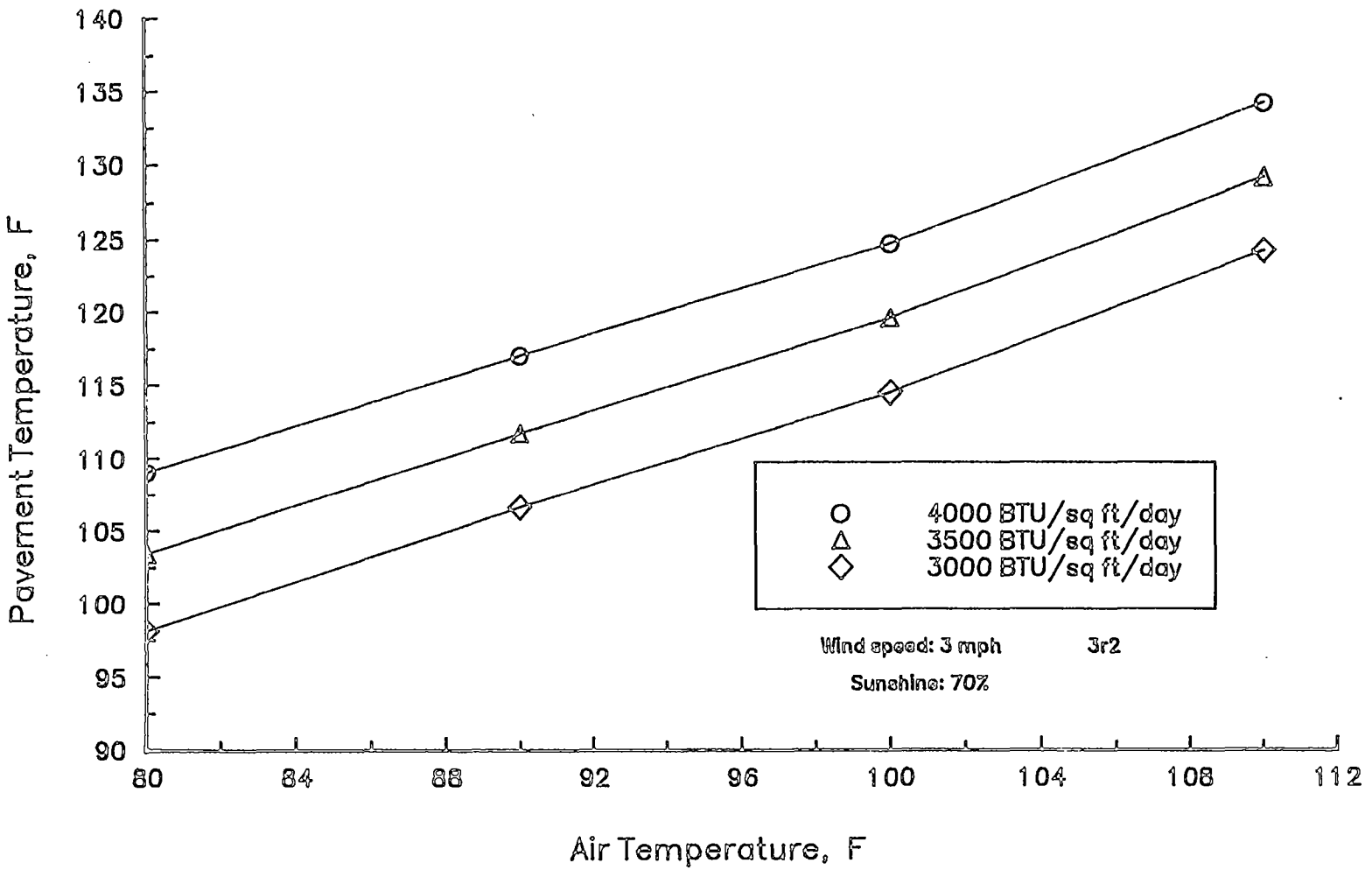

Figure I-15. Predicted Pavement Surface temperature as a Function of Air Temperature for Different Radiations.

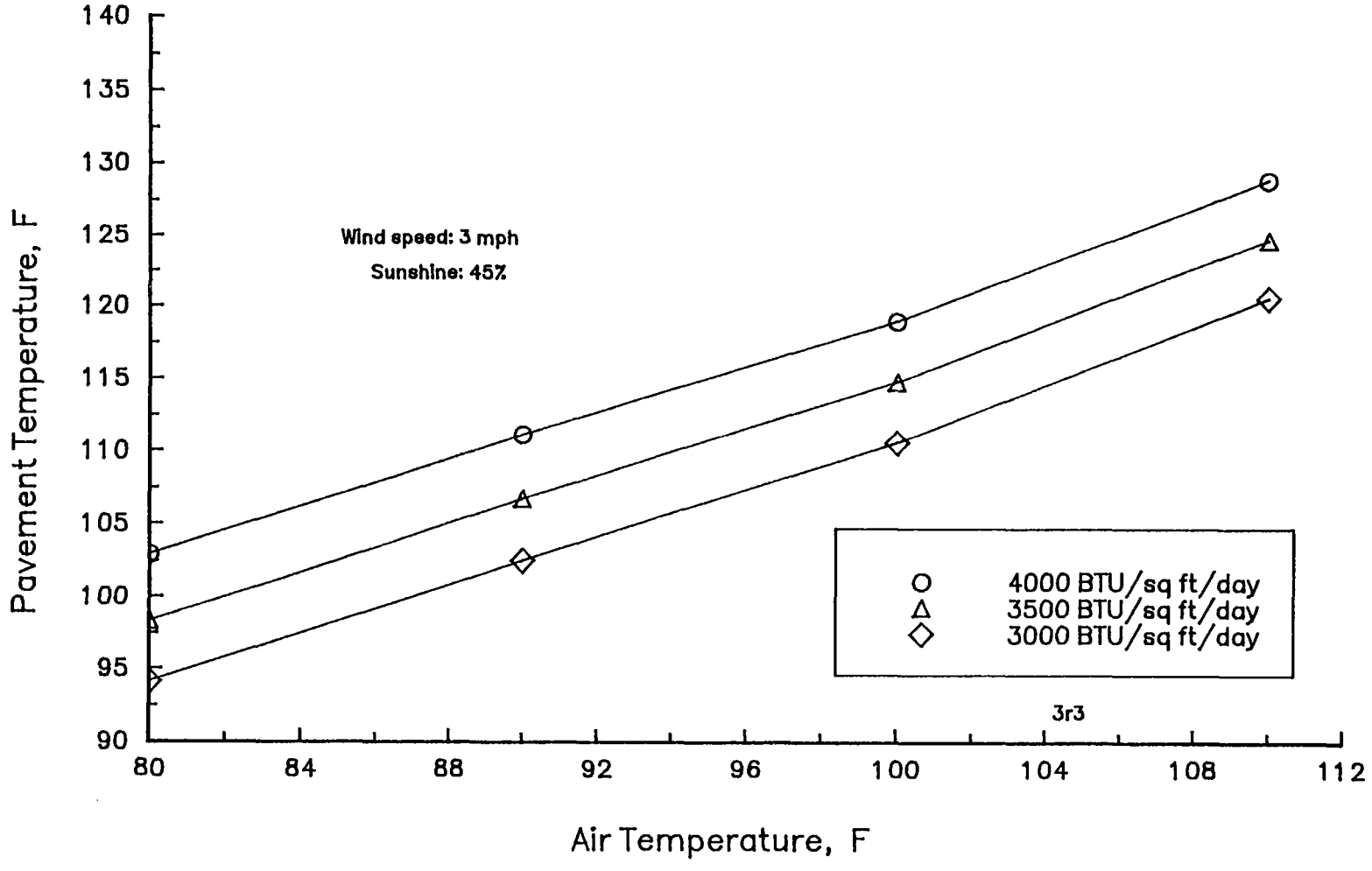

Figure I-16. Predicted Pavement Surface Temperature as a Function of Air Temperature for Different Radiations.

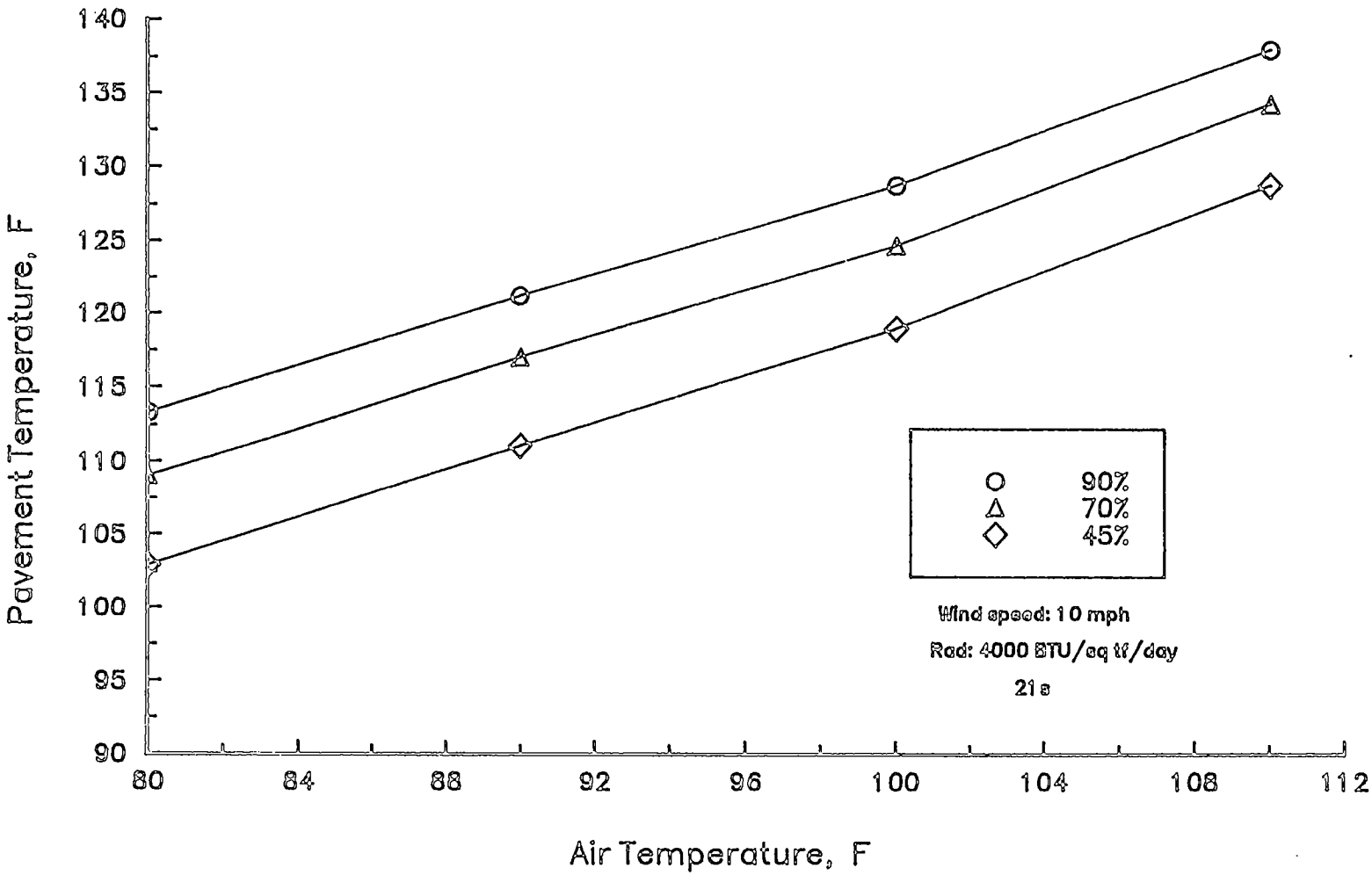

Figure I-17. Predicted Pavement Surface Temperature as a Function of Air Temperature for Different Radiations.

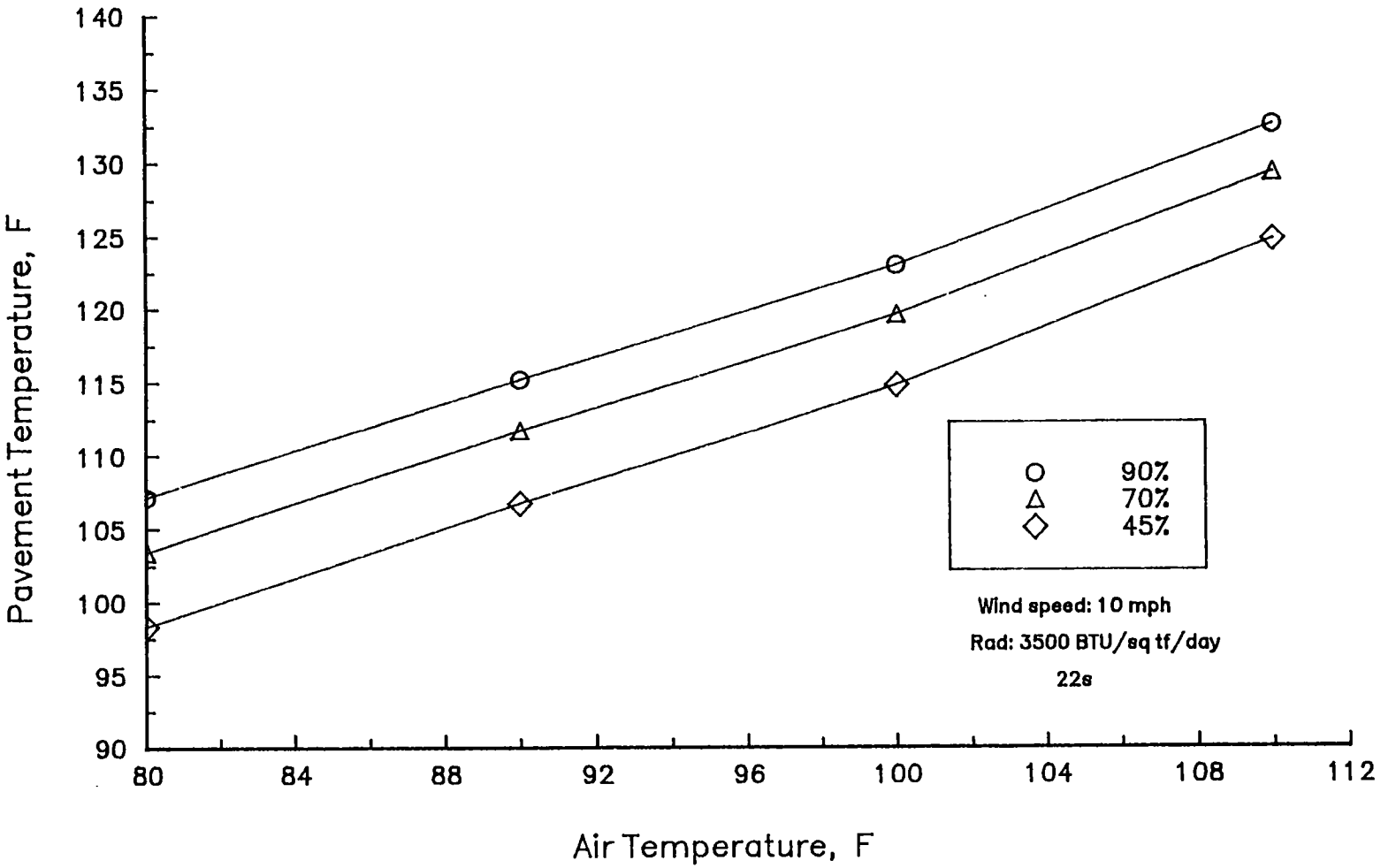

Figure I-18. Predicted Pavement Surface Temperature as a Function of Air Temperature for Different Radiations.

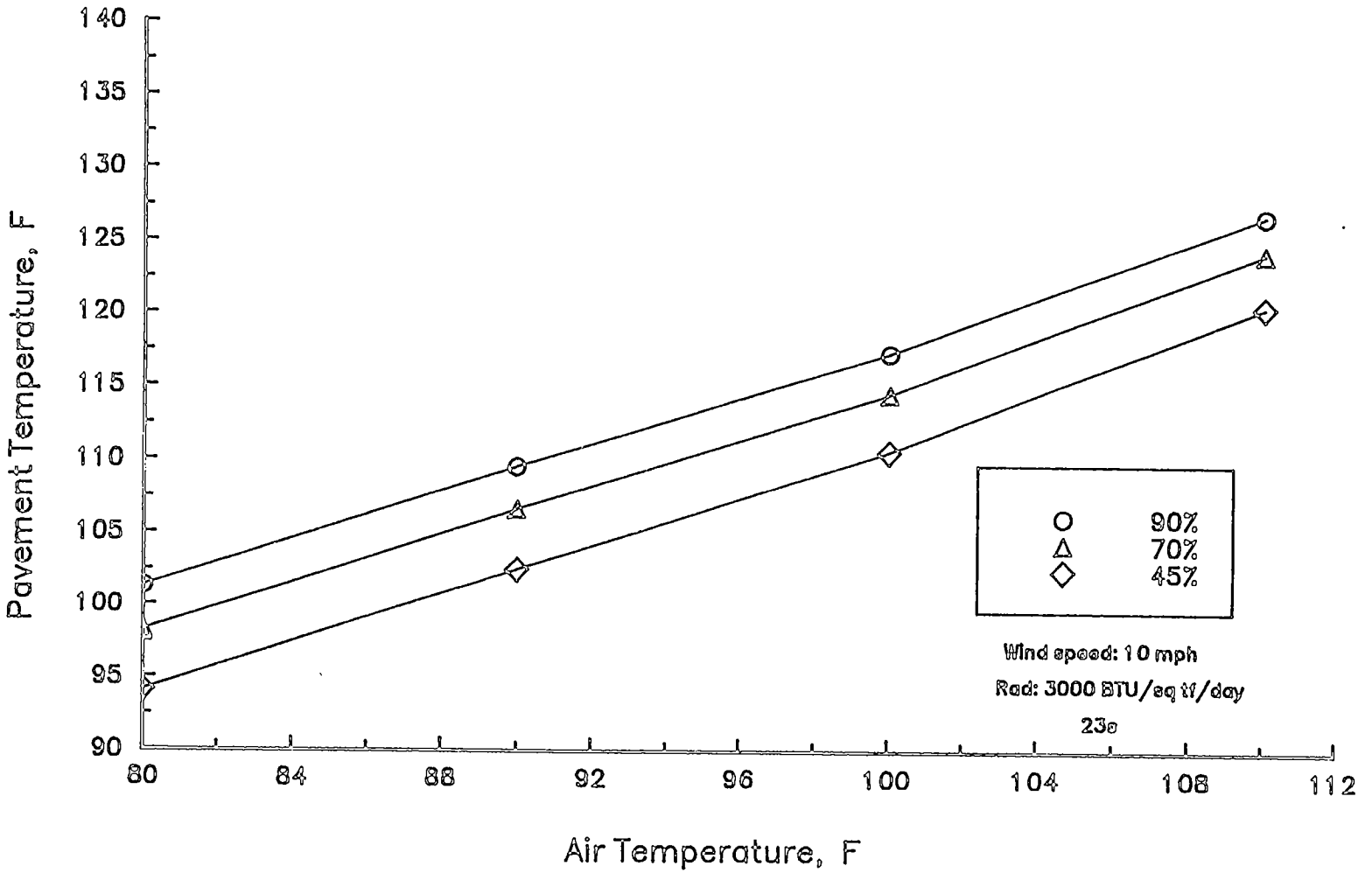

Figure I-19. Predicted Pavement Surface Temperature as a Function of Air Temperature for Different Percent Sunshine.

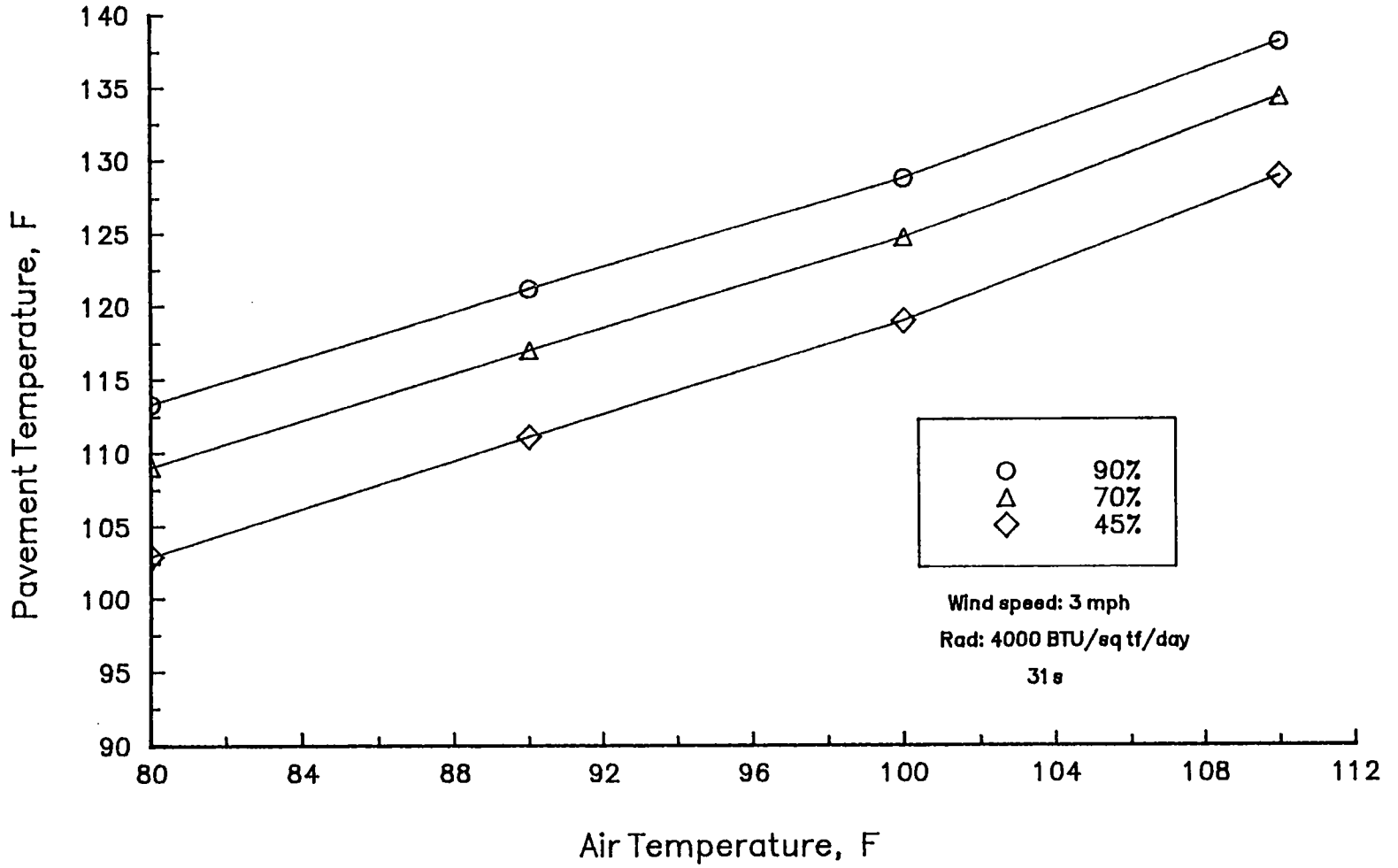

Figure I-20. Predicted Pavement Surface Temperature as a Function of Air Temperature for Different Percent Sunshine.

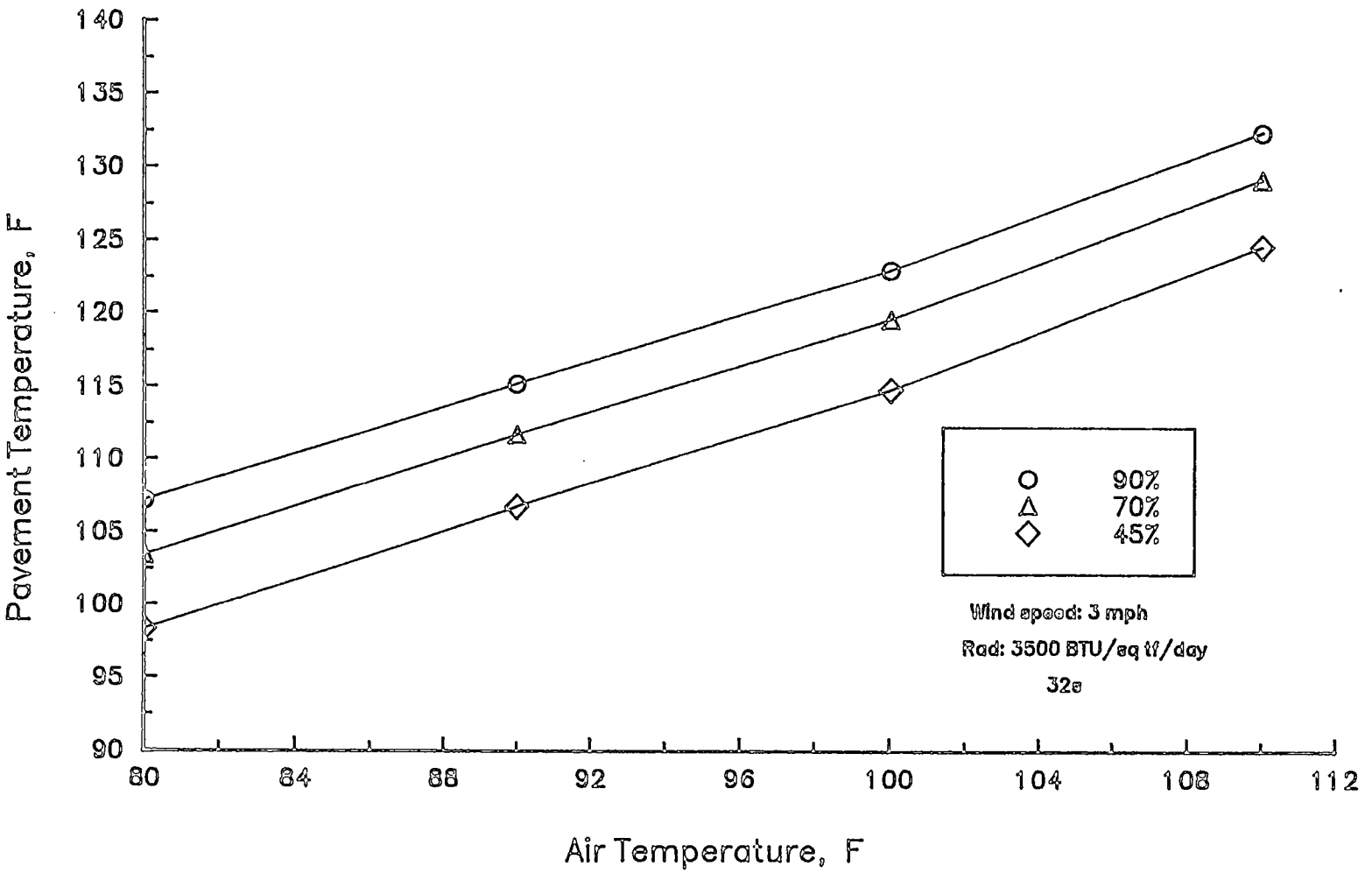

Figure I-21. Predicted Pavement Surface Temperature as a Function of Air Temperature for Different Percent Sunshine.

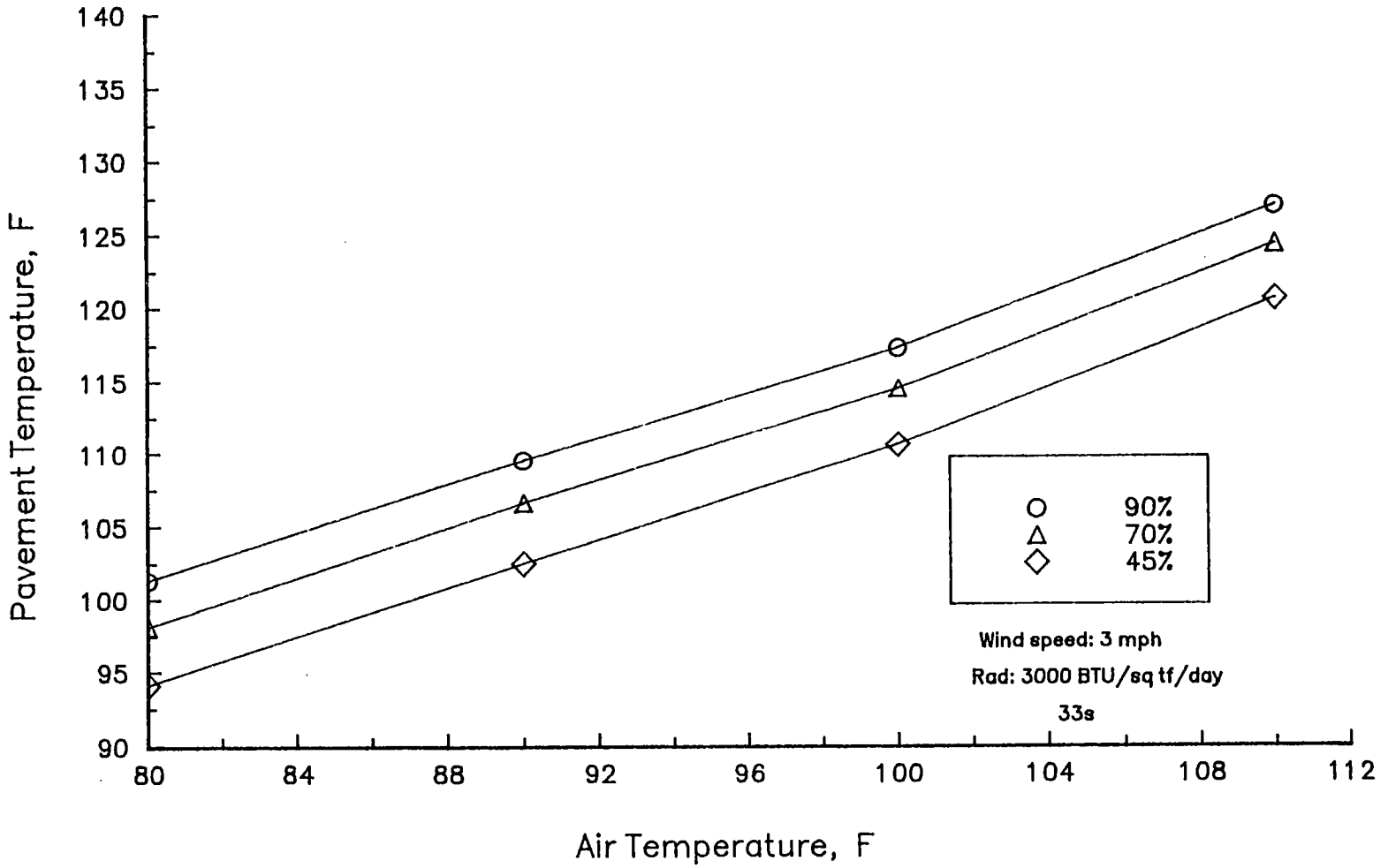

Figure I-22. Predicted Pavement Surface Temperature as a Function of Air Temperature for Different Percent Sunshine.

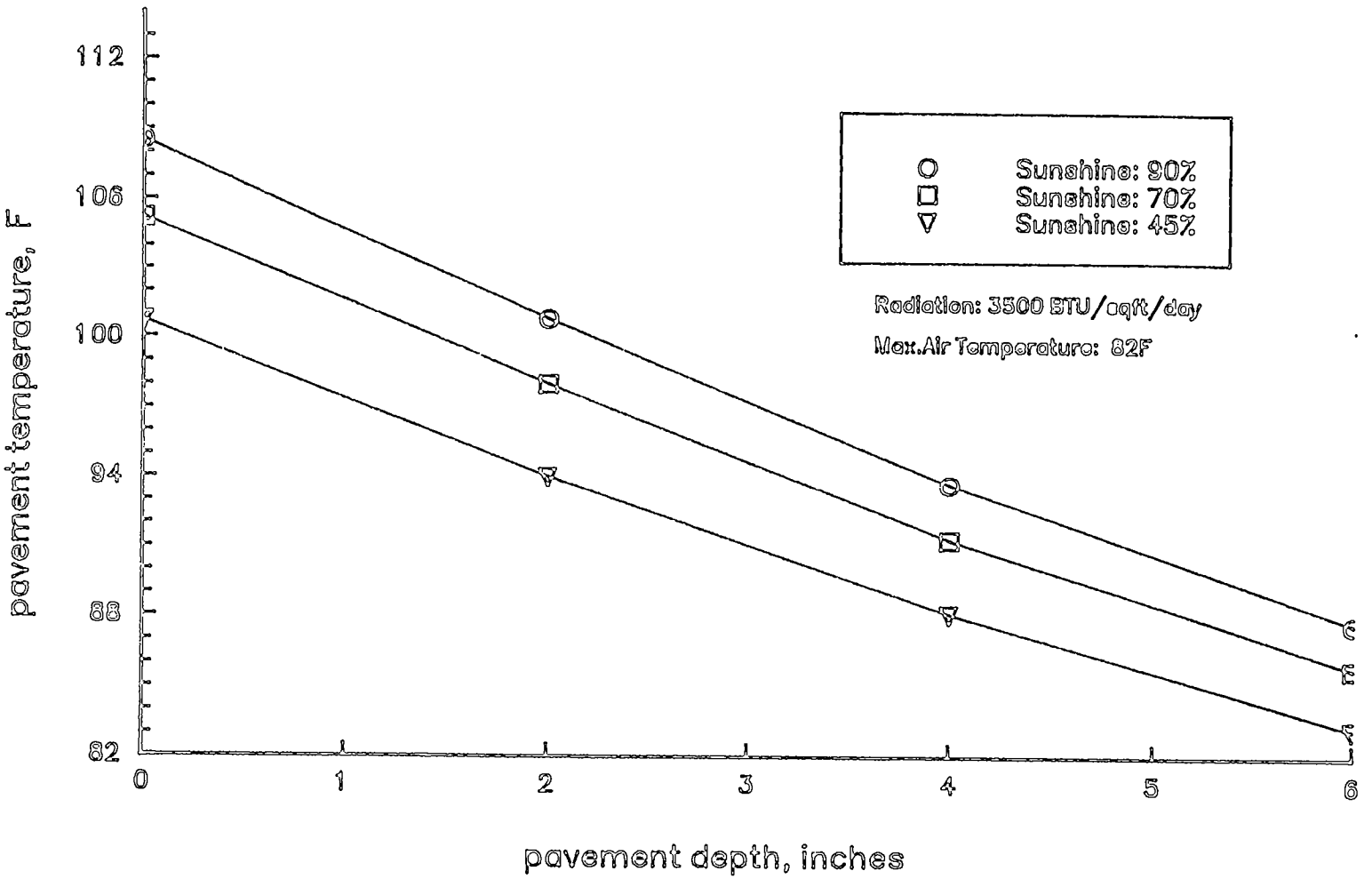

Figure I-23. Predicted Pavement Temperature Profile for Different Values of Percent Sunshine.

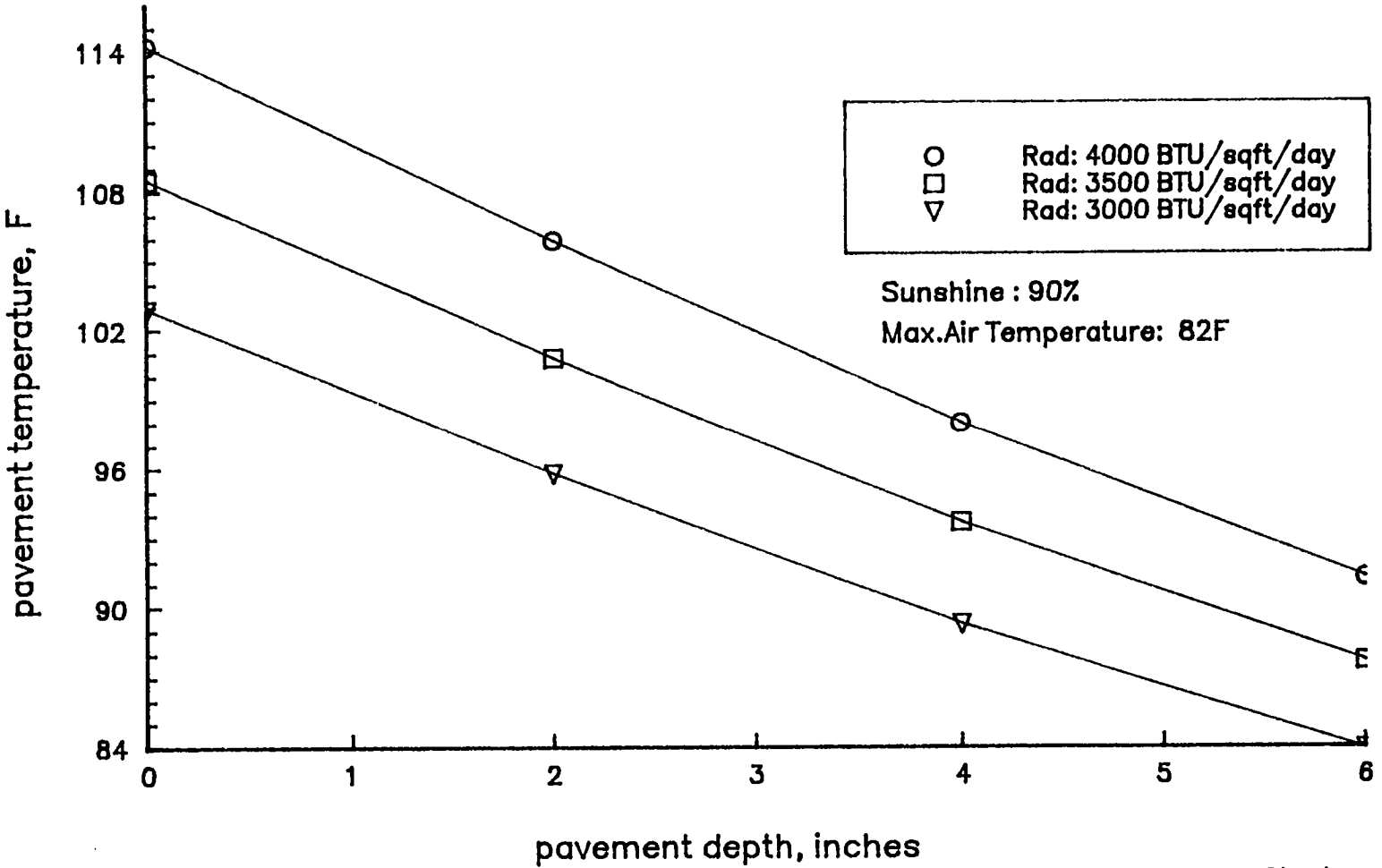

Figure I-24. Predicted Pavement Temperature Profile for Different Values of Solar Radiation.

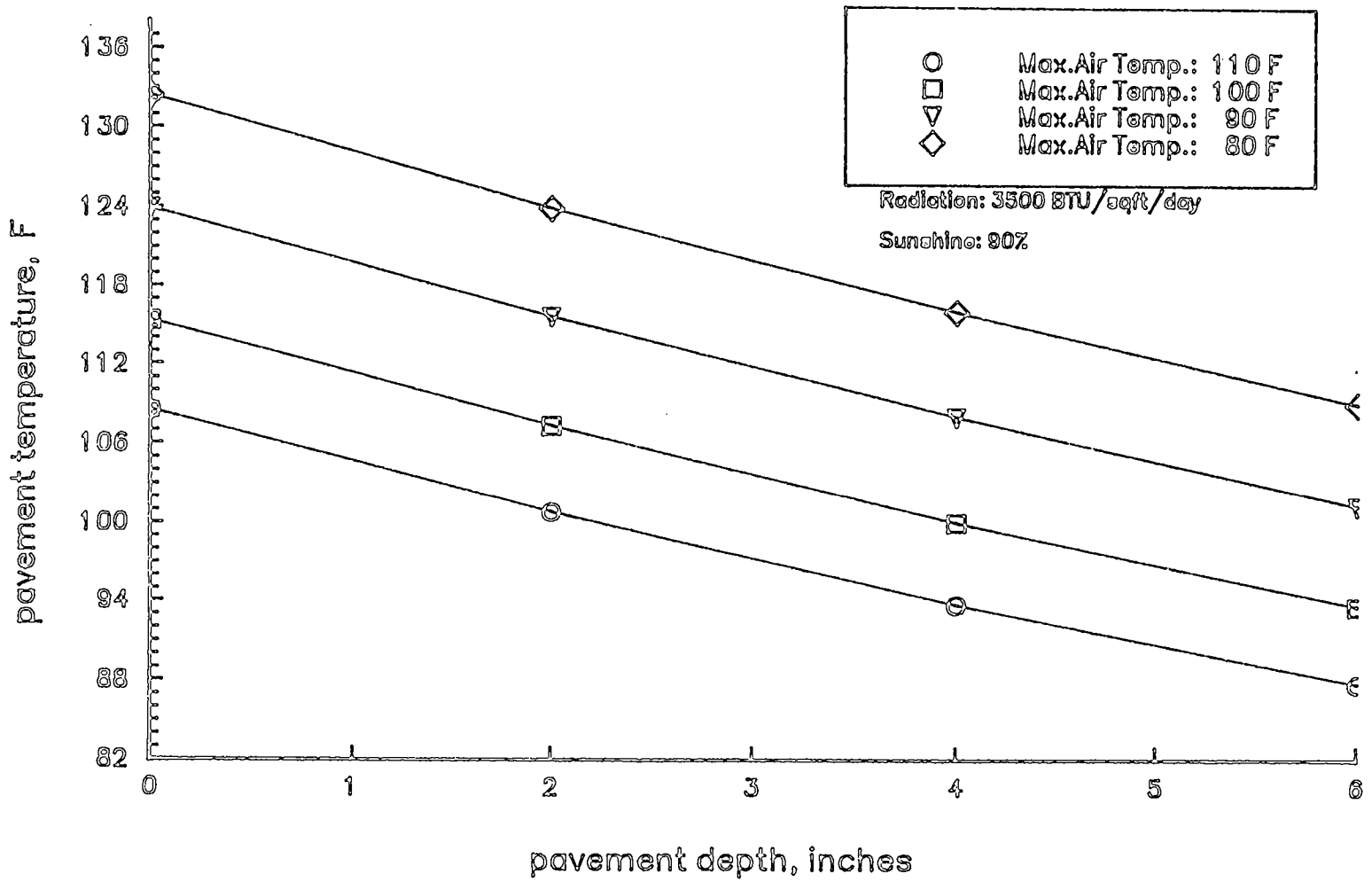

Figure I-25. Predicted Pavement Temperature Profile at Different Values of Maximum Air Temperature.

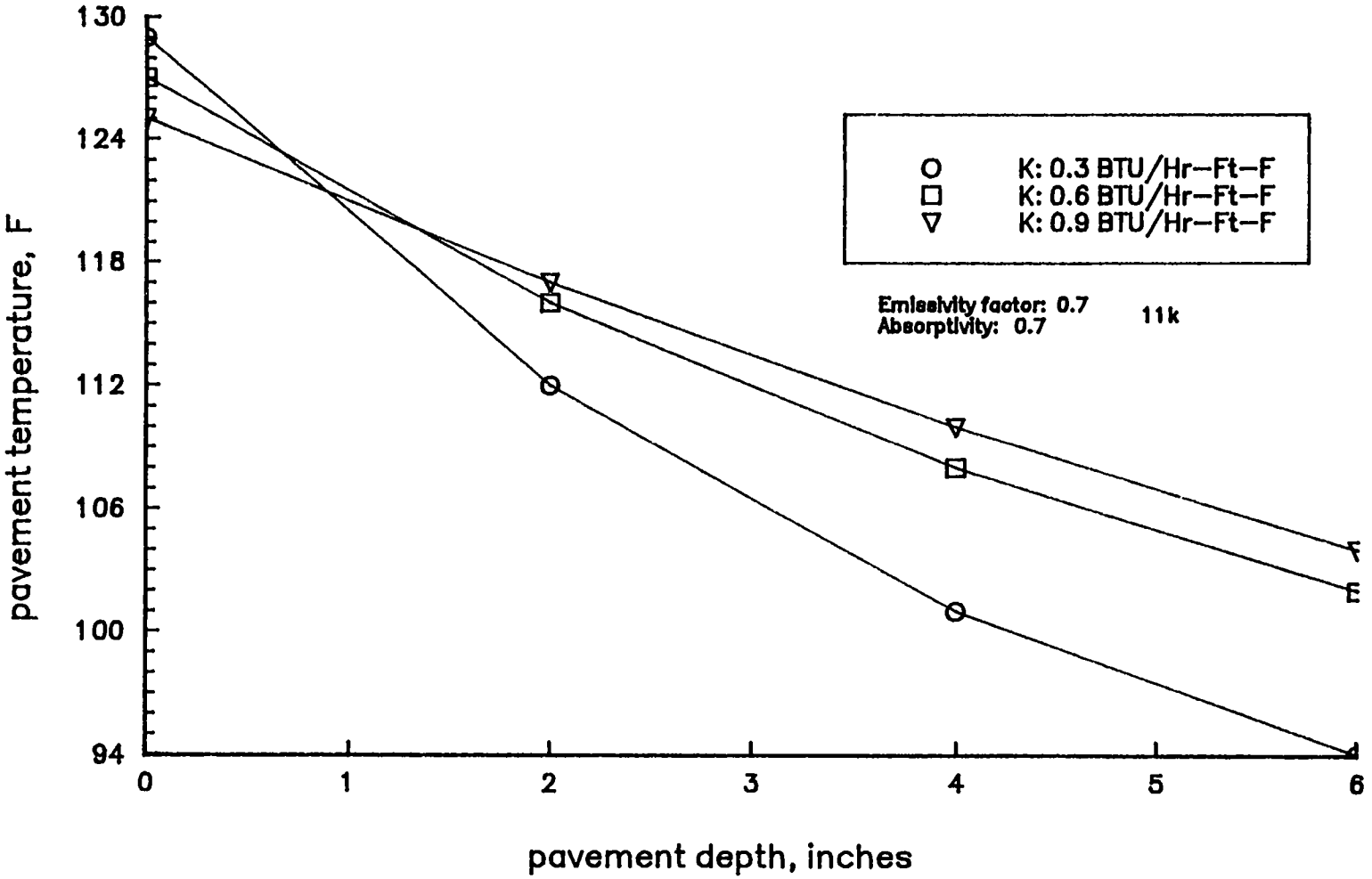

Figure I-26. Predicted Pavement Temperature Profile for Different Thermal Conductivities.

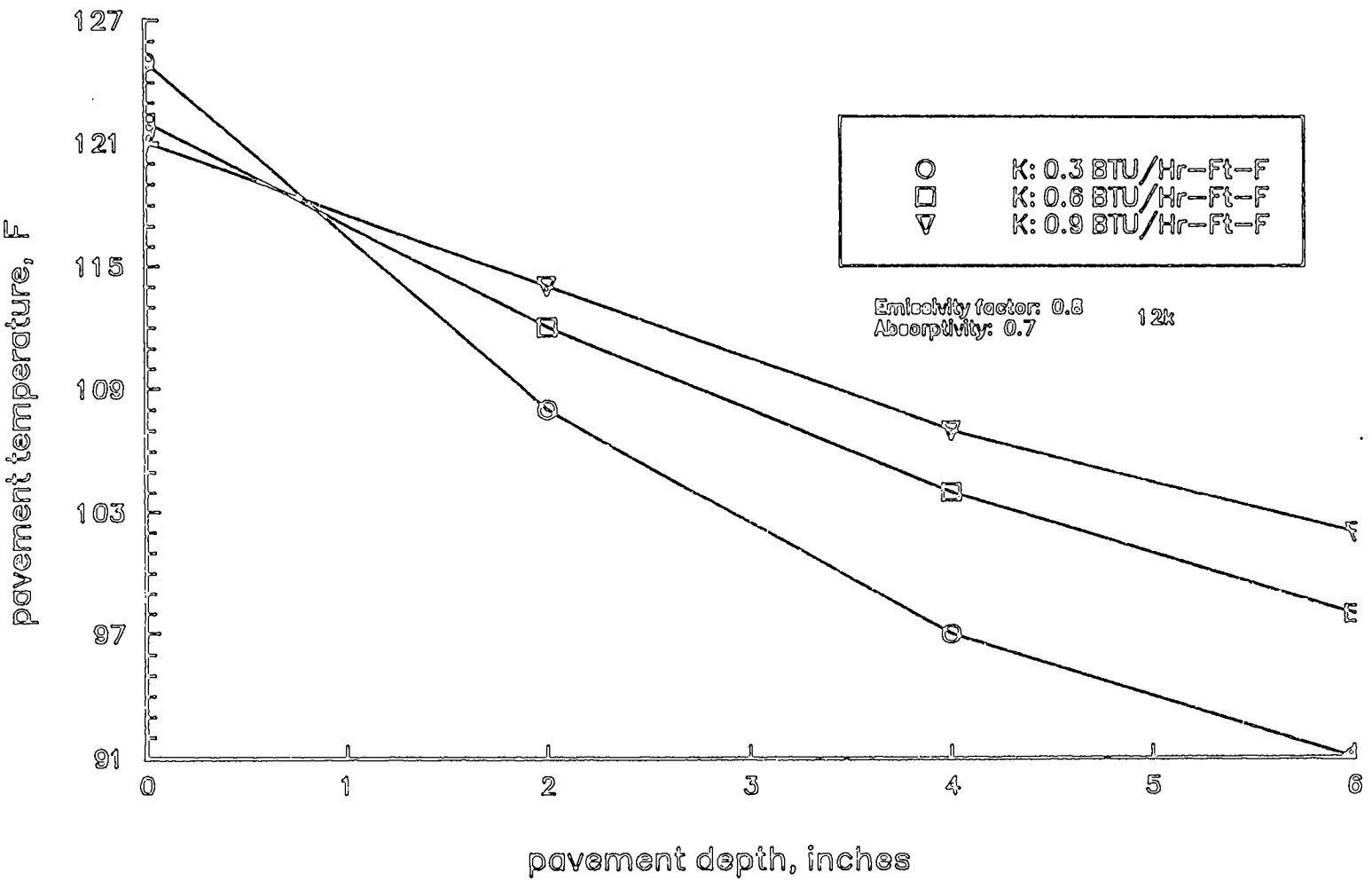

Figure I-27. Predicted Pavement Temperature Profile for Different Thermal Conductivities.

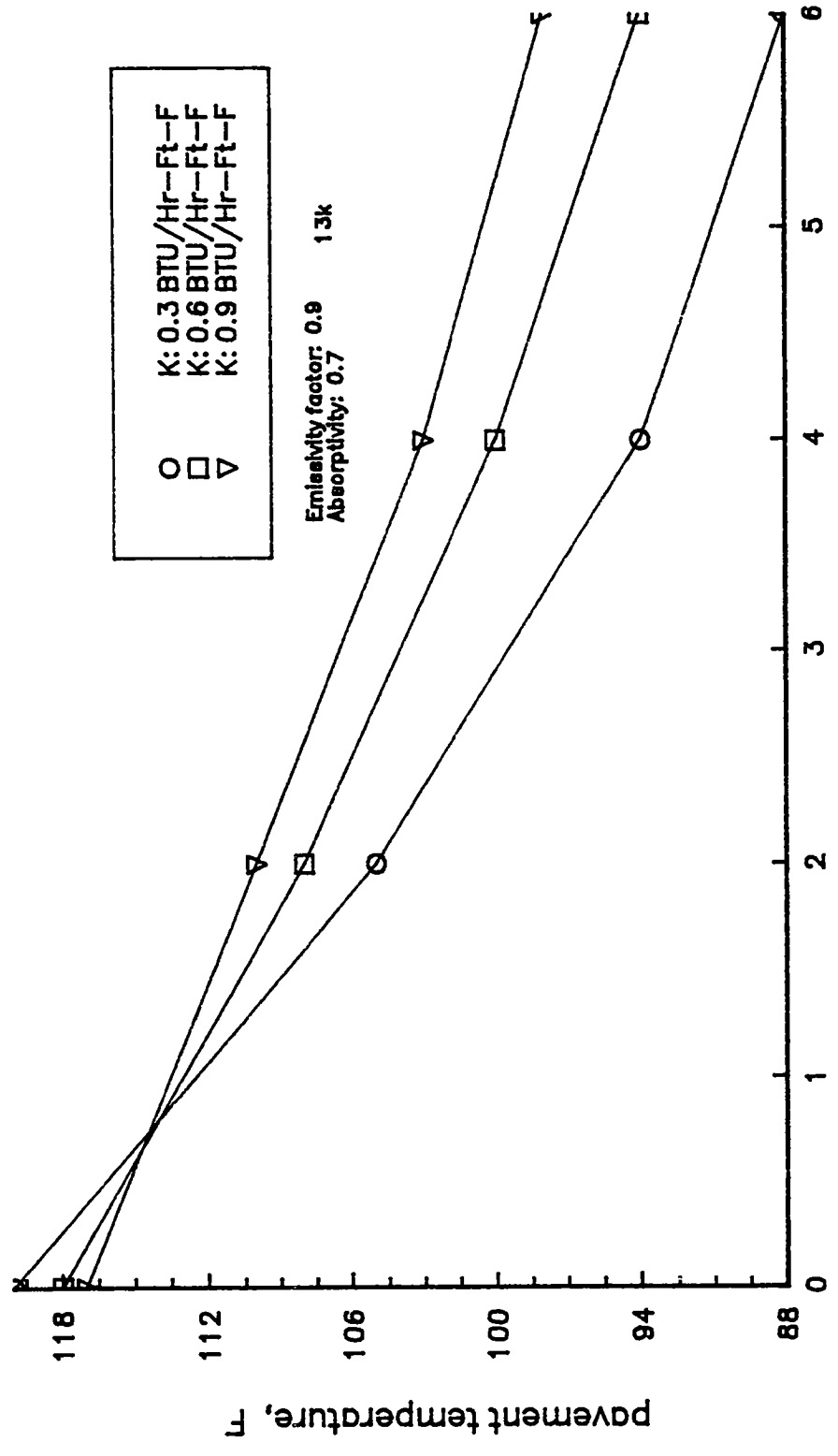

Figure I-28. Predicted Pavement Temperature Profile for Different Thermal Conductivities.

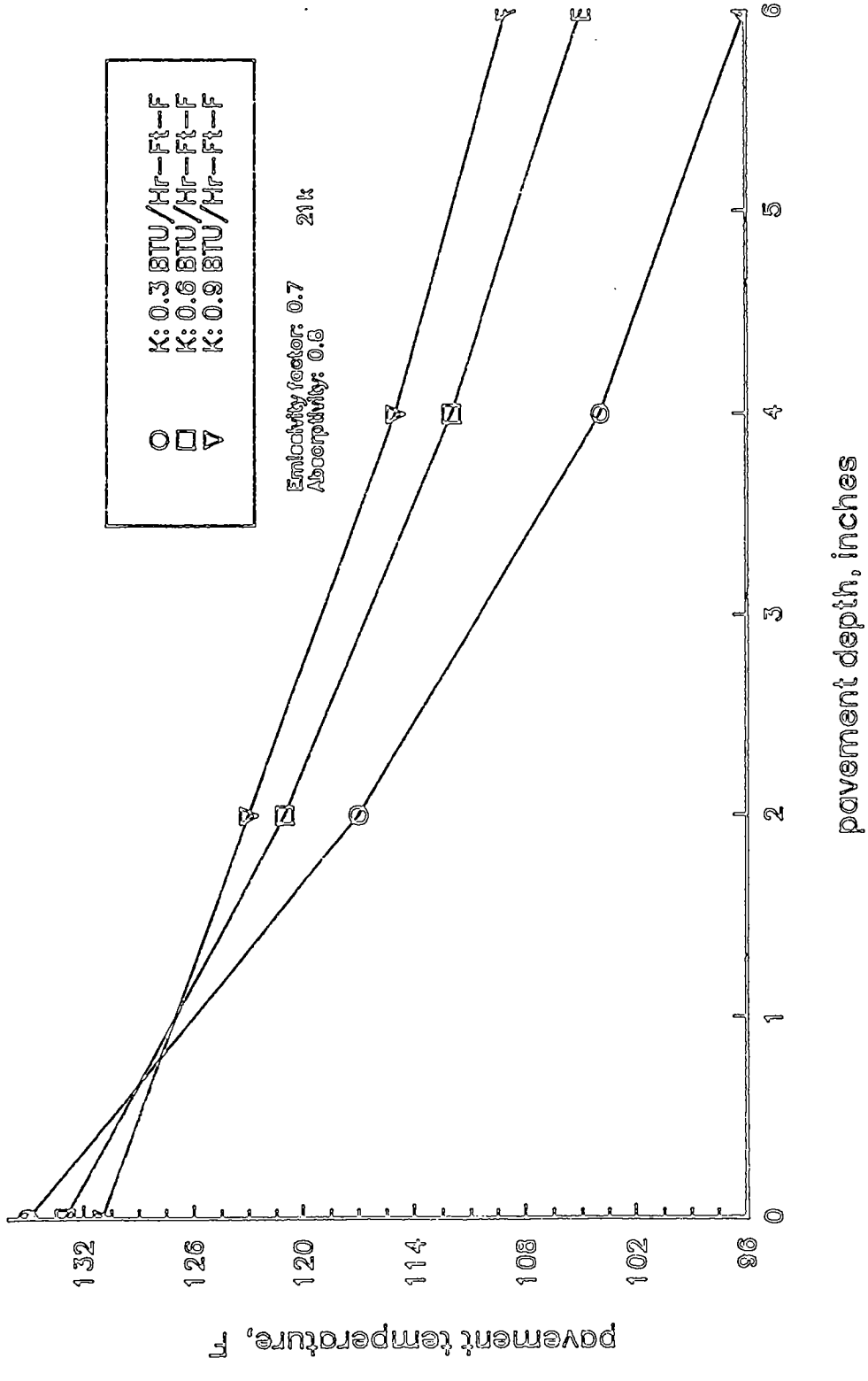

Figure I-29. Predicted Pavement Temperature Profile for Different Thermal Conductivities.

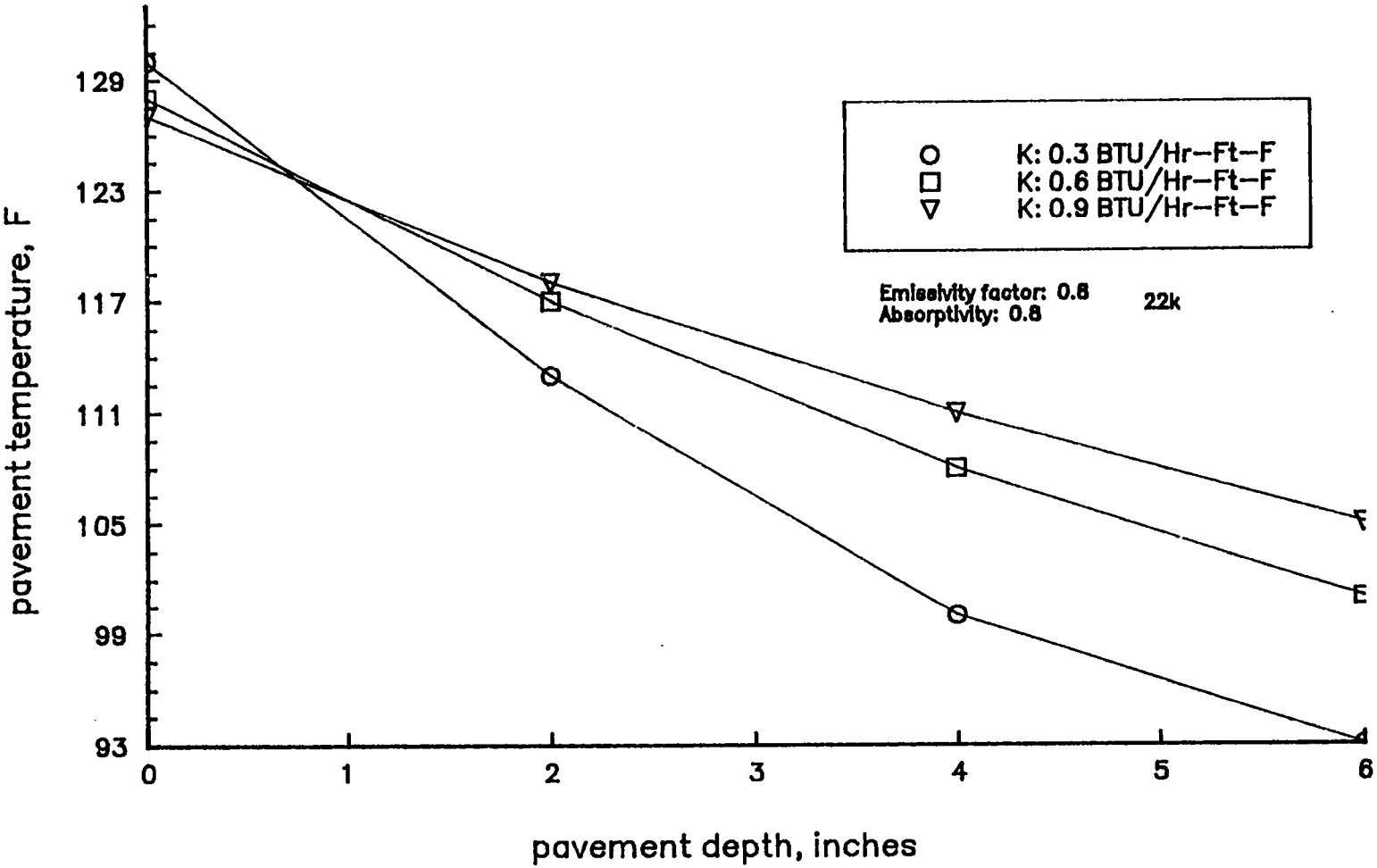

Figure I-30. Predicted Pavement Temperature Profile for Different Thermal Conductivities.

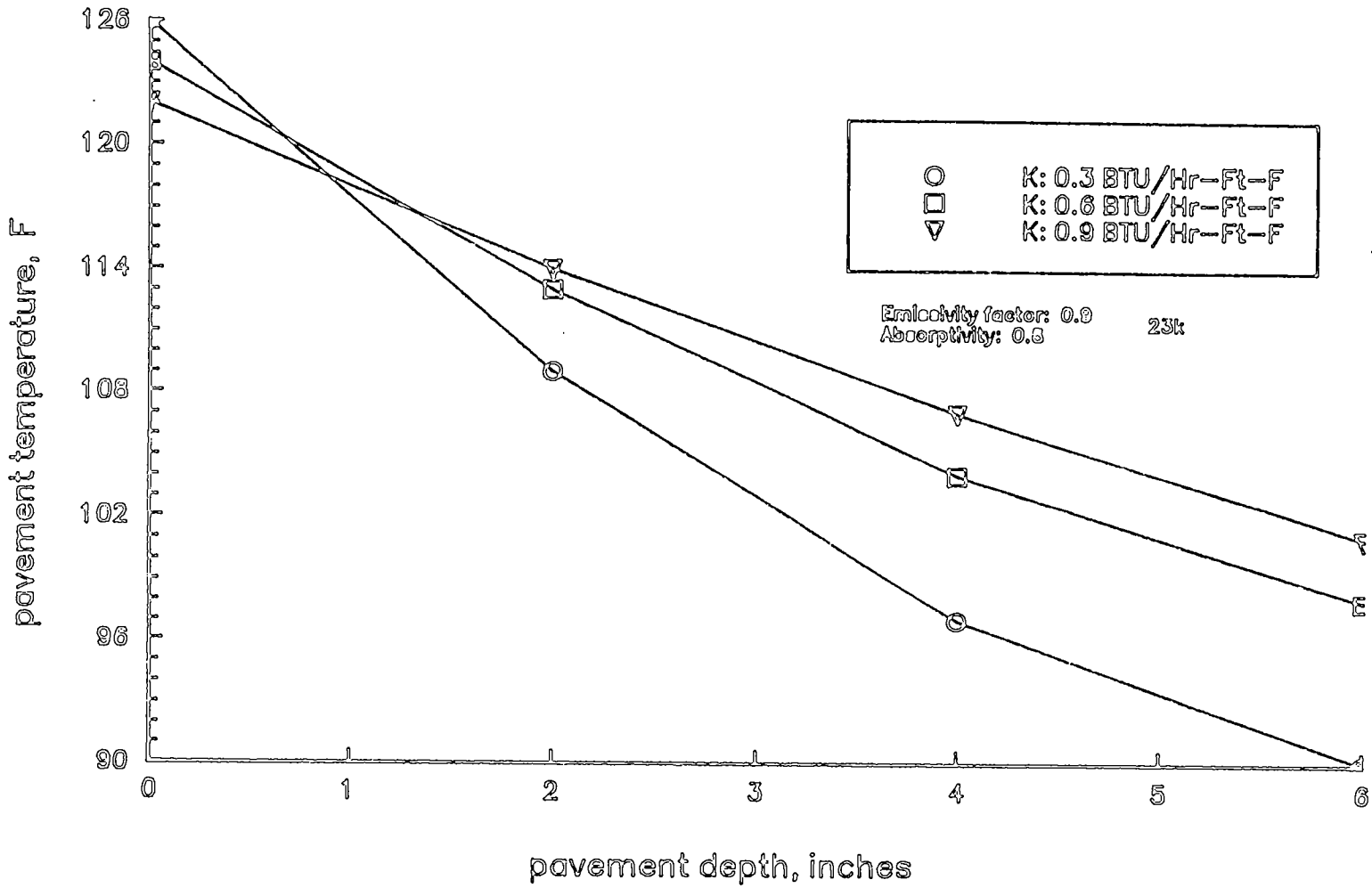

Figure I-31. Predicted Pavement Temperature Profile for Different Thermal Conductivities.

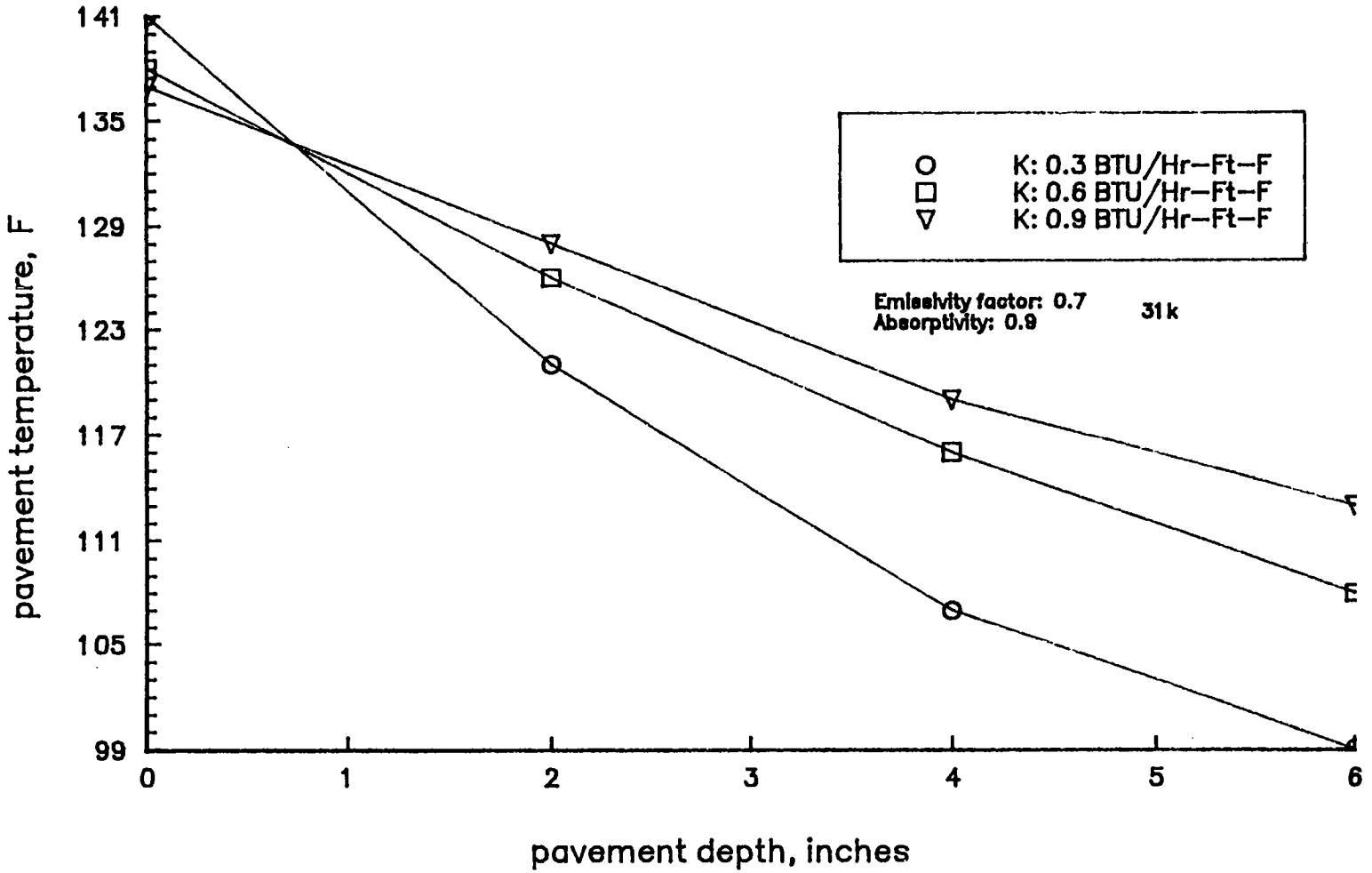

Figure I-32. Predicted Pavement Temperature Profile for Different Thermal Conductivities.

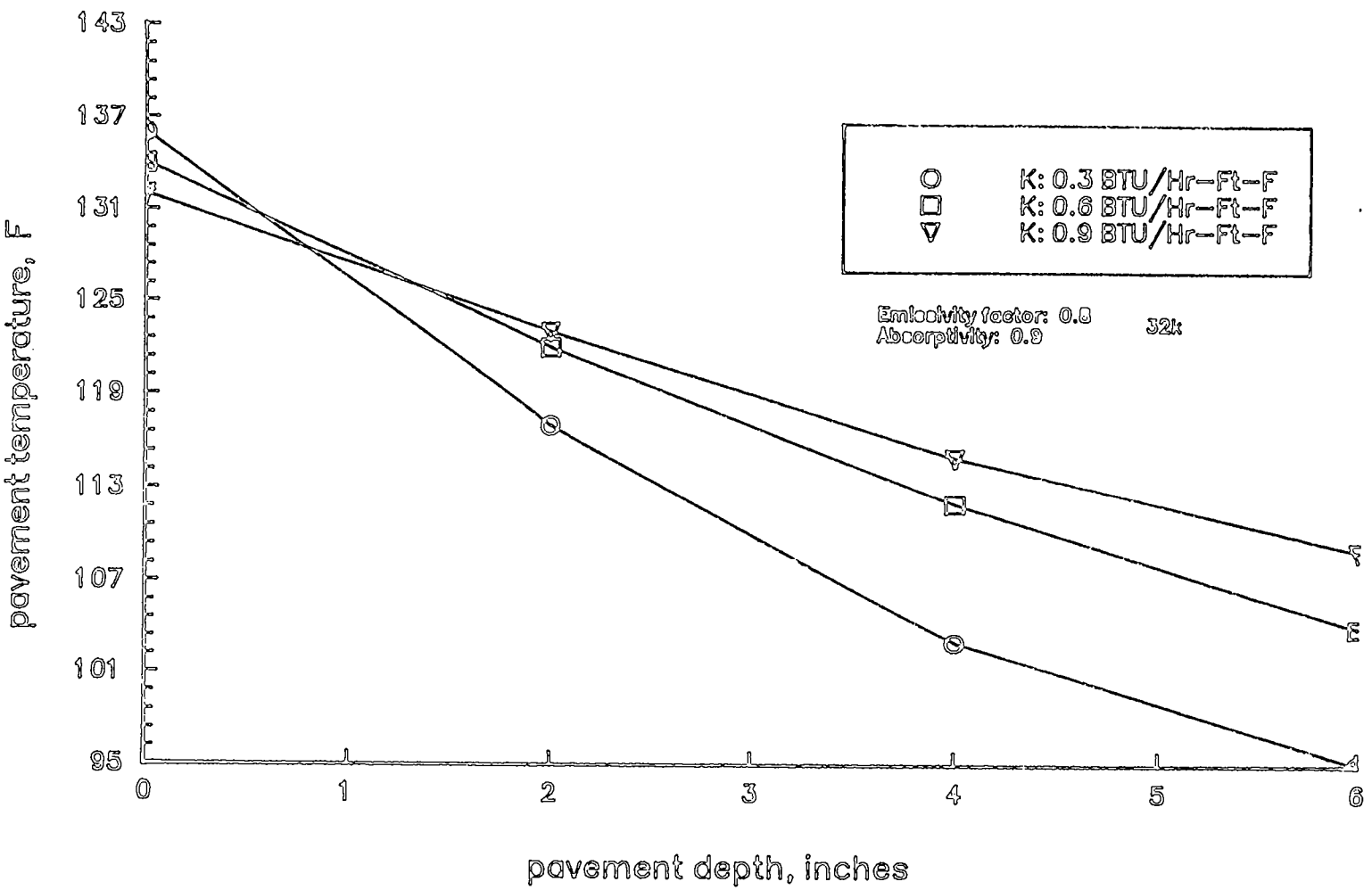

Figure I-33. Predicted Pavement Temperature Profile for Different Thermal Conductivities.

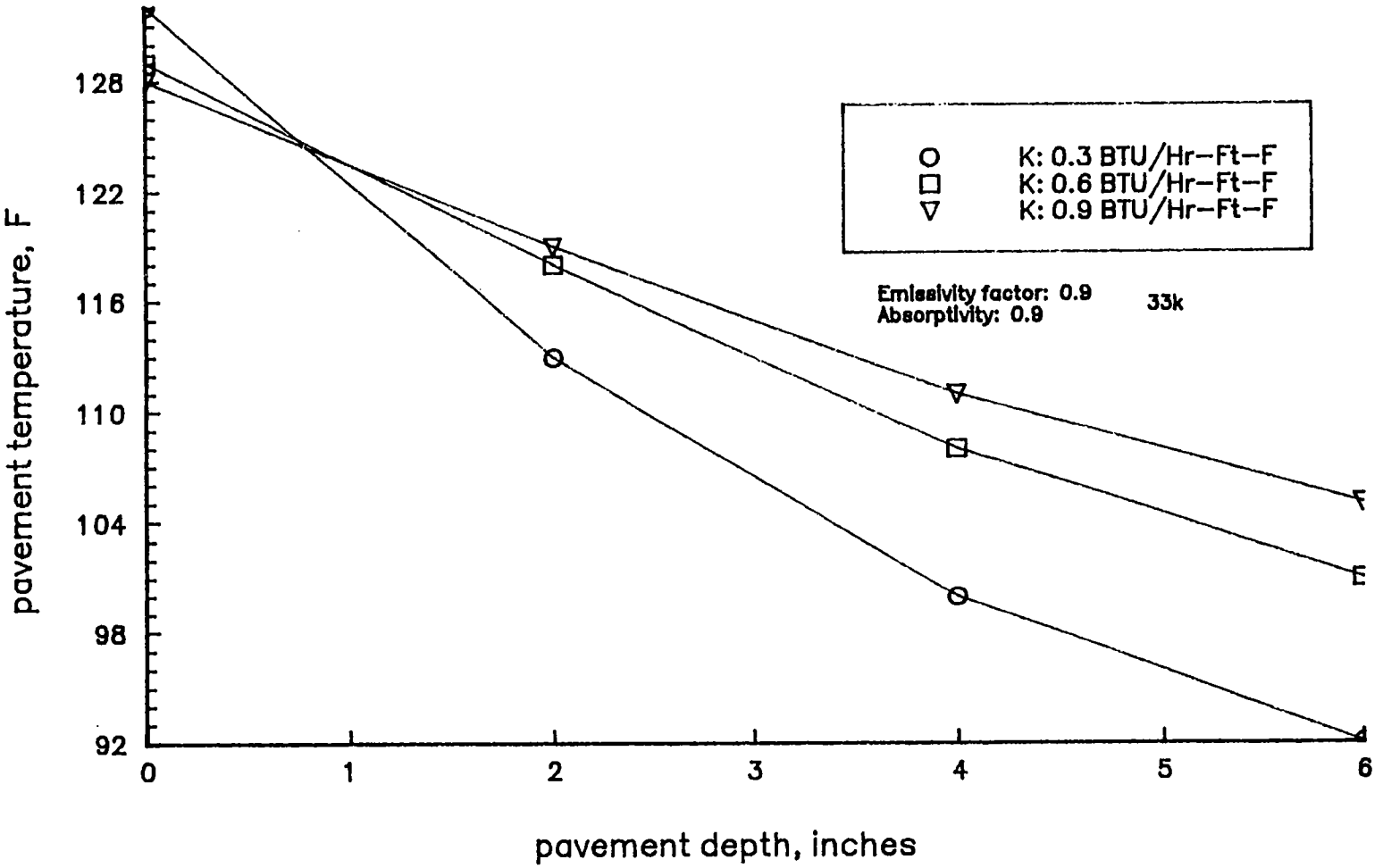

Figure I-34. Predicted Pavement Temperature Profile for Different Thermal Conductivities.

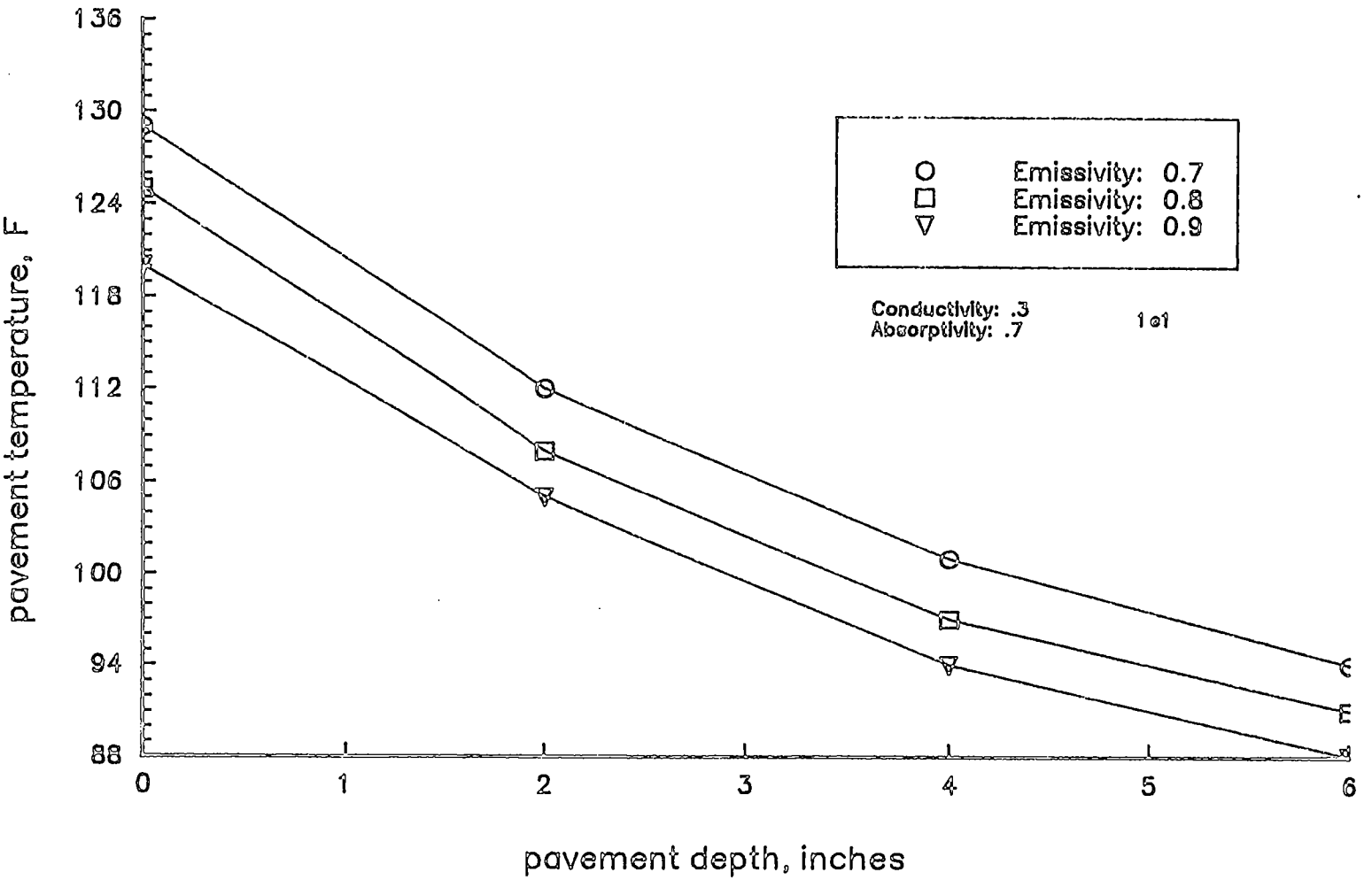

Figure I-35. Predicted Pavement Temperature Profile for Different Emissivity Factors.

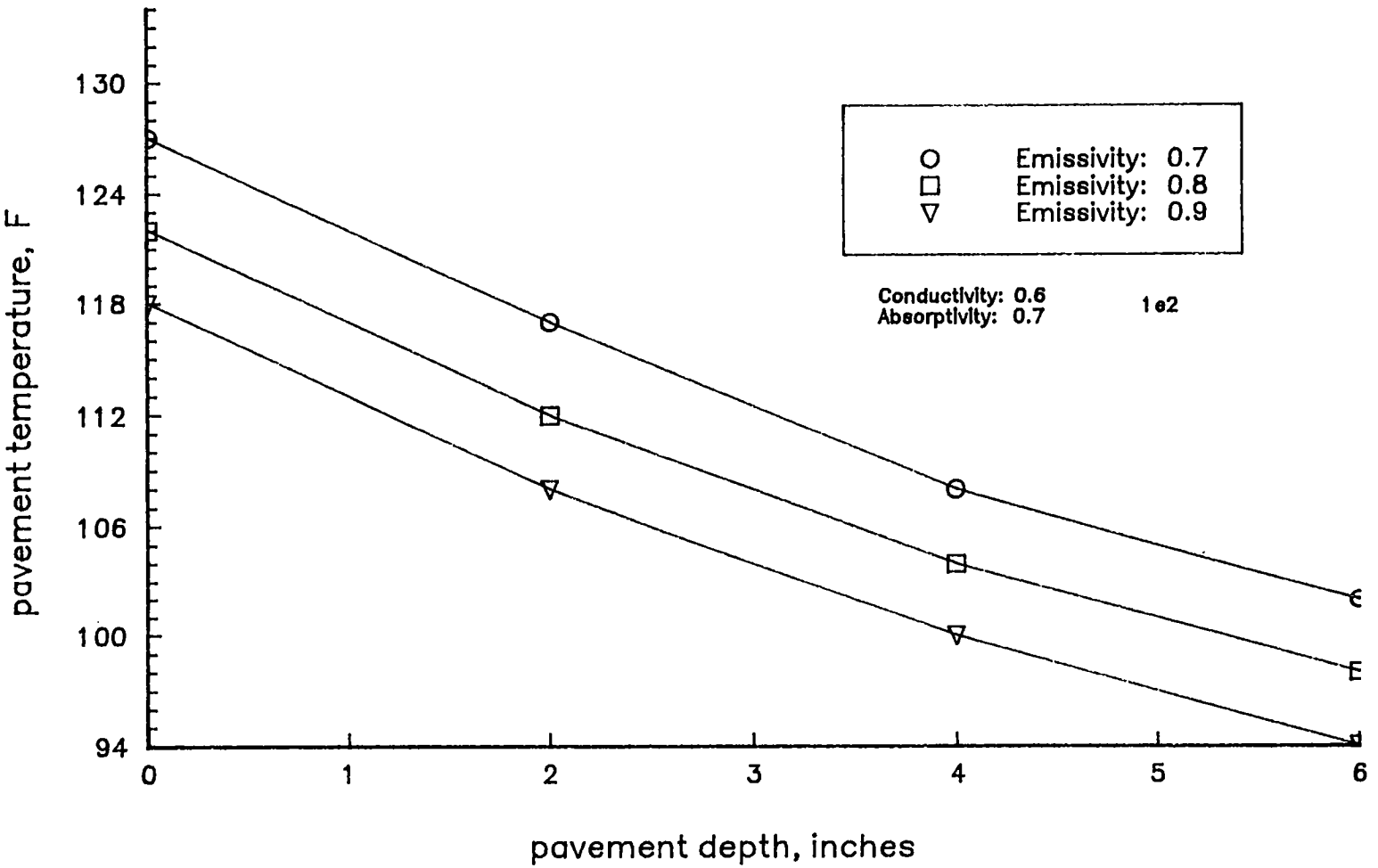

Figure I-36. Predicted Pavement Temperature Profile for Different Emissivity Factors.

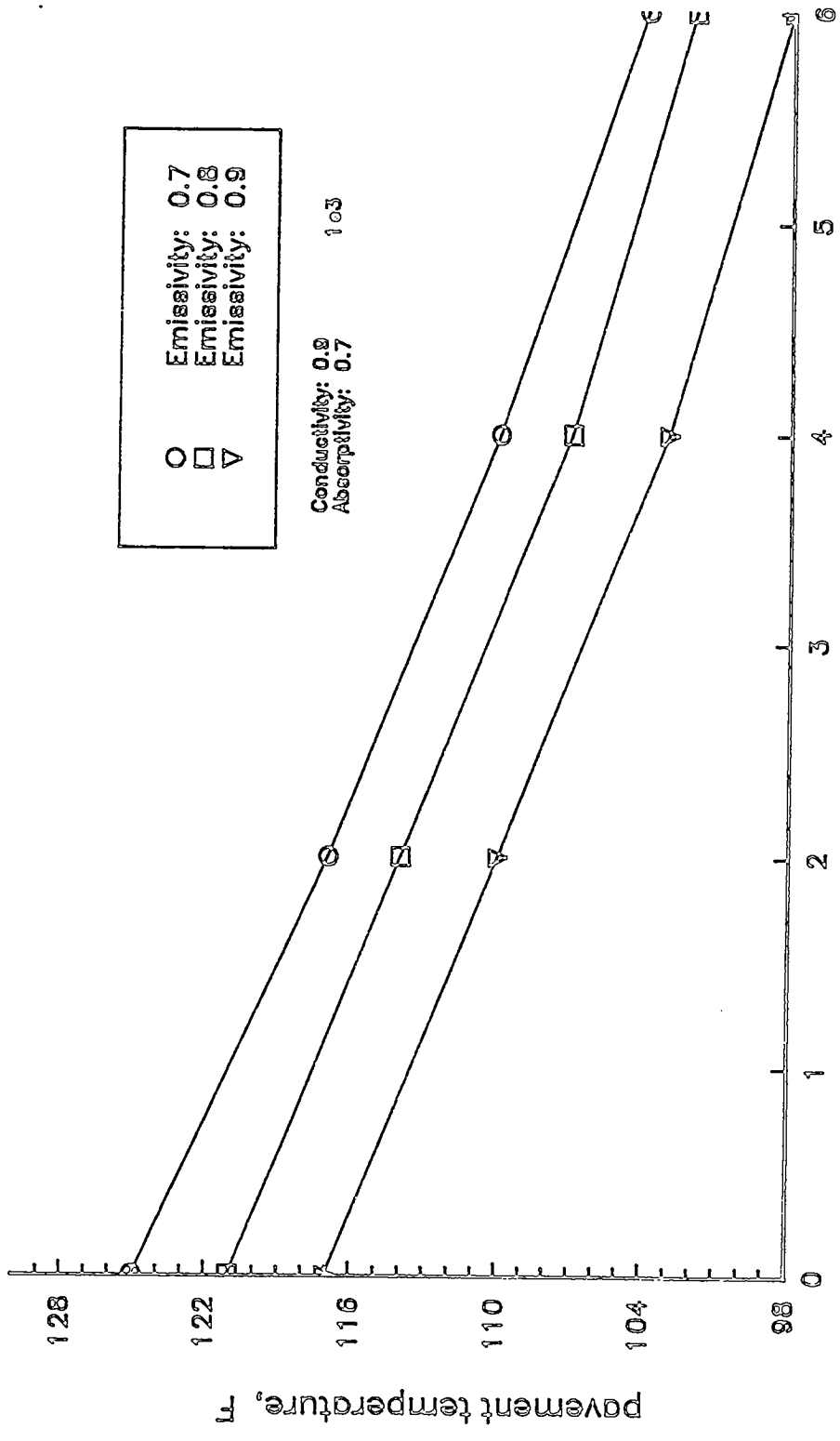

Figure I-37. Predicted Pavement Temperature Profile for Different Emissivity Factors.

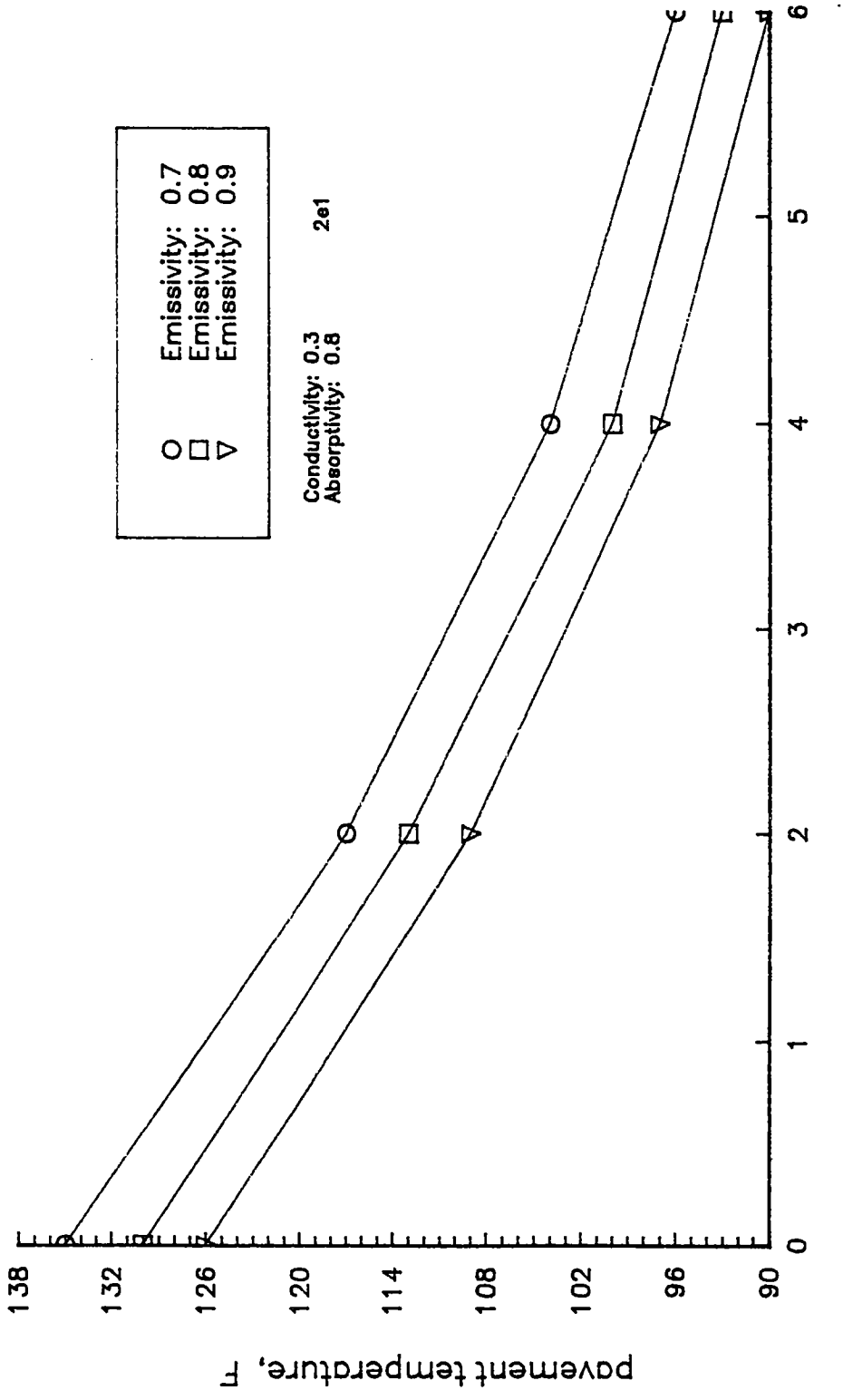

Figure I-38. Predicted Pavement Temperature Profile for Different Emissivity Factors.

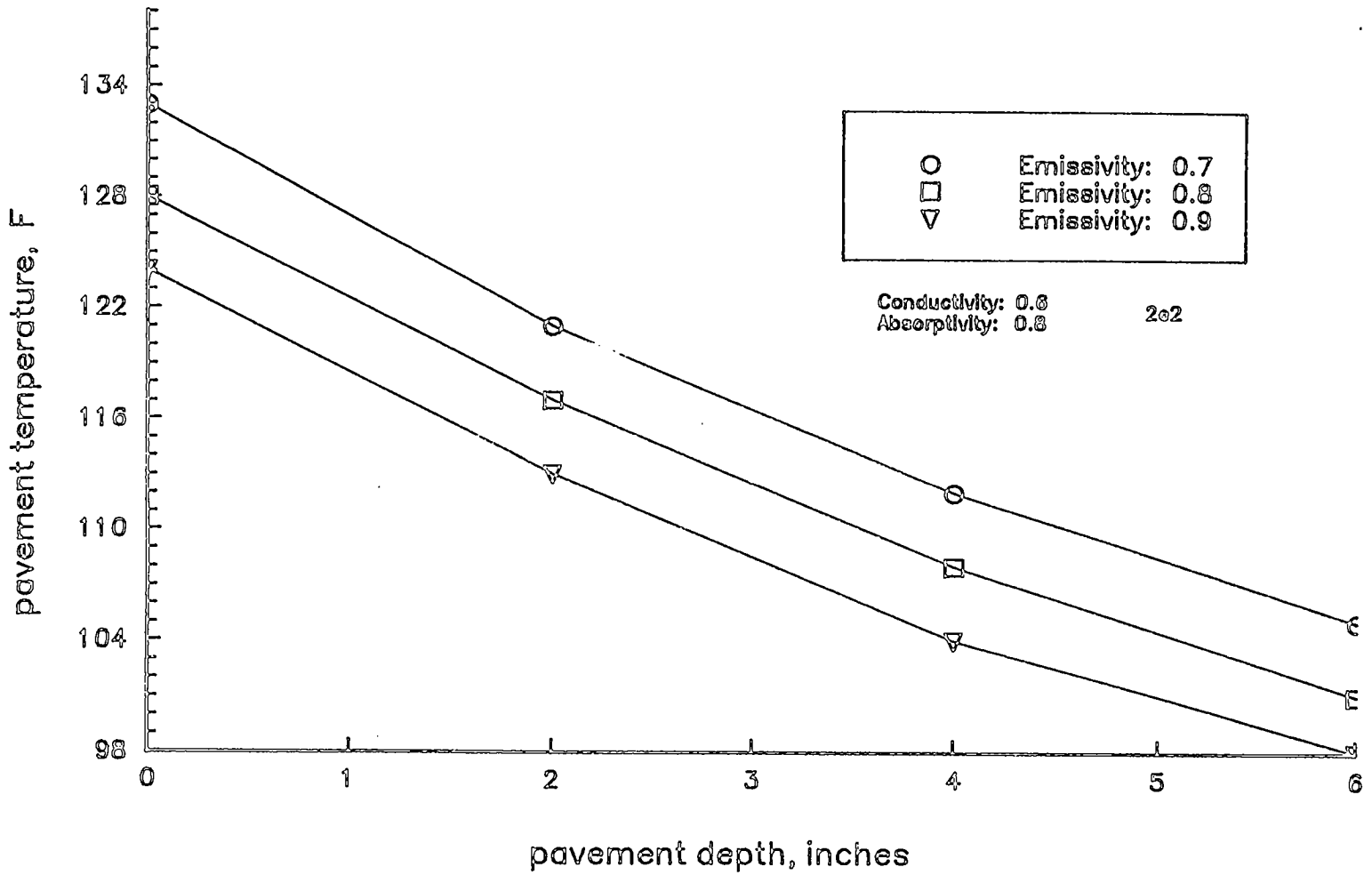

Figure I-39. Predicted Pavement Temperature Profile for Different Emissivity Factors.

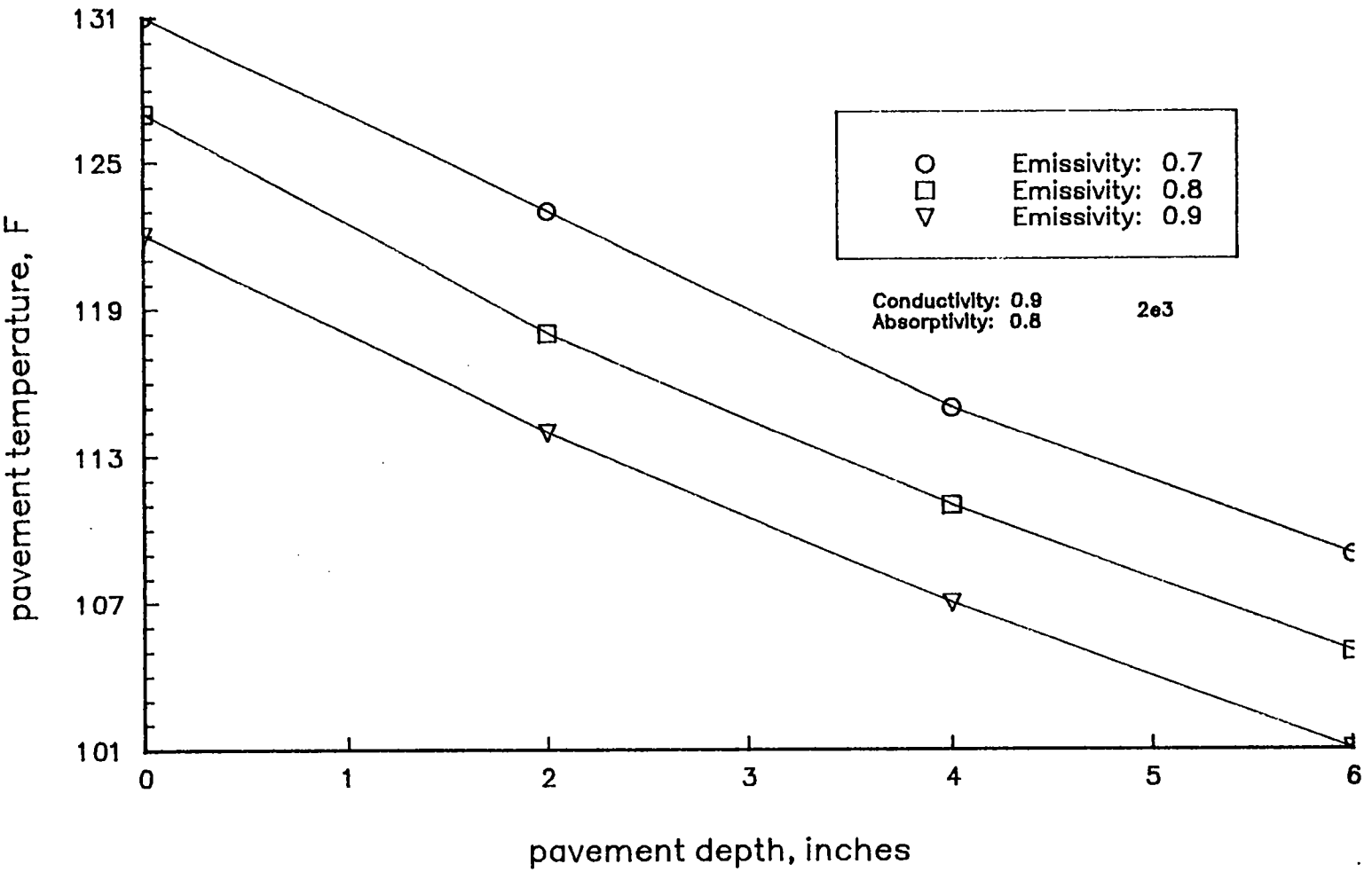

Figure I-40. Predicted Pavement Temperature Profile for Different Emissivity Factors.

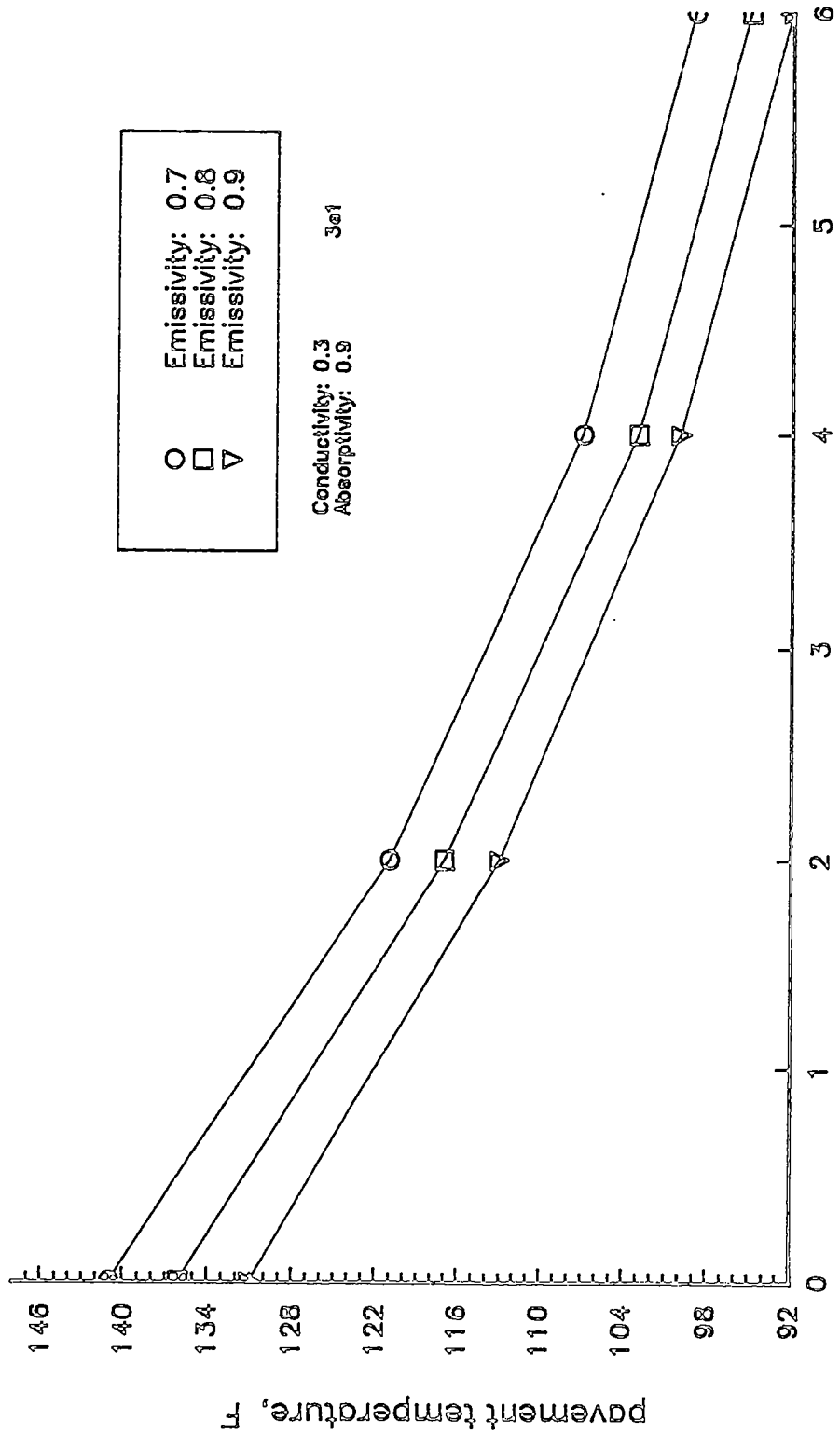

Figure I-41. Predicted Pavement Temperature Profile for Different Emissivity Factors.

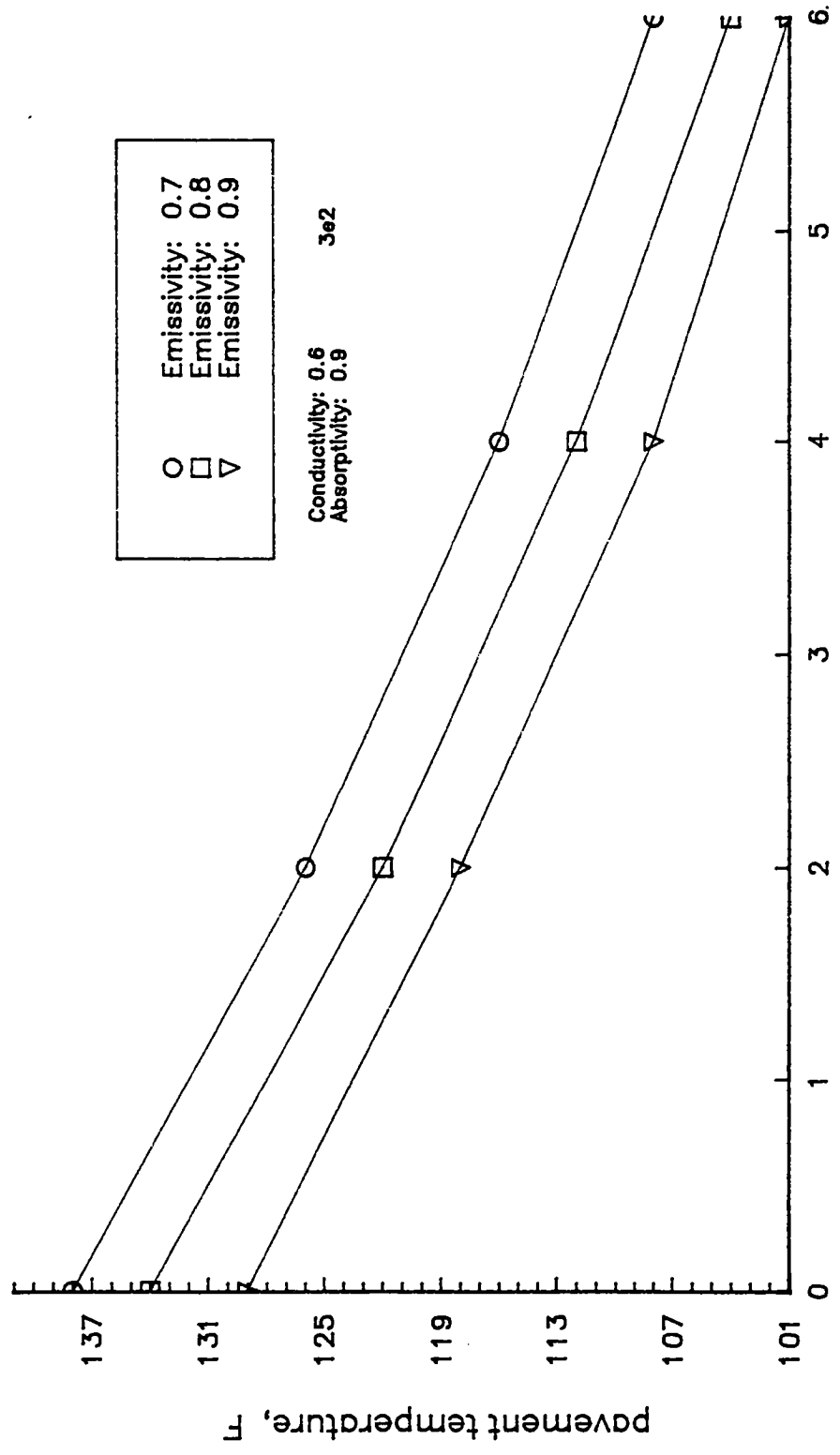

Figure I-42. Predicted Pavement Temperature Profile for Different Emissivity Factors.

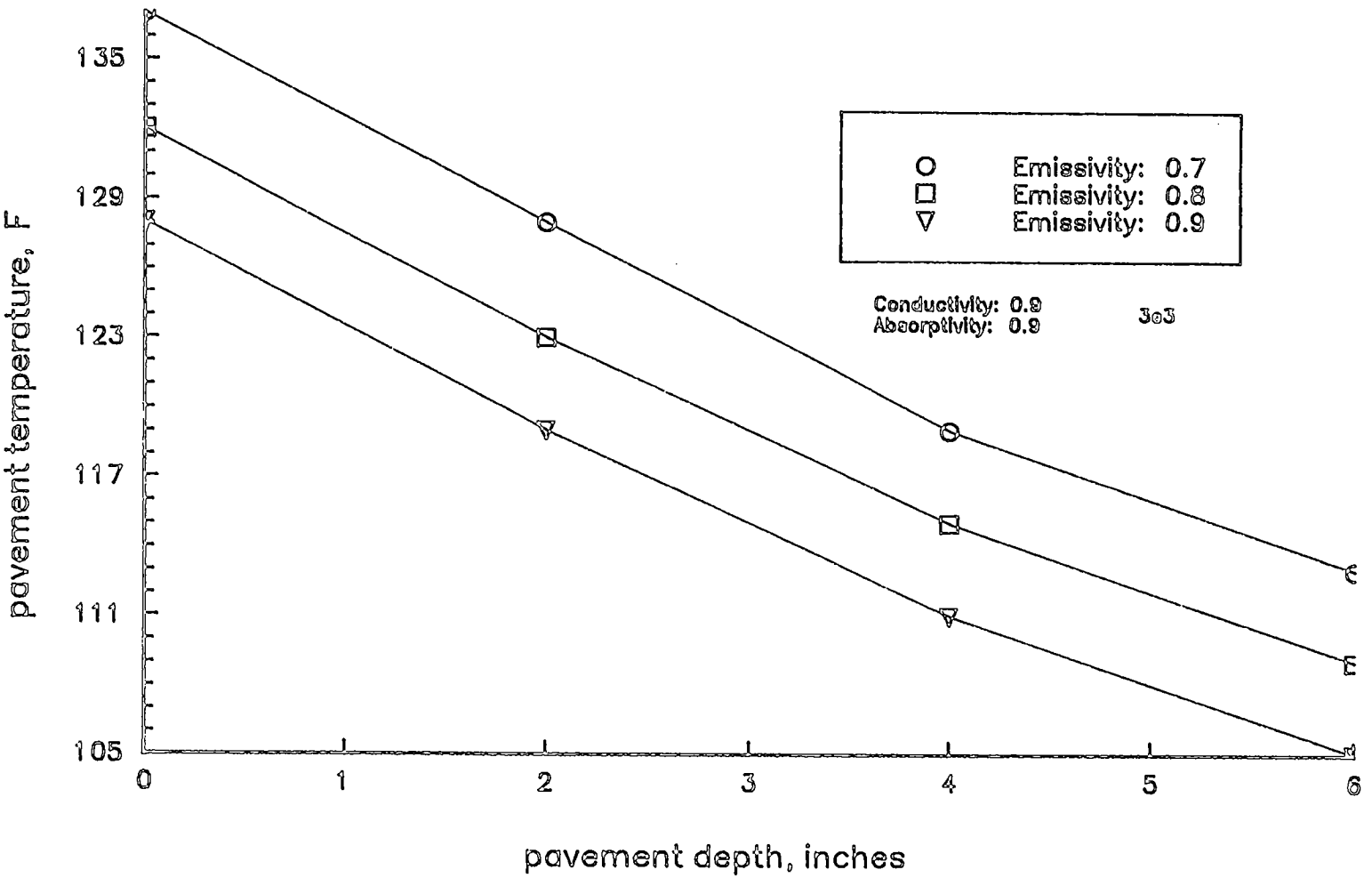

Figure I-43. Predicted Pavement Temperature Profile for Different Emissivity Factors.

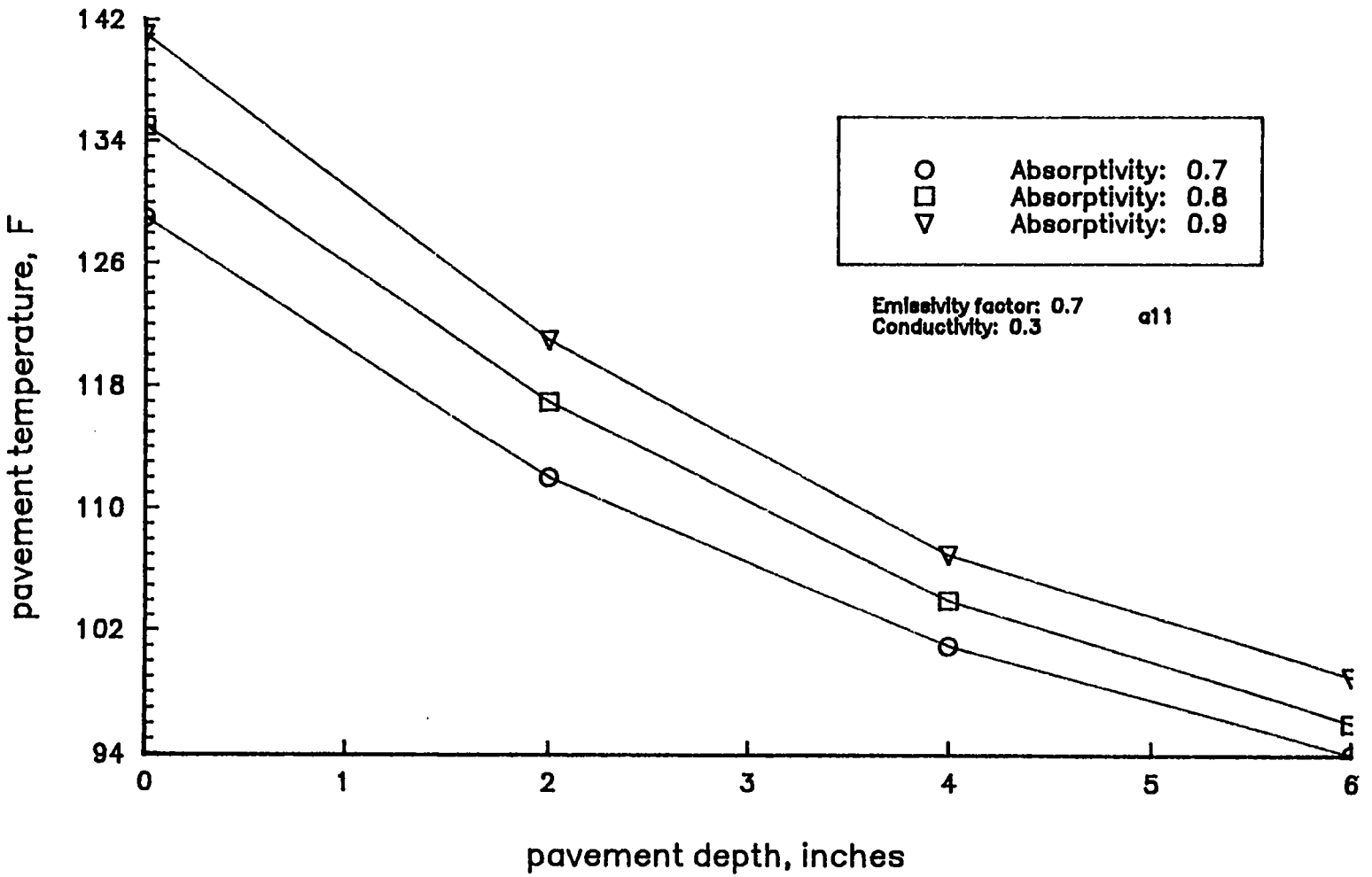

Figure I-44. Predicted Pavement Temperature Profile for Different Surface Short-wave Absorptivities.

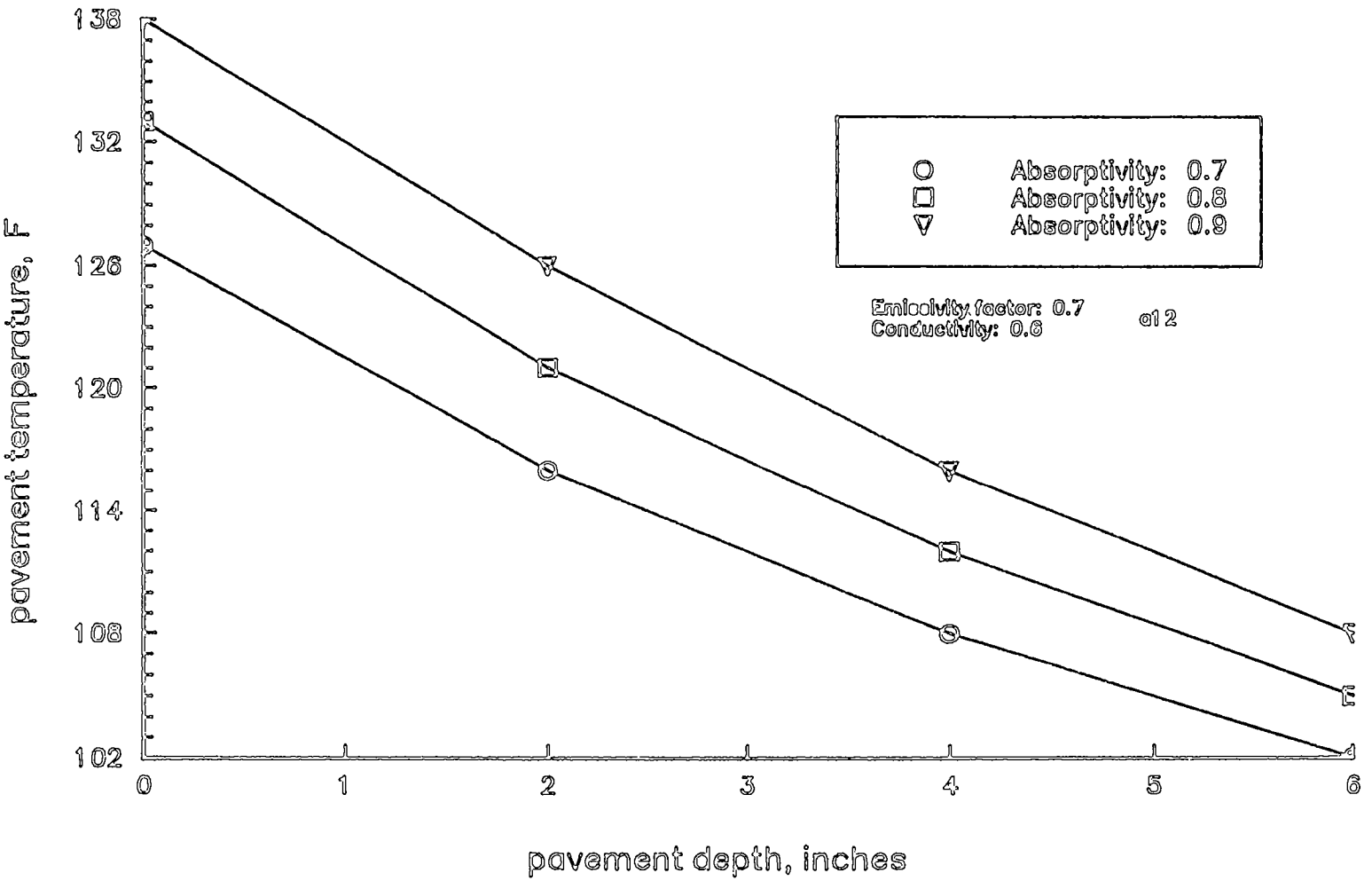

Figure I-45. Predicted Pavement Temperature Profile for Different Surface Short-wave Absorptivities.

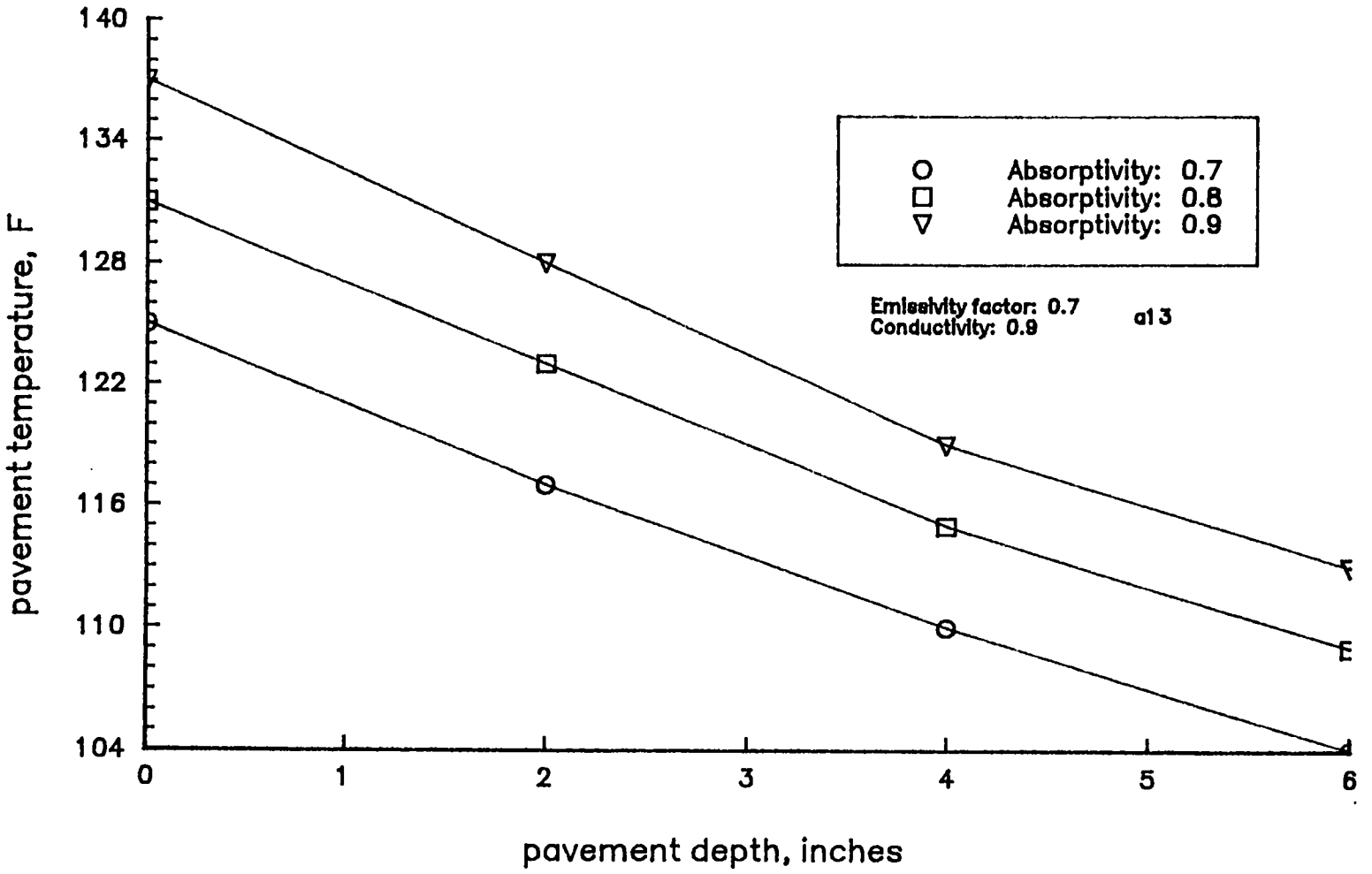

Figure I-46. Predicted Pavement Temperature Profile for Different Surface Short-wave Absorptivities.

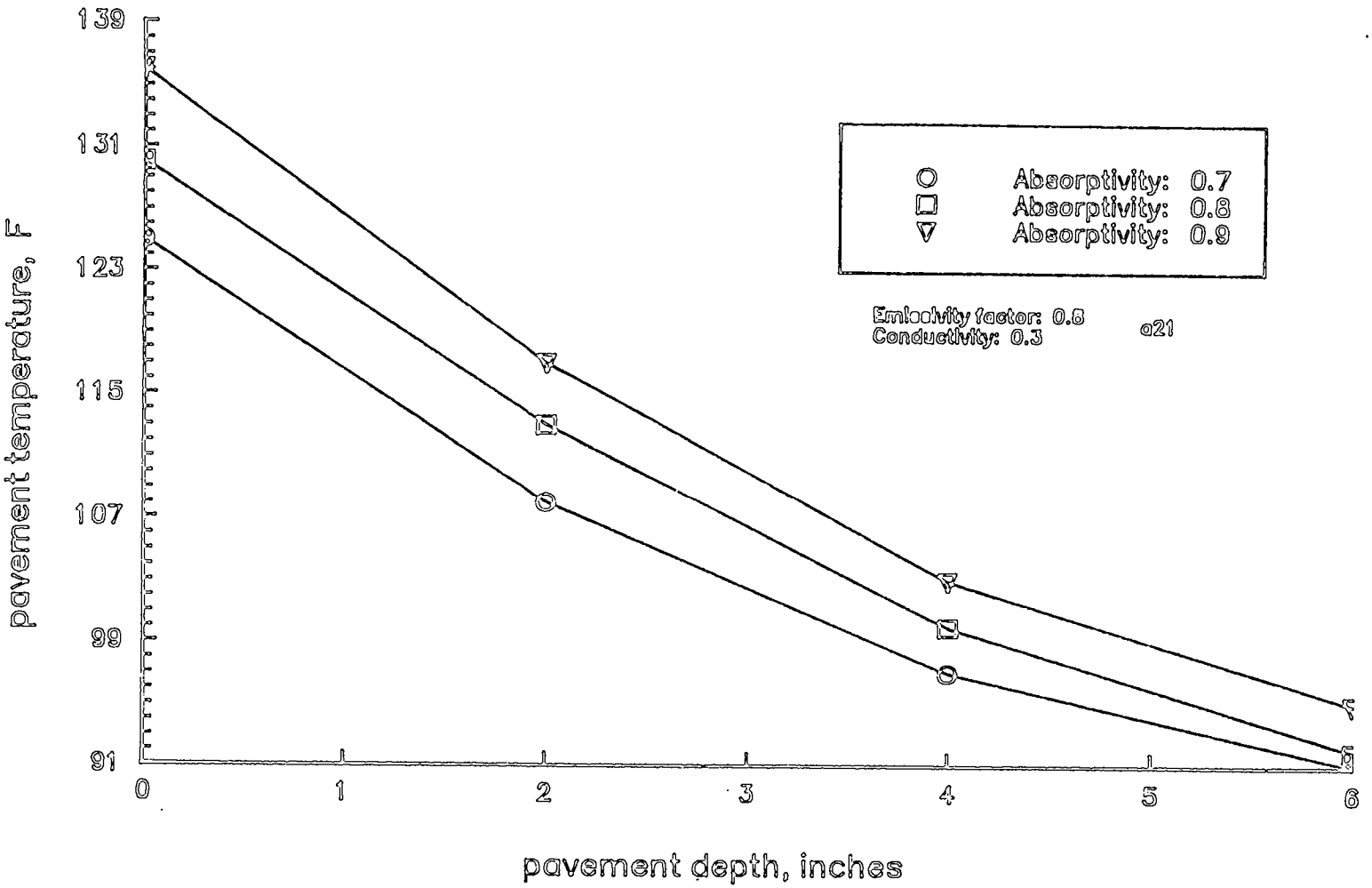

Figure I-47. Predicted Pavement Temperature Profile for Different Surface Short-wave Absorptivities.

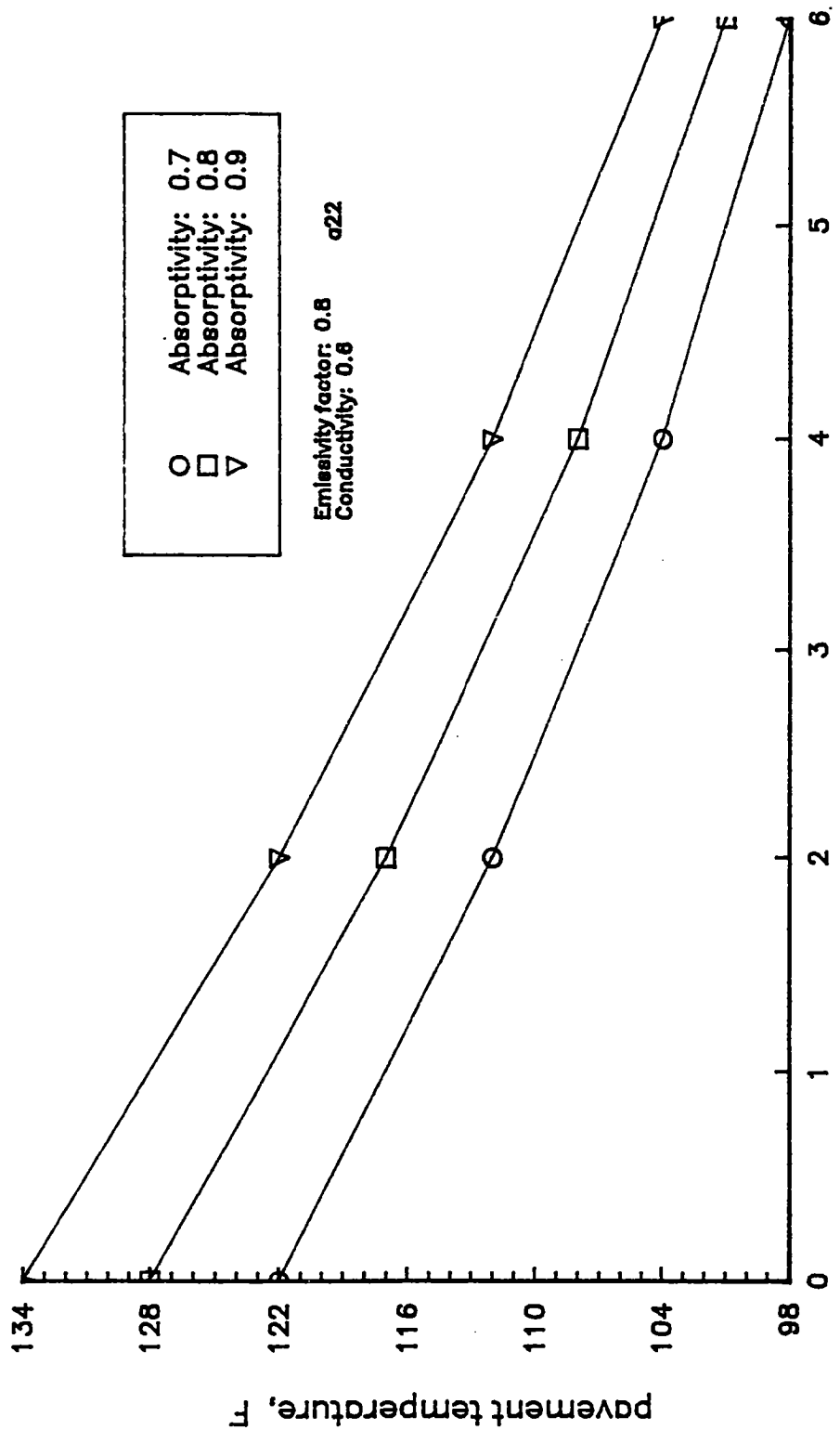

Figure I-48. Predicted Pavement Temperature Profile for Different Surface Short-wave Absorptivities.

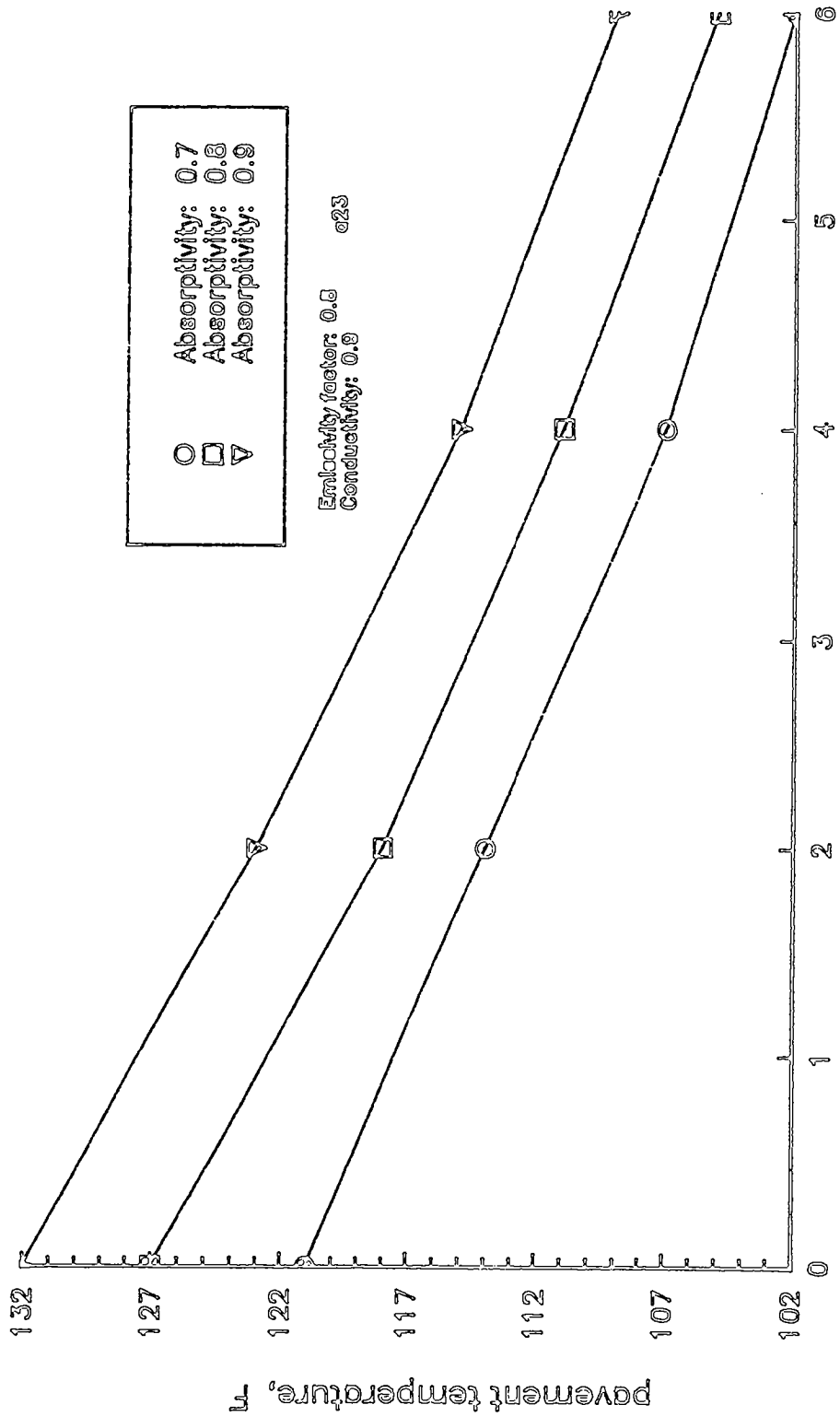

Figure I-49. Predicted Pavement Temperature Profile for Different Surface Short-wave Absorptivities.

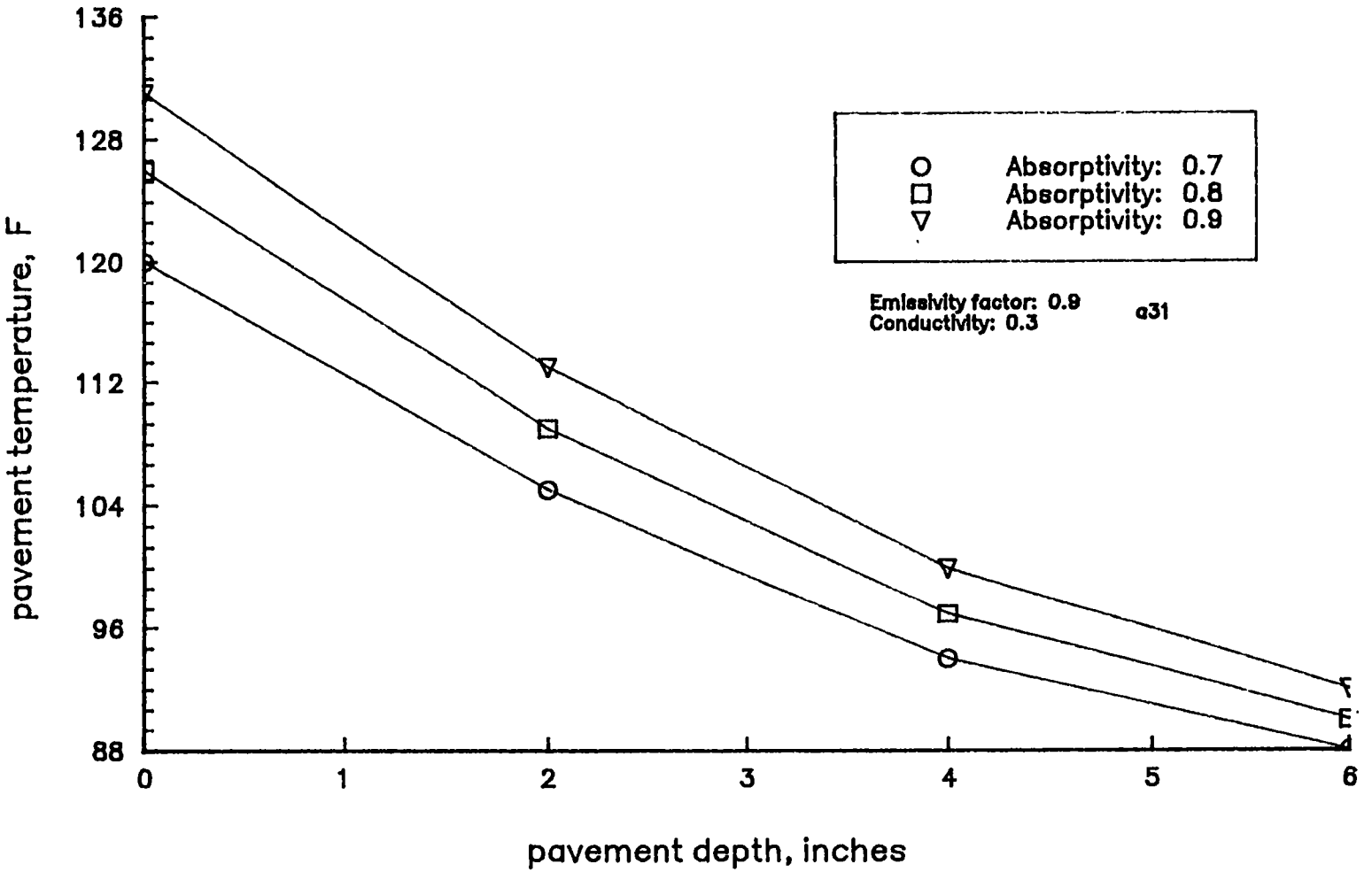

Figure I-50. Predicted Pavement Temperature Profile for Different Surface Short-wave Absorptivities.

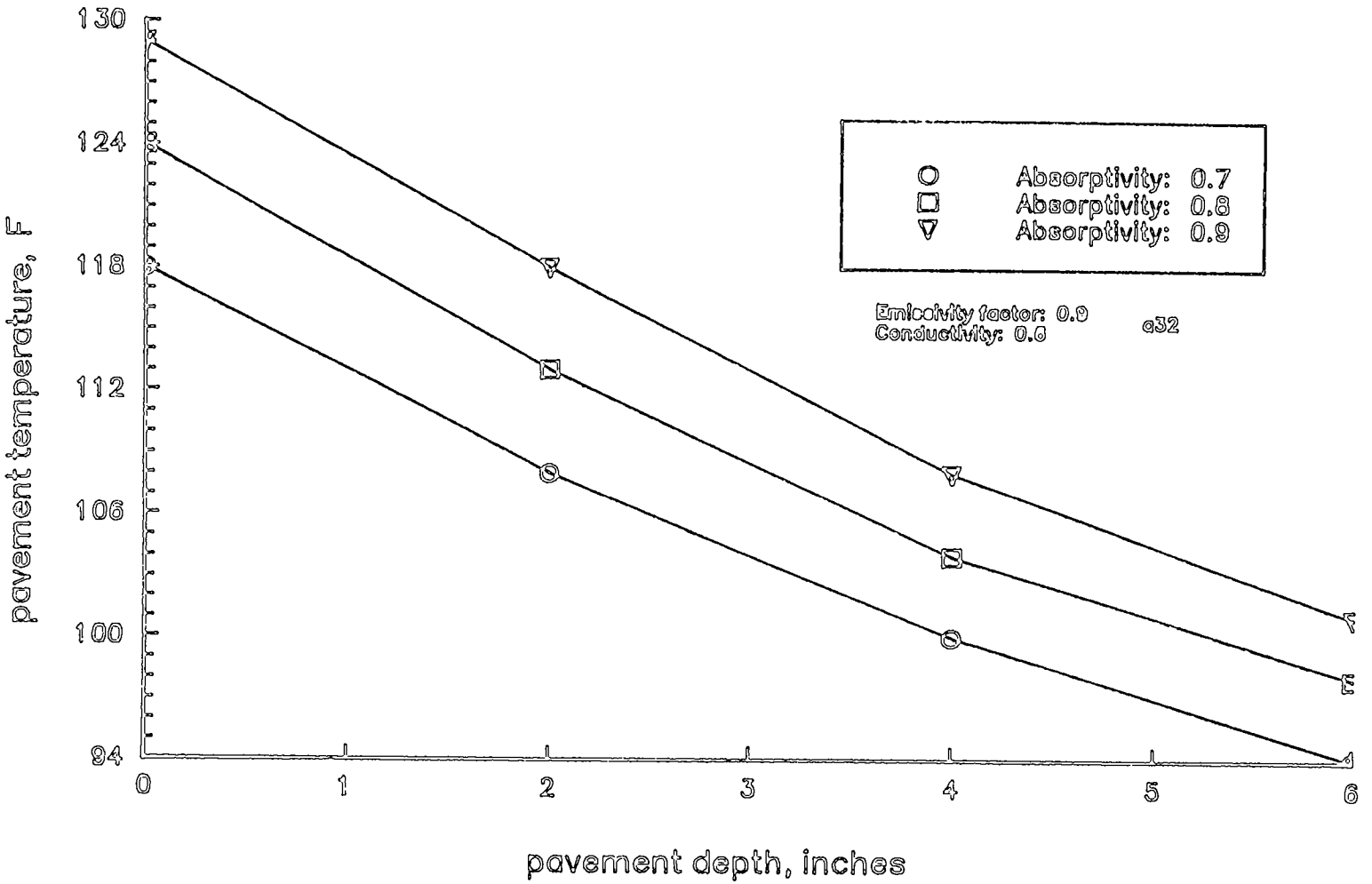

Figure I-51. Predicted Pavement Temperature Profile for Different Surface Short-wave Absorptivities.

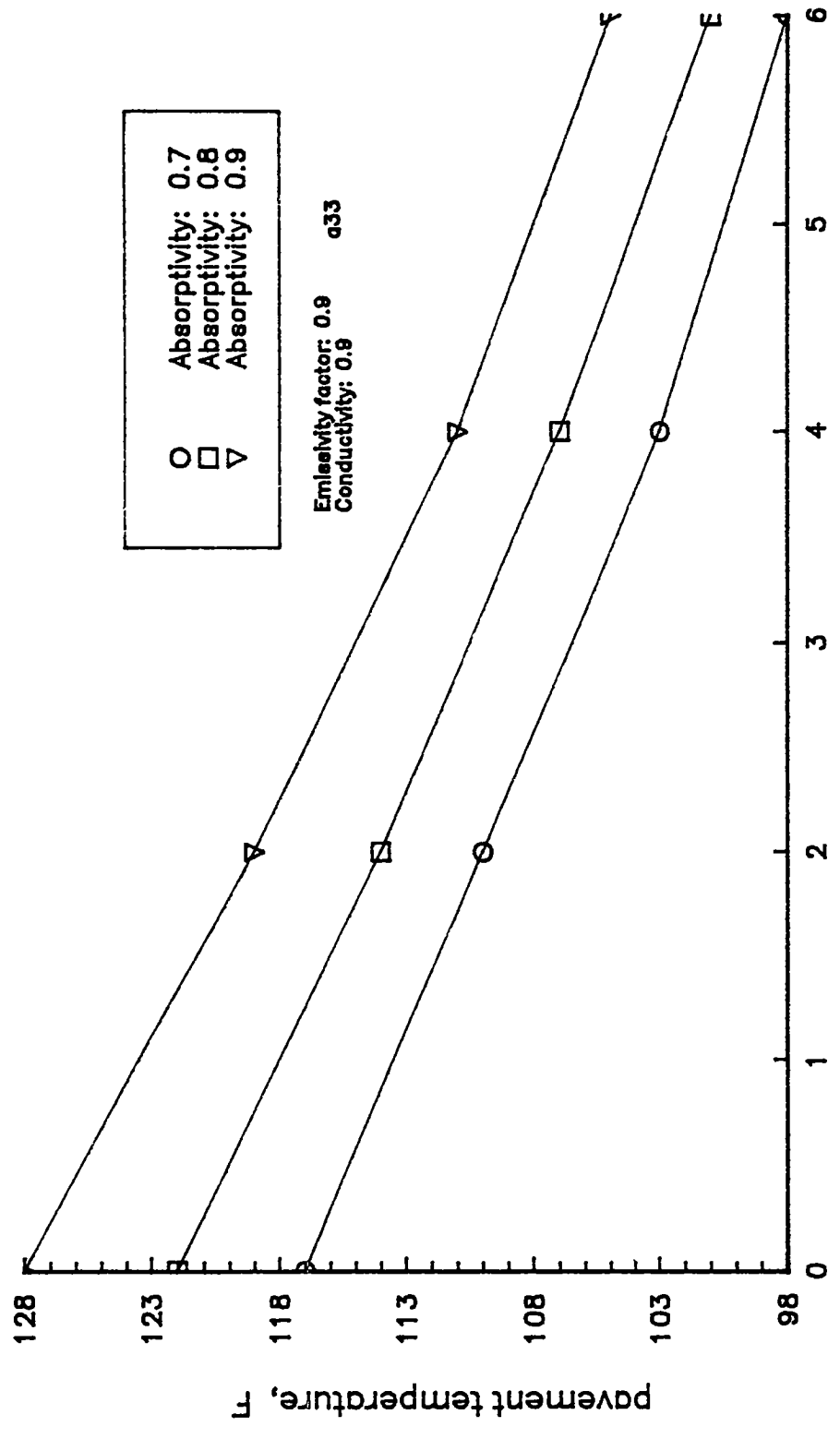

Figure I-52. Predicted Pavement Temperature Profile for Different Surface Short-wave Absorptivities.

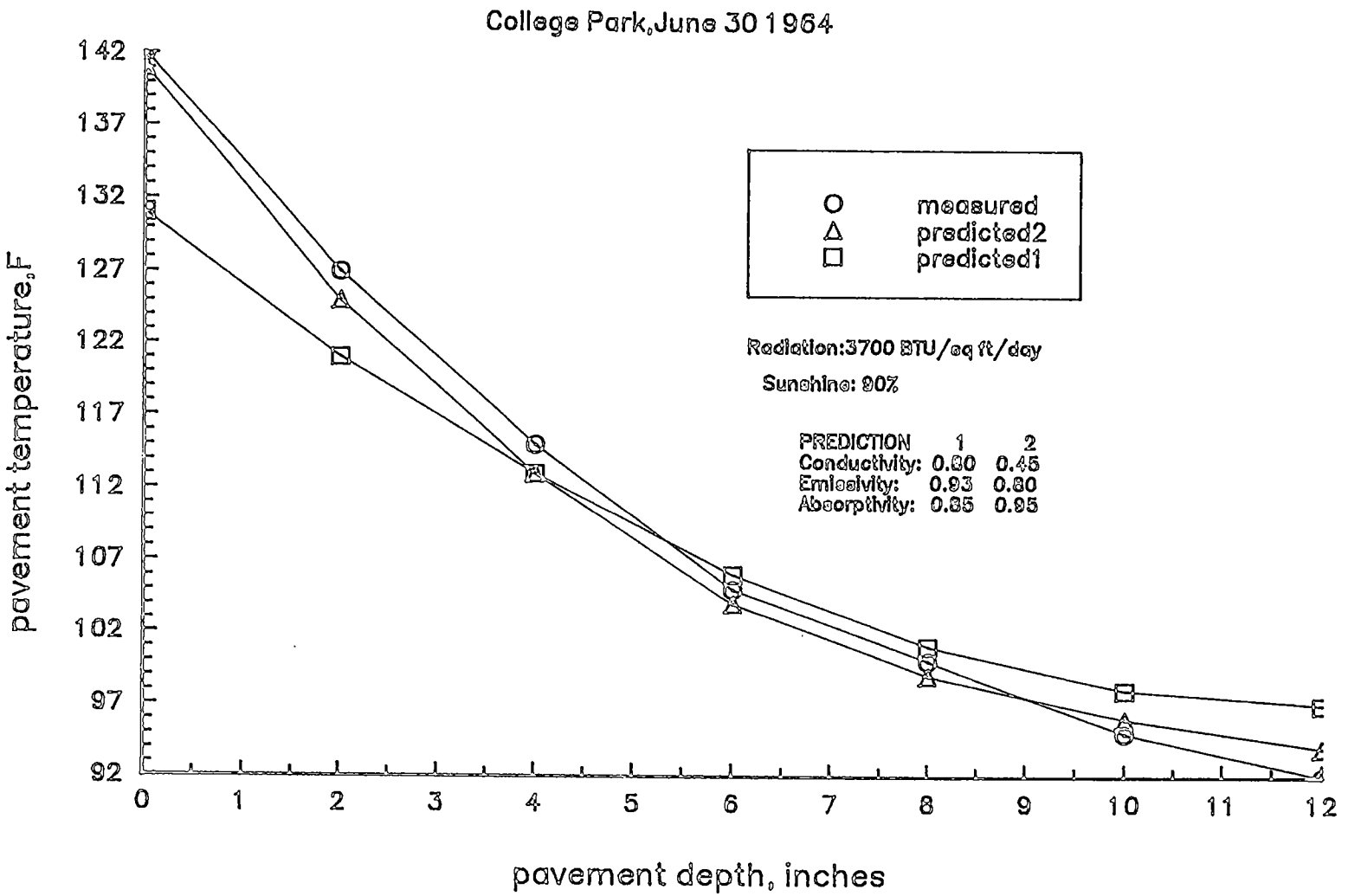

Figure II-1. Measured and Predicted Pavement Temperature Profile at College Park, Maryland.

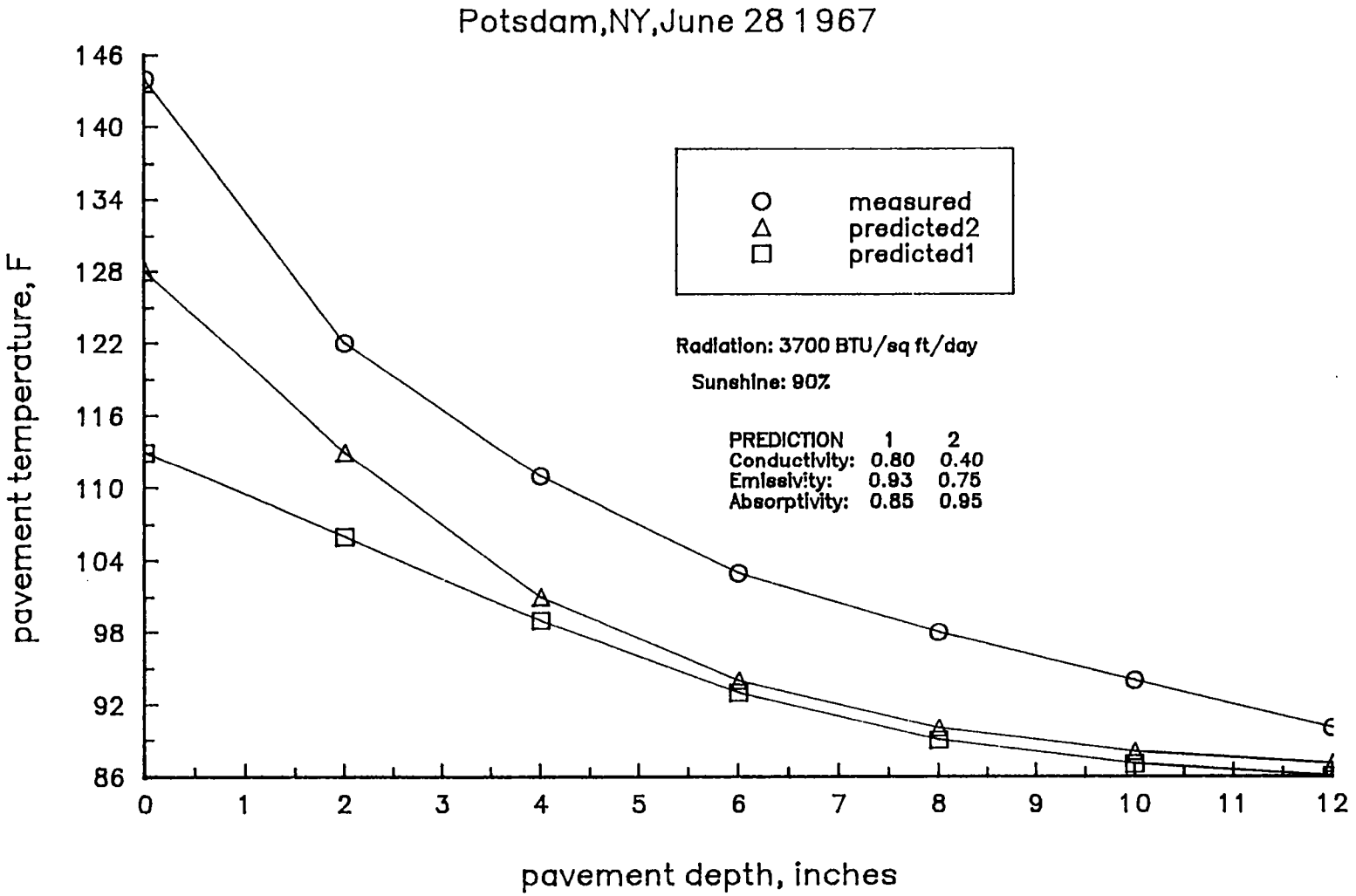

Figure II-2. Measured and Predicted Pavement Temperature Profile at Potsdam, NY.

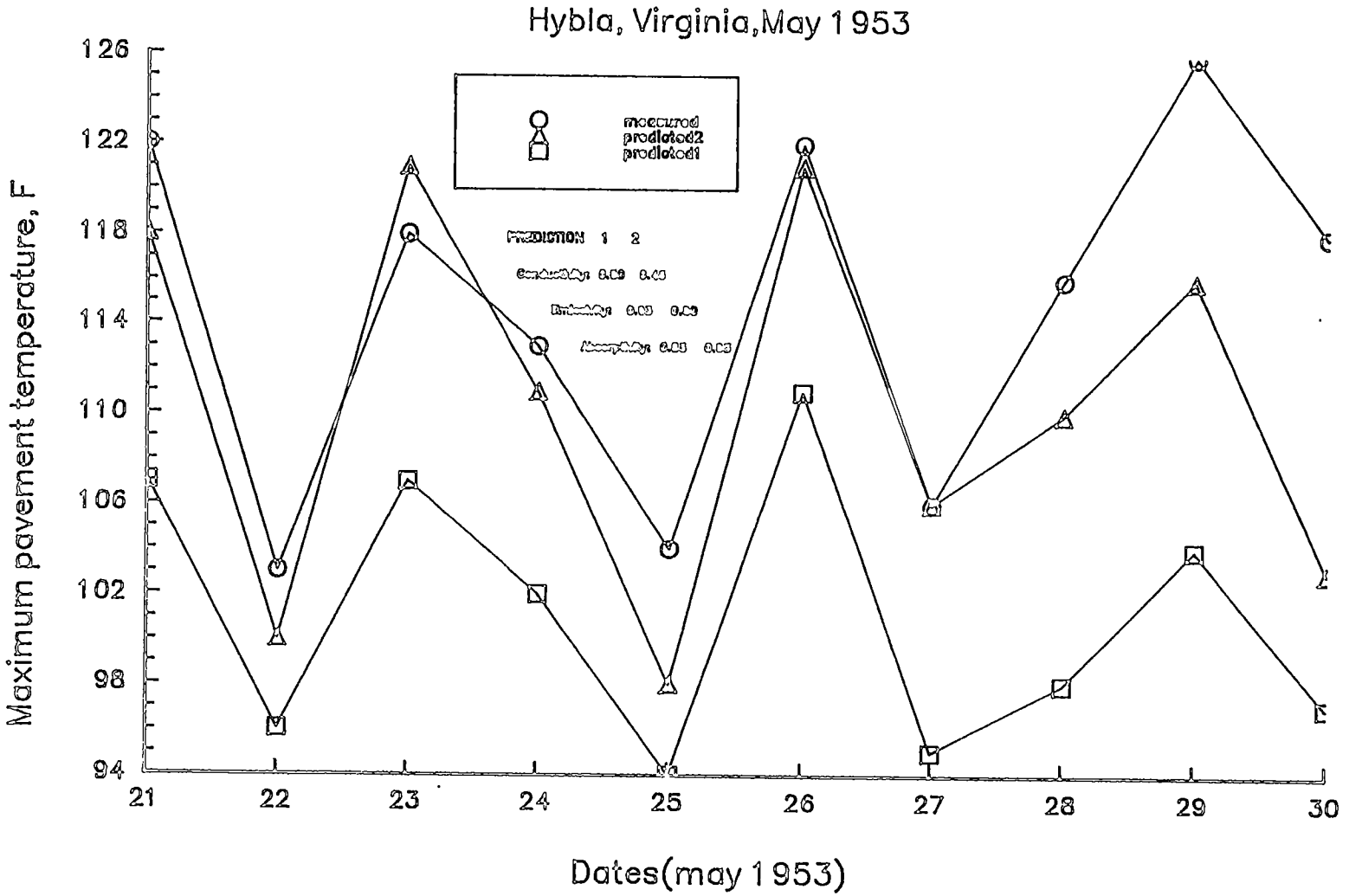

Figure II-3. Measured and Predicted Pavement Temperature Profile at Hybla, Virginia.

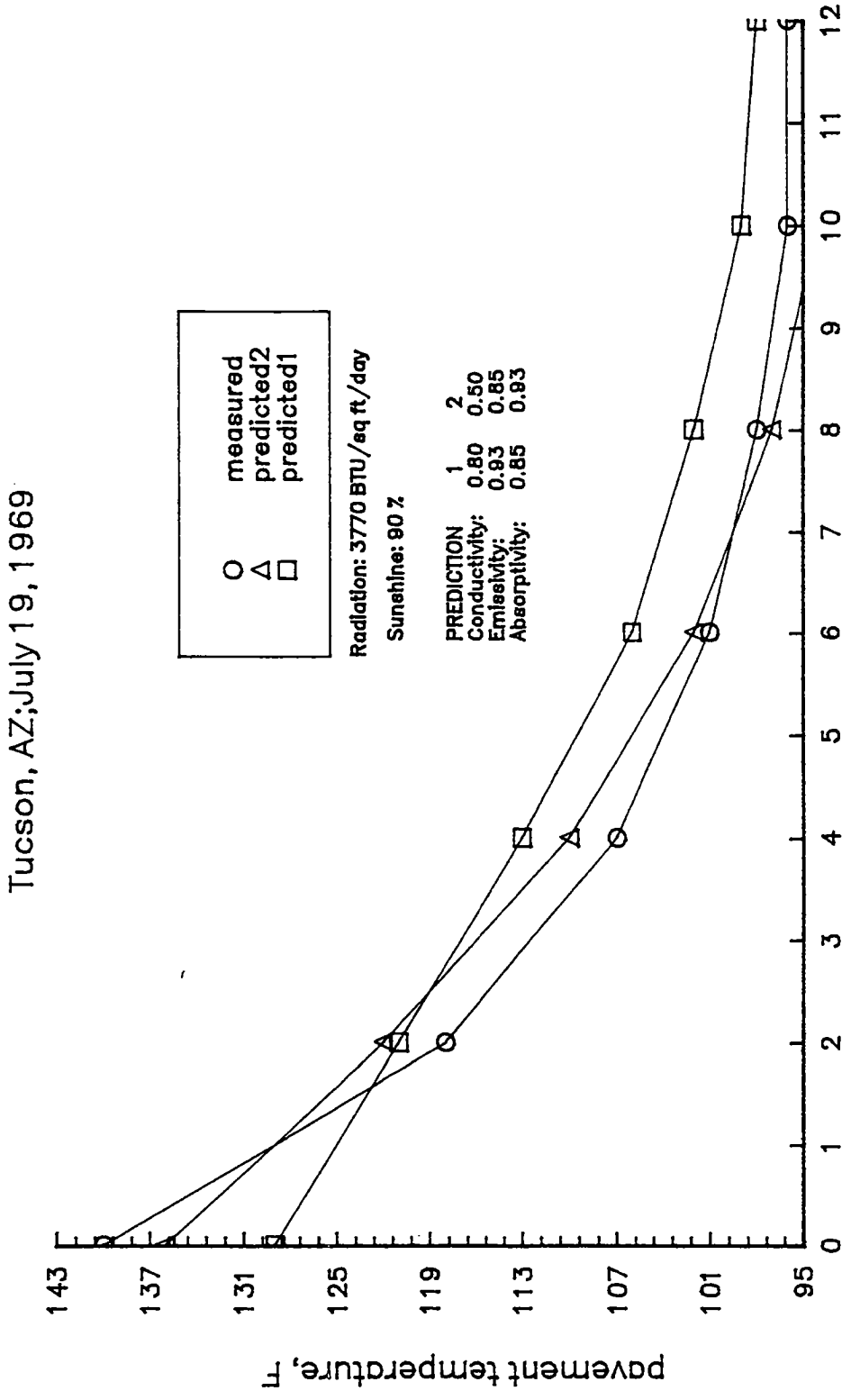

Figure II-4. Measured and Predicted Pavement Temeprature Profiles at Tuscon, Arizona.

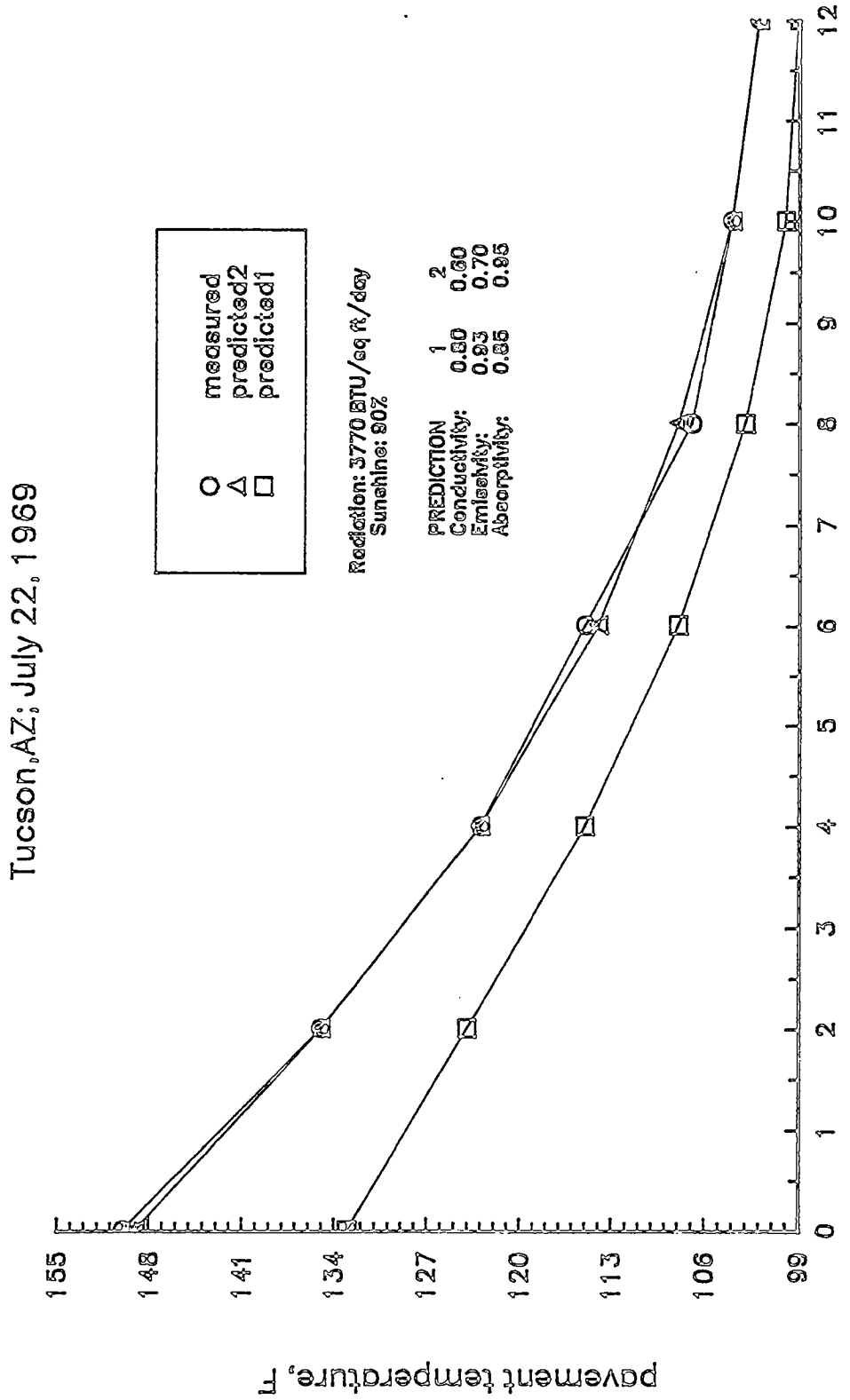

Figure II-5. Measured and Predicted Pavement Temperature Profiles at Tucson, Arizona.

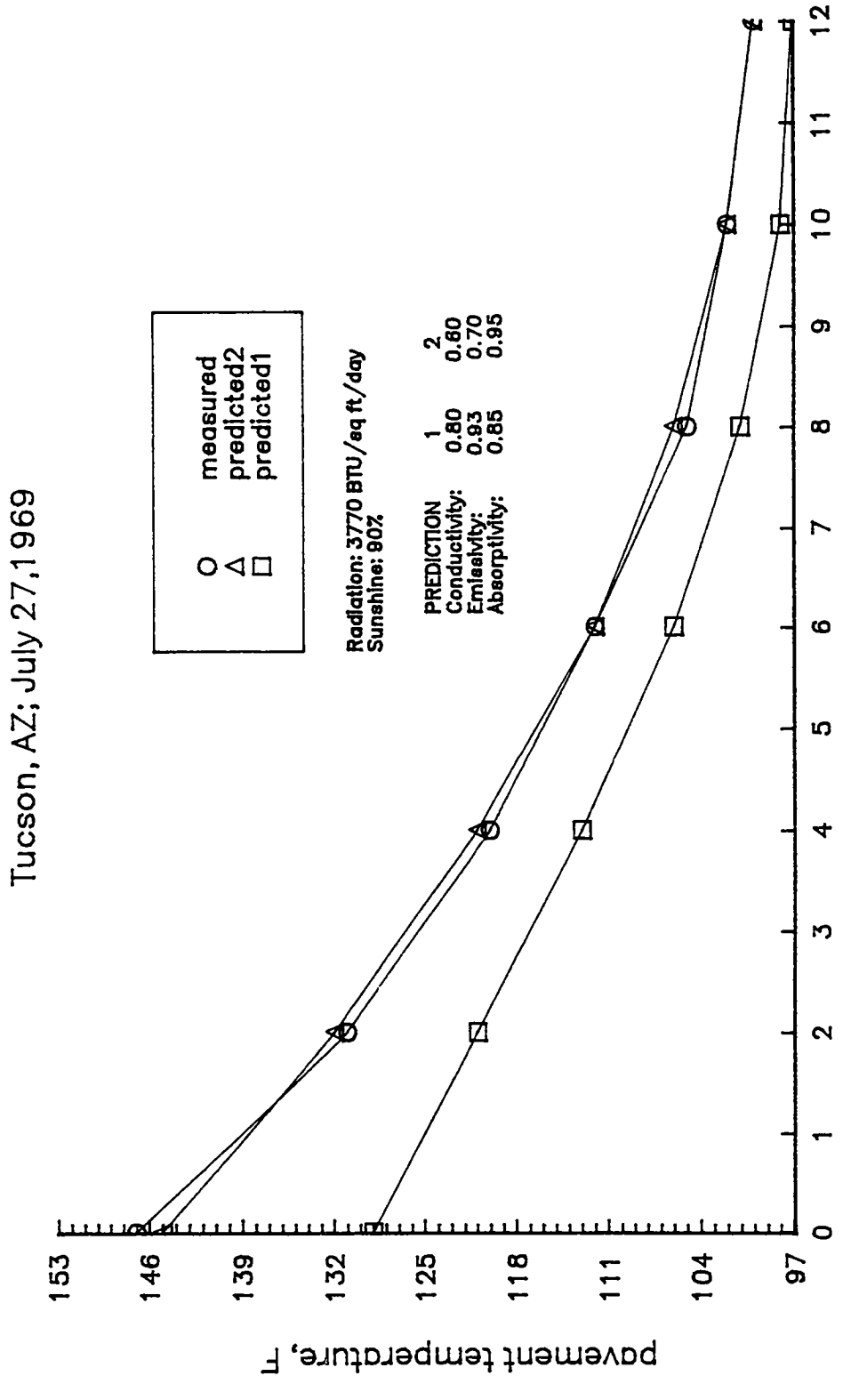

Figure II-6. Measured and Predicted Pavement Temperature Profiles at Tucson, Arizona.

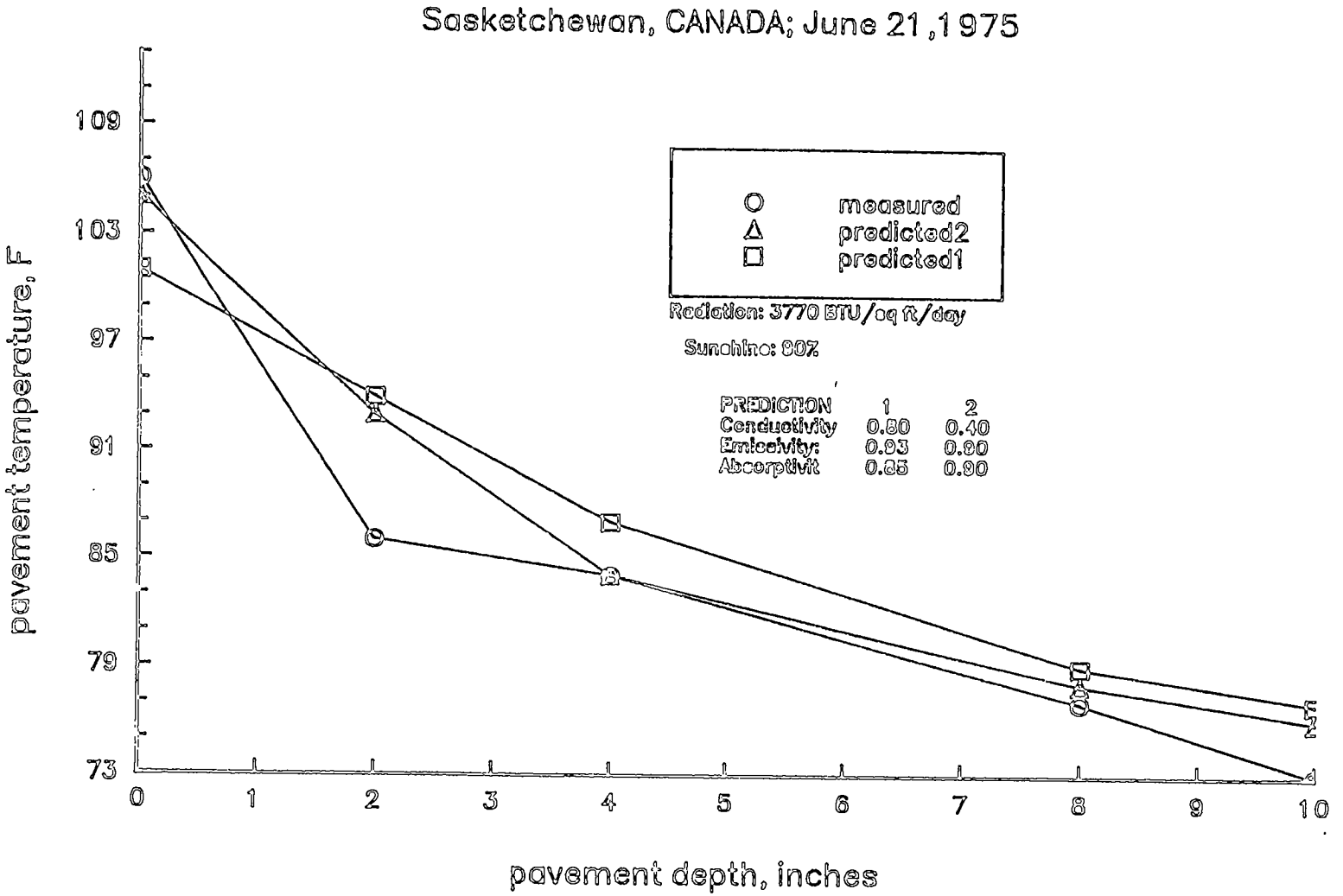

Figure II-7. Measured and Predicted Pavement Temperature Profiles at Saskatchewan, Canada.

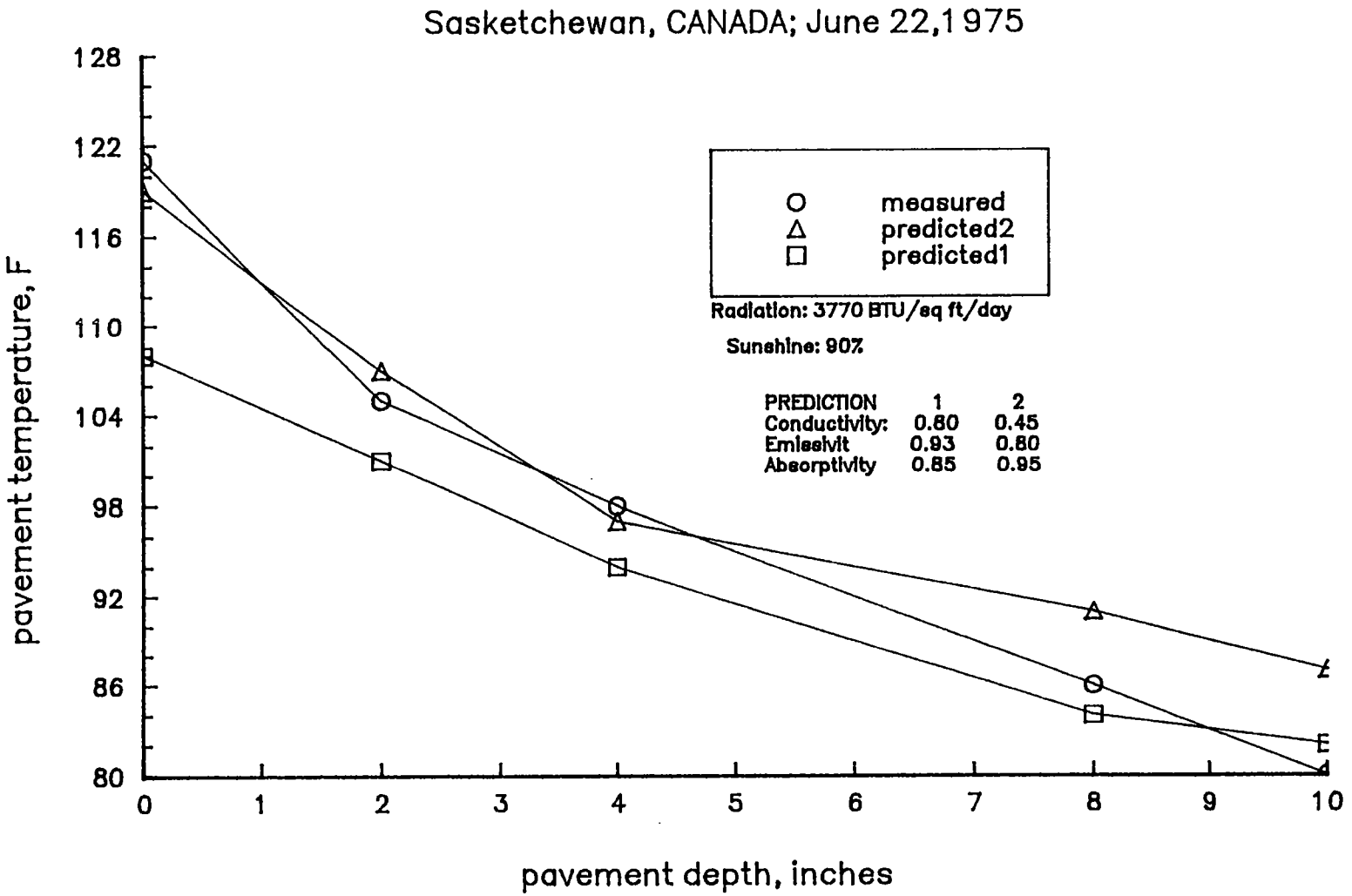

Figure II-8. Measured and Predicted Pavement Temperature Profiles at Saskatchewan, Canada.

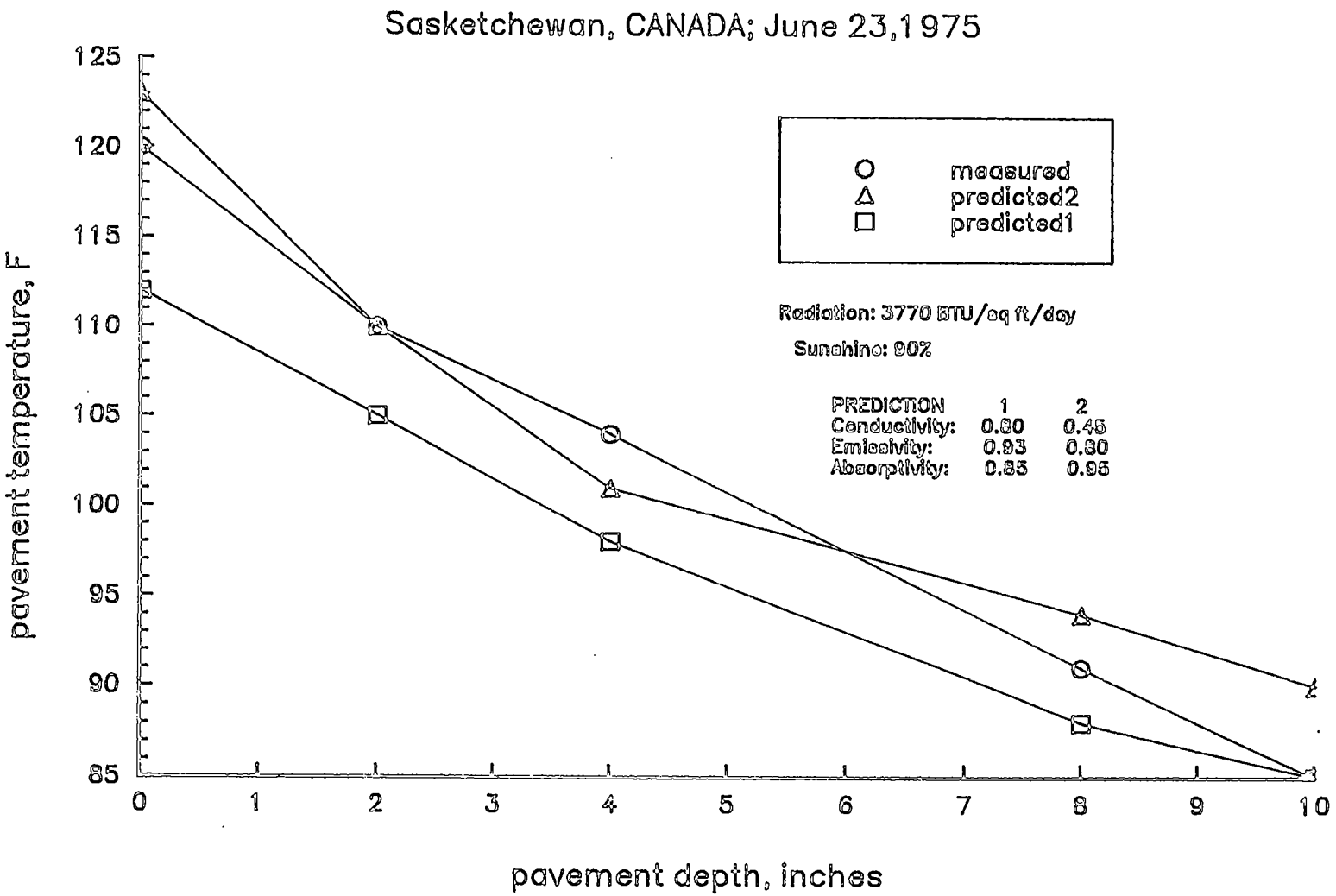

Figure II-9. Measured and Predicted Pavement Temperature Profiles at Saskatchewan, Canada.

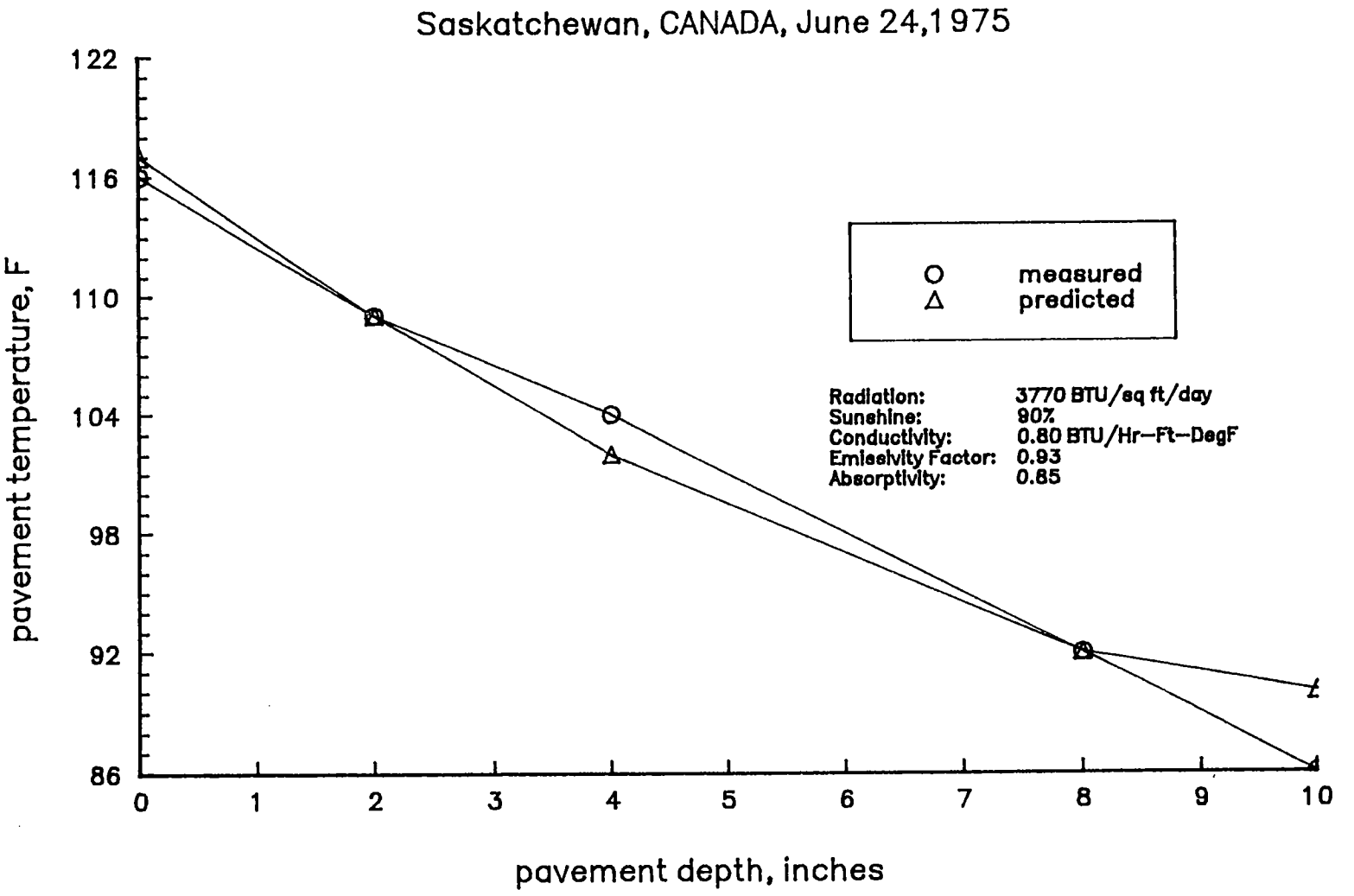

Figure II-10. Measured and Predicted Pavement Temperature Profiles at Saskatchewan, Canada.

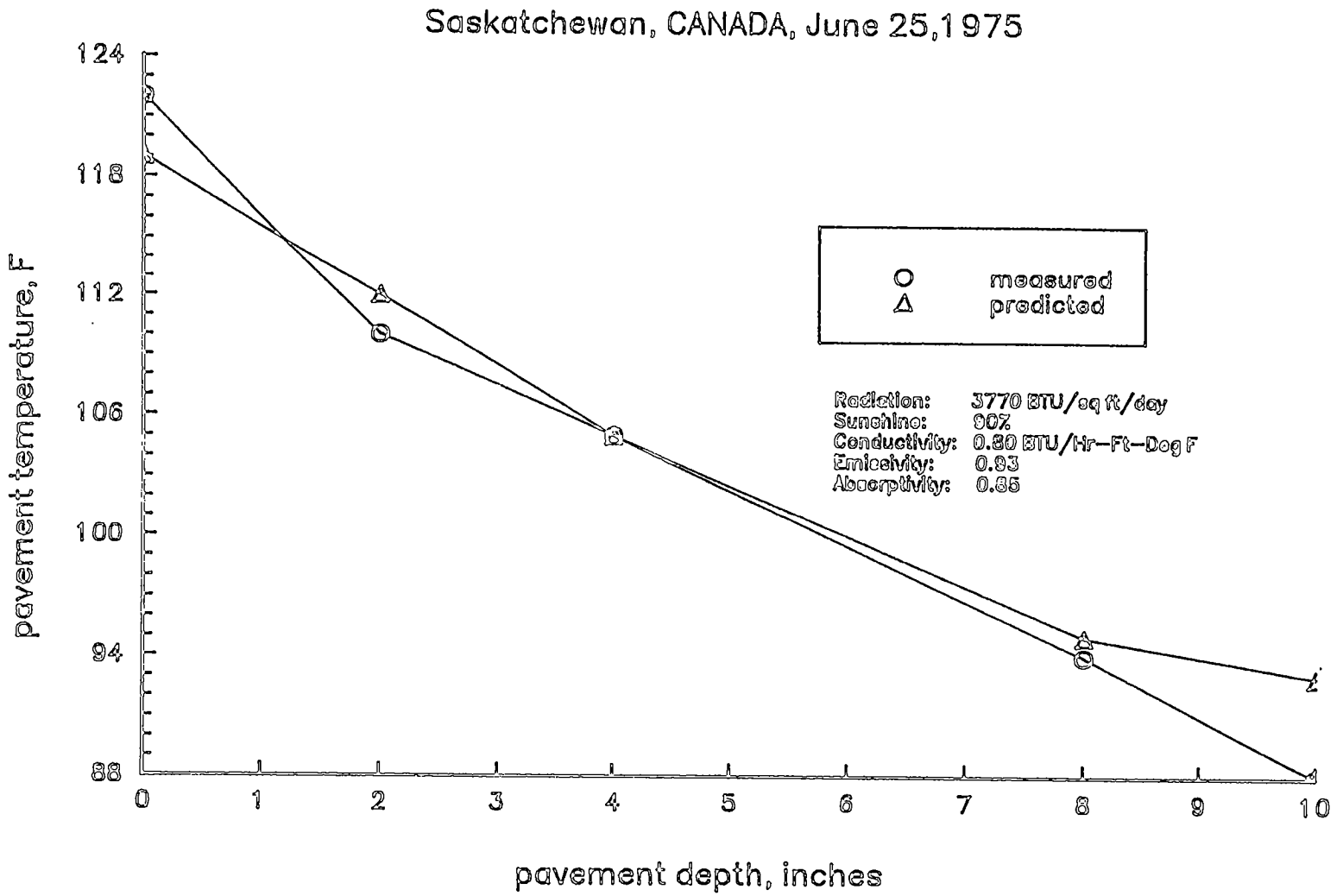

Figure II-11. Measured and Predicted Pavement Temperature Profiles at Saskatchewan, Canada.

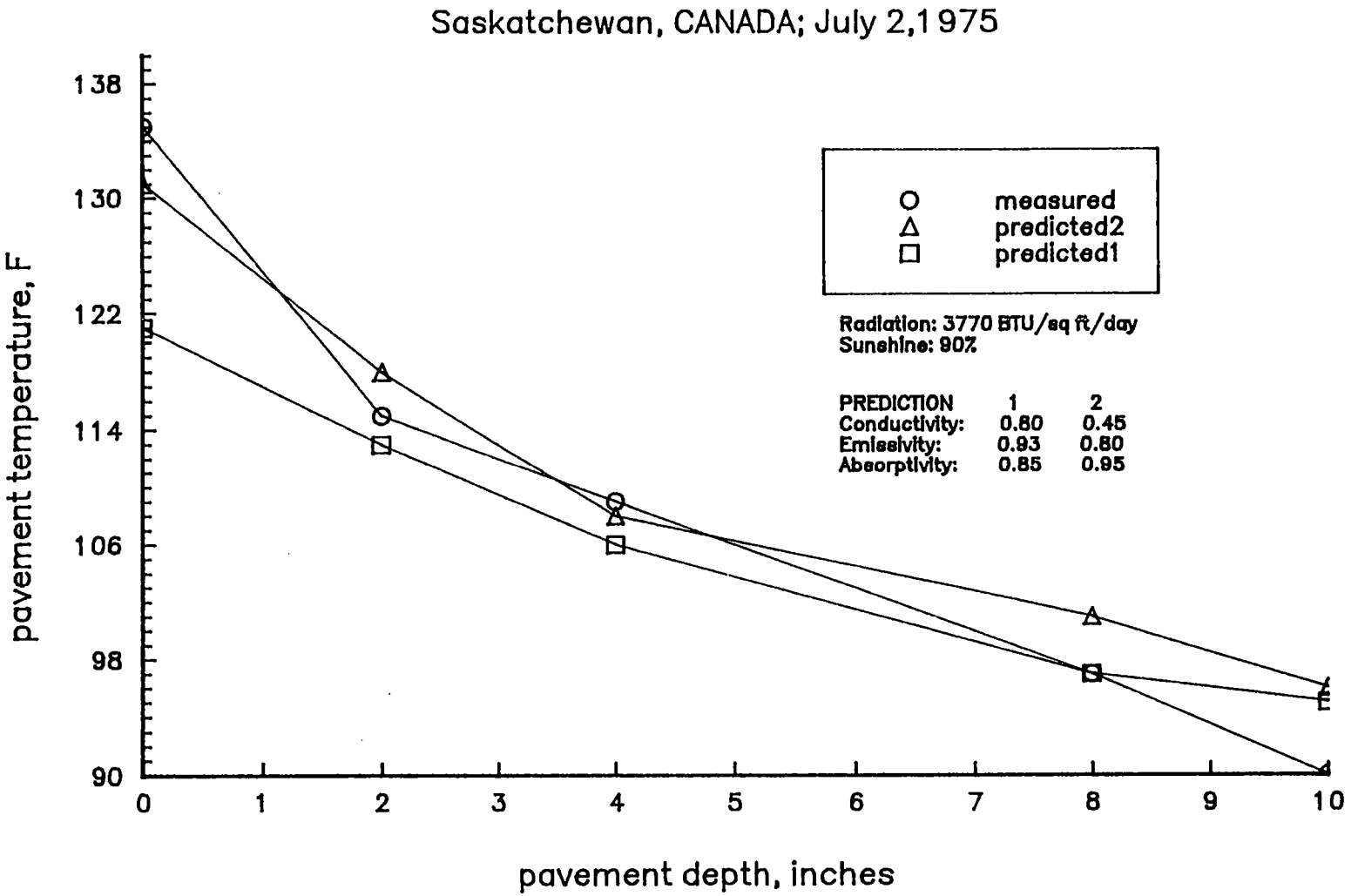

Figure II-12. Measured and Predicted Pavement Temperature Profiles at Saskatchewan, Canada.

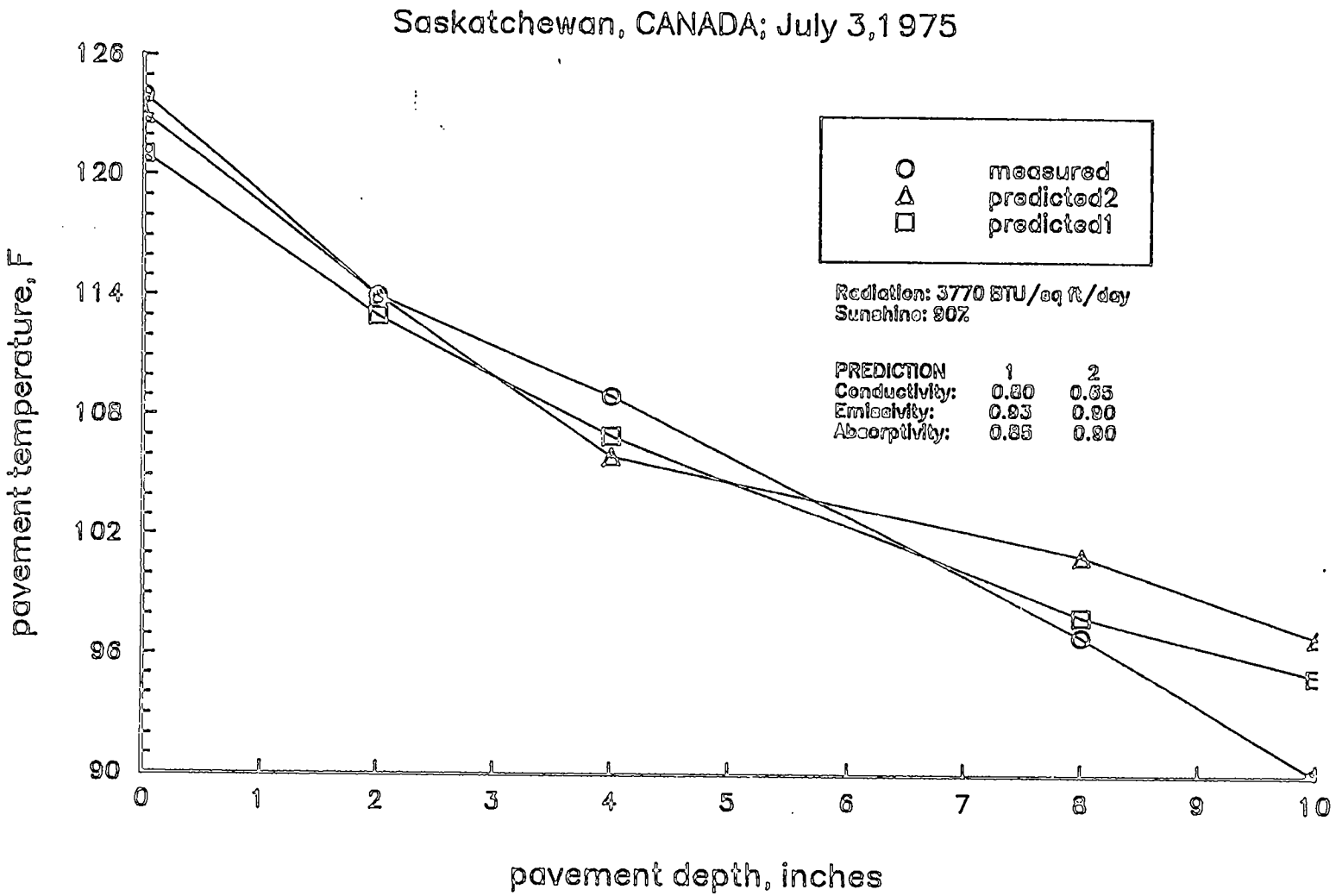

Figure II-13. Measured and Predicted Pavement Temperature Profiles at Saskatchewan, Canada.

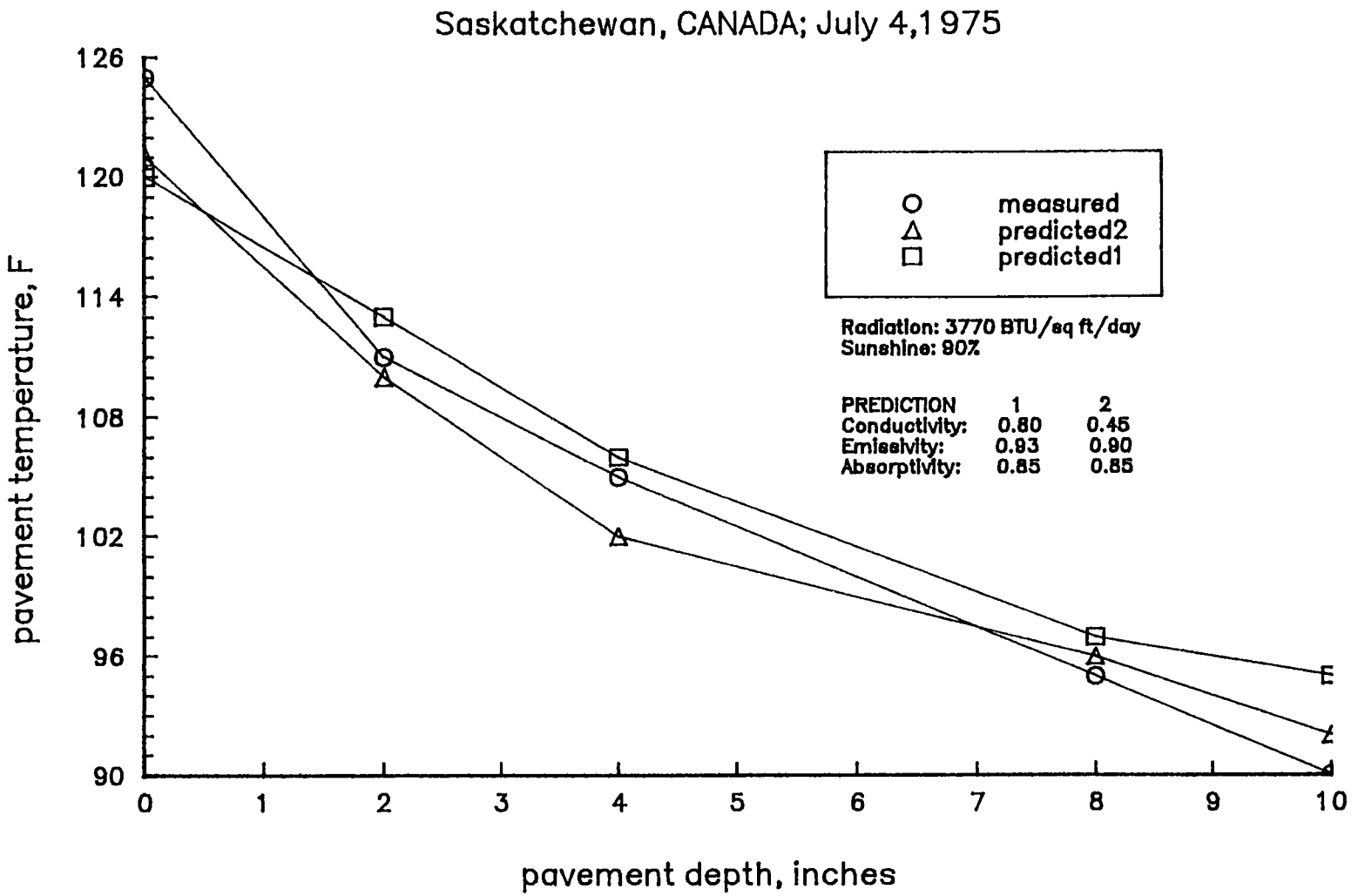

Figure II-14. Measured and Predicted Pavement Temperature Profiles at Saskatchewan, Canada.

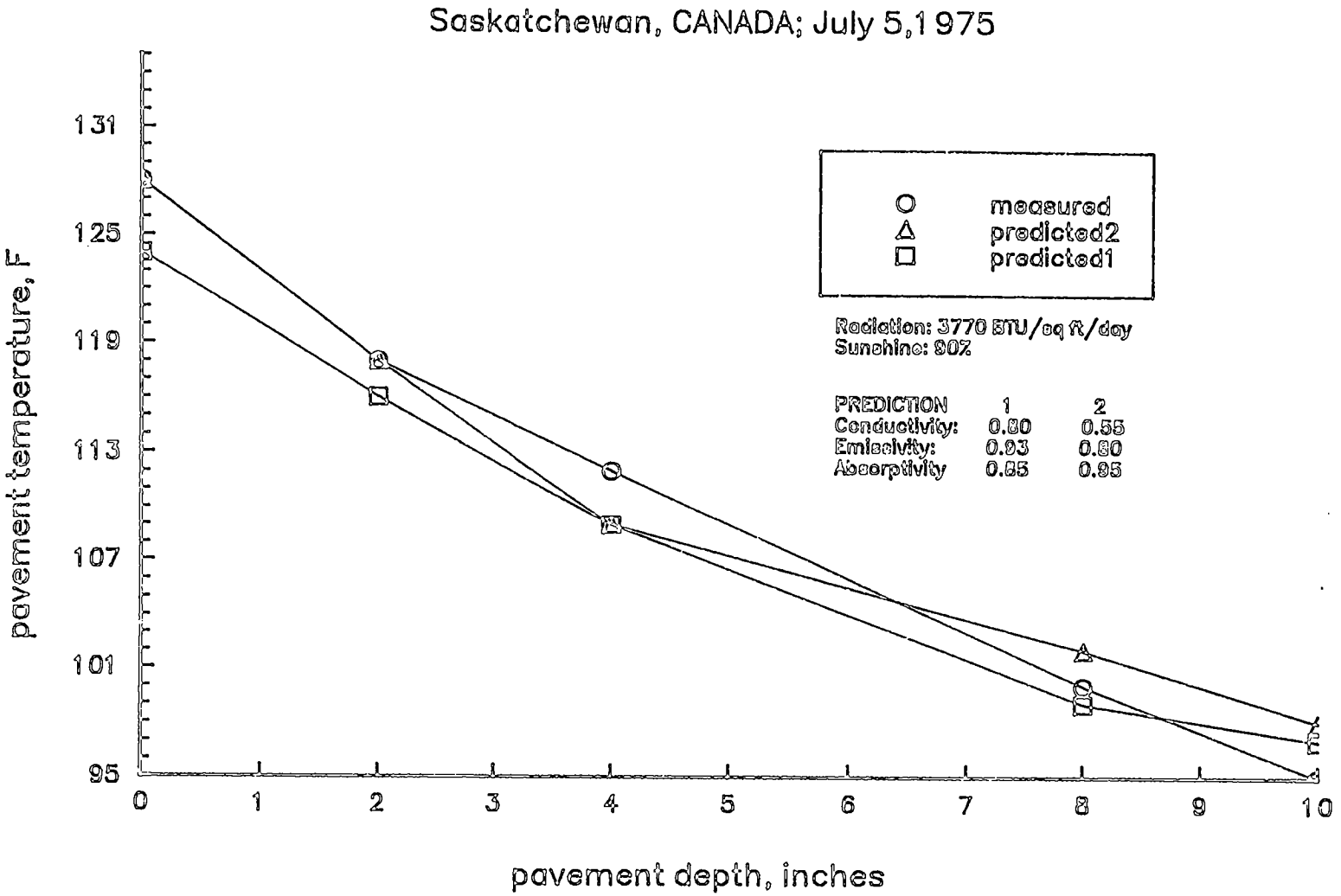

Figure II-15. Measured and Predicted Pavement Temperature Profiles at Saskatchewan, Canada.

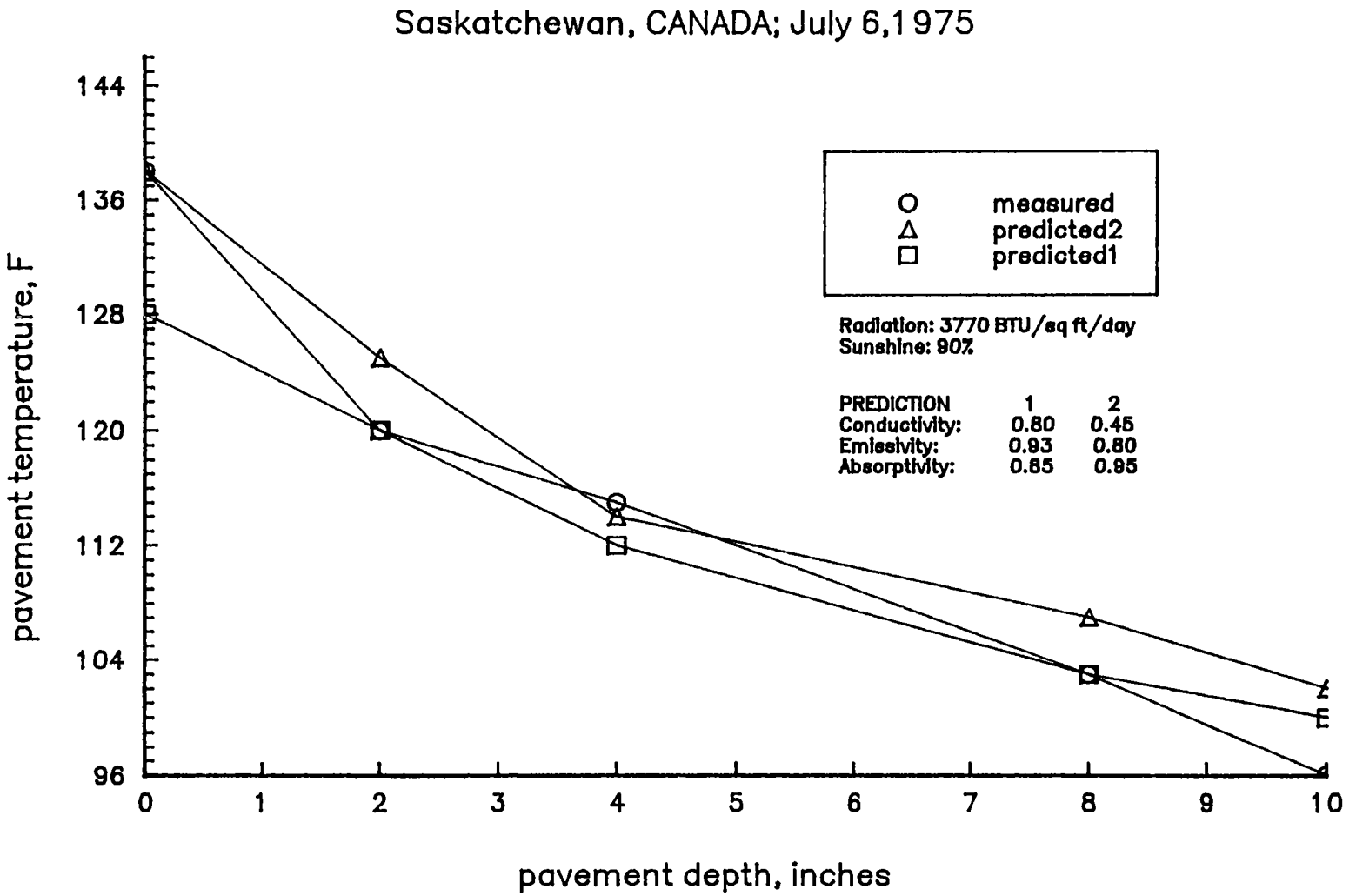

Figure II-16. Measured and Predicted Pavement Temperature Profile at Saskatchewan, Canada.

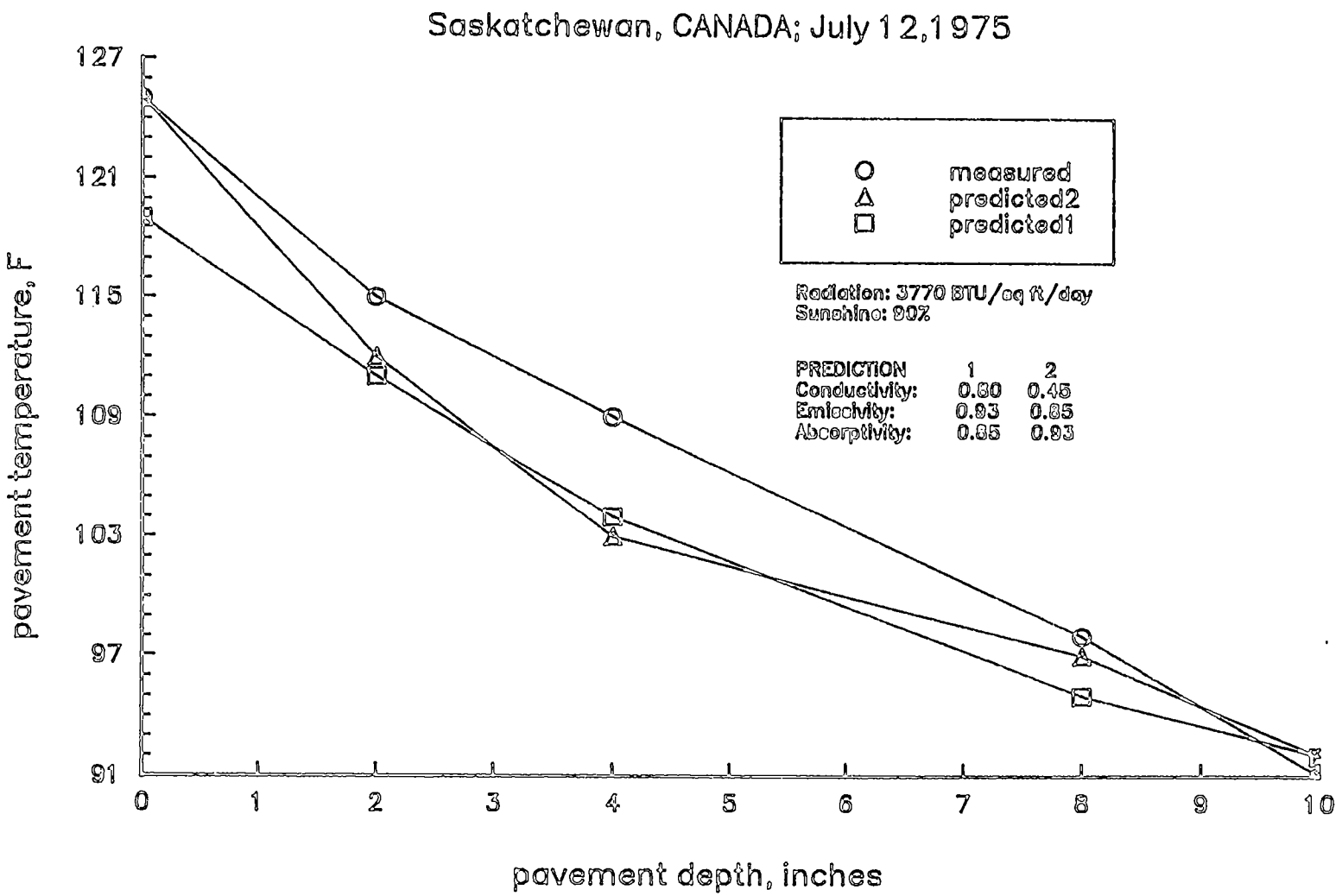

Figure II-17. Measured and Predicted Pavement Temperature Profiles at Sakatchewan, Canada.

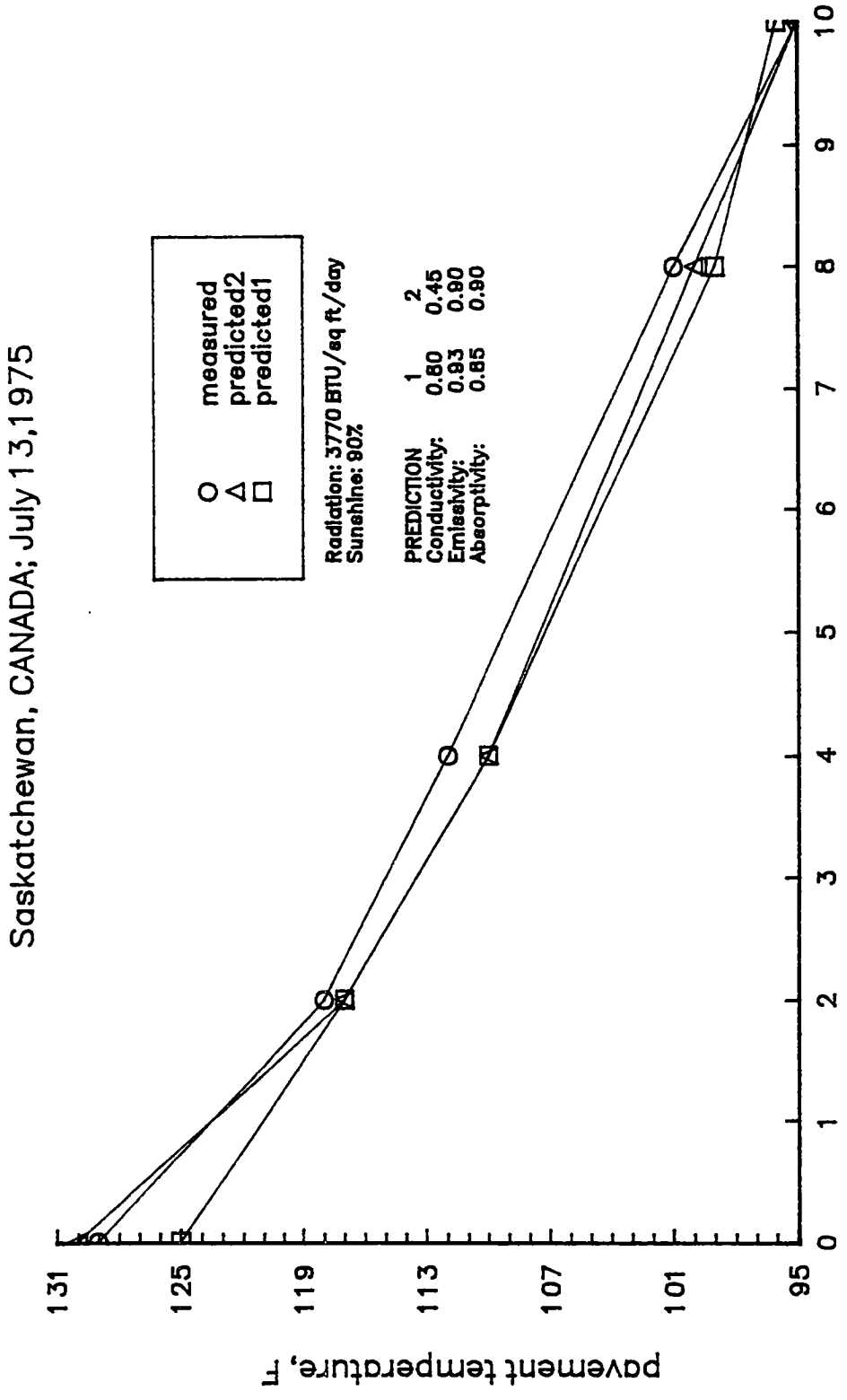

Figure II-18. Measured and Predicted Pavement Temperature Profiles at Saskatchewan, Canada.

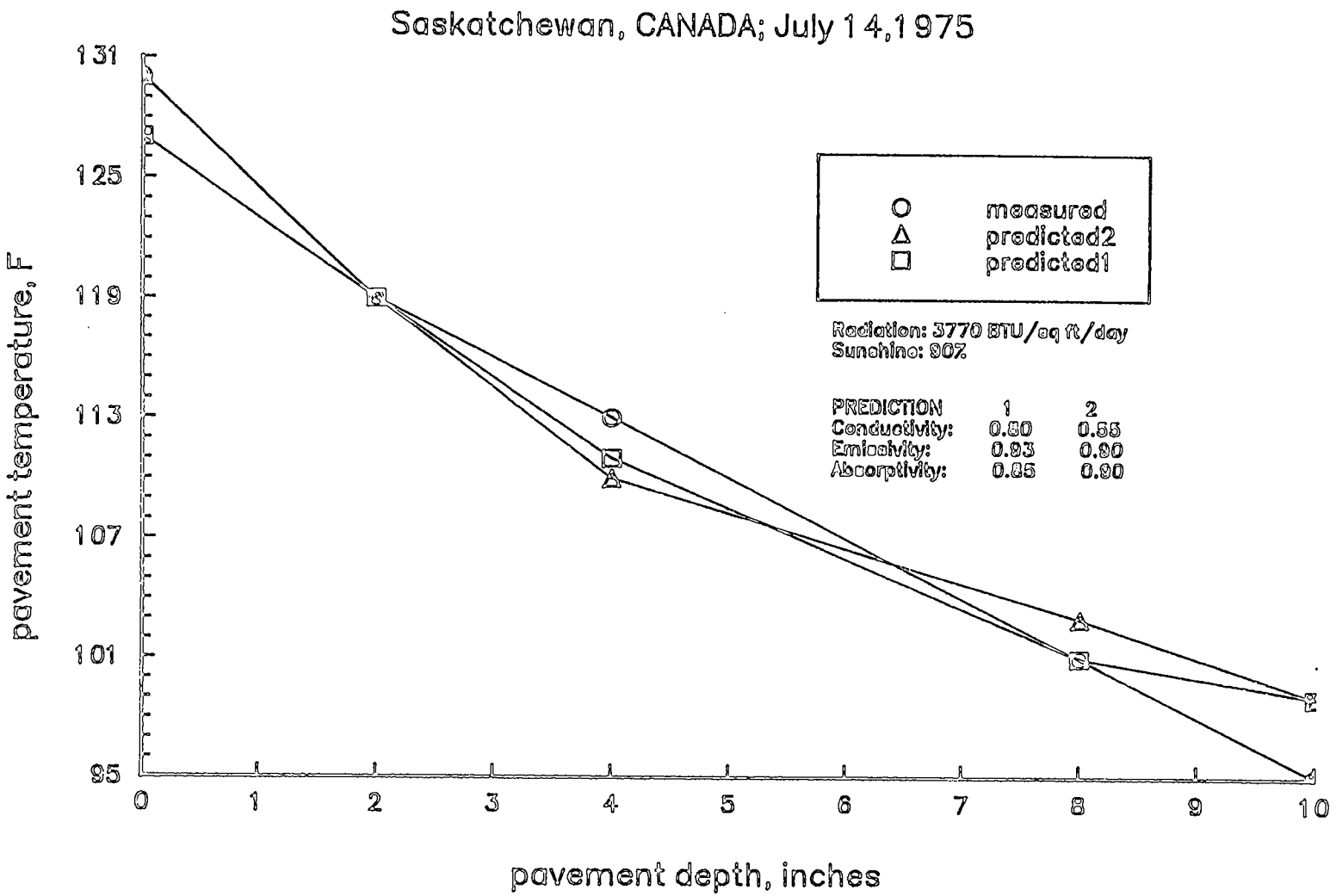

Figure II-19. Measured and Predicted pavement Temperature Profiles at Saskatchewan, Canada.

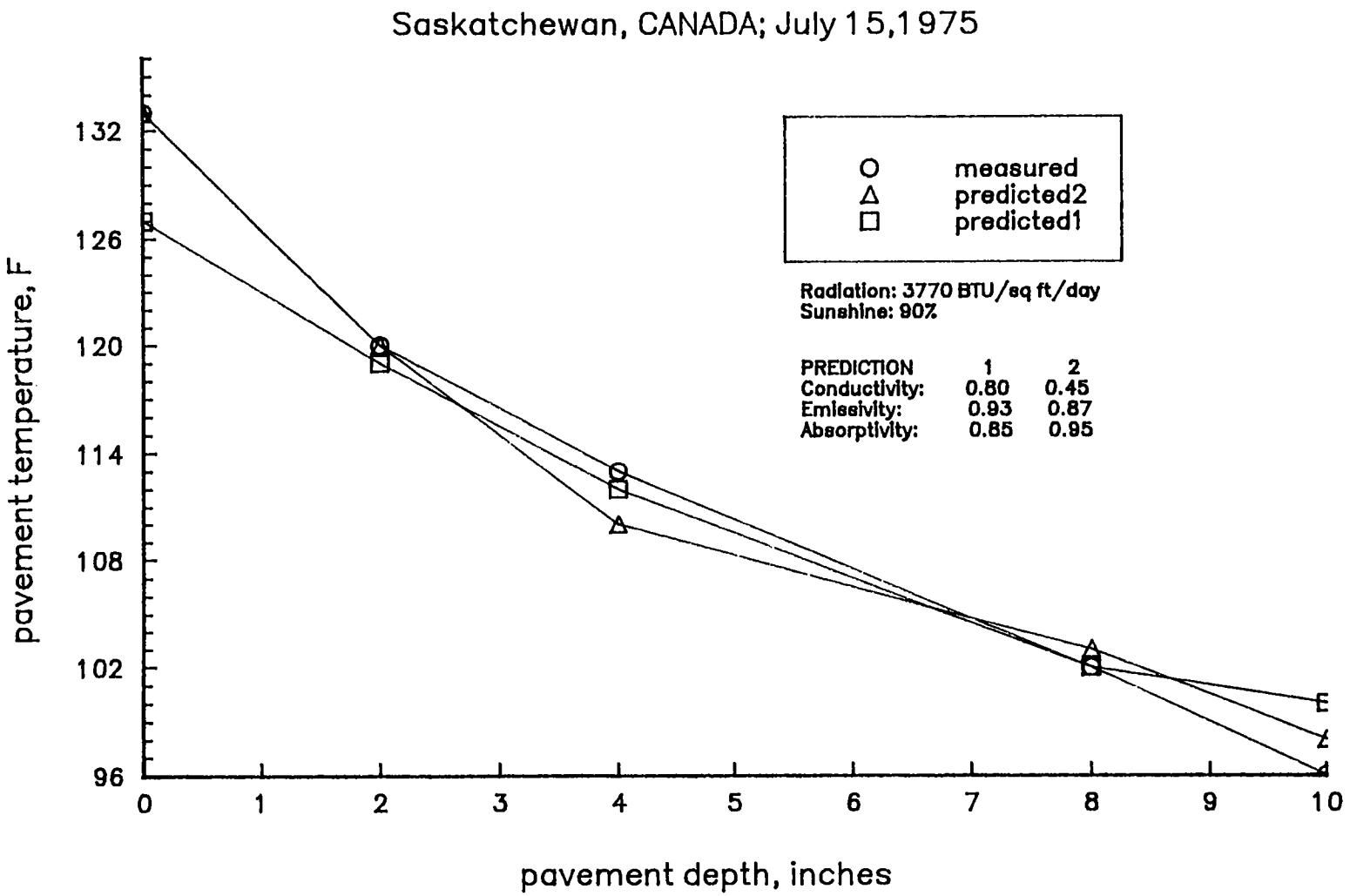

Figure II-20. Measured and Predicted Pavement Temperature Profiles at Saskatchewan, Canada.

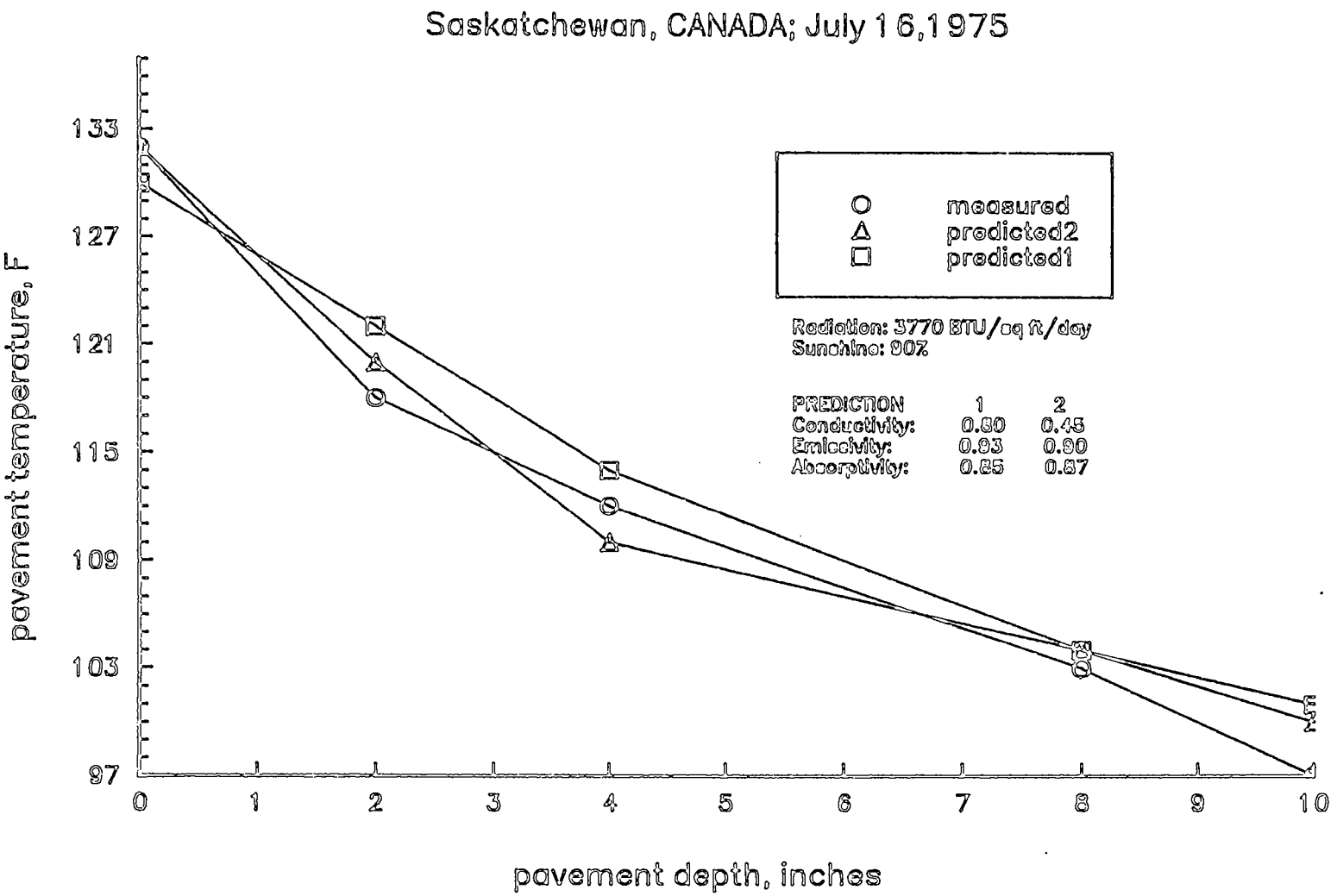

Figure II-21. Measured and Predicted Pavement Temperature Profiles at Saskatchewan, Canada.

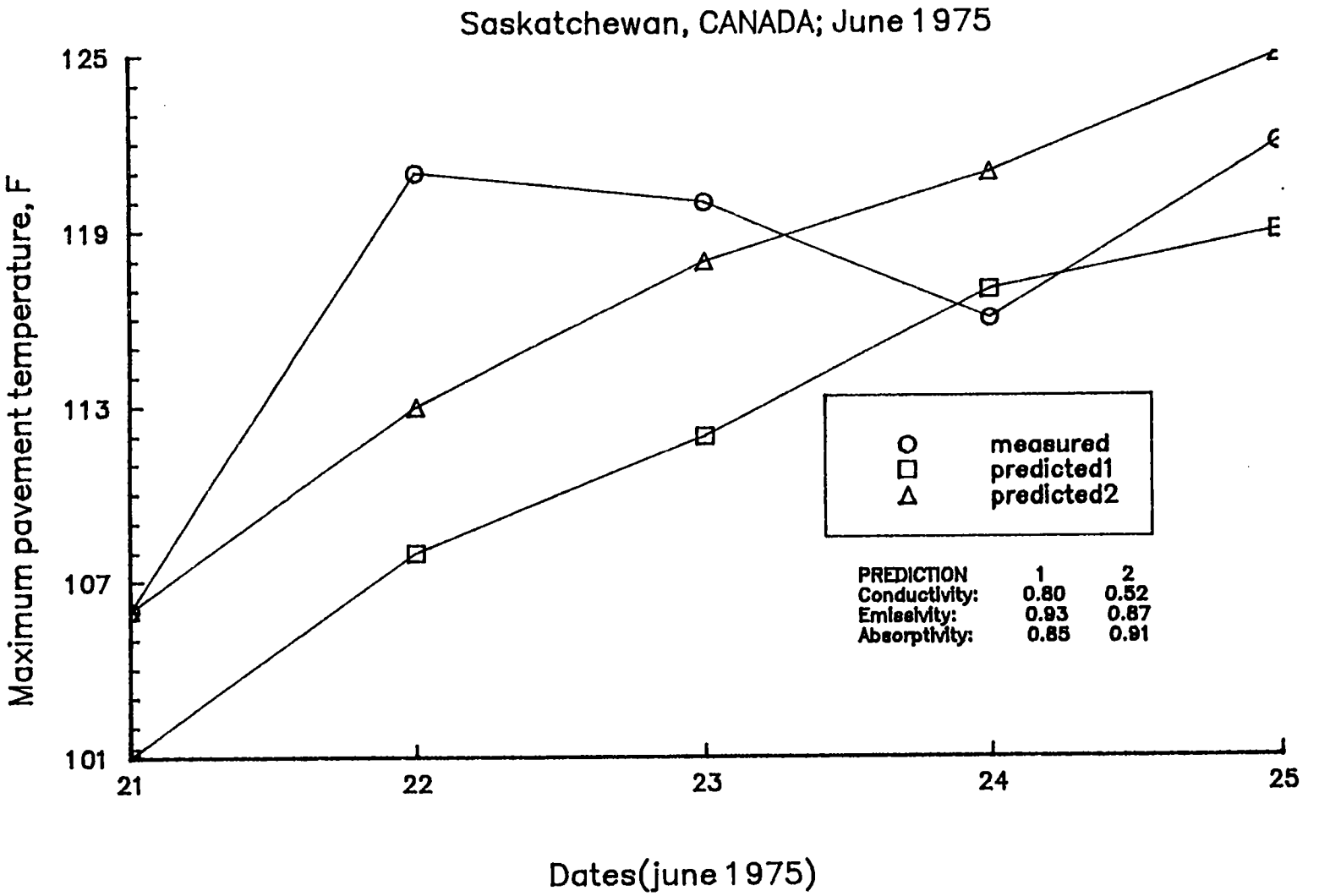

Figure II-22. Measured and Predicted Pavement Surface Temperature at Saskatchewan, Canada.

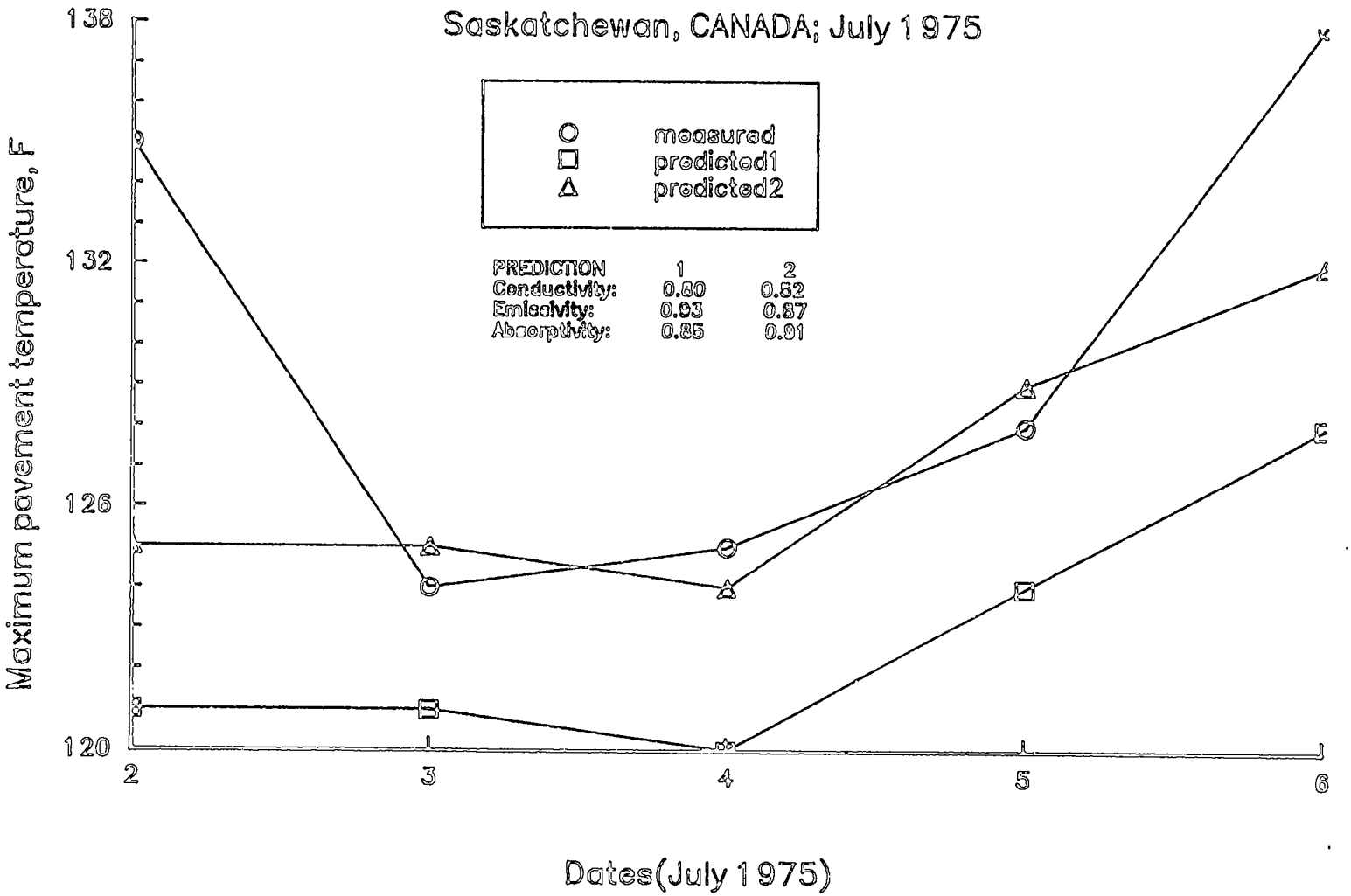

Figure II-23. Measured and Predicted Pavement Temperature Profiles at Saskatchewan, Canada.

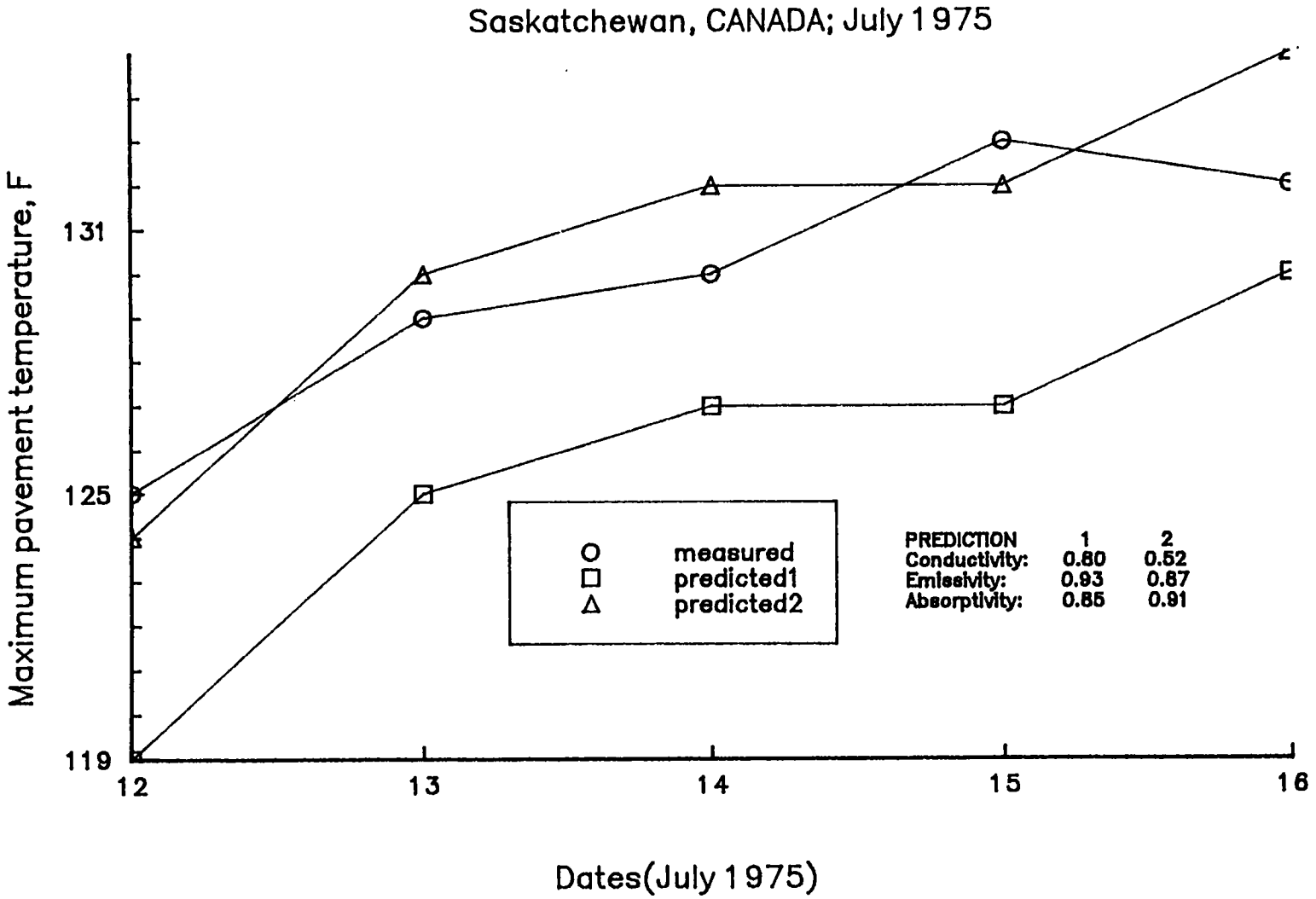

Figure II-24. Measured and Predicted Pavement Temperature Profile at Saskatchewan, Canada.

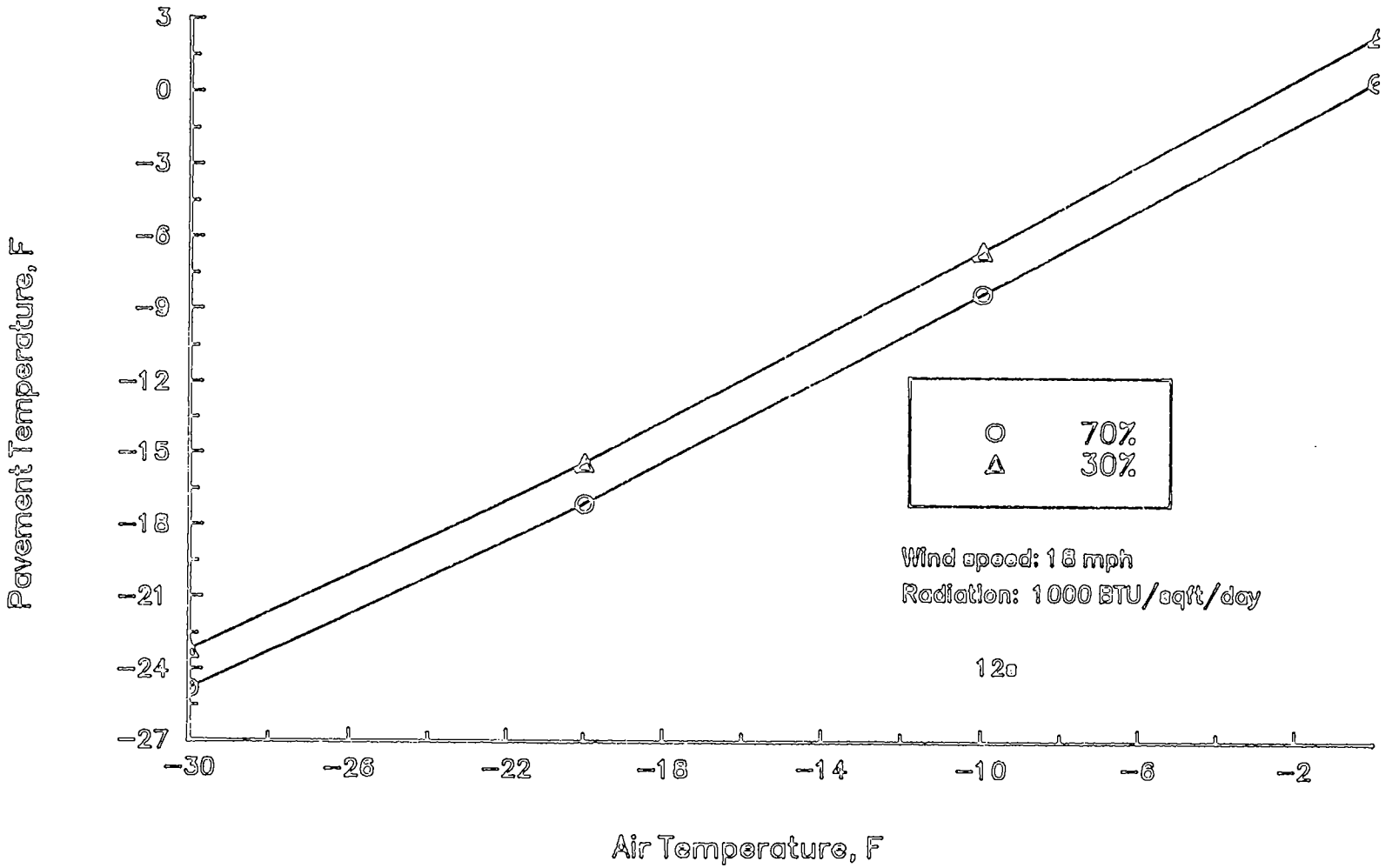

Fig. III-1. Predicted Pavement Surface Lowest Temperature as a Function of Lowest Air Temperature for Different Percent Sunshine.

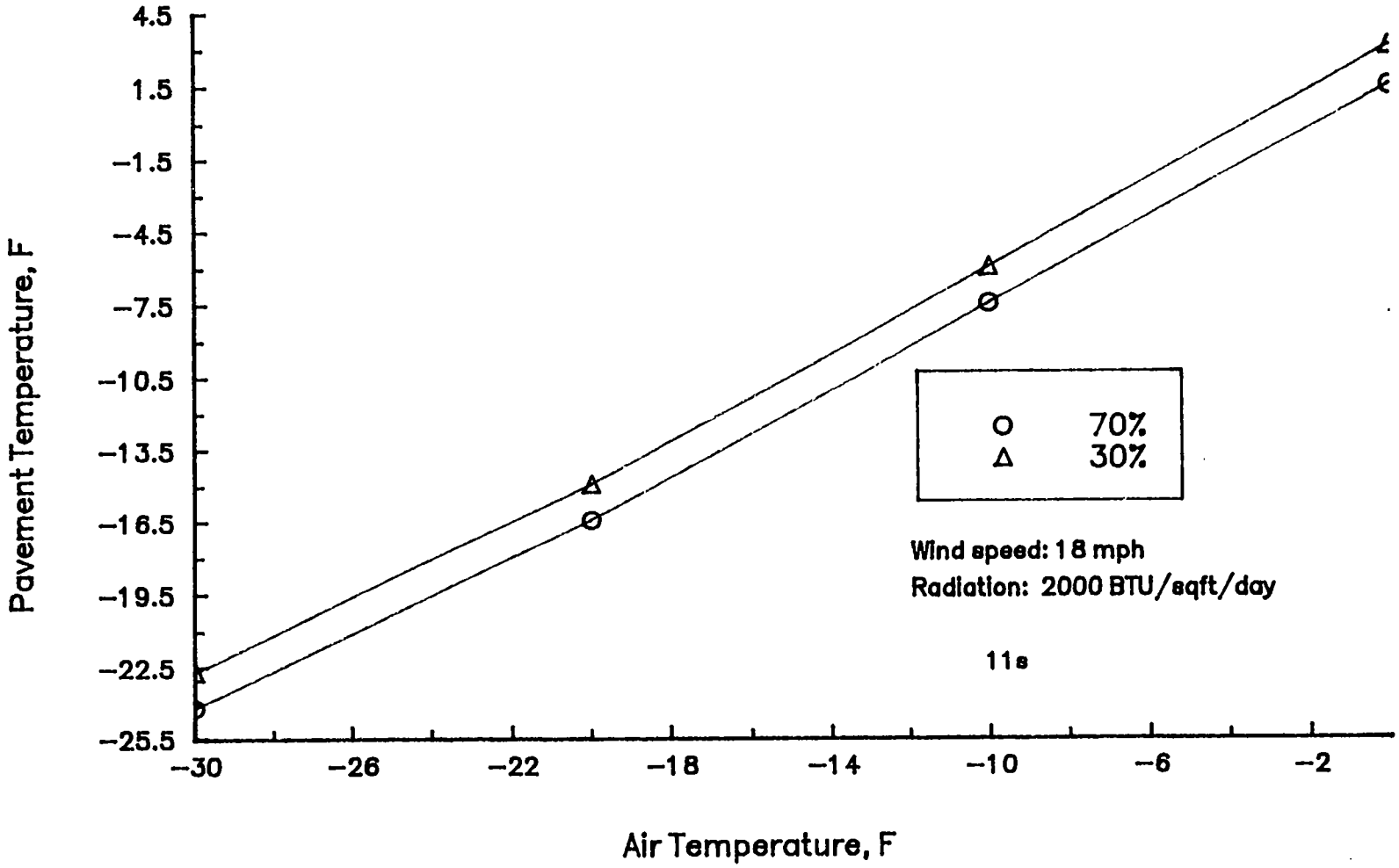

Fig. III-2. Predicted Pavement Surface Lowest Temperature as a Function of Lowest Air Temperature for Different Percent Sunshine.

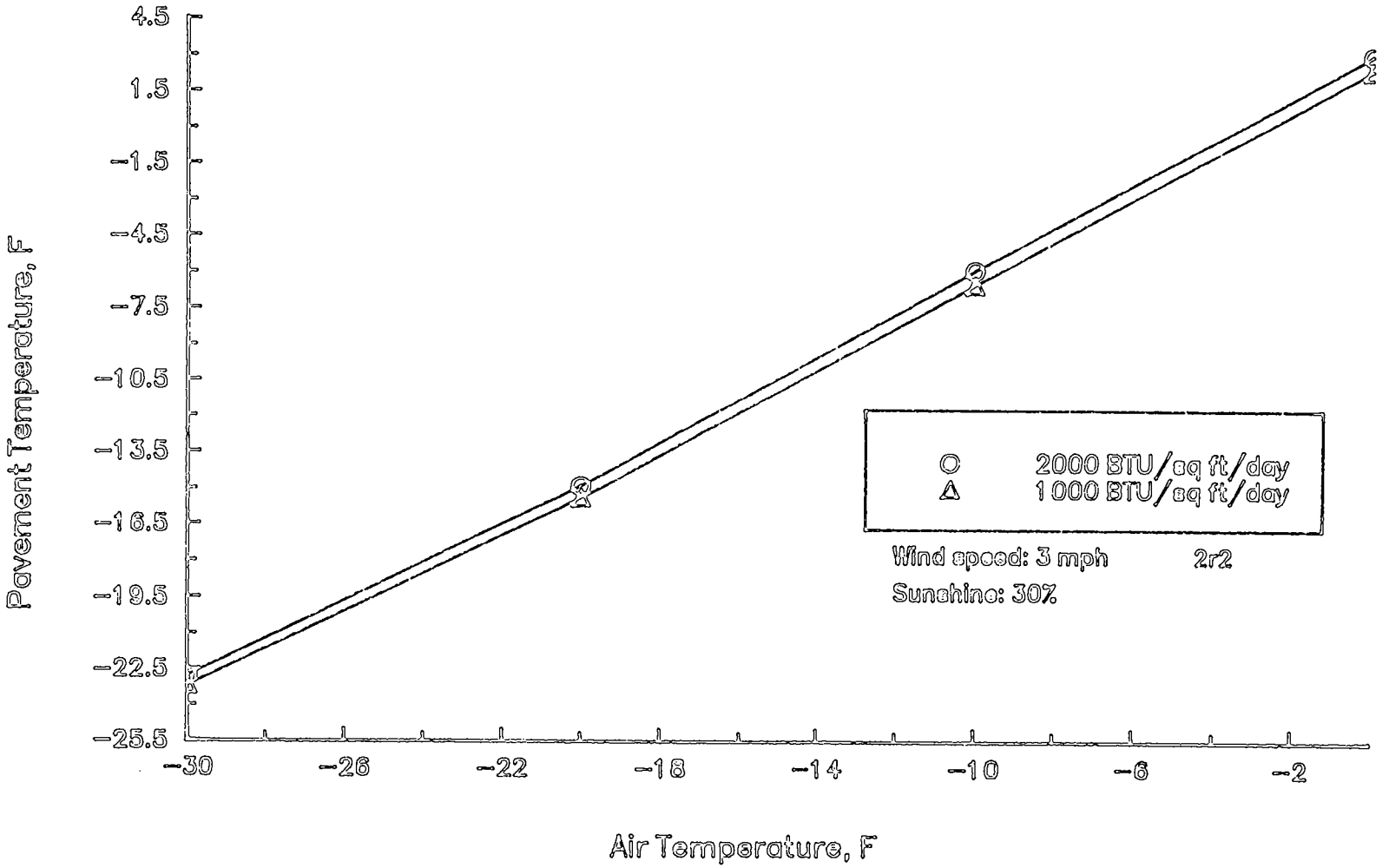

Fig. III-3. Predicted Pavement Surface Lowest Temperature as a Function of Lowest Air Temperature for Different Values of Radiation.

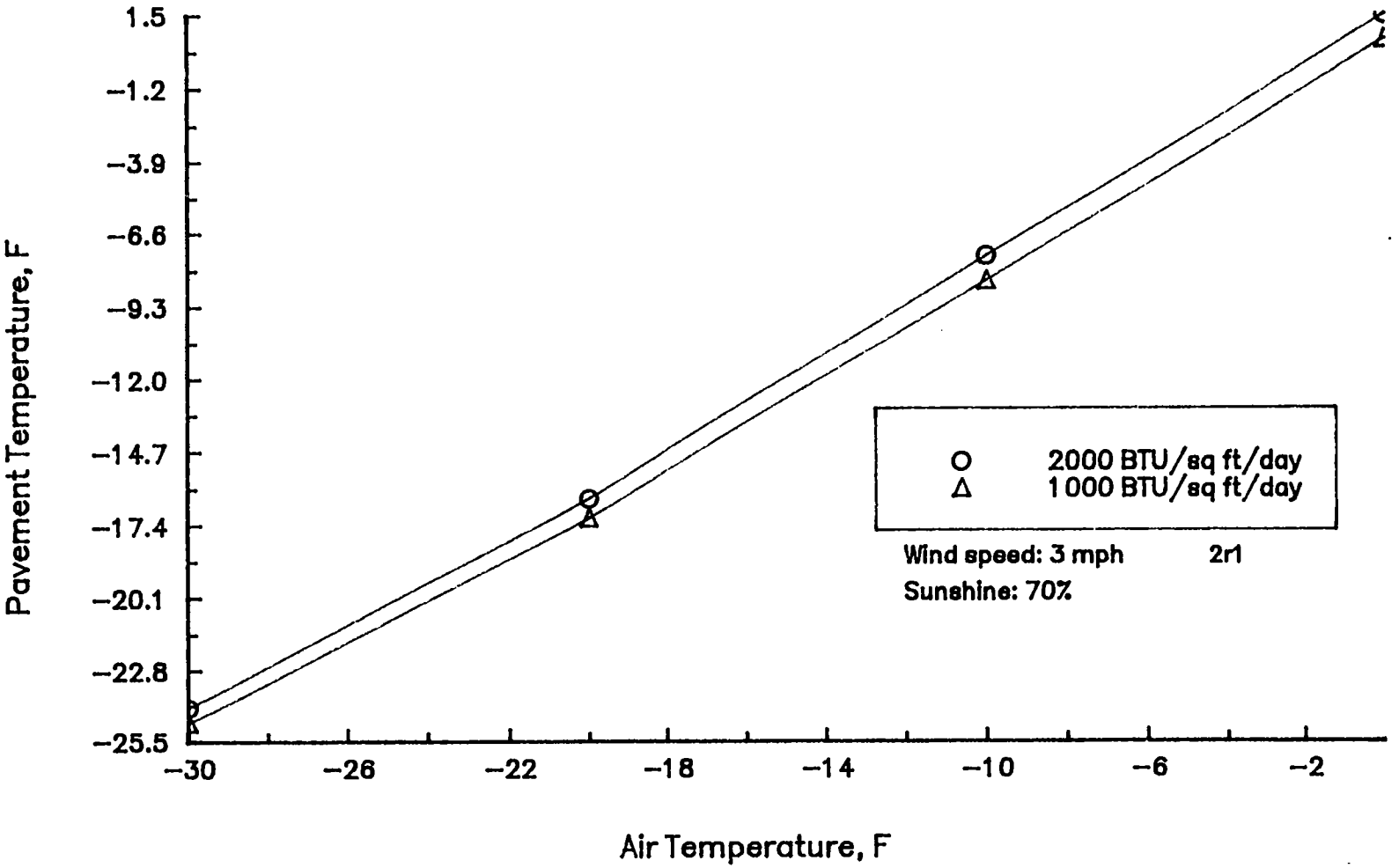

Fig. III-4. Predicted Pavement Surface Lowest Temperature as a Function of Lowest Air Temperature in Different Values of Radiation.

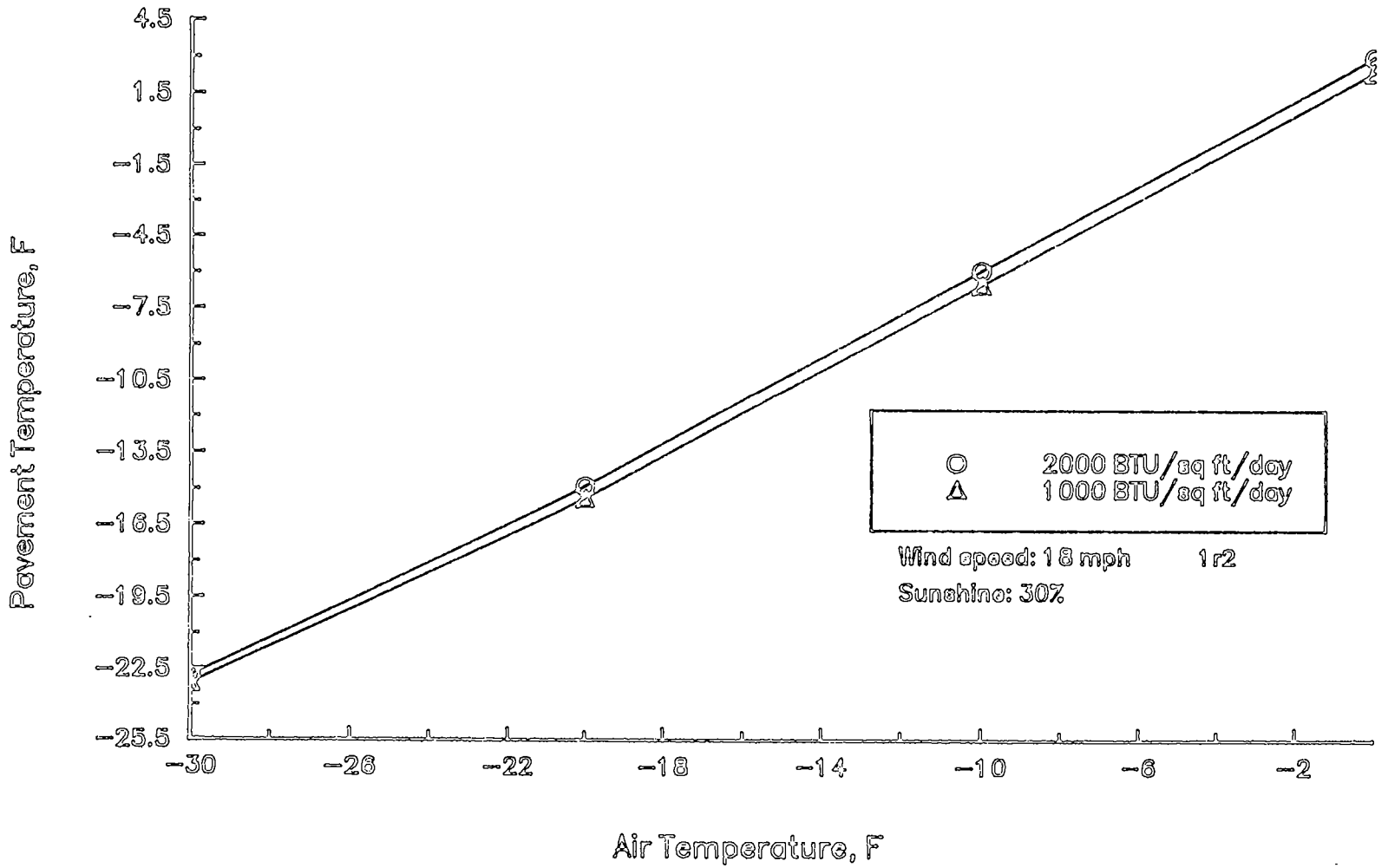

Fig. III-5. Predicted Pavement Surface Lowest Temperature as a Function of Lowest Air Temperature in Different Values of Radiation.

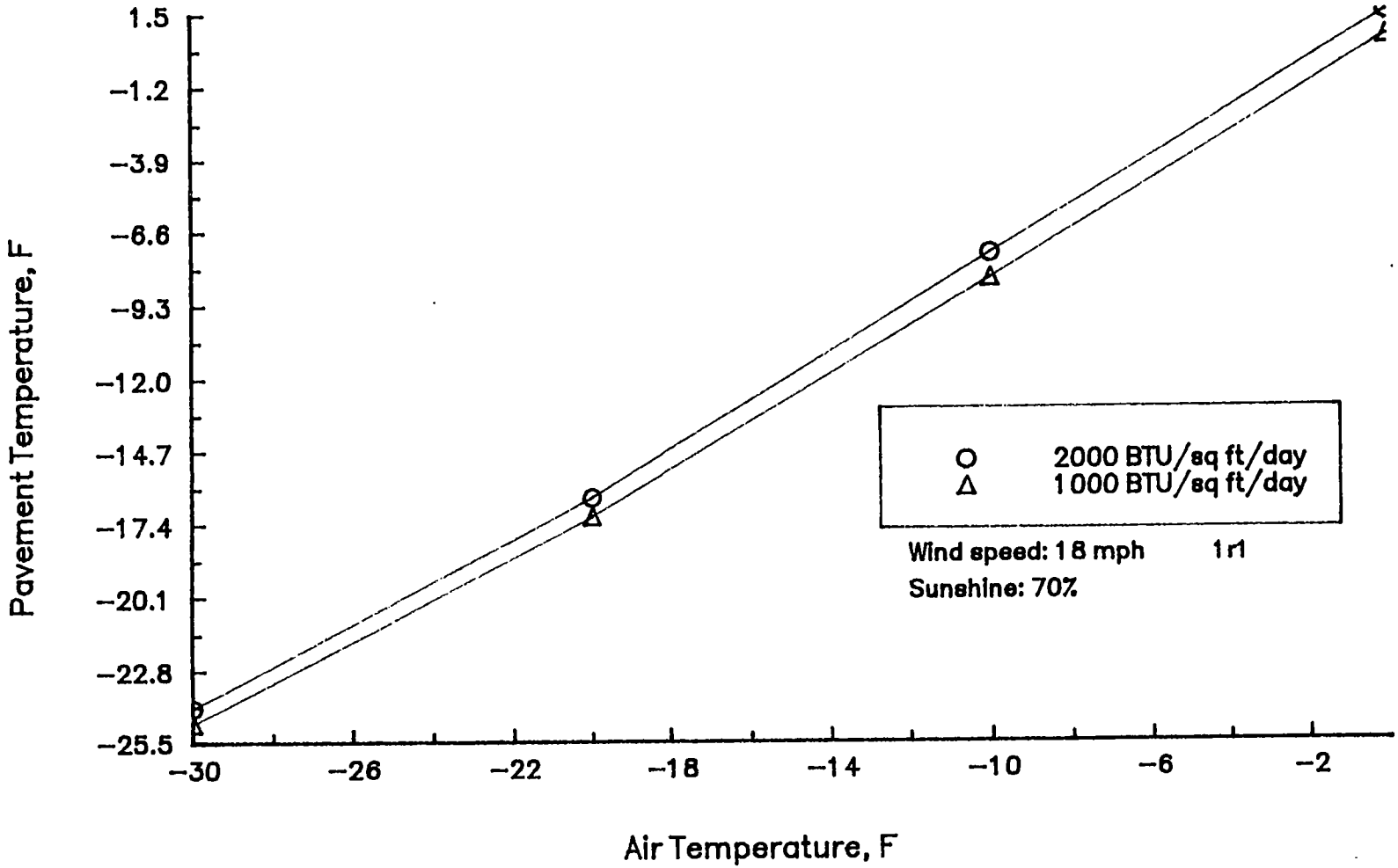

Fig. III-6. Predicted Pavement Surface Lowest Temperature as a Function of Lowest Air Temperature for Different Values of Radiation.

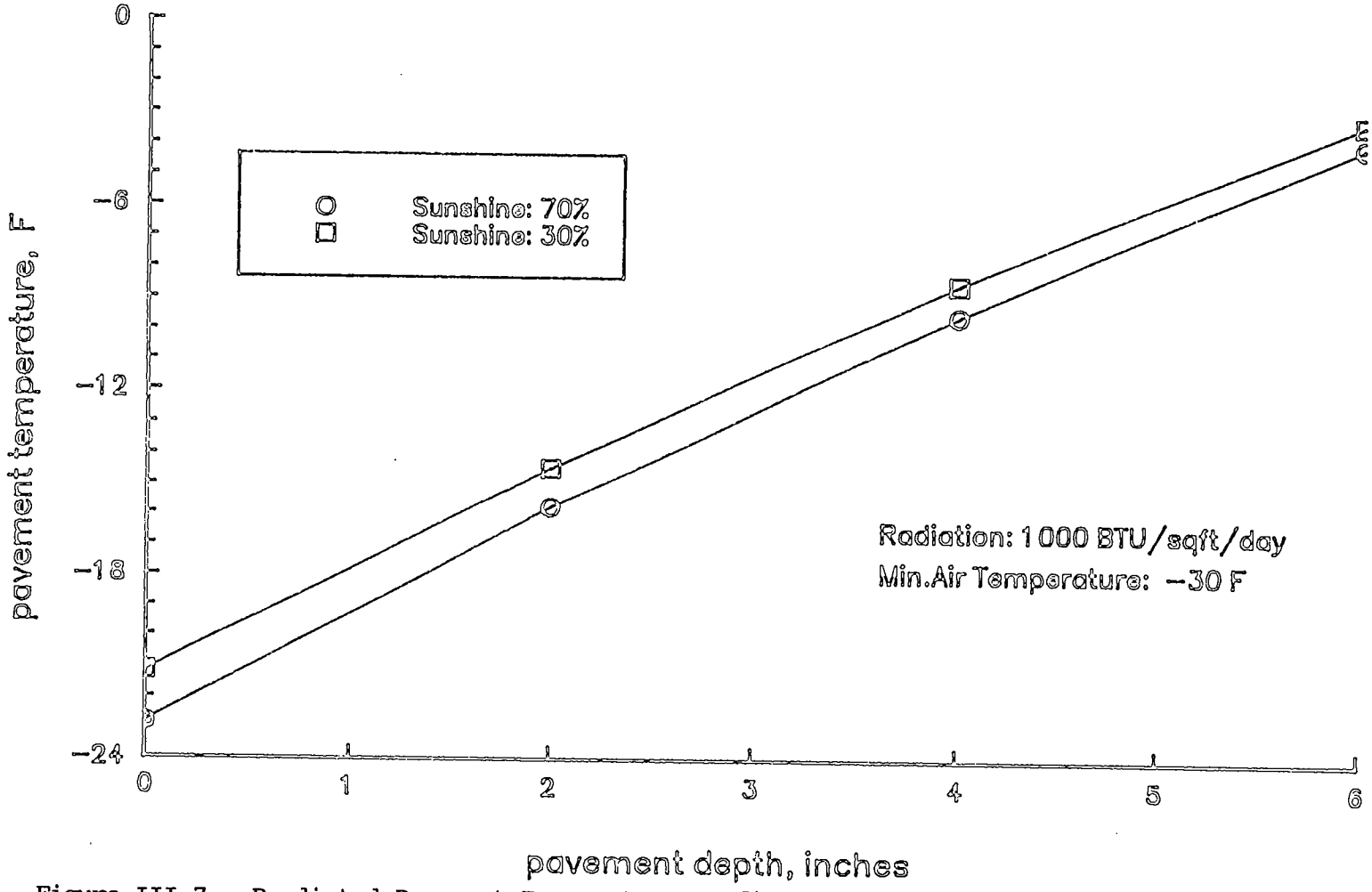

Figure III-7. Predicted Pavement Temperature Profile for Different Values of Percent Sunshine.

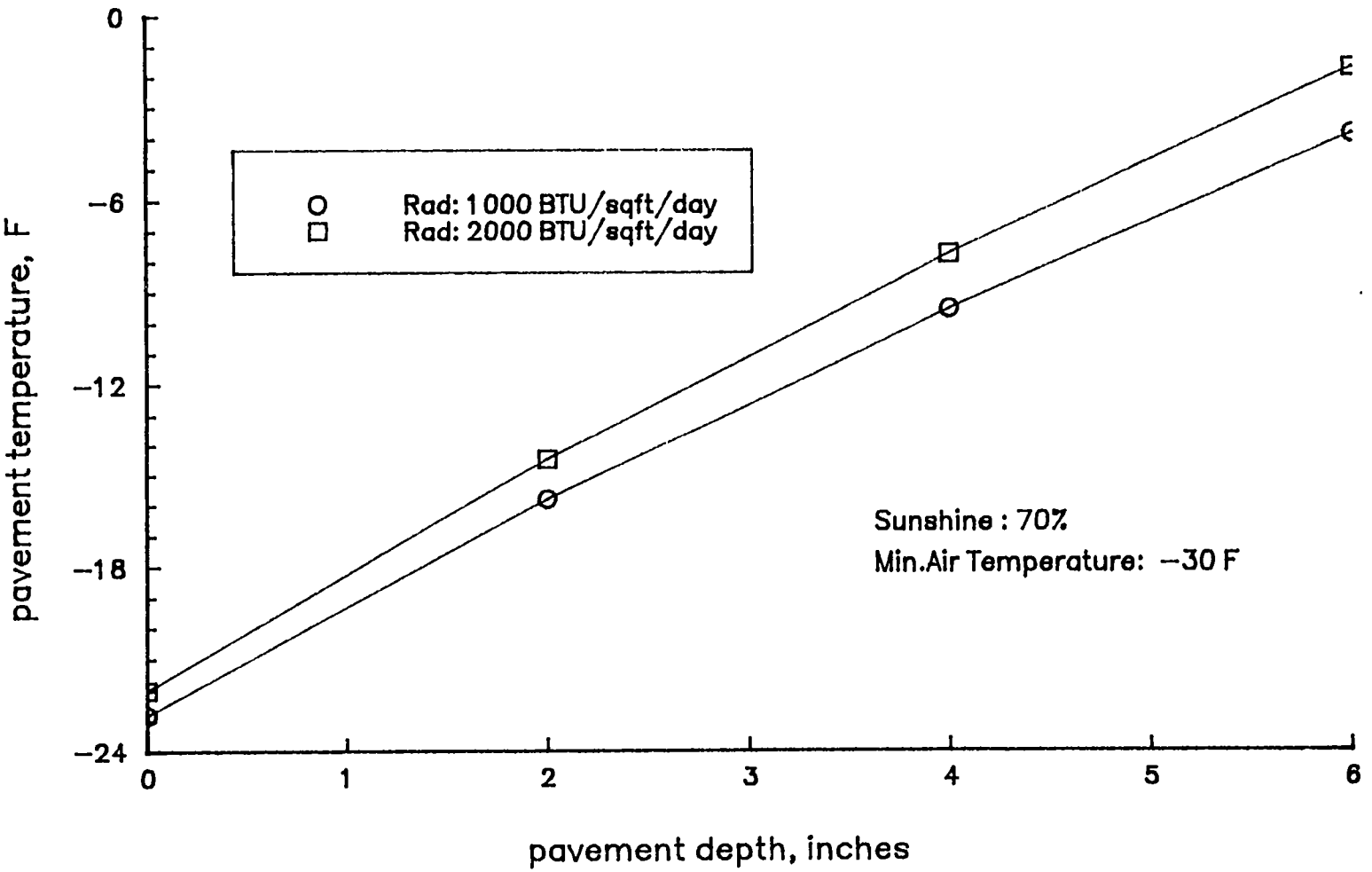

Figure III-8. Predicted Pavement Temperature Profile for Different Values of Radiation.

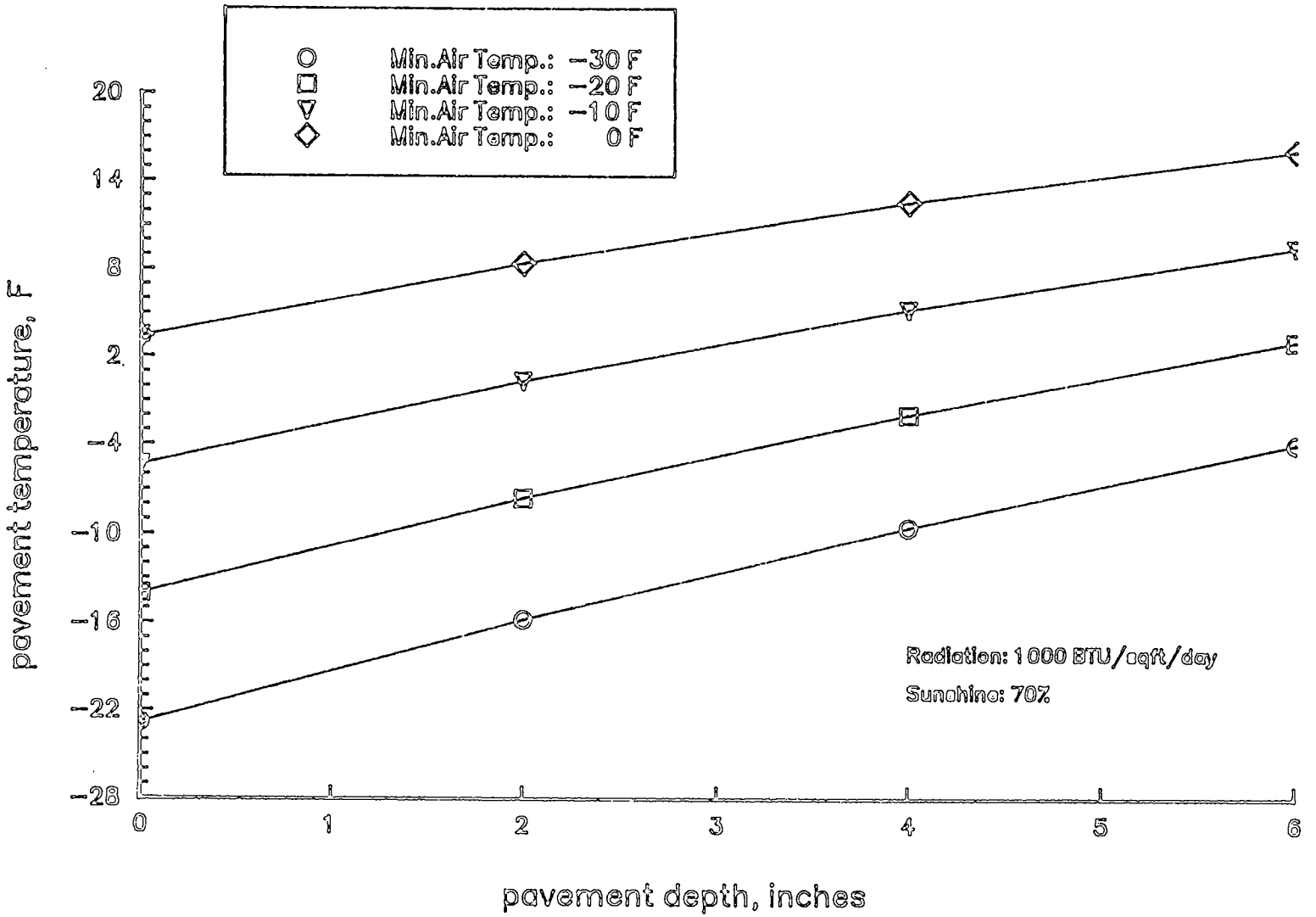

Figure III-9. Predicted Pavement Temperature Profile for Different Values of Minimum Air Temperature.

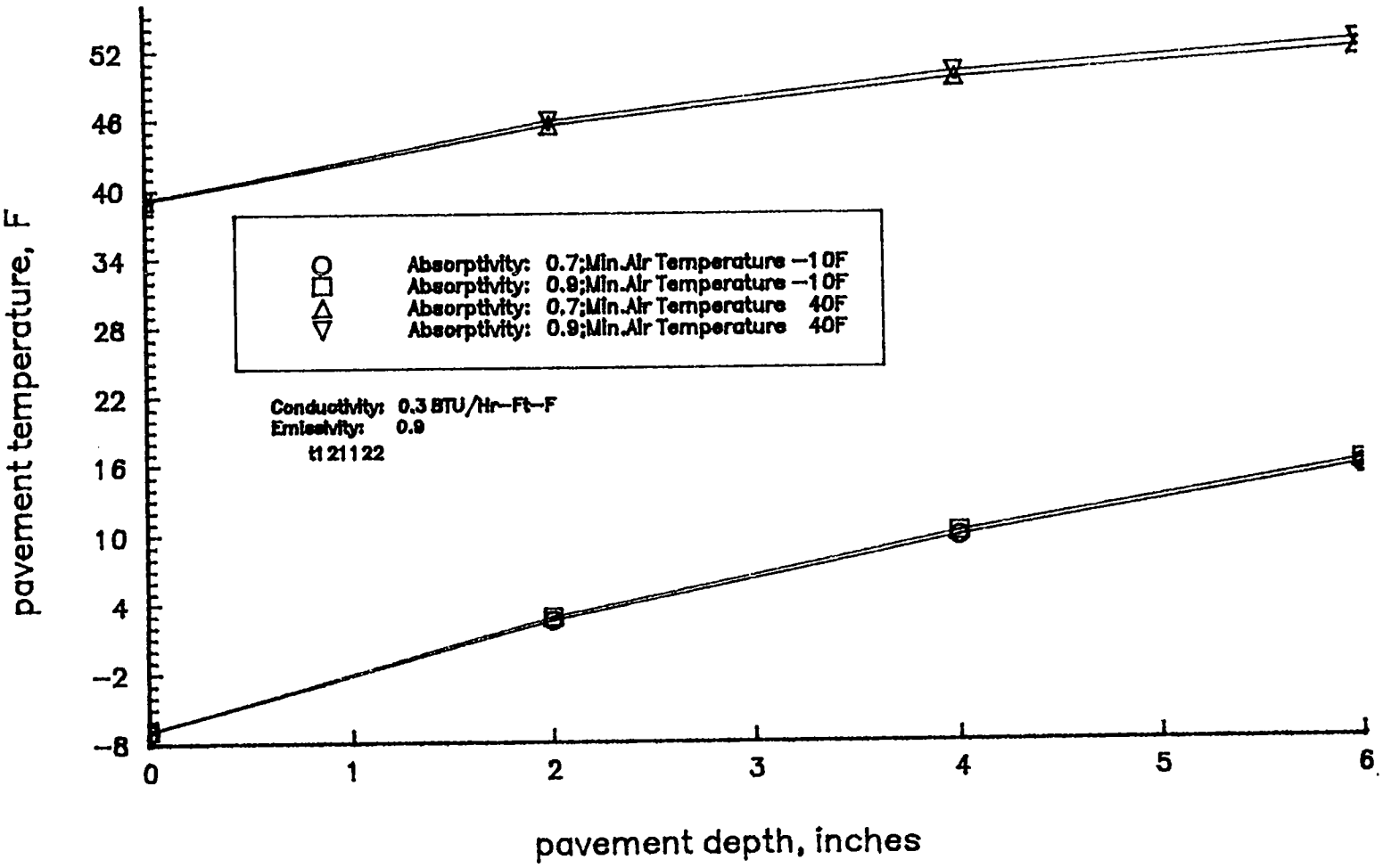

Figure III-10. Predicted Pavement Lowest Temperature Profile for Different Surface Short-wave Absorptivities at Two Different Levels of Minimum Air Temperatures.

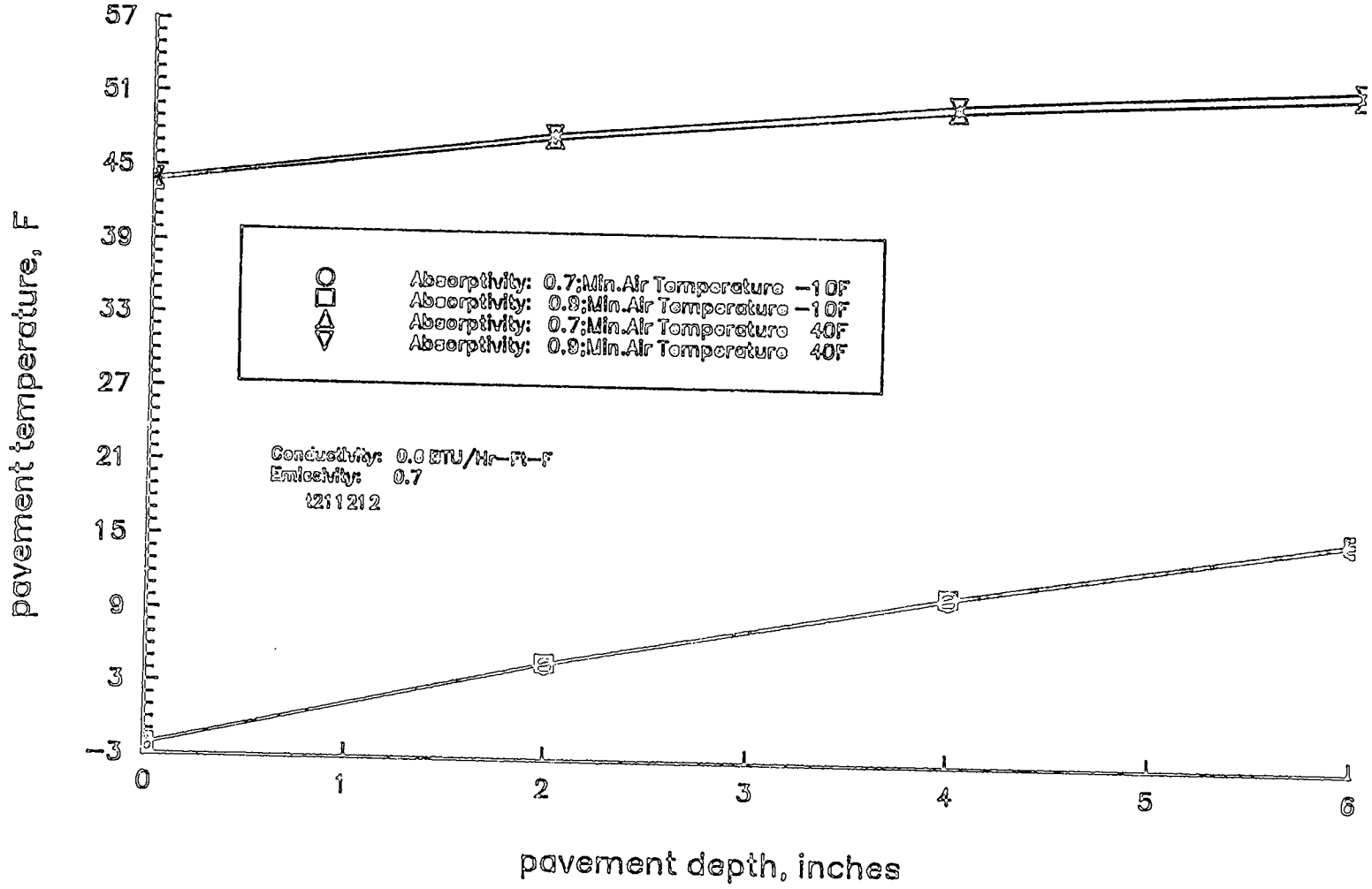

Figure III-11. Predicted Pavement Lowest Temperature Profile for Different Surface Short-wave Absorptivities at Two Different Levels of Minimum Air Temperatures.

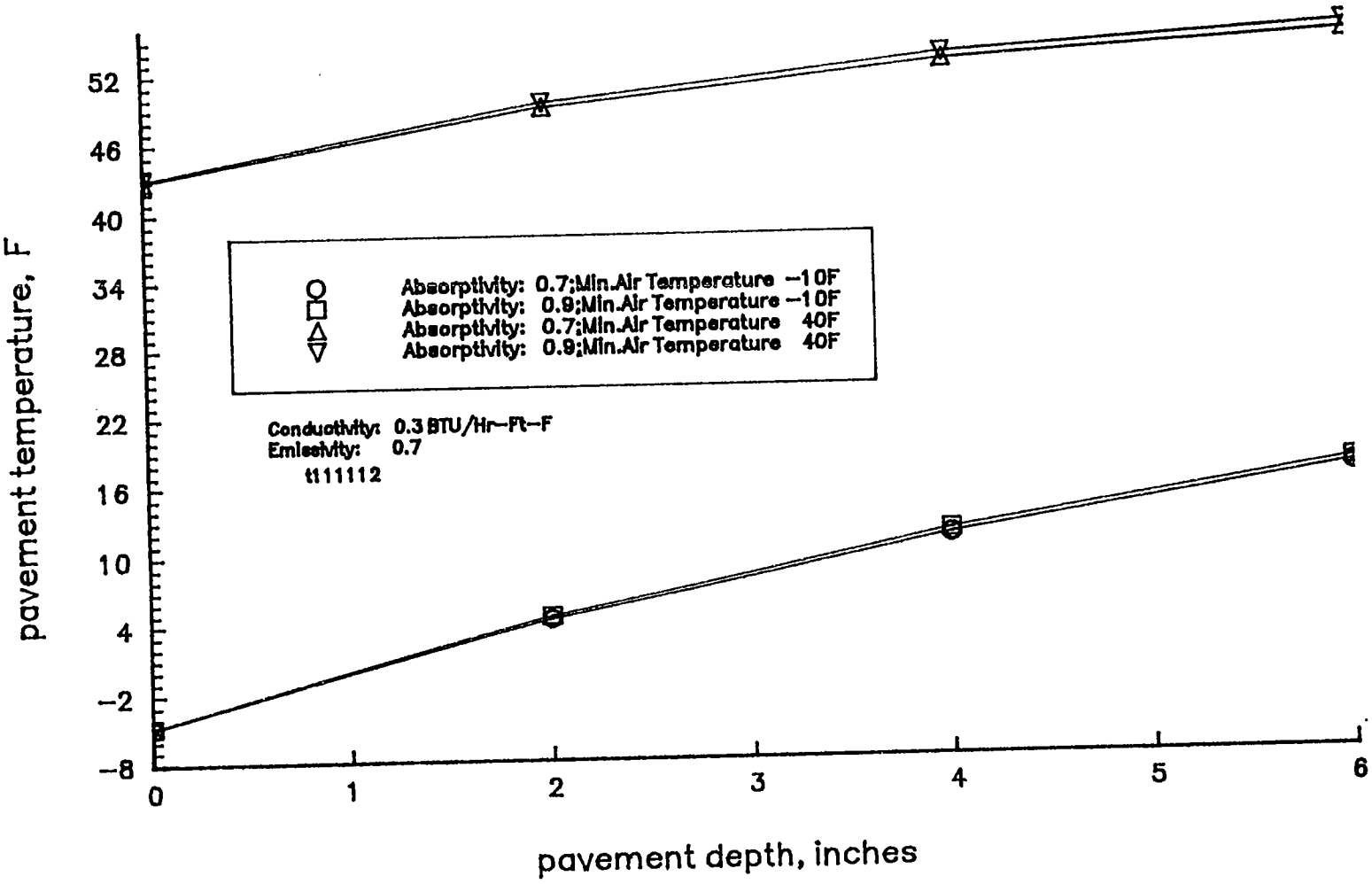

Figure III-12. Predicted Pavement Lowest Temperature Profile for Different Surface Short-wave Absorptivities at Two Different Levels of Minimum Air Temperatures.

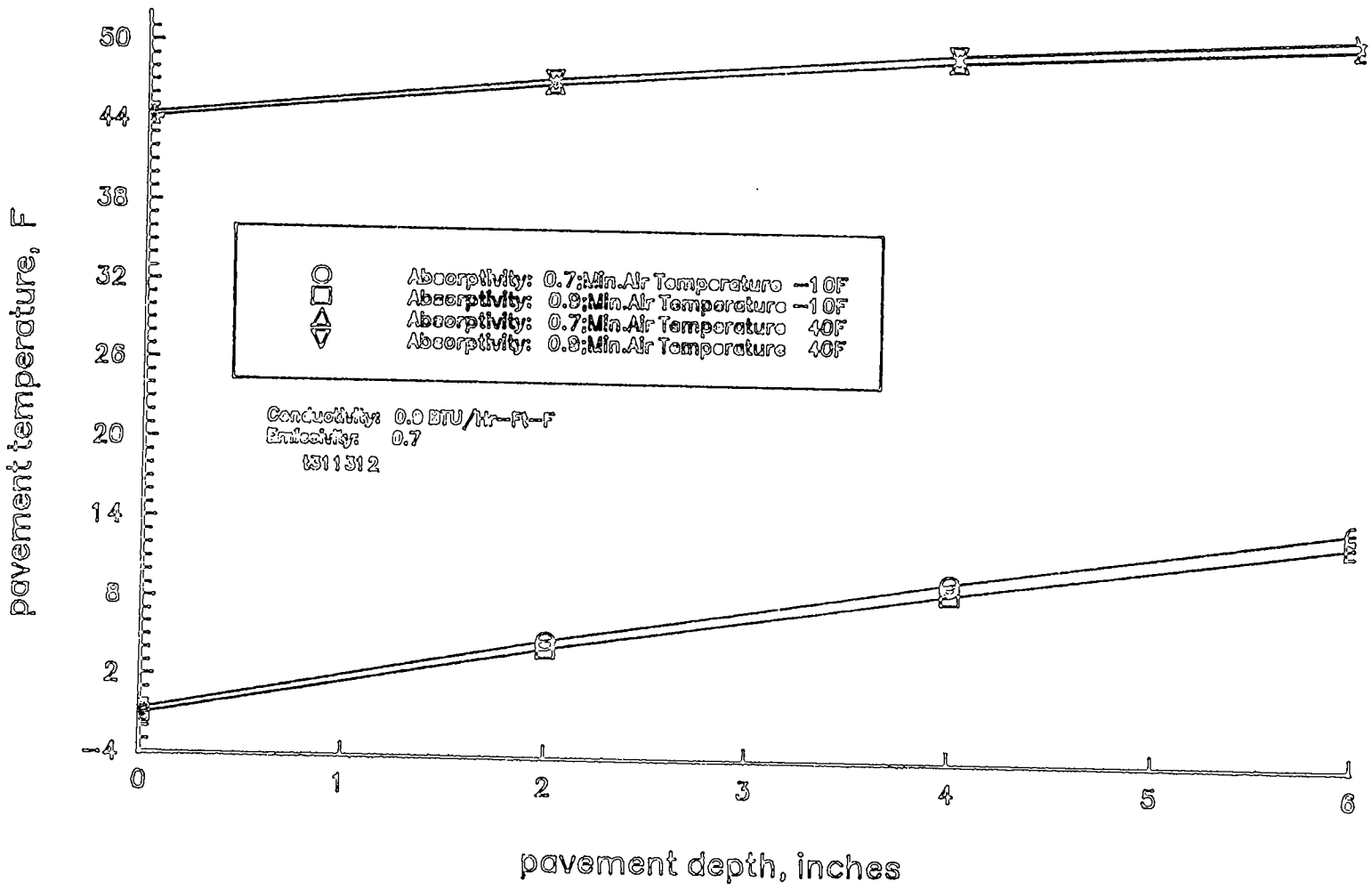

Figure III-13. Predicted Pavement Lowest Temperature Profile for Different Surface Short-wave Absorptivities at Two Different Levels of Minimum Air Temperatures.

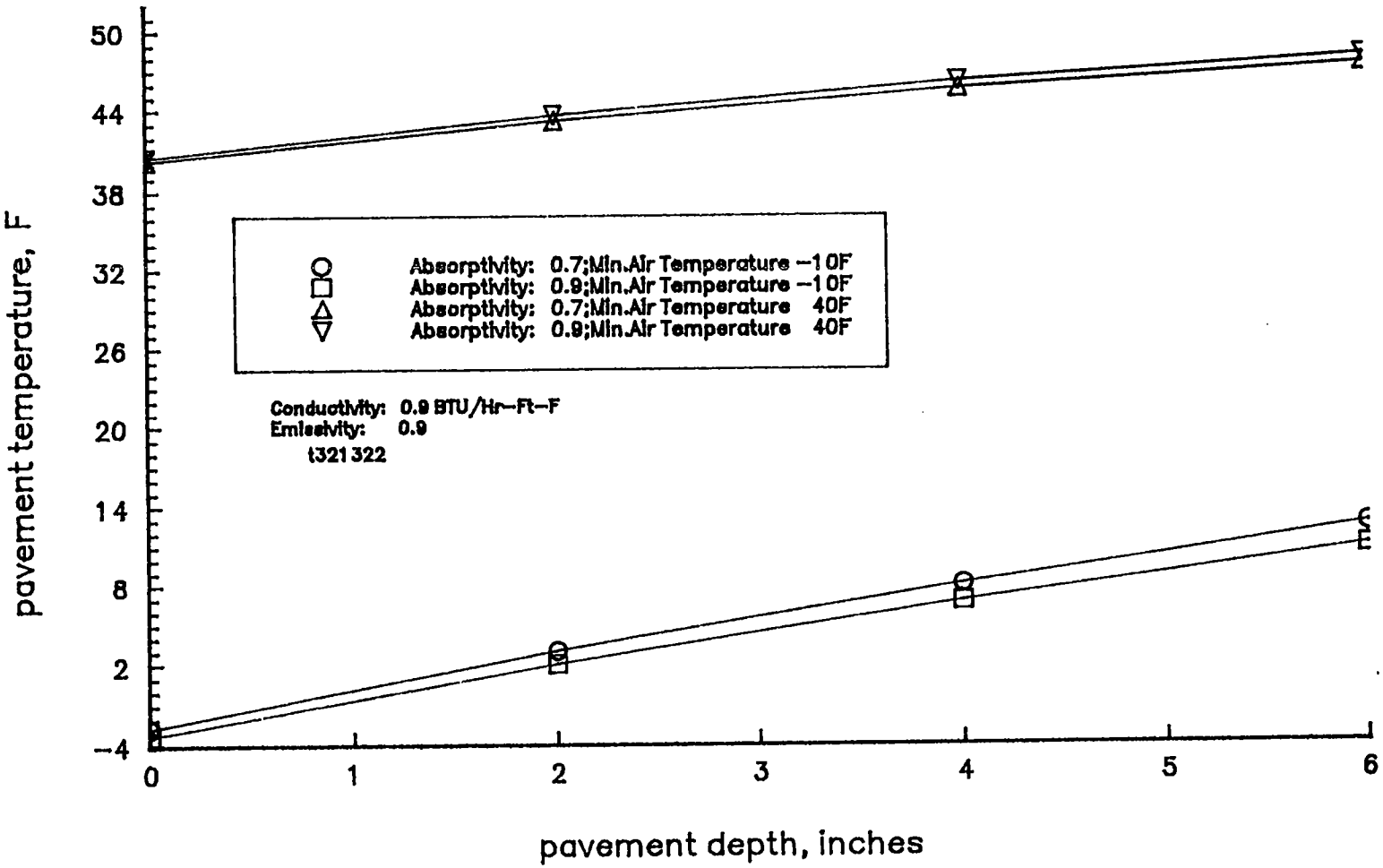

Figure III-14. Predicted Pavement Lowest Temperature Profile for Different Surface Short-wave Absorptivities at Two Different Levels of Minimum Air Temperatures.

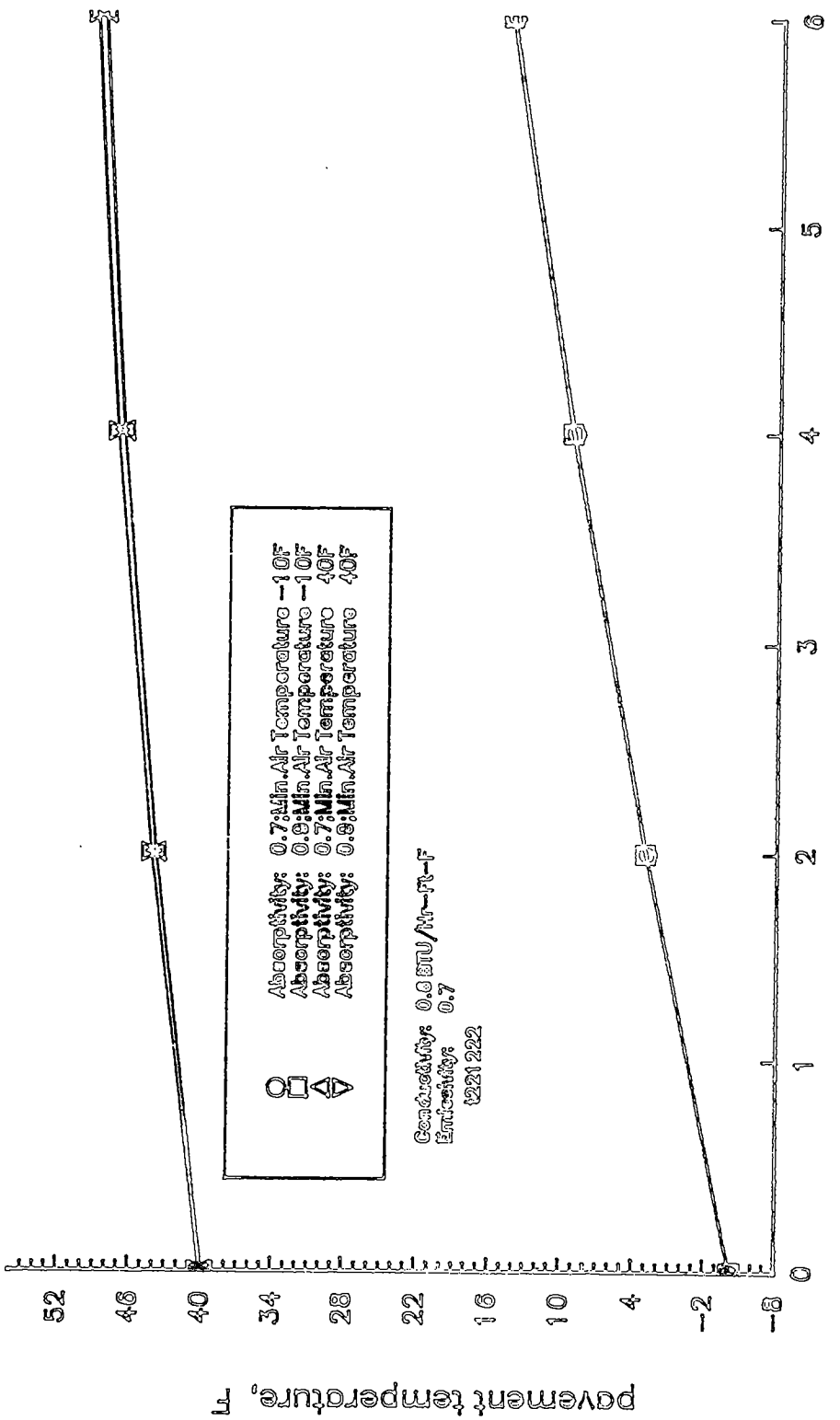

Figure II-15. Predicted Pavement Lowest Temperature Profile for Different Surface Short-wave Absorptivities at Two Different Levels of Minimum Air Temperatures.

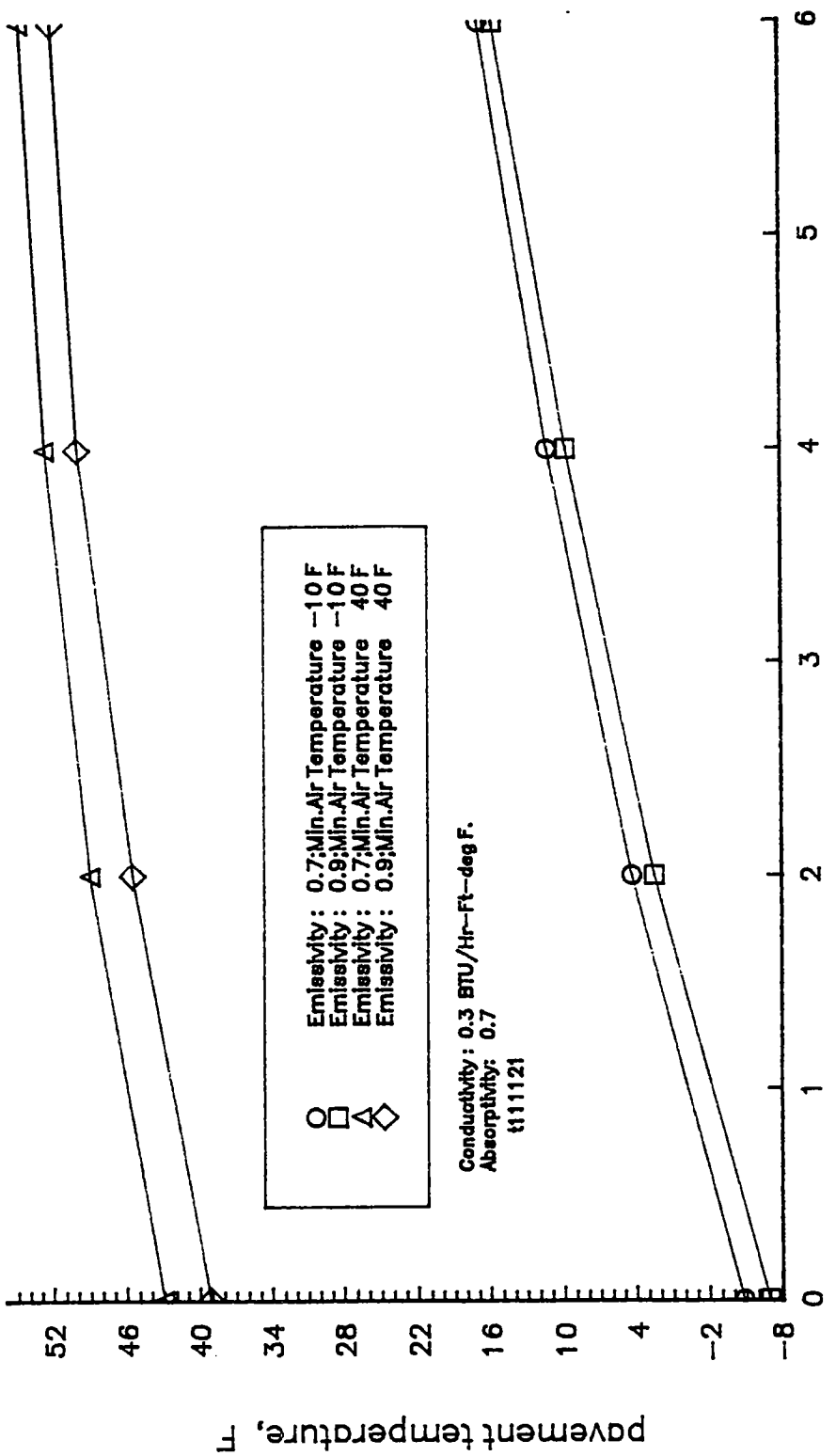

Figure III-16. Predicted Pavement Lowest Temperature Profile for Different Emissivity Factors at Two Levels of Minimum Air Temperatures.

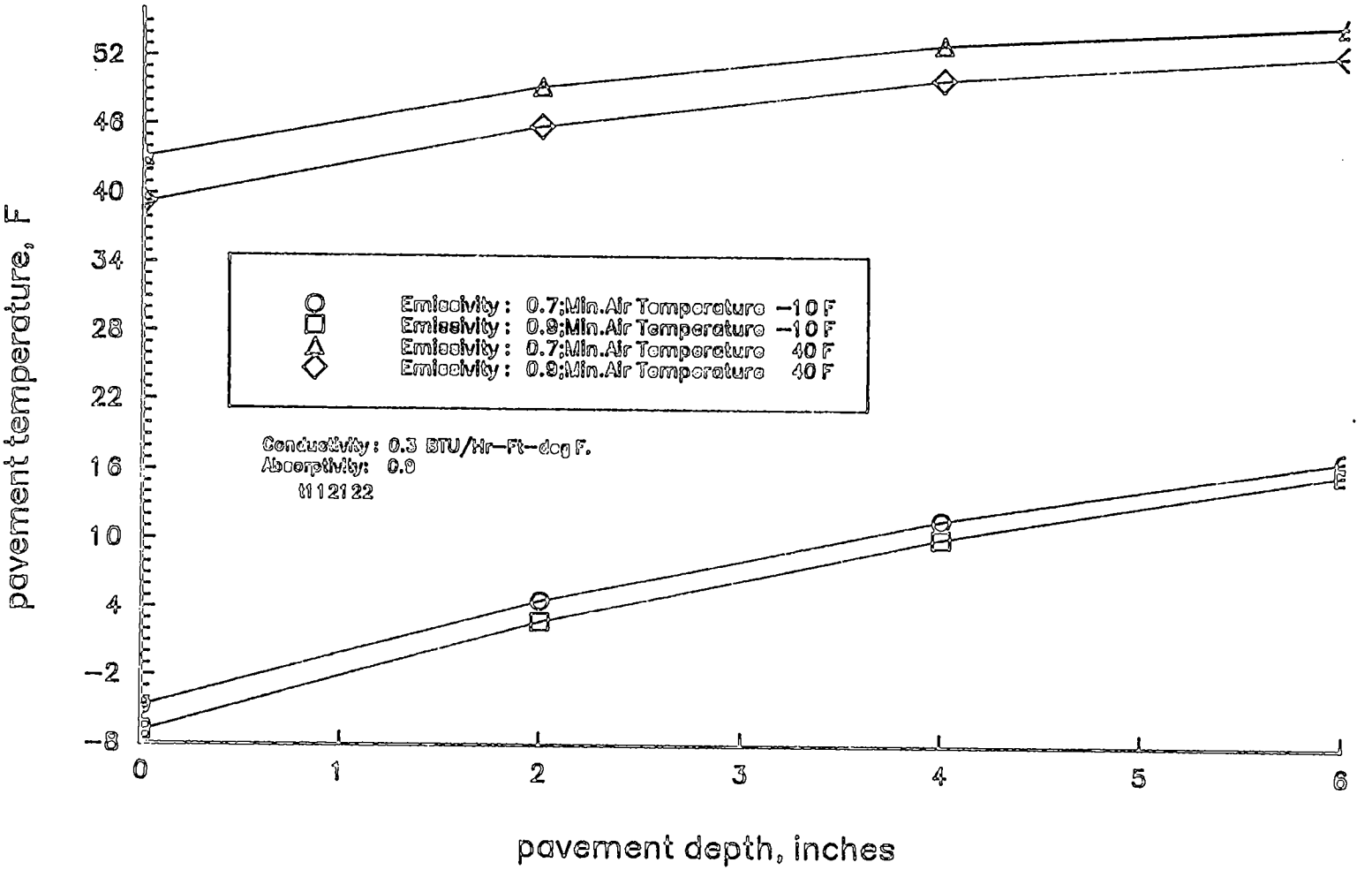

Figure III-17. Predicted Pavement Lowest Temperature Profile for different Emissivity Factors at Two Levels of Minimum Air Temperatures.

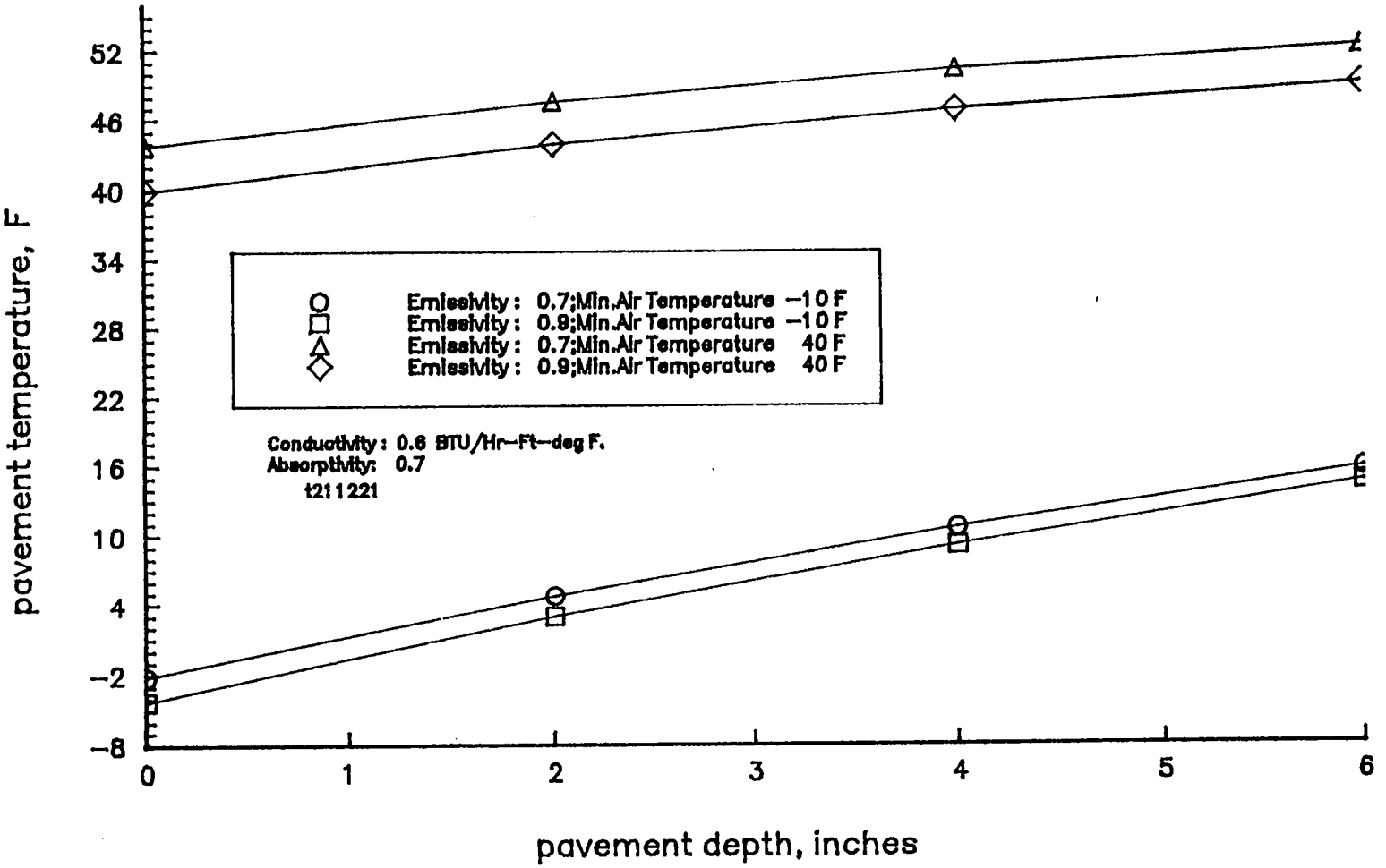

Figure III-18. Predicted Pavement Lowest Temperature Profile for Different Emissivity Factors at Two Levels of Minimum Air Temperatures.

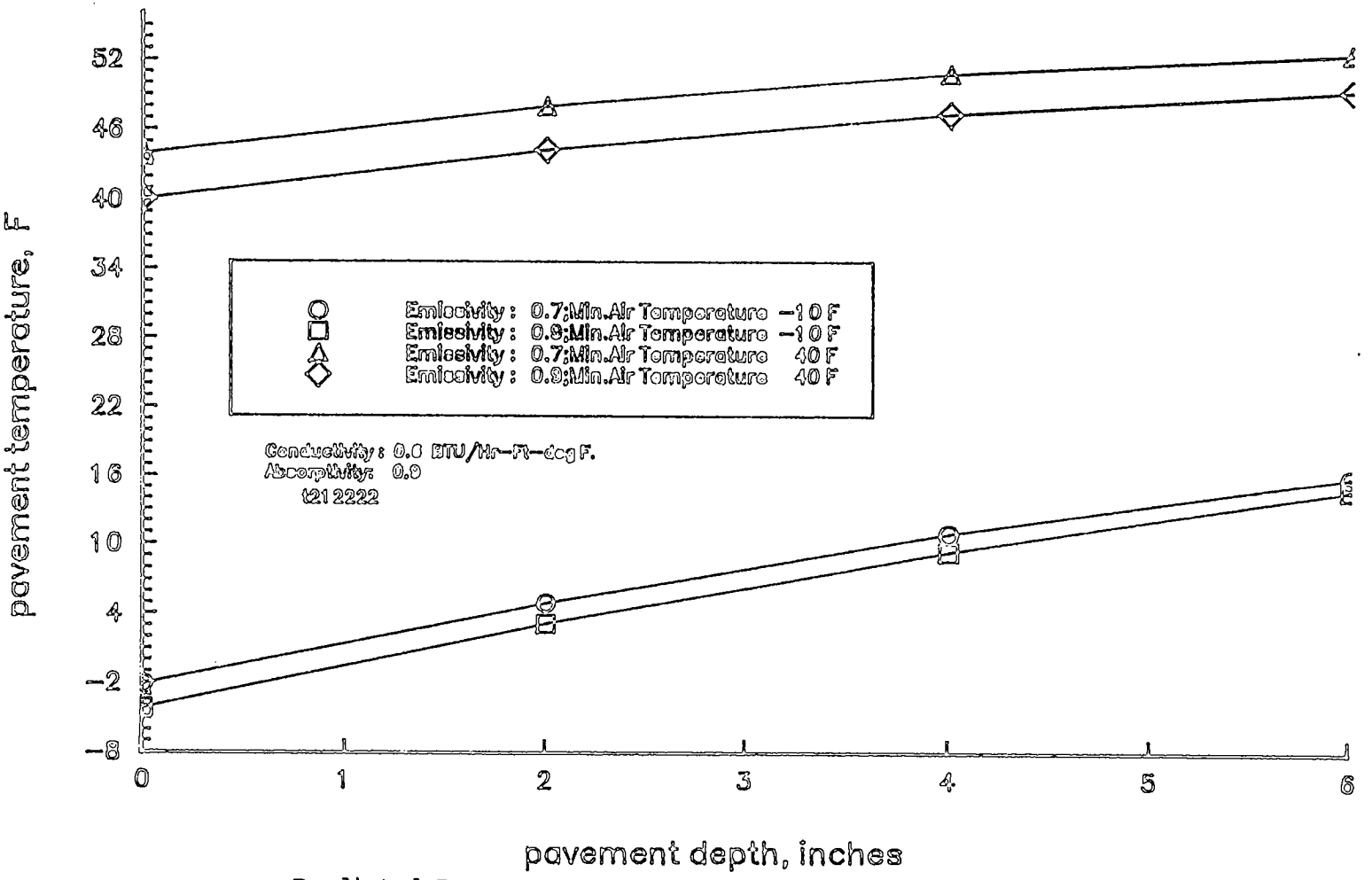

Figure III-19. Predicted Pavement Lowest Temperature Profile for Different Emissivity Factors at Two Levels of Minimum Air Temperatures.

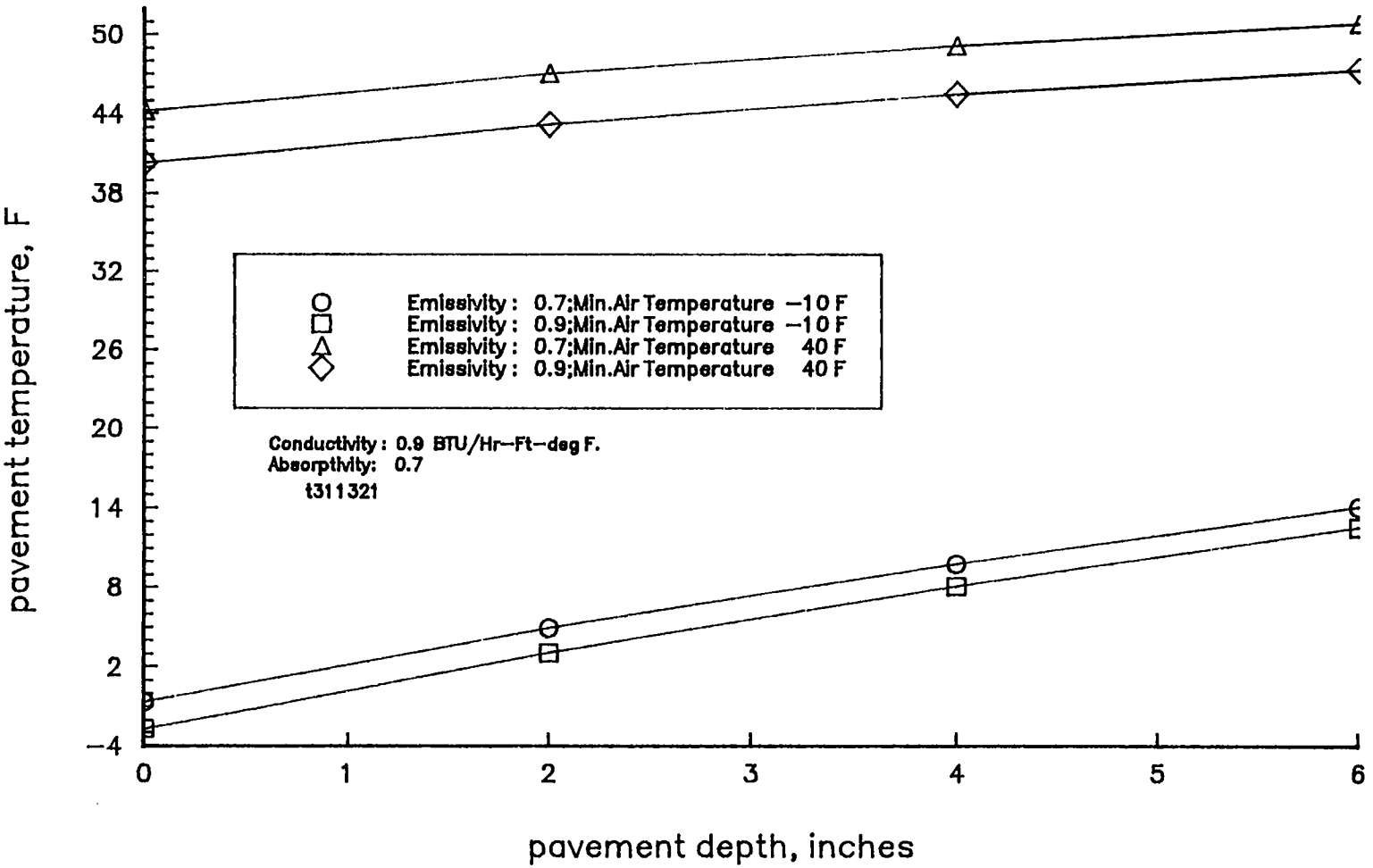

Figure III-20. Predicted Pavement Lowest Temperature Profile for Different Emissivity Factors at Two Levels of Minimum Air Temperatures.

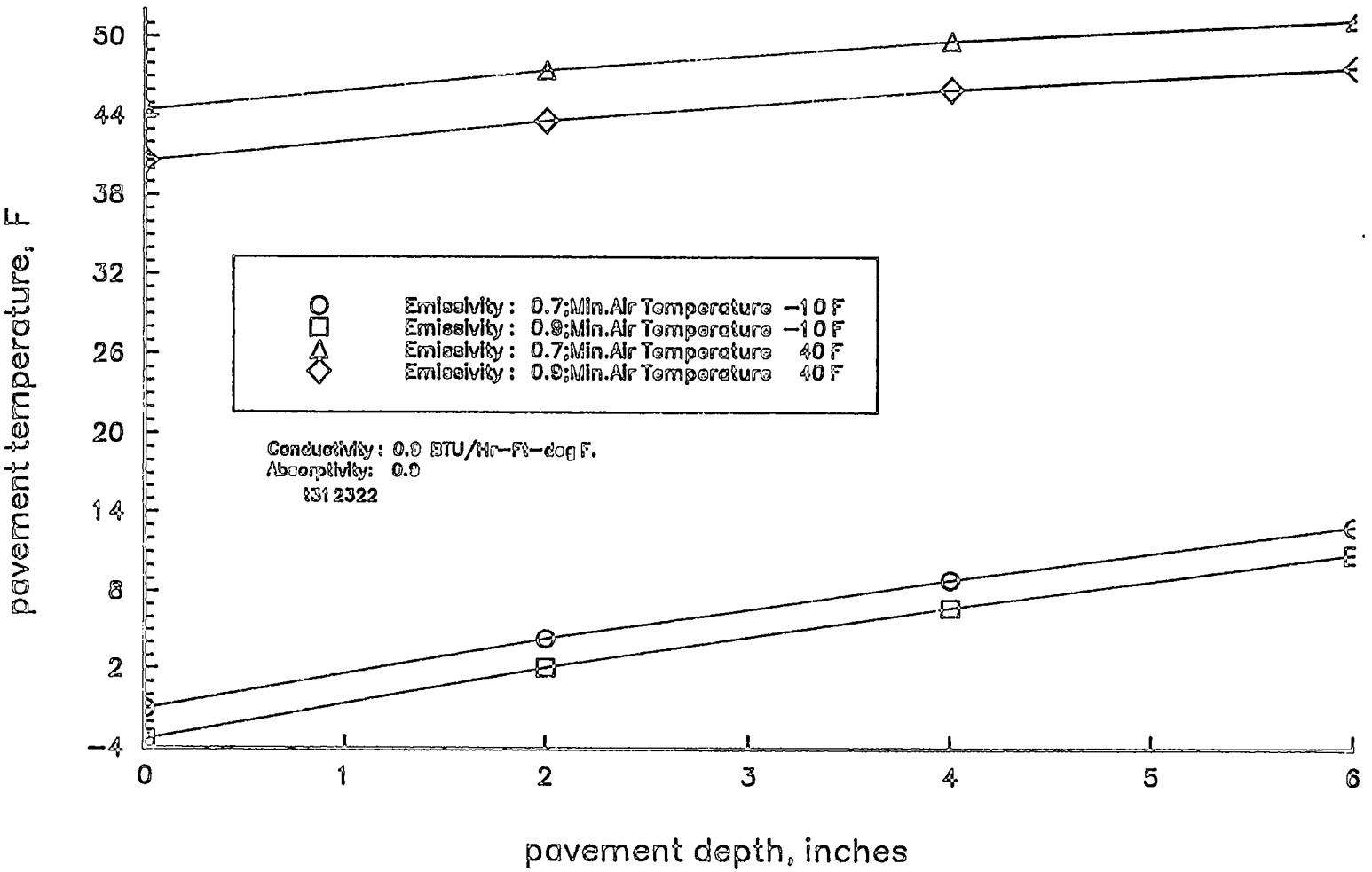

Figure III-21. Predicted Pavement Lowest Temperature Profile for Different Emissivity Factors at Two Levels of Minimum Air Temperatures.

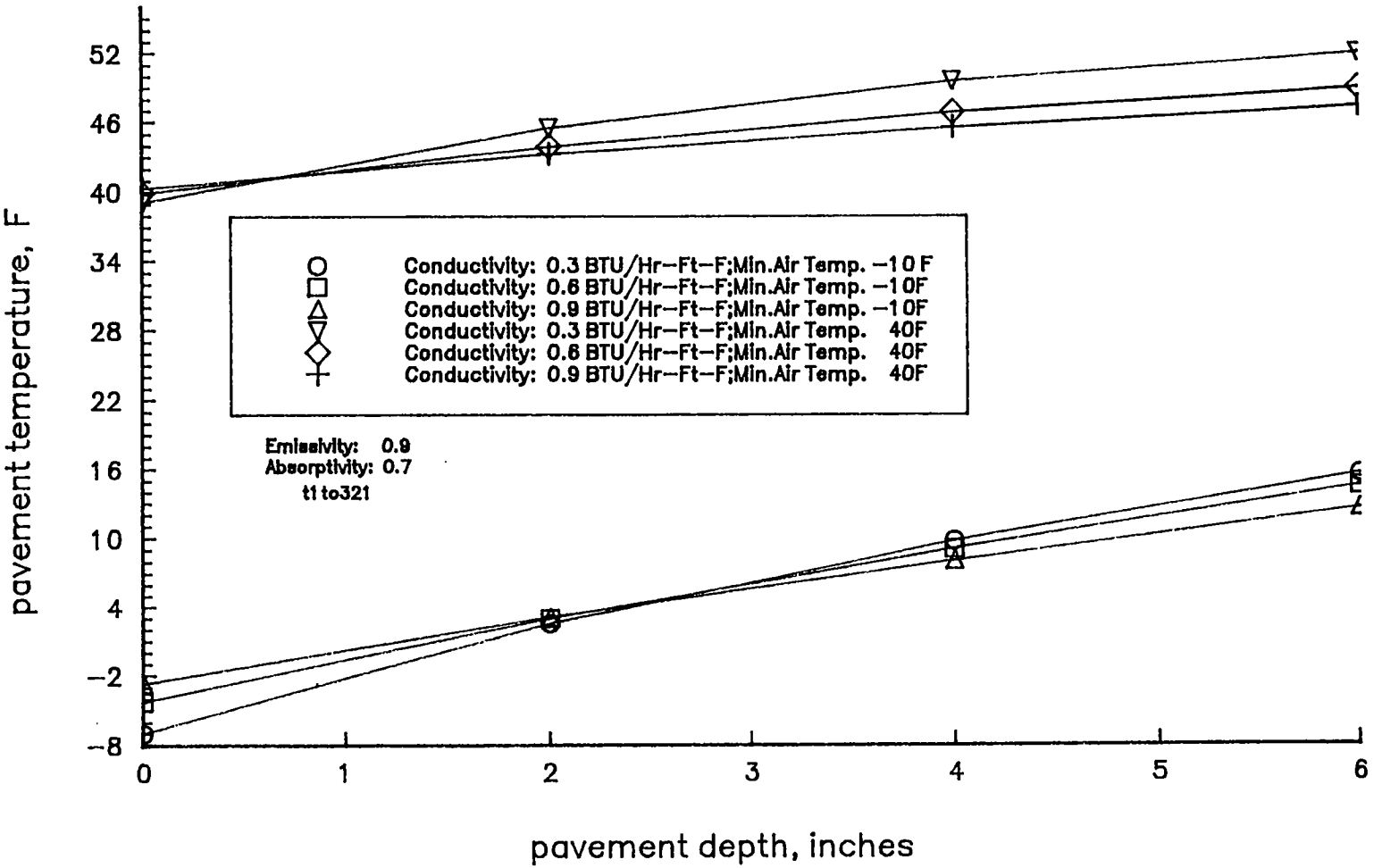

Figure III-22. Predicted Pavement Lowest Temperature Profile for Different Thermal Conductivities at Two Levels of Minimum Air Temperatures.

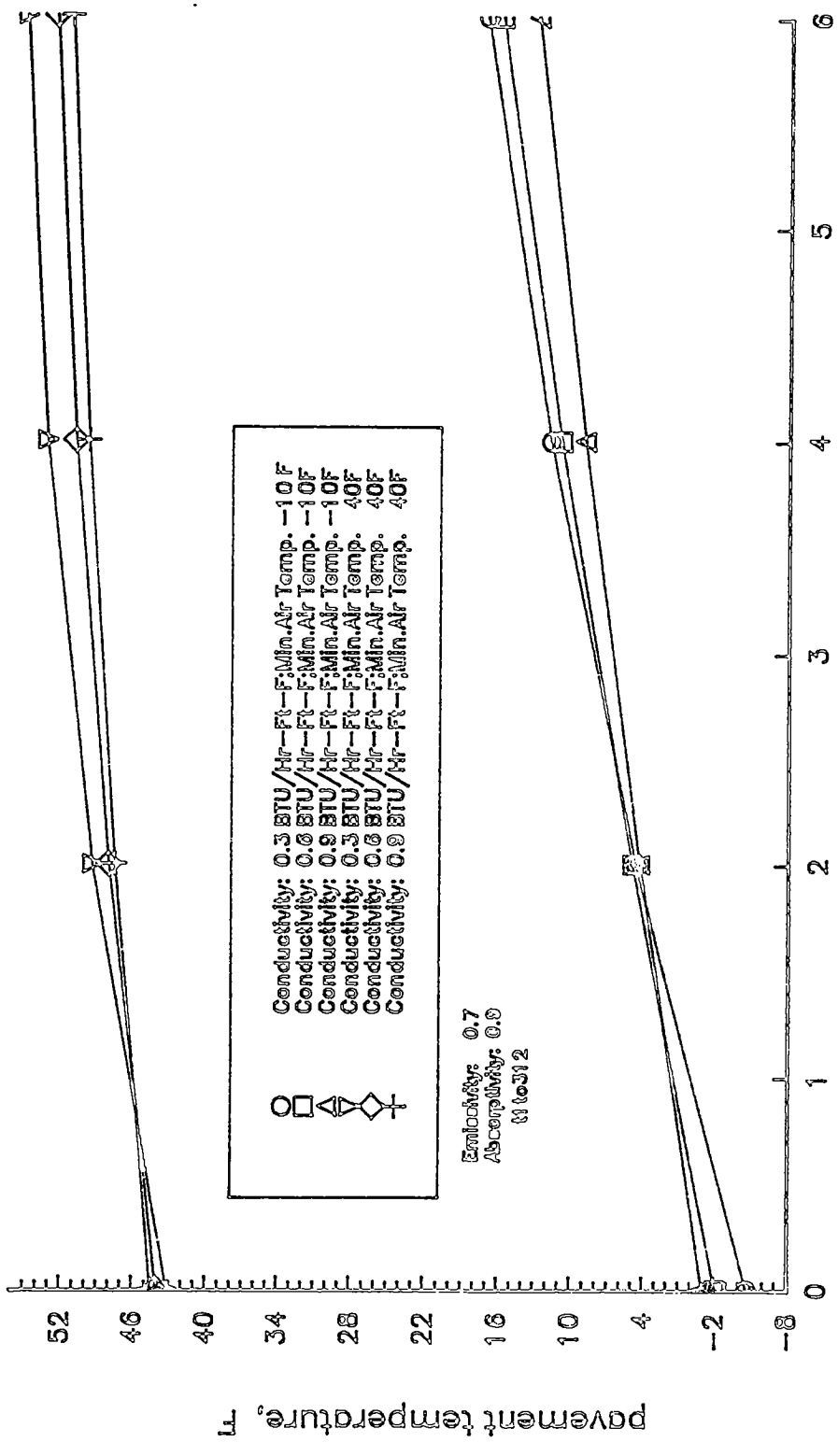

Figure III-23. Predicted Pavement Lowest Temperature Profile for Different Thermal Conductivities at Two Levels of Minimum Air Temperatures.

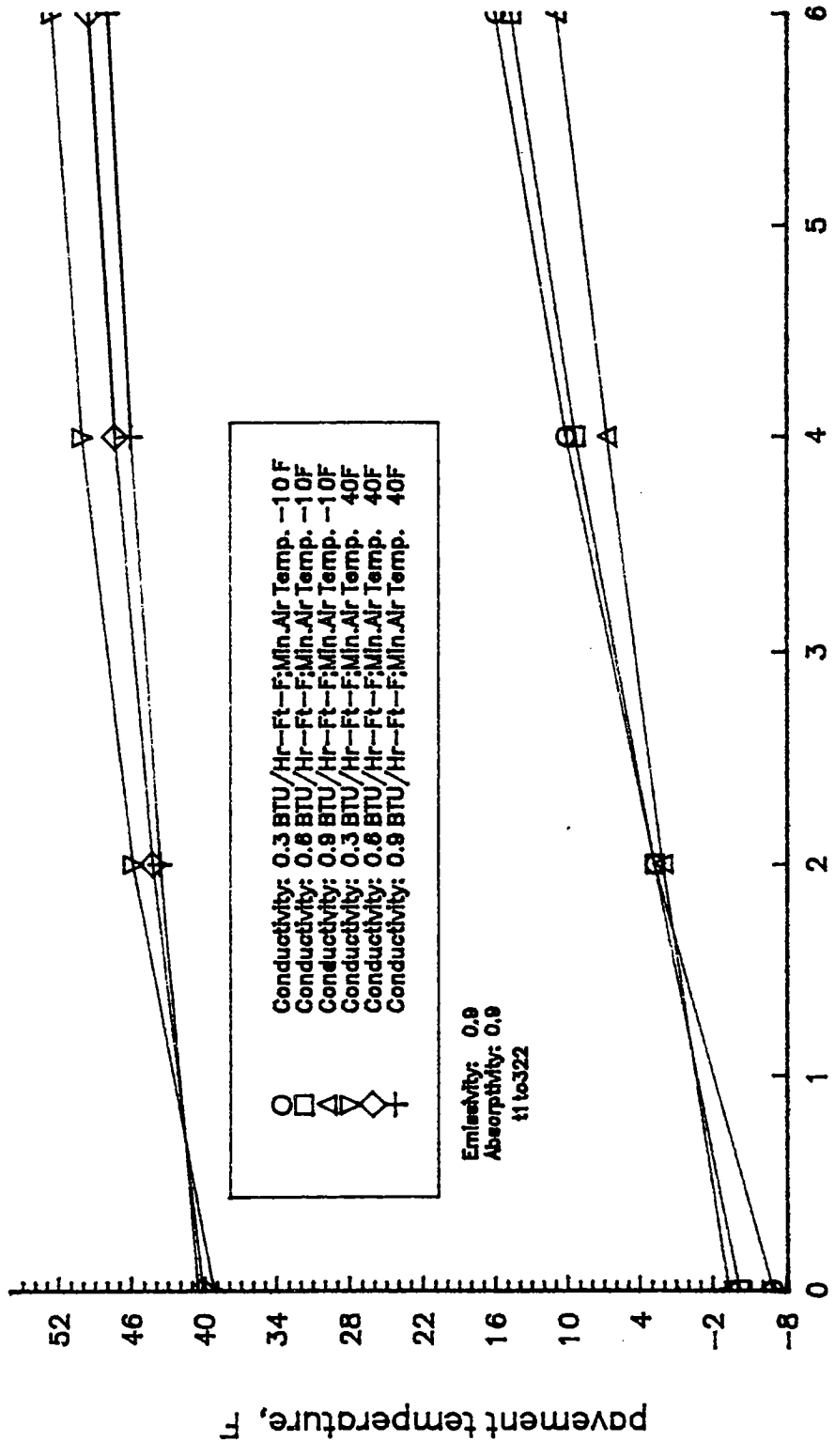

Figure III-24. Predicted Pavement Lowest Temperature Profile for Different Thermal Conductivities at Two Levels of Minimum Air Temperatures.

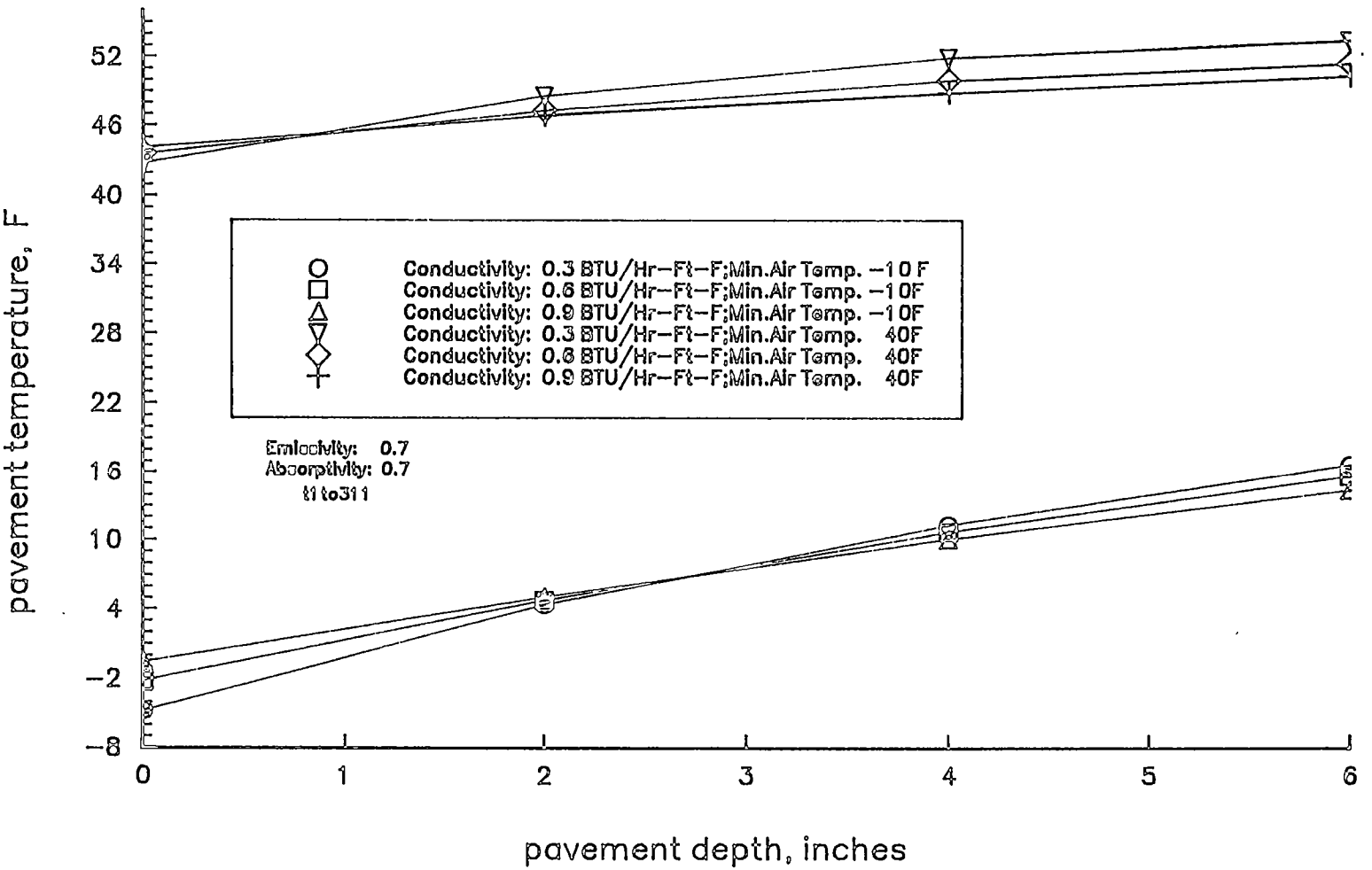

Figure III-25. Predicted Pavement Lowest Temperature Profile for Different Thermal Conductivities at Two Levels of Minimum Air Temperatures.

Fig. IV-1. Measured and Predicted Pavements Lowest Temperature Profiles at College Park, Maryland.

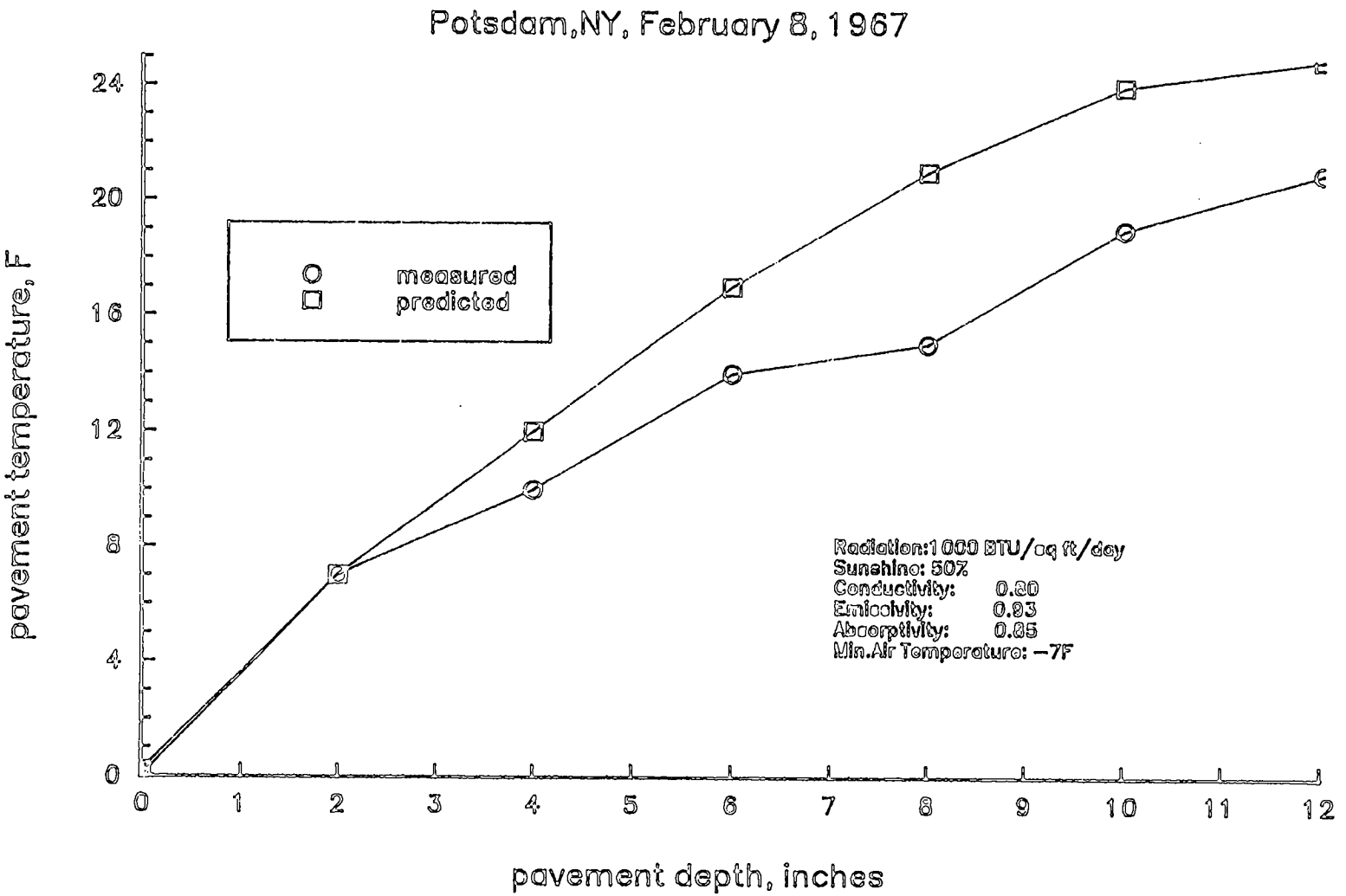

Fig. IV-2. Measured and Predicted Pavement Lowest Temperature Profiles at Potsdam, New York.

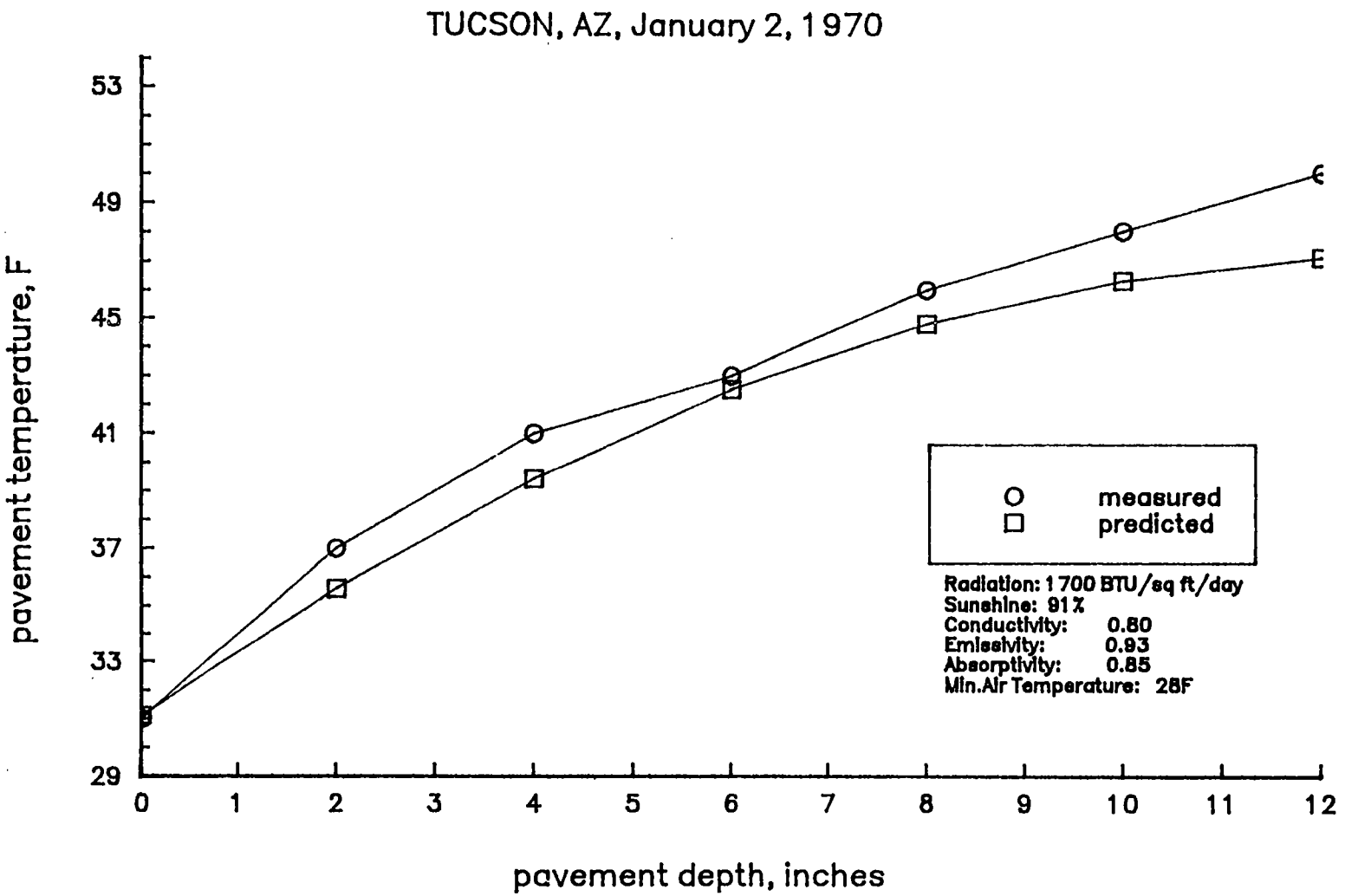

Fig. IV-3. Measured and Predicted Pavement Lowest Temperature Profiles at Tucson, Arizona.

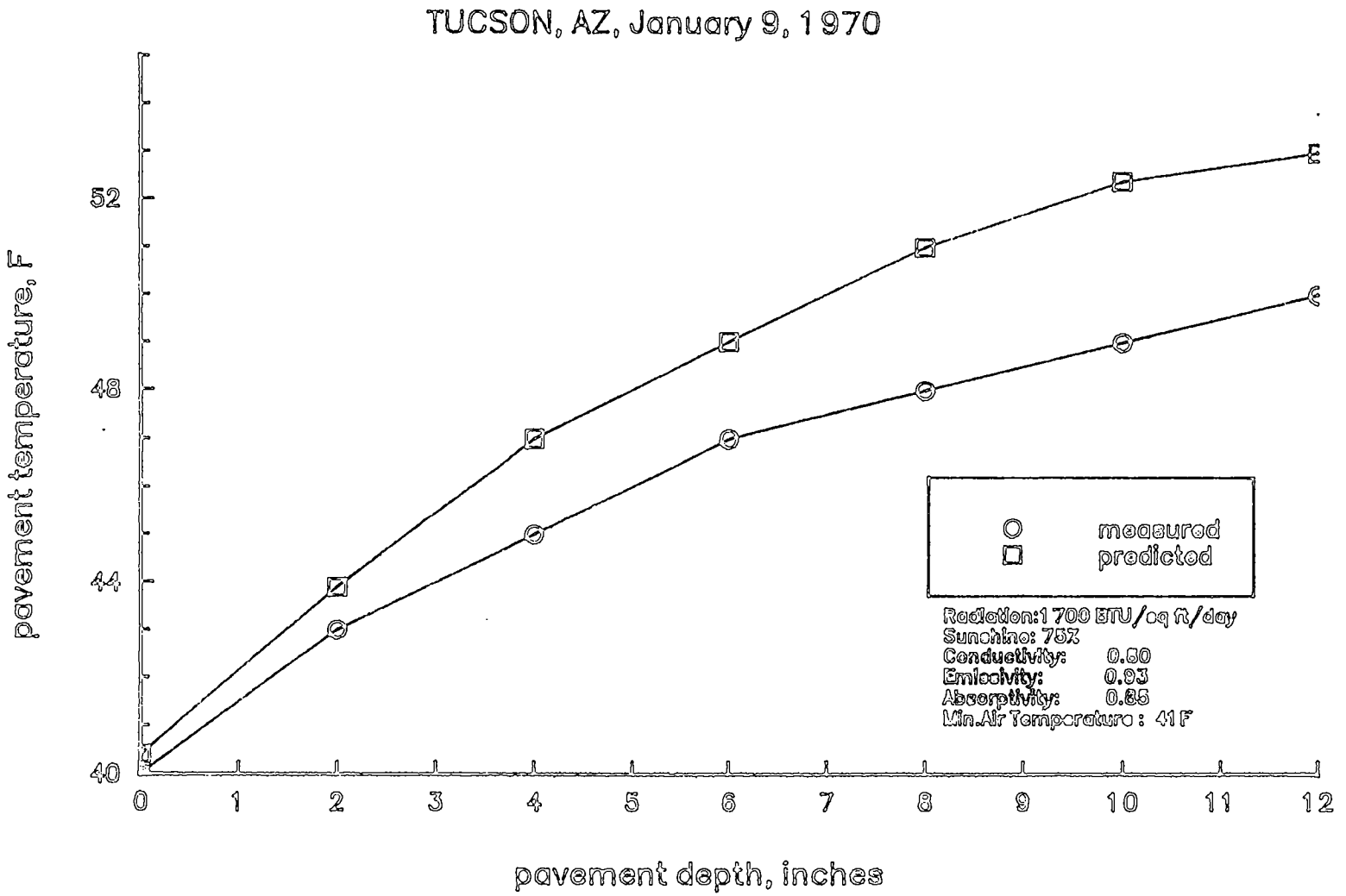

Fig. IV-4. Measured and Predicted Pavement Lowest Temperature Profiles at Tucson, Arizona.

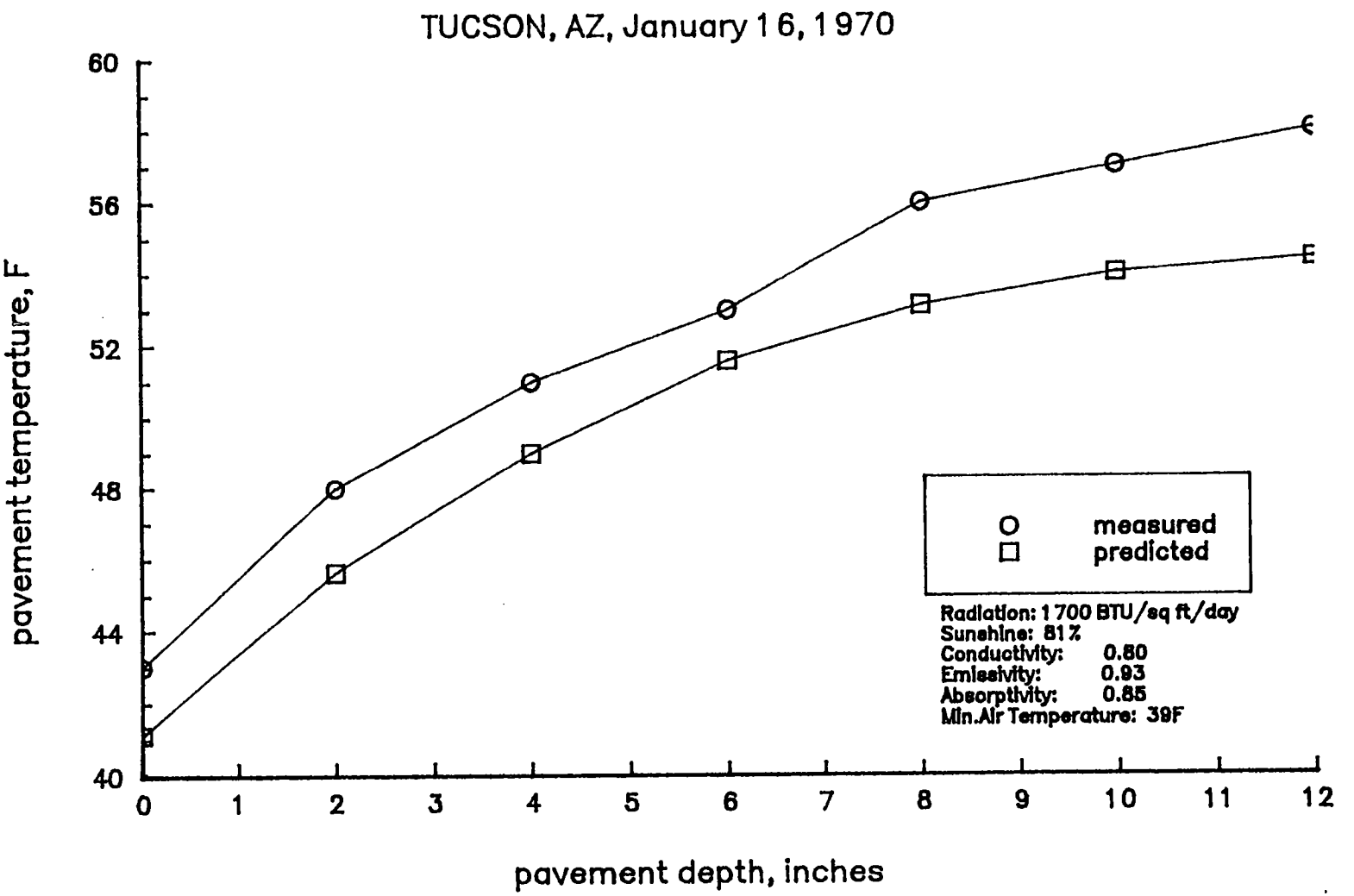

Fig. IV-5. Measured and Predicted Pavement Lowest Temperature Profiles at Tucson, Arizona.

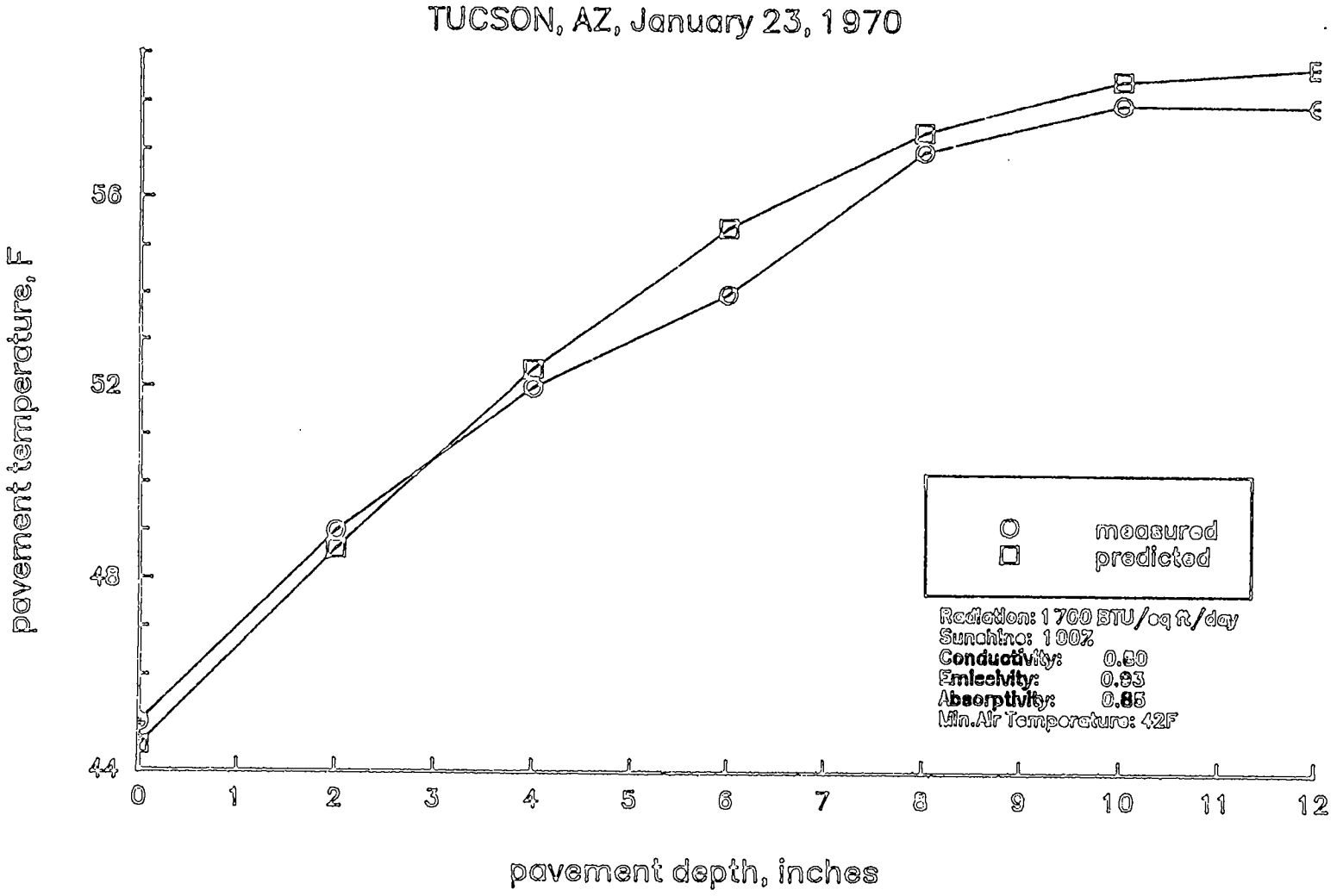

Fig. IV-6. Measured and Predicted Pavement Lowest Temperature Profiles at Tucson, Arizona.

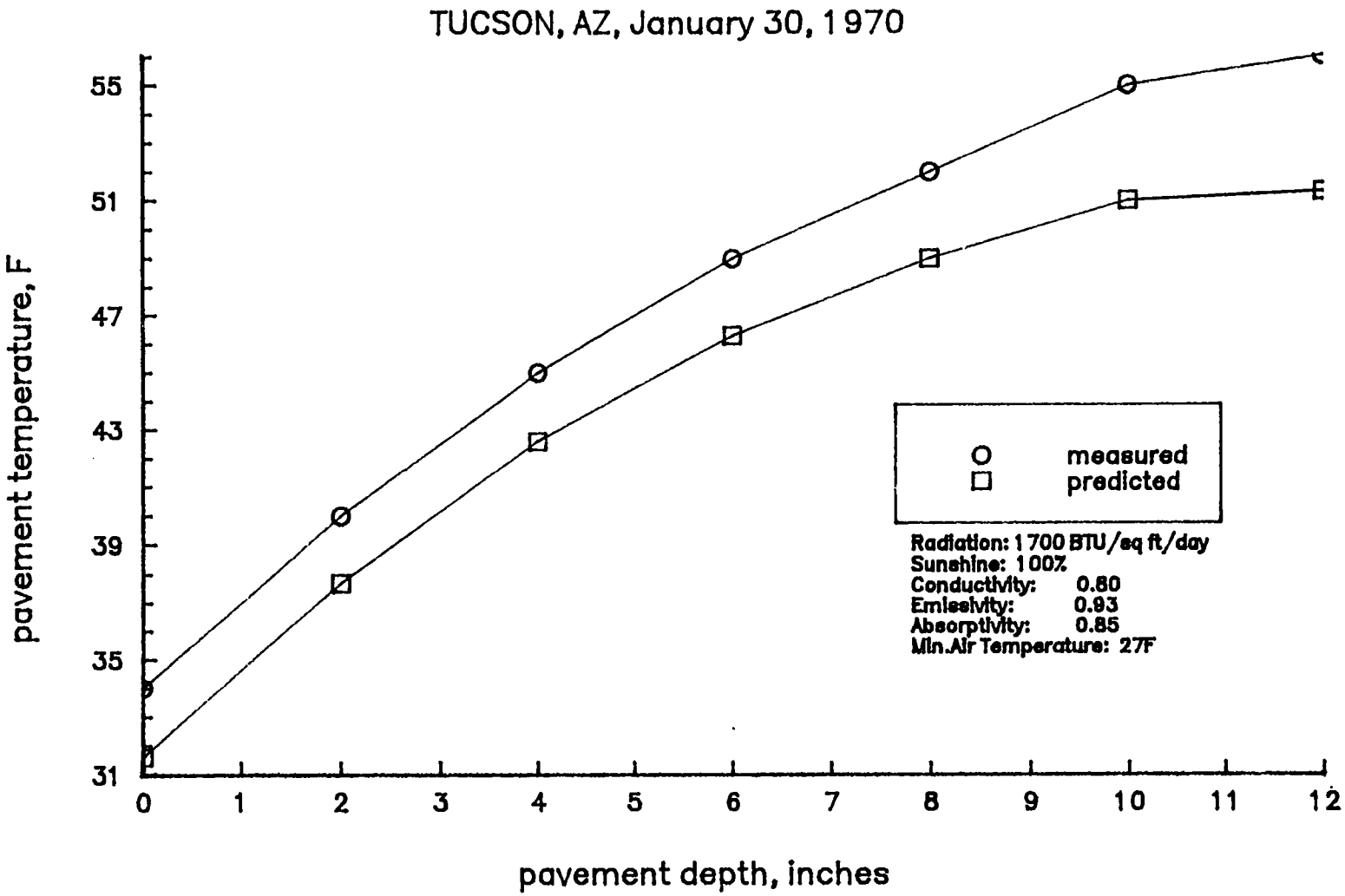

Fig. IV-7. Measured and Predicted Pavement Lowest Temperature Profiles at Tucson, Arizona.

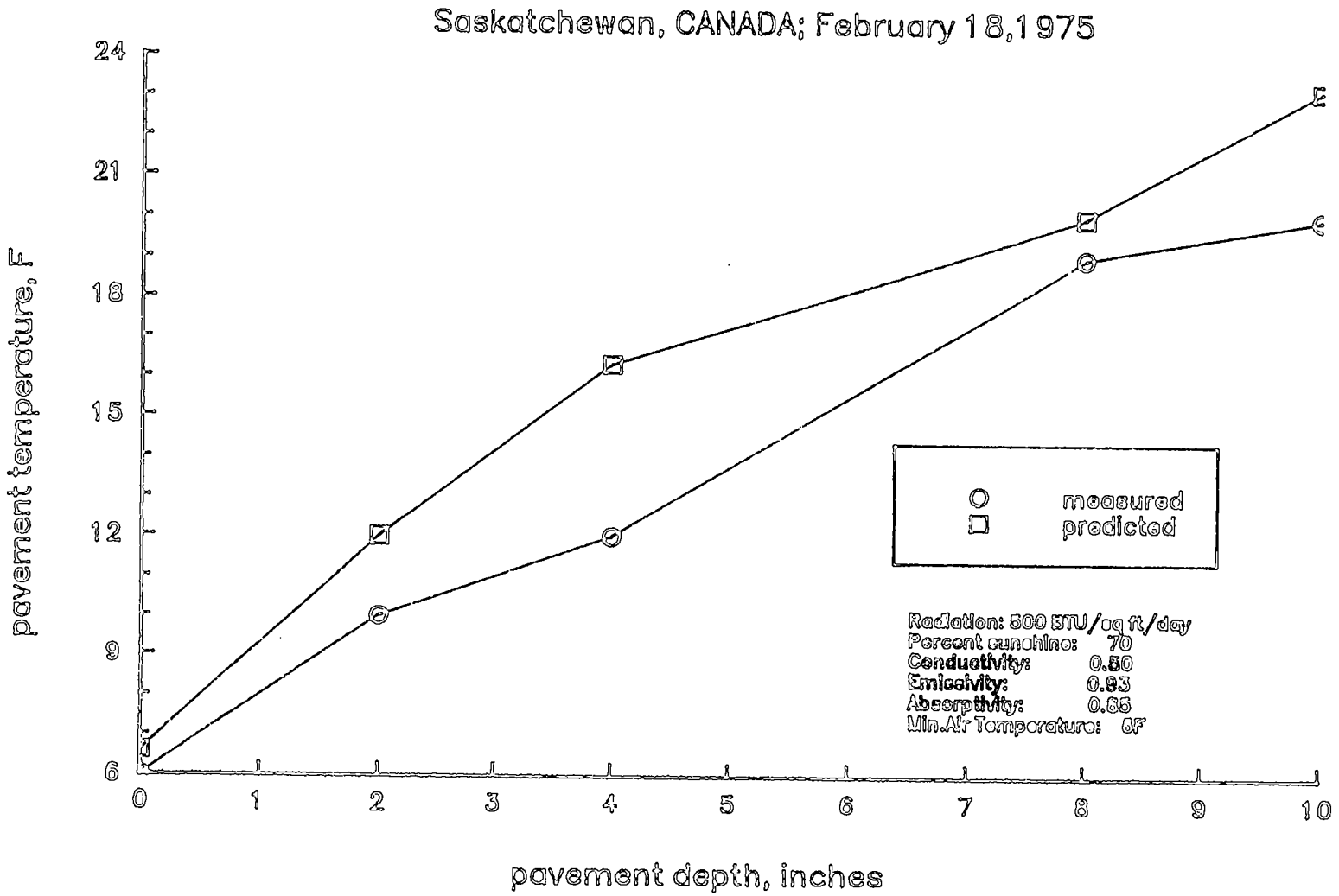

Fig. IV-8. Measured and Predicted Pavement Lowest Temperature Profiles at Saskatchewan, Canada.